Optical Coherence Tomography: a new imaging technique for neovascular age-related macular degeneration

This thesis is submitted in accordance with the requirements of the University of Liverpool for the degree of Doctor of Medicine

by

Jayashree Nair Sahni

October 2008

UNIVERSITY OF LIVERPOOL

DECLARATION

This thesis is the result of my own work. The material contained in this thesis has not been presented, either wholly or in part for any other degree or qualification.

The clinical observations and investigations were undertaken at the Clinical Eye Research Centre under the auspices of the Department of Ophthalmology, University of Liverpool and St Paul's Eye Unit, Liverpool.

Signed.

Jayashree Nair Sahni

ACKNOWLEDGEMENTS

This thesis was made possible due to the help, advice and support of many people and I would like to take this opportunity to thank them.

First and foremost I had like to my supervisor, Simon Harding, Professor of Ophthalmology & Consultant Ophthalmologist, St Paul's Eye Unit, University of Liverpool for his advice, guidance, inspiration, encouragement and support throughout the research and at all stages of this thesis.

Paulo Stanga, Consultant Ophthalmologist, Manchester Royal Eye Hospital, whose advice was invaluable and pivotal in the initial formulation of this research project. He also provided me with the initial training in the acquisition and interpretation of the optical coherence tomography scans.

Alison MacKay, Scientist, Clinical Engineering Department, University of Liverpool, who worked alongside me collecting, analysing and interpreting the data for the multifocal electroretinogram study.

The consultants, Ian Pearce and Michael Briggs, the associate specialist, Pauline Lenfestey and junior doctors at the Clinical Eye Research Centre, St Paul's Eye Unit for their assistance with the clinical examination of the research patients.

Andrew Tompkin, Valerie Tompkin and the Department of Optometry at St Paul's Eye Unit, for conducting all the vision assessments for this study.

The nurses (Sandra Taylor, Catherine Moore, Julie McNally, Samantha Kaye) of the Clinical Eye Research Centre who cared for the patients

Jerry Sharp and Martin Hodson, Imaging Technicians, St Pauls Eye Unit, Liverpool for providing photographic services.

Claire Kelly, clerk, Clinical Eye Research Centre who helped to identify the patients at the baseline visit and also with the throughput of the patients through a busy and often chaotic department.

Lindy Gee, Research Secretary to Professor Harding, who helped to co-ordinate the meetings and also helped with acquiring finances for the various incidentals.

David Wong, Professor of Ophthalmology & Consultant Ophthalmologist, St Paul's Eye Unit, University of Liverpool for his advice and encouragement.

Ian Grierson, Professor of Ophthalmology, University of Liverpool for encouragement and support.

The Foundation for Prevention of Blindness, and the PDT fund who provided financial support for this research.

The patients, their relatives and carers who participated in the studies for their courage and co-operation.

And finally my husband, Vishal Sahni, who was a beacon of unconditional support and encouragement during the preparation of this manuscript.

TABLE OF CONTENTS

APPENDICES

Appendix 1 OCT Grading Protocol

Appendix 2 OCT examples

Appendix 3 List of publications and presentations.

Appendix 4 Sahni J, Stanga PE, Wong D, Harding SP. Optical Coherence Tomography in photodynamic therapy for subfoveal choroidal neovascularisation secondary to age-related macular degeneration: a cross-sectional study. Br J Ophthalmol. 2005;89:316-20.

Appendix 5 Sahni J, Harding SP. Optical coherence tomography of the vitreomacular interface in photodynamic therapy. Br J Ophthalmol. 2005;89:929.

Appendix 6 Sahni J, Stanga PE, Kent D, Wong D, Harding SP. Morphometric Analysis of End-stage Choroidal Neovascularisation after Photodynamic Therapy for Age-related Macular Degeneration using Optical Coherence Tomography. Clin Experiment Ophthalmol. 2007;35:13-7.

Abstract

OPTICAL COHERENCE TOMOGRAPHY: A NEW IMAGING TECHNIQUE FOR NEOVASCULAR AGE-RELATED MACULAR DEGENERATION

Jayashree Sahni

April 2008

Introduction

Neovascular age-related macular degeneration (AMD) is becoming an increasing socio-economic problem as the proportion of the aged population is continuously increasing. Optical coherence tomography (OCT), which was only introduced in ophthalmology a decade ago, has been rapidly accepted in the field of retinal imaging and AMD management. However, studies on the clinical relevance and effectiveness of the OCT systems in clinical practice are lacking.

Aim

To determine the value of OCT in the management of patients with subfoveal choroidal neovascularisation (CNV) secondary to AMD by studying the effect of PDT on the morphology and function of the retina.

Methods

Patients were recruited prospectively from a population with subfoveal predominantly classic CNV attending St Paul's Eye Unit for PDT, between 2002 and 2004. All patients underwent best-corrected visual acuity (BCVA) measurement, OCT scans at the fovea, FA and slit lamp biomicroscopy. No changes were made to the established treatment plan with PDT.

Results

Overall, 264 eyes of 217 patients met the eligibility criteria. Good quality scans passing through the fovea could be obtained in 90% of the eyes.

New terminology was defined and a protocol for interpreting OCT images was developed. The protocol was validated and found to have acceptable interobserver concordance in eyes with neovascular AMD.

Using FA as the reference standard OCT had a sensitivity of 86% and specificity of 57% in detecting fluid (intra and sub retinal fluid (IRF and SRF).

There was an association between neuroretinal foveal thickness (NFT) on OCT and BCVA at baseline, but this was lost following treatment with PDT. There was an association between outer high reflectivity band thickness (OHRBT) on OCT and BCVA.

A 3-stage OCT based classification system based on the response of the retina and CNV to a course of PDT was developed.

Conclusion

The protocol developed for this study can be used to interpret OCT scans in eyes with neovascular AMD, with a high level of interobserver agreement.

The low specificity of the OCT in detecting leakage on FA may be due to the inherent differences between the two techniques. FA can detect leakage whereas OCT detects collection of the fluid (IRF or SRF). In the presence of a functioning RPE, fluid may not collect. Difficulty in distinguishing between staining and leakage on FA may lead to an underestimation of the incidence of fluid at the macula.

The lack of association between NFT and BCVA may be because patients with subfoveal CNV can have eccentric non-foveal fixation. Also eyes with extensive disruption of the retinal architecture may still have normal NFT that may not reflect the viability of the photoreceptors.

Reduced vision in eyes with thicker OHRBT on OCT is supported by histologic studies, which suggest that eyes with thicker disciform scars are associated with more severe photoreceptor loss.

In the management of neovascular AMD, an OCT based classification can provide valuable data that can contribute to the effective decision-making.

Chapter 1

INTRODUCTION

This chapter introduces my research and places it within the context of the historical development of retinal imaging.

In it I describe the impact of age-related macular degeneration (AMD) and its consequence on the aging population.

Finally I describe the layout of the thesis and present the aims of this research in investigating the optical coherence tomography features of neovascular AMD.

1.1 HISTORICAL PERSPECTIVE

The advancement of ophthalmology has been linked with the development of instruments and techniques. Fundus imaging has become an essential requirement for clinical research, teaching and patient care in the medical retina speciality. Therefore, it is appropriate that a study on the use of a new imaging technique should look back to the historical development of retinal imaging.

1.1.1 Ophthalmoscope

One of the most exciting inventions in the study of retinal diseases was the invention of the ophthalmoscope in 1851. Hermann von Helmholtz's ophthalmoscope consisted of an "eye-mirror" made of plates of glass and used a flickering candle as a source of illumination (Figure 1.1).[1] This invention revolutionised ophthalmology. He demonstrated that there were 3 essential elements to the working of an ophthalmoscope: a source of illumination, a reflecting surface to direct light towards the eye and a means of correcting an out-of-focus image on

the fundus. Prior to his invention, ophthalmologists could not view the posterior section of the eye and struggled to explain certain classes of eye disease in which there was a dimness or loss of vision. "*In the whole history of medicine there is no more beautiful episode than the invention of the ophthalmoscope, and physiology has few greater triumphs*," wrote American ophthalmologist Edward Loring in the opening paragraph of his *Textbook of Ophthalmology* in 1892.[2] The introduction of this ophthalmoscope into clinical ophthalmology by Albert von Graefe in Berlin, Edward Jaeger in Vienna and William Bowman in London served to increase the knowledge and understanding of many eye conditions including the recognition of "senile macular degeneration".

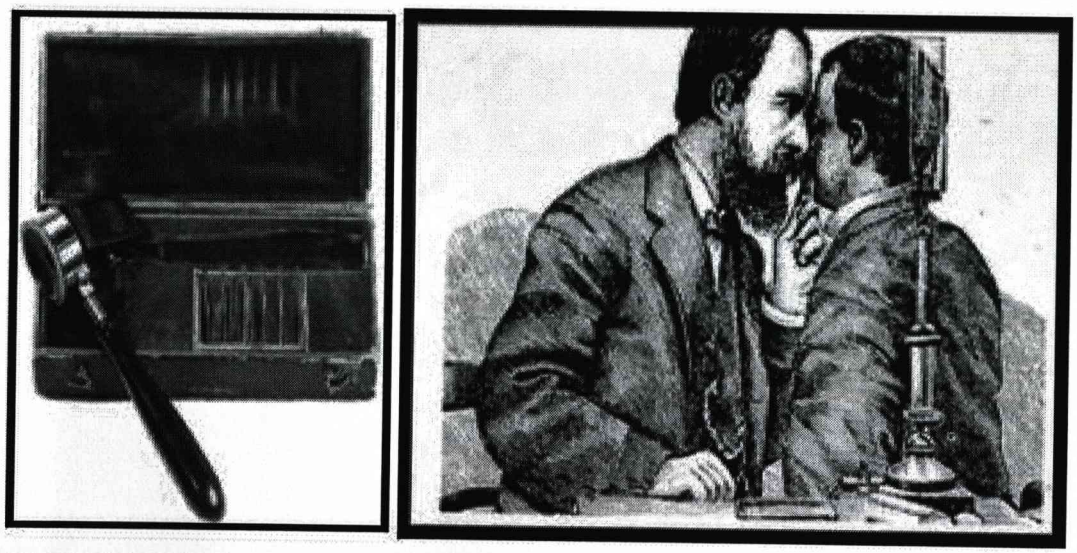

Figure 1.1 : Helmholtz's ophthalmoscope, 1851. (British Journal of Ophthalmology 2002;86:602-603). Helmholtz used a flickering candlelight as a source of illumination.

1.1.2 Slit lamp biomicroscope[3]

Another landmark invention in the development of ophthalmology was the invention of the slit lamp biomicroscope by Allvar Gullstrand, a professor of ophthalmology at the University of Uppsala in Sweden (Figure 1.2). In 1911 he won the Nobel Prize in Medicine for his achievement. An extension of the slit-lamp

microscope was developed by Koeppe who, by using a contact-glass, succeeded in examining the fundus.

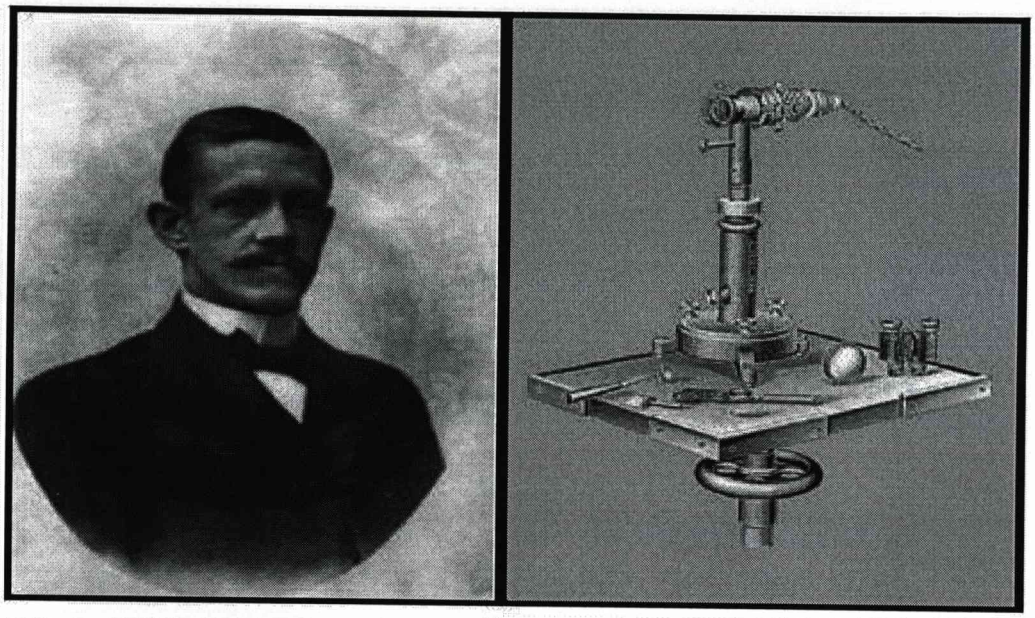

Figure 1.2: Professor Allvar Gullstrand(1862-1930) & Nernst slit lamp designed by Gullstrand in 1912.

1.1.3 Fundus photography

Medical illustration has a long history of depicting the eye, going as far back as the ancient Greeks (Figure 1.3).[4] But realistic depictions of the eye were only possible following the invention of the ophthalmoscope. Duke –Elder (1967) credits the first realistic graphic representation of the retina and the first coloured printed illustration of the fundus of the eye to Adrian Christopher Van Trigt and the drawing appeared in his thesis of '*Dissertatio Ophthalmologica Inauguralisde Speculo Oculi'* in 1853 (Figure 1.4).[5]

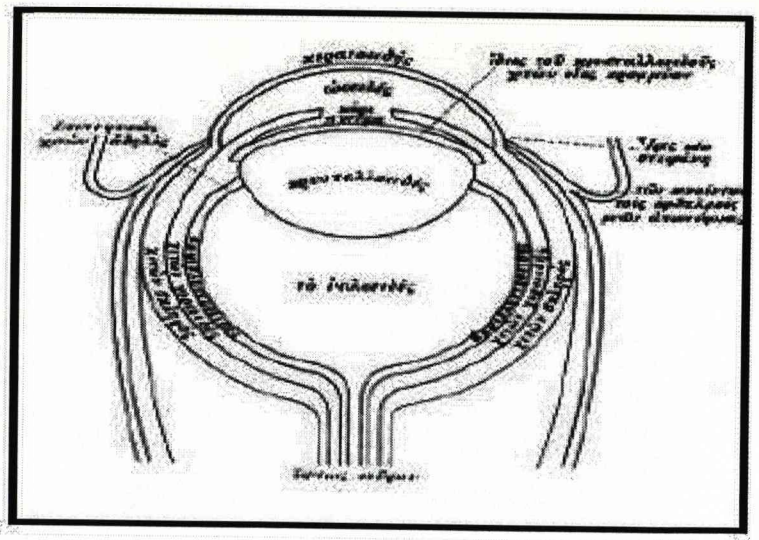

Figure 1.3: Galen's eye from about 150 AD. (Duke-Elder, 1961)

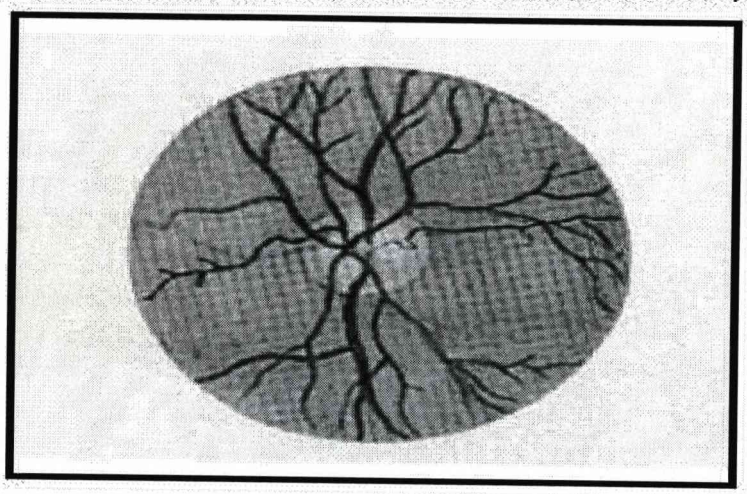

Figure 1.4: The realistic illustration of the fundus of the eye by Van Trigt in 1853. The original was in colour. (from Duke-Elder, 1967).

Fundus photography was developed in pursuit of an accurate and specific graphic representation of the retina. The first published photograph of in-vivo human retina was by Jackman and Webster in the Philadelphia Photographer in 1888 (Figure 1.5).[6] The prototype camera was fixed to the patient's head, and a 2.5 minute exposure was used (Figure 1.6). Although the apparatus showed only the largest details of the retinal anatomy and the images were extremely blurred it was groundbreaking in allowing photographic documentation of retinal findings. Fundus

photography's initial impact on ophthalmology was to replace tedious drawings and paintings of the retina.

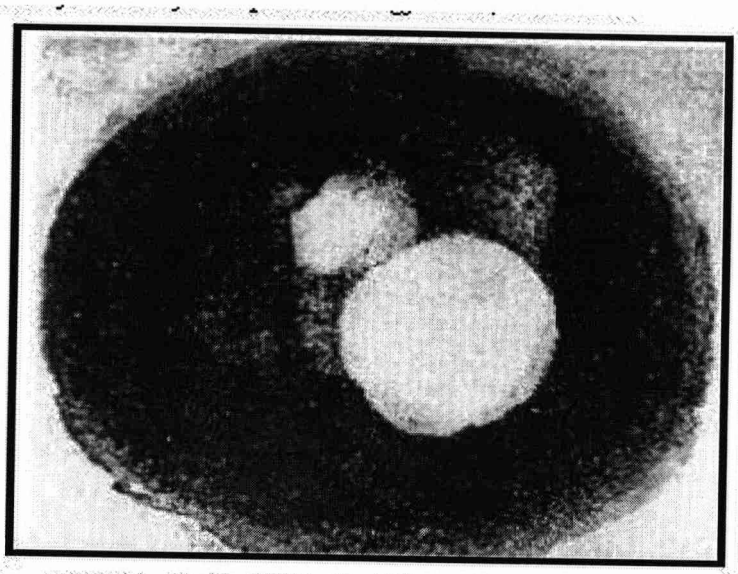

Figure 1.5: The first published photograph of in-vivo human retina by Jackman and Webster in the 'Philadelphia Photographer' in 1888. The small white area on the top is the optic disc, and the lower, larger light area is an artifact. Blood vessels cannot be identified. (reproduced from Mann, 1970).

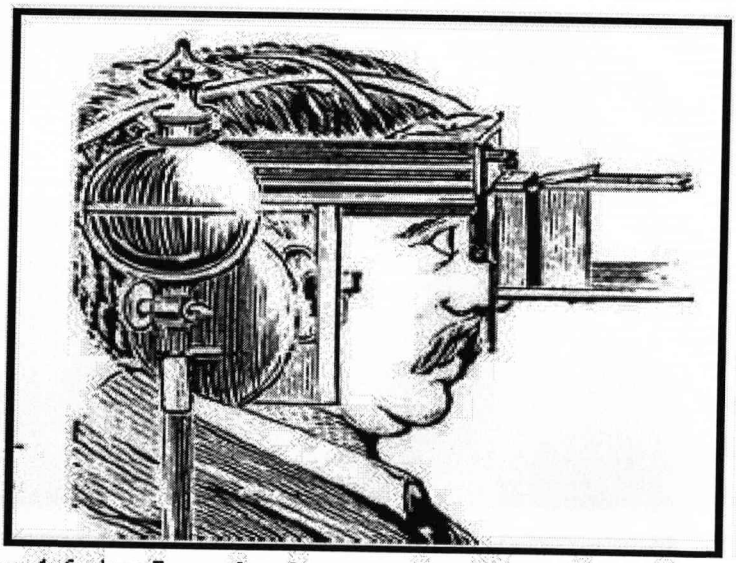

Figure 1.6: An albo-carbon burner such as the one shown here was used to acquire the first published human fundus photograph and required a 2.5 minute exposure. (reproduced from Mann, W.A. History of photography of the eye. Survey of Ophthalmology 1970;15:179-189.

In 1891, Gerhoff used flash powder to illuminate a low magnification fundus photograph (Figure 1.7 & 1.8). This helped to produce clearer retinal photographs. Dimmer in 1927, using carbon arc illumination was able to obtain high quality black

and white images and is said to have "electrified" the Ninth International Congress in 1899 with his marvellous pictures".[7] He also went on to publish the first fundus photography atlas.

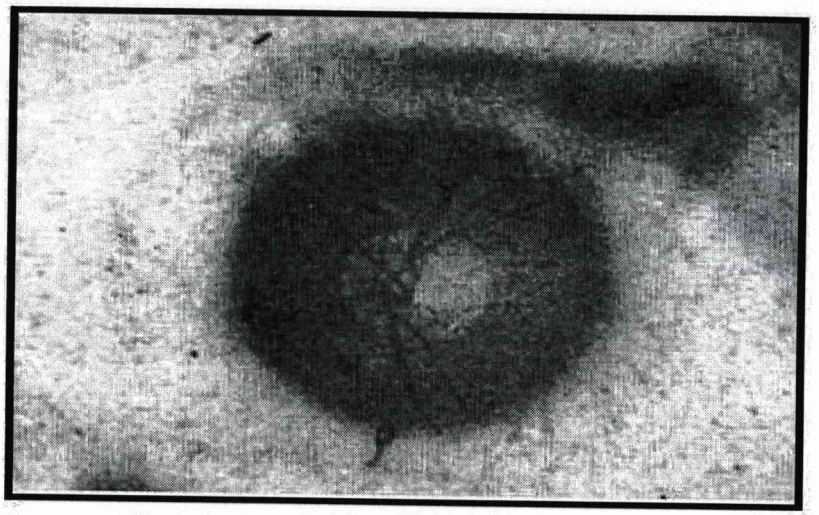

Figure 1.7: Gerloff was considered as a pioneer in fundus photography. This retinal photograph taken in 1891 is much clearer than the earlier images and shows the optic disc and blood vessels.

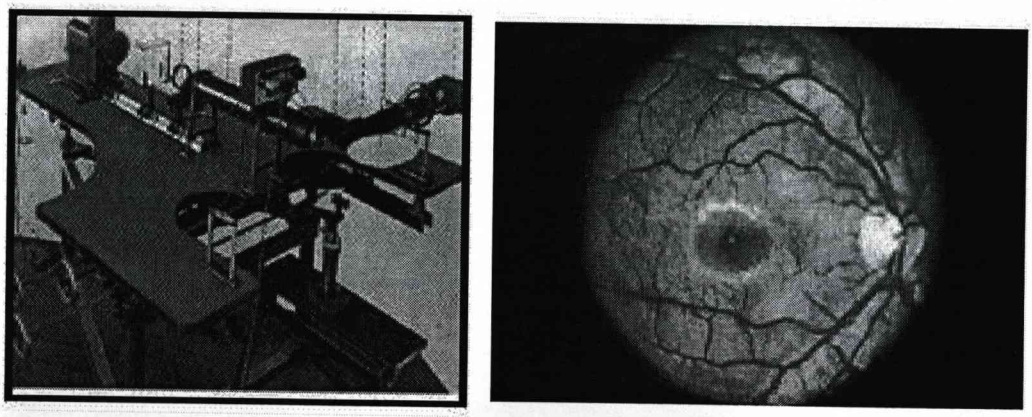

Figure 1.8: This photograph of the retina is from the first fundus photography atlas published by Dimmer in 1927. (Same PJ. Landmarks in the historical development of fluorescein angiography. Journal of Ophthalmic Photography 1993;15:17-23)

Nordenson introduced a camera based on Gullstrand's principles in 1925. The Carl Zeiss Company marketed Nordenson's design as the first commercially available fundus camera in 1926 (Figure 1.9). This camera had a 10° field of view and required a 1/2 second exposure with colour film.

Figure 1.9: An advertisement for the Zeiss fundus camera from 1932. (American Journal of Ophthalmology, 1932)

1.1.4 Fluorescein angiography

The modern photographic technique of fluorescein angiography (FA) was developed in the late 1950's by two young doctors, a medical student, Harold Novotny, and an intern, Dr. David Alvis, while working on determining the oxygen saturation in retinal arterioles. It was thought that the observation of fluorescence might make it easier to make that determination, and sodium fluorescein was one of the dyes used. A Kodak filter book was used to choose appropriate exciter and barrier filters. Dr Alvis, reportedly on the toss of a coin, became the first person to have the first modern fluorescein angiogram (Figure 1.10). It is interesting to note that their work when submitted to the American Journal of Ophthalmology in 1960 was rejected. In July of 1961, the utilisation of a fundus camera equipped with an exciter filter, barrier filter and an electronic flash to sequentially document the retinal blood flow following a sodium fluorescein injection was outlined in their landmark article published in the journal *Circulation*.[8] Most of the techniques they described are still in use today. Ocular angiography has since become an essential tool in the field of ophthalmology.

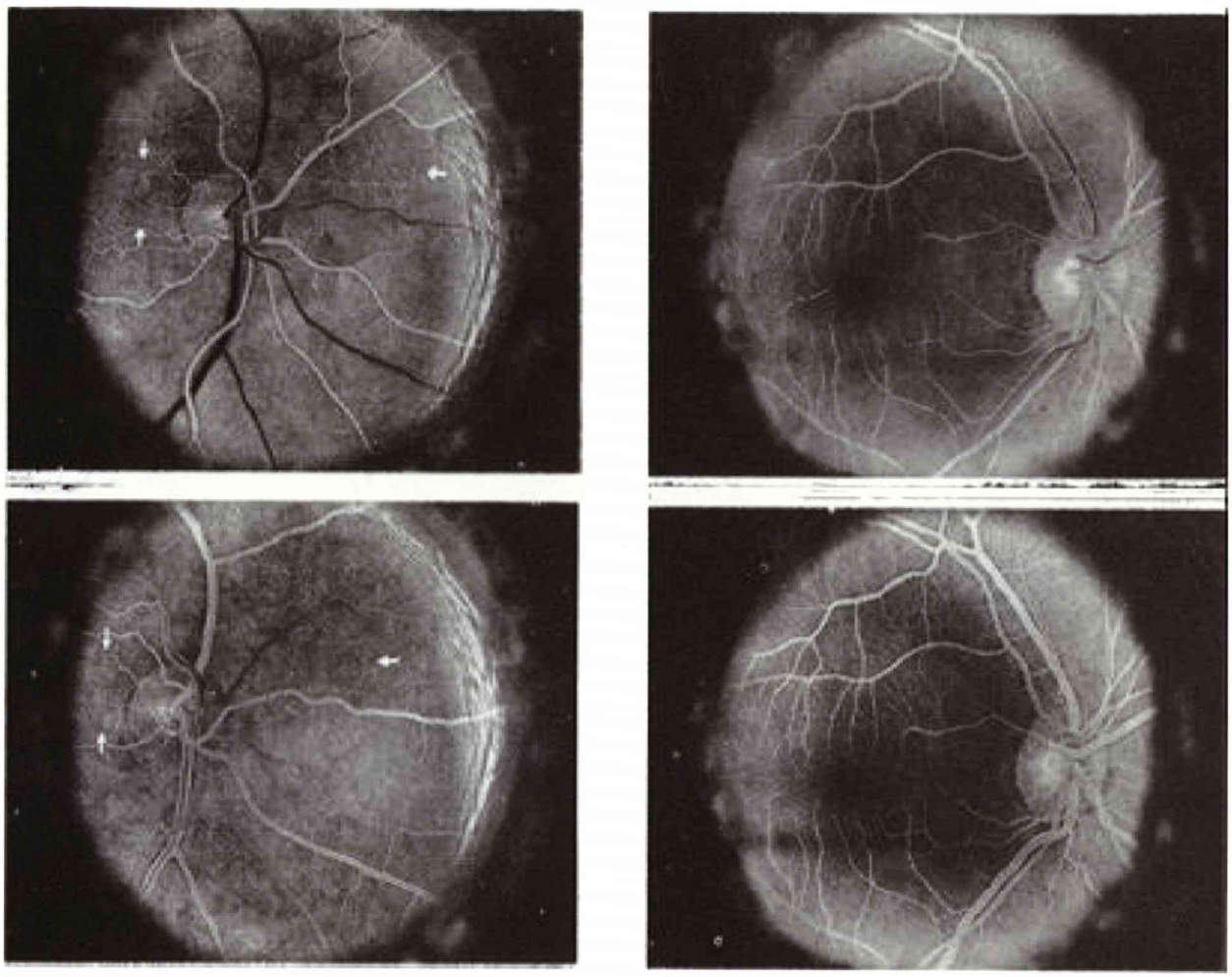

Figure 1.10: These are the first photographs of fluorescein angiogram taken by Novotny and Alvis and published in Circulation in 1961. These images of a normal eye were described as showing arteriolar (top images) and venous filling filling phase (bottom images).

1.1.5 Ophthalmic fundus imaging today

FA as a new diagnostic adjunct was a welcome addition in the 1960s to provide better understanding of the pathological meaning and the natural course of clinical manifestations. Its importance was recognized by Dr Donald Gass who, eventually refined and studied the technique and published landmark monographs. In the 1970's Dr J Donald Gass's *Stereoscopic Atlas of Macular Diseases*[9] set new standards in fundus diagnosis and image acquisition. Technology for acquisition of these images was designed and developed to enhance resolution, stereopsis and field of view. Stereo imaging served to segregate the retinal from the choroidal circulations and to separate anatomical compartments in the fundus, allowing visualisation of lesions such as detachment of the retinal pigment epithelium and neurosensory retina and cystic spaces in the retina itself.

The conversion from stereo film-based photographs to digital images has evolved slowly but progressively over the past decade. Advances in digital camera technology, improvements in computer storage and enhanced photographic evaluation techniques have resulted in the creation of an imaging system superior in many respects to the traditional film-based techniques of the past. Medical-retinal specialists today rely on imaging for clinical research, teaching and patient care in their subspecialty.

History continues to be written with the invention of the optical coherence tomography, heralding a new era, the cross-sectional imaging of the eye. This novel method is expected to provide a different perspective on diagnosis and management. The potential of this new technique to yield insights into the pathophysiology of retinal diseases is yet to be completely explored.

1.2 IMPACT OF AMD

Age-related macular degeneration (AMD) is the most common cause of adult blindness in Western, developed countries.[10, 11] Fletcher et al estimate that somewhere between 182,000 and 300,000 people in the United Kingdom are blind or partially sighted as a result of AMD.[12]

Late stage AMD exists in two forms: atrophic and neovascular or exudative. The atrophic form is more common than the more sight threatening exudative form, affecting about 85% of people with age related macular degeneration.[13] Exudative AMD is more threatening to vision and is responsible for 90% of severe visual loss in people with AMD. Blood or serum leakage resulting from choroidal neovascularisation (CNV) may occur precipitously and is often associated with an abrupt loss or distortion of vision. Once exudative AMD has developed in one eye the other eye is at high risk of developing the same (cumulative estimated incidence is 10% at one year, 28% at three years and 42% at five years).[14] The burden of ocular morbidity and visual disability due to AMD is expected to increase further with an increasingly older population. This is reflected in a steady increase in the number of people registering as blind in most Western countries.

The major public health outcome of AMD is blindness. Vision loss is associated with increased morbidity, including an increased risk of falls and hip fractures.[15, 16] Recent research has shown how vision impairment compromises quality of life and limits social interaction and independence.[17] Vision impairment caused by AMD has also been shown to interfere with the person's ability to care for themselves and others indicating need for community and vision related support.[18] Vision loss from AMD [is] reported to be associated with depression in about 30% of cases.[19] Disability

resulting from neovascular AMD led to greater use of health care resources and more need for help with activities of daily living than was reported by controls.

There is also a considerable economic burden of AMD. People with visual loss from AMD experience considerable difficulty in obtaining employment and may have decreased earnings compared with those who have no disabilities.[20] Disability payments, healthcare expenses, caregiver costs and transport costs will further add to this burden.

In summary, the substantial public health burden of AMD includes both its adverse effects upon quality of life and upon the economy. There is a need for early detection and treatment of AMD to arrest vision loss and preserve the patient's independence and well being. Interventions that improve the morbidity caused by AMD have the potential to greatly benefit the quality of life of individual patients as well as the overall economic well being of the country.

1.3 INTRODUCTION TO THESIS

My work commenced in June 2002 when, based on the treatment of age-related macular degeneration with photodynamic therapy (TAP) study,[21, 22] photodynamic therapy (PDT) was being introduced into the UK as a treatment for classic and predominantly classic subfoveal CNV secondary to AMD. At the time, there was very little evidence of the effect of PDT on the morphology and function of the macula and FA with its associated limitations was the mainstay of diagnosis and management. The Optical Coherence Tomography (OCT) had been made available for clinical use only a few years earlier. While there were a few anecdotal and descriptive papers on its general use in other macular diseases, literature of its application in macular degeneration was not available. It was thought that the

Stratus Optical Coherence Tomography (OCT3), with its ability to take cross-sectional images of the retina, could measure retinal and CNV thickness and identify and quantitatively assess intra retinal oedema and subretinal fluid more effectively than biomicroscopy or angiography and the response to PDT could be objectively monitored.

The research presented in this thesis was undertaken between June 2002 and June 2004. As the principle investigator, under the tutelage of Professor Harding, I conducted a detailed review of the literature, designed the study, performed the OCT scans, collected and analysed the data and prepared this manuscript.

1.4 THESIS AIMS

The aim of my MD thesis is to evaluate the role of OCT in the management of patients with subfoveal neovascular AMD. Specifically:

(i) To test the feasibility of doing OCT in an aging population with this disabling eye disease.

(ii) To define macular features of AMD on OCT and validate the technique of interpreting OCT scans in AMD.

(iii) To define the relationship of the findings on OCT to overall disease processes, by relating the scans to visual outcome and FA.

(iv) To determine if OCT can be used to monitor the response of the retina to a course of treatment.

(v) To develop diagnostic and analysis criteria for OCT based on our observations.

To provide a thorough evaluation four studies were carried out.

1. Development of relevant terminology and measurements to analyse OCT scans and quantitative assessment of the reproducibility of the terminology between observers in the analysis of the scans.
2. A cross-sectional study to apply the new terminology in the assessment of eyes with neovascular AMD and comparison of OCT with stereo FA in identifying clinical features of CNV.
3. A cross-sectional OCT analysis of bilateral end stage CNV where one eye is treated with PDT.
4. A longitudinal study to investigate the response of the retina and CNV to a course of PDT and identify OCT features associated with worse outcome in PDT for subfoveal predominantly classic CNV secondary to AMD.

I present this thesis in 8 chapters. The highlight of each of the sections has been touched on briefly below.

Chapter 1 (this chapter) introduces my thesis and reviews the published landmarks in the historical development of retinal imaging.

Chapter 2 will review the relevant literature on neovascular AMD and its treatment with PDT, and retinal imaging with particular emphasis on OCT.

In Chapter 3, I will discuss the methodology used in the studies presented in this thesis.

Chapters 4 to 7 will present the results and discussion of a series of investigations performed within the framework of the thesis to answer the research questions.

Chapter 8, the final chapter, will discuss the overall outcome and conclusions of the research. In this chapter I will also discuss the developments in the management of neovascular AMD since the completion of my work.

Chapter 2

REVIEW OF PUBLISHED LITERATURE

2.1 INTRODUCTION

Although recognised since at least 1875 and the subject of in excess of 9000 publications, the sub classification, pathogenesis, and particularly, the management of age-related macular degeneration (AMD) remains controversial. Over the years developments in retinal imaging have sought to address some of these issues. Against this background, the purpose of this chapter is to review the literature on the role of imaging in the management of neovascular AMD.

In this chapter, I discuss the controversy surrounding the definition, nomenclature and the classification of AMD; the morphological and fluorescein angiography findings in exudative AMD; and the treatment options available at the commencement of this study. As there is a large amount of literature on this topical disease, I have only included the information relevant to my thesis.

I have also summarised and critically appraised the current knowledge on the application of OCT in the diagnosis and treatment of AMD.

2.2 AGE RELATED MACULAR DEGENERATION

2.2.1 Nomenclature

The terms macula lutea, macula, posterior pole, area centralis, fovea and foveola have created confusion among both anatomists and clinicians. The word macula (Latin, *small yellow spot or blemish*) was initially used by Pagenstecher to describe

the yellow area at the posterior pole of the enucleated eye.[23] Hogan et al defined the macula histologically as that area centred on the fovea in which the ganglion cell layer is more than one-cell in thickness, an area approximately 5 to 5.5mm in diameter.[24] The term fovea derived from Latin and meaning '***small pit'***, is the concave central retinal depression approximately 1.5mm in diameter and evident ophthalmoscopically (in young patients) as an elliptical light reflex that arises from the slope of the thickened internal limiting membrane of the retina. The ***foveola*** is the central depression within the fovea approximately 0.35mm in diameter. The photoreceptor layer at the foveola is made up almost entirely of cones, this is thought to account for the most acute vision (Figure2.1).

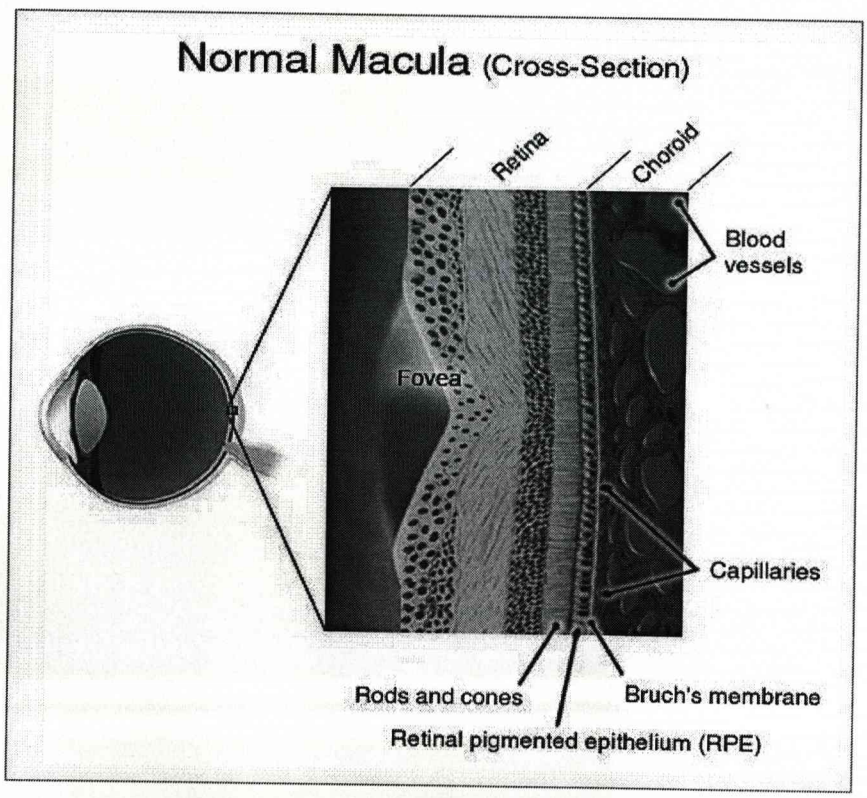

Figure 2.1: Diagrammatic representation showing the cross-section of a normal macula with the central depression of the fovea.

This confusion regarding nomenclature has extended into the definition of AMD as well. Numerous terms have been coined to describe the different stages in what is

now recognised as a process that continually evolves from one phase to another. As a result there are several names and descriptions of AMD. It was first described and illustrated in the literature in 1875 by Pagenstecher and Genth.[25] They termed the condition '***chorioidioretinitis in regione maculae luteae***'. Hutchinson and Tay[26] in 1875 were probably the first ophthalmologists in the English literature to describe the symmetrical fundal changes in senile patients. Yarr recognized the disc-like configuration of the macular lesion and termed it "***central choroidoretinitis resembling an optic disc***" (Yarr 1898-1899). Oeller in 1905 first used the name "diskiform" degeneration (***degeneratio maculae luteae disciformis***)[27] to describe the same process, which he had previously called "***chorioretinitis anastomosis arteriovenosa***". The term disciform came into disrepute when it was realised that it was not an aetiological diagnosis, but a clinicopathologic entity common to many different processes and mainly a morphological description. This term is now reserved for the cicatricial end-stage of the pathological process.

Otto Haab[28] is credited with coining the term called "***senile macular degeneration (SMD)***" in 1885. He observed bilateral "pigmented" and "light" spots at the macula associated with severely reduced vision occurring in old people and attributed it to pigment epithelial atrophy. This term 'senile macular degeneration' was widely accepted by generations of ophthalmologists to describe the macular changes observed in the elderly. By the 1980's, the word senile had acquired pejorative connotation of mental decline that replaced its original meaning - "associated with old age".

The term ***age-related macular degeneration (AMD)*** is relatively recent in history and was proposed at the Macular Society symposium at the American Academy of Ophthalmology annual meeting 25 years ago. The controversy surrounding the

nomenclature exists to this day, with the terms ***age-related maculopathy (ARM)*** and AMD being used interchangeably. In this thesis I will be using the term AMD as defined and classified by the Age-Related Eye Disease Study (AREDS).[29]

The final word of the title "***degeneration***," implies an abiotrophic as opposed to an inflammatory or atrophic aetiology. Thus the term degeneration may be appropriate for types of age-related macular degeneration but not for acute processes such as trauma, histoplasmosis or other inflammatory disorders.[30]

2.2.2 Definition

AMD is defined as a disorder of the macula characterised by one or more of the following:

- Drusen
- Retinal pigment epithelium (RPE) abnormalities (hypopigmentation or hyperpigmentation)
- Geographic atrophy of the RPE and choriocapillaris involving the centre of the fovea
- Neovascular (exudative) maculopathy

The two main types of AMD are non-exudative AMD and exudative AMD, referred to colloquially as dry AMD and wet AMD, respectively.

2.2.3 Classification from epidemiological studies

Despite extensive past and ongoing research in AMD, there is currently no universally accepted classification of AMD in the literature. The problem is further compounded by differences in methodology used in the various epidemiological studies, making comparisons between them difficult. The classification systems

discussed here were used by investigators interested in the analysis of genetic, epidemiological, and morphological features of AMD and are based on photographic assessment of the macula.

In an effort to develop a unified classification system, the ***International Age-related Maculopathy Epidemiological Study Group*** published the International Classification and Grading System in 1995.[31] This study relied exclusively on colour fundus photographs and used the term age-related maculopathy (ARM) to define early lesions that are not attributable to any other cause (e. g., ocular trauma, retinal detachment, high myopia, chorioretinal infective or inflammatory process, choroidal dystrophy, etc).

Early ARM was defined by the presence of

- Drusen defined as ''discrete whitish-yellow spot"; or
- Areas of hyperpigmentation associated with drusen; or
- Areas of hypopigmentation associated with drusen.

The late stages were termed AMD or late ARM and was subdivided into dry and wet AMD

Dry AMD (or ''geographic atrophy'')

- Eyes showing sharply demarcated areas of hypopigmentation in which choroidal vessels are more visible than in surrounding areas and which are at least 175 μm in diameter

Wet AMD (''neovascular,'' ''disciform,'' or ''exudative''AMD)

- Retinal Pigment Epithelial (RPE) detachments, which may be associated with neurosensory retinal detachment.

- Subretinal or sub-RPE neovascular membranes.
- Epiretinal, intraretinal, subretinal, or subpigment epithelial scar/ glial tissue or fibrin like deposits.
- Subretinal haemorrhages not related to other retinal vascular disease.
- Hard exudates (lipid) related to other ARM findings and not related to other vascular diseases.

The ***Age-Related Eye Disease Study (AREDS)***, a large, multicentre cohort study, investigated the clinical course of AMD and the effect of high-dose antioxidant vitamins and zinc on the progression of ARM and cataract formation.[32] The AREDS classification is based on the fundus features assessed by evaluating stereo colour photographs and classified AMD.

No AMD (AREDS category 1): no or few small drusen (<63 microns in diameter).

Early AMD (AREDS category 2): the size of a druse was ≥63μ and/ or the total drusen area was > 5 small drusen.

Intermediate AMD (AREDS category 3): the presence of extensive intermediate drusen (63-125 microns), at least one large druse (≥125 microns in diameter), or geographic atrophy not involving the centre of the fovea. (125 microns is the width of a large vein at the disc margin)

Advanced AMD (AREDS category 4): characterised by one or more of the following:

- Geographic atrophy ≥1/6 disc area of the RPE and choriocapillaris involving the centre of the fovea
- Neovascular maculopathy such as:

- Choroidal neovascularisation (CNV)
- Serous and/or hemorrhagic detachment of the sensory retina or RPE
- Lipid exudates (a secondary phenomenon resulting from chronic leakage from any source)
- Subretinal and sub-RPE fibrovascular proliferation
- Disciform scar

In 2006, Seddon et al[33] proposed the ***Clinical Age-Related Maculopathy Staging (CARMS)*** system, as a grading system for clinical practise and clinical research protocols. The CARMS system divides patients into 5 mutually exclusive categories based on slit-lamp assessment of drusen, RPE irregularities, geographic atrophy, retinal pigment epithelial detachment (RPED), and CNV.

Table 2.1: The Clinical Age-Related Maculopathy Staging (CARMS) system.

Grade of maculopathy	Clinical Features
1	No drusen or <10 small drusen without pigment abnormalities
2	a. Approximately ≥10 small drusen or 1 to 15 intermediate drusen
	b. RPE changes (hyperpigmentation and hypopigmentation)
	c. Both drusen and RPE changes
3	a. Approximately ≥15 intermediate drusen or any large drusen
	b. Drusenoid PED
4	Central geographic atrophy or noncentral geographic atrophy at least 350 μm in diameter
5	Exudative AMD
	a. Serous RPED, without CNV
	b. CNV or disciform scar

There continue to be attempts to simplify the classification of AMD further. As future studies provide further insight into the pathogenesis of the disease and new imaging techniques permit more accurate and quantitative analysis of the retina and subretinal deposits, there will be a need to incorporate new subcategories or change the classification.

AMD is a complex disorder with multiple phenotypes. Absence of common disease descriptors and uniform reading and grading systems make comparison between the classifications difficult. Also the great number of subtypes within each of the above classifications and absence of visual acuity measurements in these classifications makes it difficult to apply clinically. None of the above classifications have been tested for inter or intraobserver reliability as interpretation is dependent on grader experience. Further assessment needs to be done before accepting any one in a clinical or research scenario.

2.2.4 Prevalence and Incidence

Because the definition of ARM and AMD varies widely between different epidemiological studies, comparisons between populations based on these data are difficult. This is particularly true when early signs of ARM are included. Prevalence rates are more consistent for advanced AMD (atrophic or neovascular). A reasonable overall estimate of the prevalence of AMD in persons aged 65-74 years is 1%, increasing to 5% in persons aged 75-84 years, and 13% after 85 years of age.[34]

Few studies have been done to evaluate the incidence of AMD. The Beaver Dam Eye Study, a census of the population of Beaver Dam, Wisconsin, determined the 5-year cumulative incidence of developing early and late AMD in a population of

3583 adults (age range, 43-86 years). For early AMD, this increased from 16% in persons aged 65 to 74 years to 22.8% for persons aged 75 and older and for late AMD increased from 1.3% in persons aged 65 to 74 years to 5.4% for persons aged 75 and older.[35] The Visual Impairment Project of Melbourne, Australia, described the 5-year incidence in a population of 3271 participants aged 40 years and older. The overall 5-year incidence of early ARM was 17.3% and of AMD was 0.49% in this population. The incidence appeared to be lower in the European Rotterdam Study, a population-based prospective cohort study of 6418 persons 55 years and older living in Rotterdam, the Netherlands. Age-related maculopathy was graded according to the International Classification and Grading System. Five-year estimates of early ARM was 7% for subjects aged 65-74 years and 18% for those aged over 75 years, while these age-specific incidences for late ARM were 0.6% and 2.8%.

AREDS report 18 proposed a simplified severity scale, a scaled step system that correlates the patients' current disease severity with the progression to advanced AMD (Figure 2.2).[32]The patients were categorized into 1 of 4 severity groups based on their fundus features. The scoring system assigns to each eye 1 risk factor for the presence of 1 or more large drusen (>125 μm) and 1 risk factor for the presence of any pigment abnormality. The risk factor score correlates with the patient's 5 year chance of progression from early to advanced AMD as follows:

0 factors, 0.5%; 1 factor, 3%; 2 factors, 12%; 3 factors, 25%; and 4 factors, 50%.

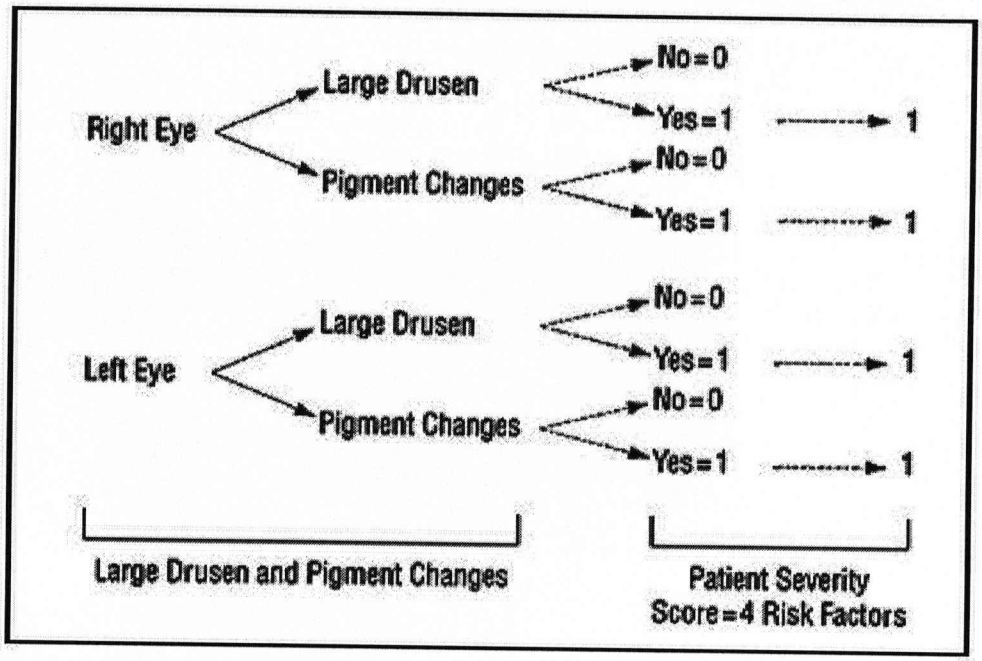

Figure 2.2: The simplified grading scheme proposed in AREDS report number 18 assigns risk factor scoring for patient with large drusen and pigment abnormalities in both eyes. (Arch Ophthalmol 2005;123:1570-1574)

2.3 NEOVASCULAR AMD

Neovascular or exudative AMD accounts for only 20% of cases of late AMD, but is responsible for 80 to 90% of cases of severe visual loss.[36]

Clinically, neovascular AMD may be associated with CNV, subretinal fluid (SRF), cystoid macular oedema (CMO), lipid exudates, or detachment of the RPE (serous and haemorrhagic). End-stage exudative AMD may be associated with the development of a fibrovascular disciform scar and loss of outer retinal tissue (Figure 2.3).

CNV represents the growth of abnormal vessels from the choroid into the subretinal or subretinal pigment epithelial (subRPE) space.[37] On fundoscopy, CNV appears as a greenish grey area often accompanied with subretinal or sub-RPE haemorrhage (Figure 2.4). CNV has been classified clinically on the basis of location and on fluorescein angiography.[38] The location of the CNV is defined in relation to the lesions proximity to the geometric centre of the foveal avascular zone (FAZ). Extrafoveal CNV is defined as a lesion situated at least 200μm from the centre of the FAZ; juxtafoveal CNV's extend to within 1μm and 199μm from the fovea and subfoveal CNV is located directly beneath the geometric centre of the FAZ.

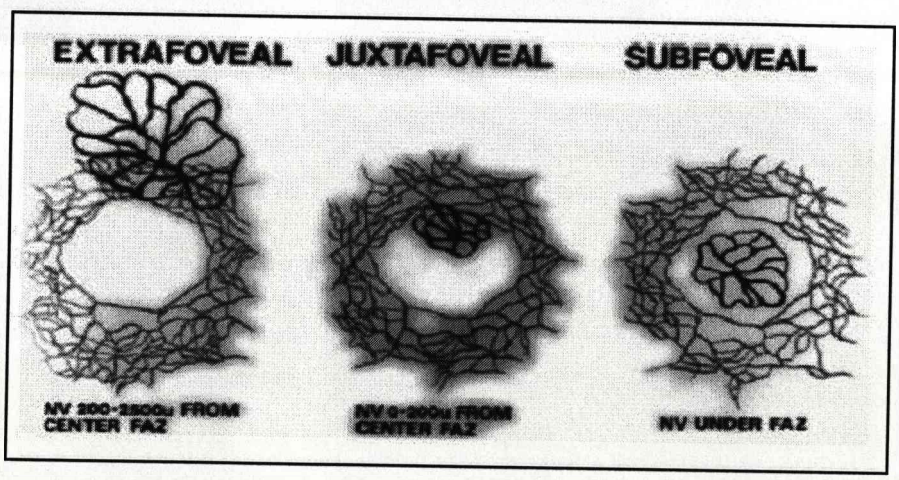

Figure 2.3: Fundus photograph of patient with end-stage age-related macular degeneration showing a fibrotic scar and areas of atrophy at the macula

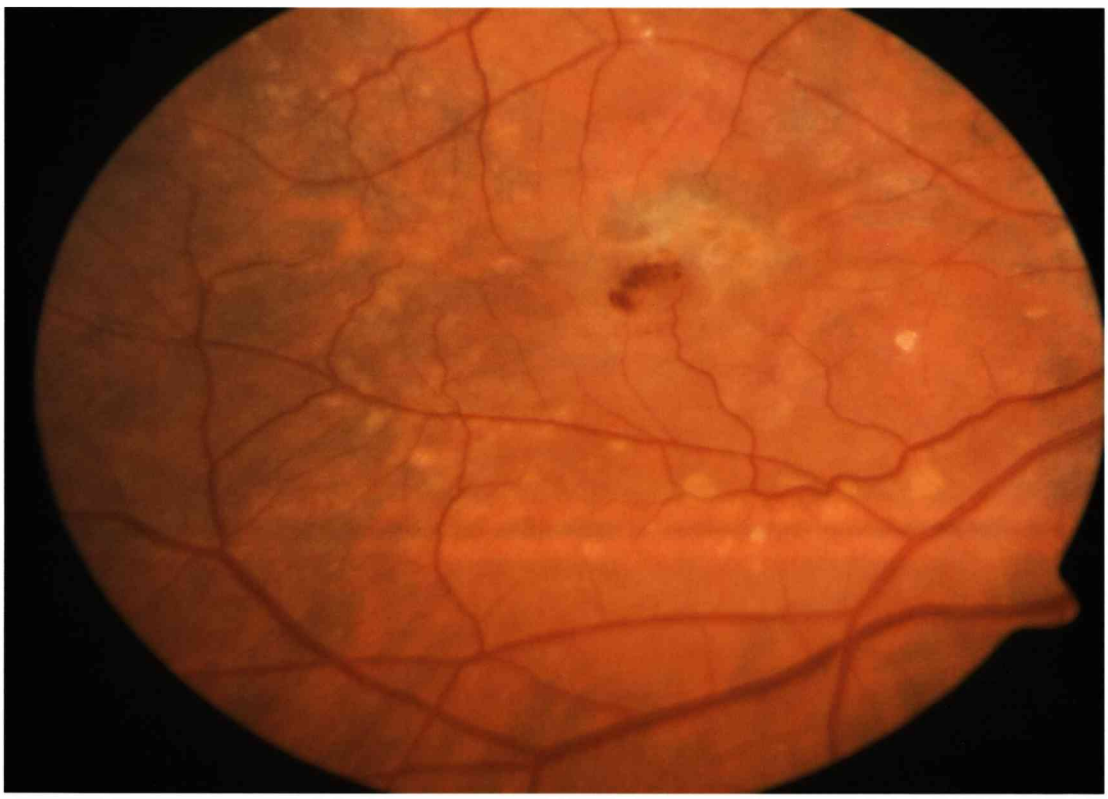

Figure 2.4: Fundus photograph of patient with subfoveal choroidal neovascularisation secondary to age-related macular degeneration showing a grey membrane and haemorrhage at the fovea.

2.3.1 Pathogenesis

Four processes: lipofuscinogenesis (with its link to oxidative stress), drusenogenesis, inflammation and neovascularisation are thought to contribute to the development of neovascular AMD. [39]. Lipofuscin accumulates in the RPE as a result of incomplete degradation of photoreceptor outer segments, and recent studies show that it is a potent source of oxidative stress.[40] Lipofuscin is purported to disrupt RPE function by mechanical disruption of cellular architecture and potentiating phototoxicity.[41] RPE senescence (and lipofuscin accumulation) or oxidative stress initiates the development of CNV by RPE, and possibly, choriocapillaris injury.[42] This may in turn elicit an inflammatory response in Bruch's membrane and the choroid.[43] RPE injury and inflammation may foster the production of an abnormal extra-cellular matrix (ECM) derived from the RPE, photoreceptor cells, choroid and substances in the systemic circulation. The abnormal ECM may result in altered RPE biological behaviour. Vascular endothelial growth factor (VEGF) production by the distressed RPE and photoreceptors may lead to choriocapillaris and/or choroidal new vessel growth. [44] This is the initiation stage of the evolution of CNV and is thought to precede the active and the involutional stages.[45] During the inflammatory active stage, the production of matrix metalloproteinases by vascular endothelium and macrophages enables the CNV to digest through tissue planes and grow in size. At some point the balance shifts toward anti-angiogenic, antiproteolytic, and anti-migratory activity and the involutional stage of the CNV. In this involutional stage, the CNV may become collagenised and form a disciform scar.[45] In this sequence of events, both the environment and multiple genes can alter a patient's susceptibility to AMD.

In addition to the above a complex interaction of metabolic, functional, genetic and environmental factors is thought to play an important role in the development of CNV. Some affected patients have been shown to have specific genetic variants of the complement factor H (*CFH*) gene, which put them at a higher risk of developing the disease. Possession of the variant Y402H polymorphism is thought to significantly increase the risk for AMD with reported odds ratios between 2.45 to 5.57.[46]

2.3.2 Histopathology

Gass et al proposed three different histological types of CNV based on studies of five surgically enucleated eyes with CNV secondary to presumed ocular histoplasmosis (POHS): type 1 CNV grows in a plane between the RPE and the Bruch's membrane (Figure 2.5); type 2 CNV grows between the retina and RPE (Figure 2.6); or a combination of both.[47]

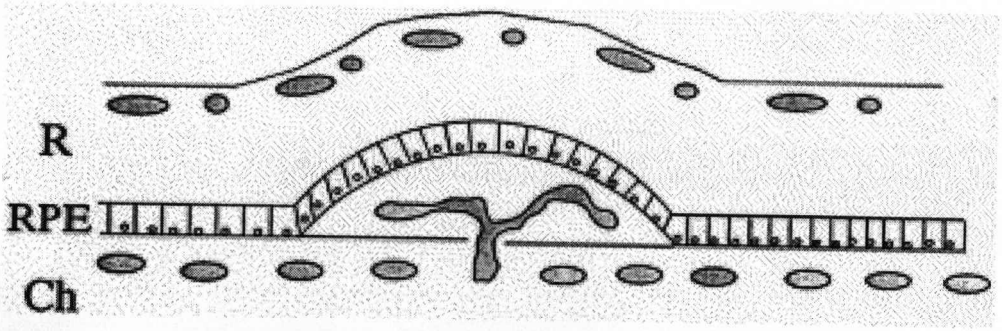

Figure 2.5: The sub retinal pigment epithelium location of type 1 CNV.

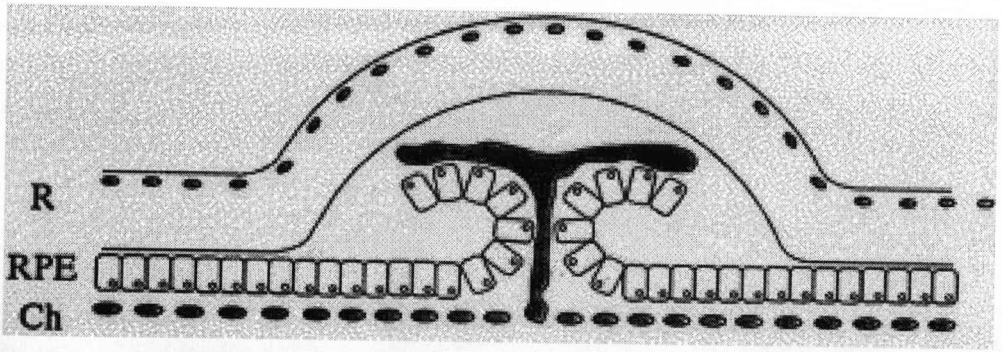

Figure2.6: The subretinal location of type 2 CNV.

Grossniklaus and Gass attempted a further clinicopathologic correlation in 10 specimens of surgically excised CNV.[48] 5 eyes had AMD and 5 had POHS. The eyes were classified as type 1 & 2 on ophthalmoscopy alone; FA was not used. The ophthalmoscopic criteria used to classify the macular lesion as type 1 were the presence of drusen or retinal pigment epithelium detachment, and absence of evidence of retinal pigment epithelium proliferation in the area of the choroidal neovascularisation. Ophthalmoscopic criteria for classification as type 2 were a subretinal pigmented halo or pigmented plaque in the area of the choroidal neovascularisation, plaque-like elevation, and sharply defined borders of the choroidal neovascularisation. They obtained a 90% match between their clinical and histological classification.

Several studies have since extrapolated these findings to the FA classification of CNV suggesting that type 1 may equate to occult and that a type 2 pattern may be present in a classic CNV.[49] La Faut et al analysed 31 CNV surgical specimens histologically. They included 19 classic, 10 occult, and two mixed membranes. 18 classic CNVs had a major subretinal fibrovascular component and 10 of these had an additional, minor fibrovascular component under the RPE. The 10 occult membranes contained a fibrovascular component under the RPE and the two mixed membranes contained fibrovascular tissue on both sides of the RPE. Fibrin and remains of outer segments tended to occur at the lateral edges of classic membranes and to cover the inner surface of occult membranes. [50]

In addition to the small numbers, these studies were all limited by the mixed case series and the clinical classification technique.

The effect of the CNV and its sequelae is obtained from a large study by Green and Enger who analysed 310 eyes with disciform scars.[51] They found that the

photoreceptor cell degeneration was progressively greater as the diameter and thickness of the disciform scar increased. In disciform scars greater than 0.2mm in thickness, only approximately 25% of the surface of the scar had some remaining photoreceptor cells. Kim et al[52] found a 70% reduction in the outer nuclear layer (ONL), but a good preservation of cells in the inner nuclear layer and ganglion cell layer, overlying disciform scars. Greater loss of the cells of the ONL appeared to be related to increased thickness of the scar, mainly its subneurosensory retinal component and loss of RPE cells on the scar surface.

2.4 FLUORESCEIN ANGIOGRAPHY

Although subretinal neovascularisation was observed histologically for years it was difficult to appreciate clinically until the advent of fluorescein angiography (FA). Despite having been developed almost half a century ago, FA remains the test of choice for the diagnosis and classification of choroidal neovascularisation and we are still learning how to interpret the various characteristics visible on the FA.

The two landmark trials that propagated the use of FA in the identification and treatment of CNV were the Macular Photocoagulation Study (MPS) and the treatment of AMD with photodynamic therapy (TAP) study.

The MPS commenced in 1979 and was the first prospective, randomised, multicentre clinical trial that evaluated laser treatment of symptomatic CNV and comprised of 3 separate studies: the Argon Macular Photocoagulation Study (1979–1988) studied extrafoveal CNV; the Krypton Macular Photocoagulation Study (1982–1991) for juxtafoveal CNV; and the Foveal Photocoagulation Study (1986–1994) for subfoveal (new or recurrent) CNV. In the MPS study, neovascular lesions were initially classified by location (extrafoveal, juxtafoveal, or subfoveal) and then by FA characteristics as classic or occult or mixed.

Classic CNV was defined as an area of choroidal hyperfluorescence with well-demarcated boundaries in the early transit phase of the angiogram that continues to leak during the mid and late phase with progressive increase in hyperfluorescence. In the later phases, pooling of the dye occurs in the overlying subretinal space and usually obscures the boundaries of the CNV (Figure 2.7).

Occult CNV was subdivided into 2 categories: fibrovascular pigment epithelial detachment (FPED), and late leakage from undetermined origin. Stereoscopic angiography is essential for the recognition of occult CNV.

Fibrovascular pigment epithelial detachment (FPED) is defined as an area of stippled hyperfluorescence with irregular elevation of the RPE (Figure 2.8). By 10 minutes there may be persistent fluorescein staining or leakage within an area of retinal pigment epithelial detachment (PED).

Late leakage of undetermined origin often appears as speckled hyperfluorescence with pooling of dye in the sub RPE space and was the term used for leakage that only became apparent 2 to 5 minutes after the fluorescein injection.

The Treatment of Age-related Macular Degeneration with Photodynamic Therapy (TAP) Study Group adapted the definitions from the MPS study and subclassified the lesions on the basis of the proportion of classic CNV. The TAP study was a large multicentre randomised clinical trial whose objective was to determine whether photodynamic therapy (PDT) with verteporfin, compared to placebo, could reduce the risk of vision loss in eyes with subfoveal CNV secondary to AMD. [21]

The lesions were determined to be

- ***predominantly classic CNV*** if the area of classic is ≥ 50% of the area of the entire lesion,
- ***minimally classic CNV*** if the area of classic is <50% but>0% of the area of the entire lesion), or
- ***occult CNV with no classic CNV.***

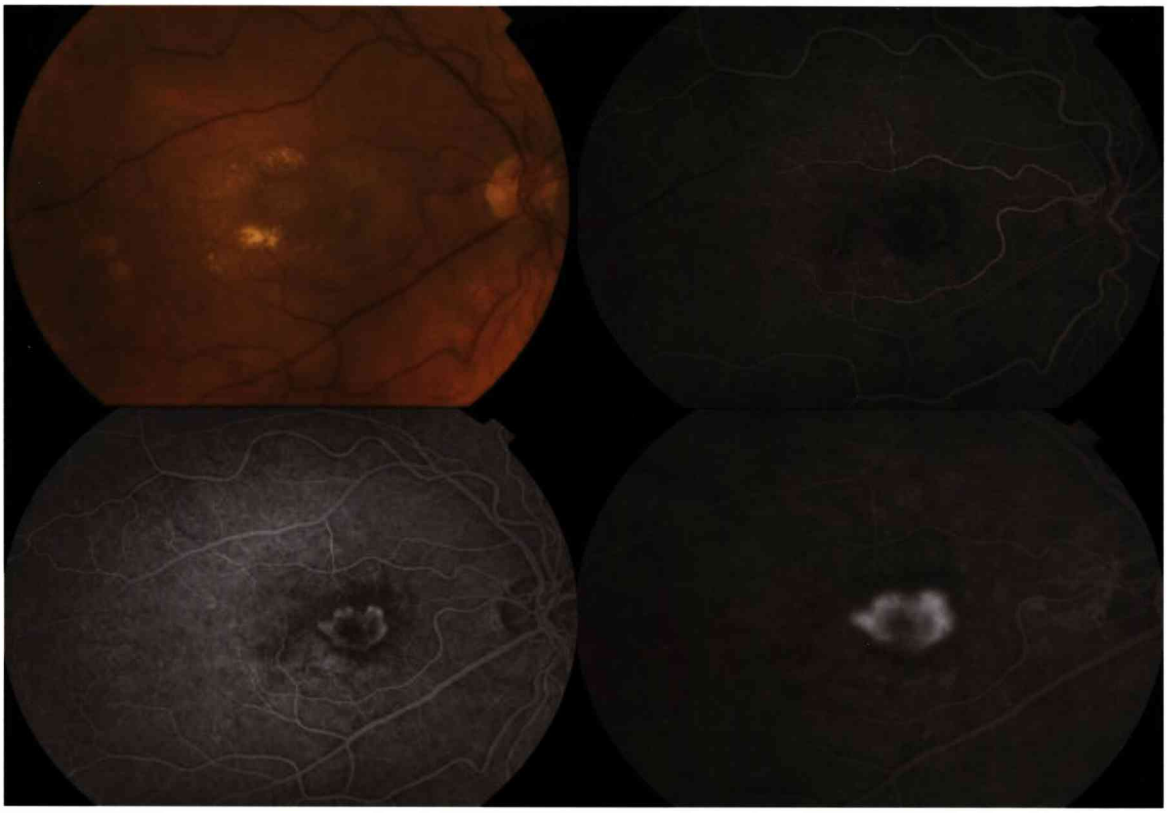

Figure 2.7: Colour fundus and fluorescein angiogram of subfoveal predominantly classic choroidal neovascularisation showing a well demarcated area of early hyperfluorescence with progressive leakage of the dye into subretinal space leading to blurring of the borders of the lesion in the late phase.

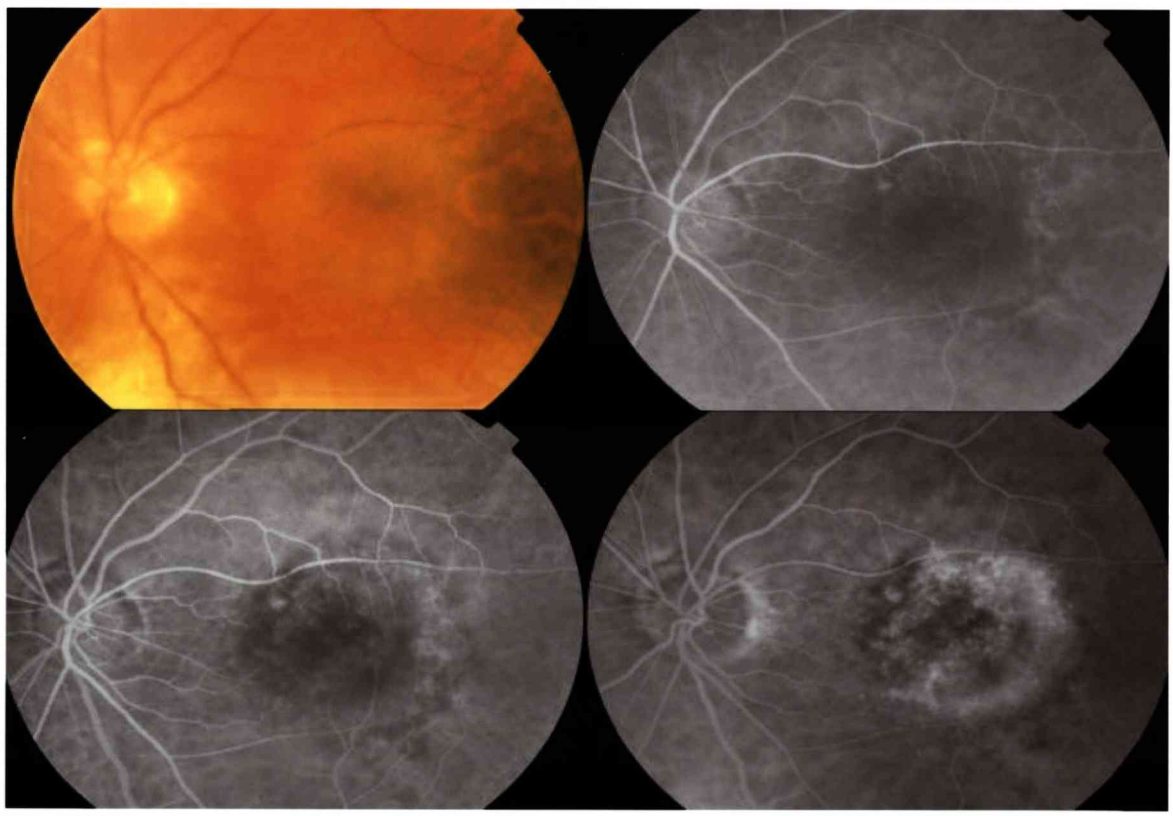

Figure 2.8: Colour fundus and fluorescein angiogram (FA) of the left eye with fibrovascular pigment epithelial detachment. FA shows stippled hyperfluorescence with irregular elevation of the retinal pigment epithelium.

Other patterns of neovascularisation:

More recently other patterns of neovascularisation have been identified and defined including retinal angiomatous proliferation and polypoidal choroidal vasculopathy.

Retinal angiomatous proliferation (RAP) (Figure 2.9) is thought to commence as an intraretinal capillary proliferation, later extending into the subretinal space, and finally terminating into a frank CNV.[53] Common clinical features of RAP include small multiple intra-retinal haemorrhages, intra-retinal oedema, vascularised pigment epithelial detachments (PEDs), and retinal choroidal anastomosis (RCA). FA sometimes reveals an ill-defined, occult choroidal neovascularisation. ICG angiography is useful in early stages because 'hot spots' can be detected before clinical or FA characteristics are present.

Polypoidal choroidal vasculopathy (PCV) (Figure 2.10), was initially described in 1982, and is characterized by RPE detachments associated with choroidal polypoidal lesions.[54] The "aneurysms," or polypoids, are clinically described as reddish-orange nodules. The temporal juxtapapillary region has been reported to be the most common location for PCV lesions;[55] however, peripheral and macular lesions have also been reported.[56] PCV lesions appeared hyperfluorescent in the early phases of both fluorescein and ICG angiography. Late-phase leakage is seen in cases associated with subretinal fluid or exudates.

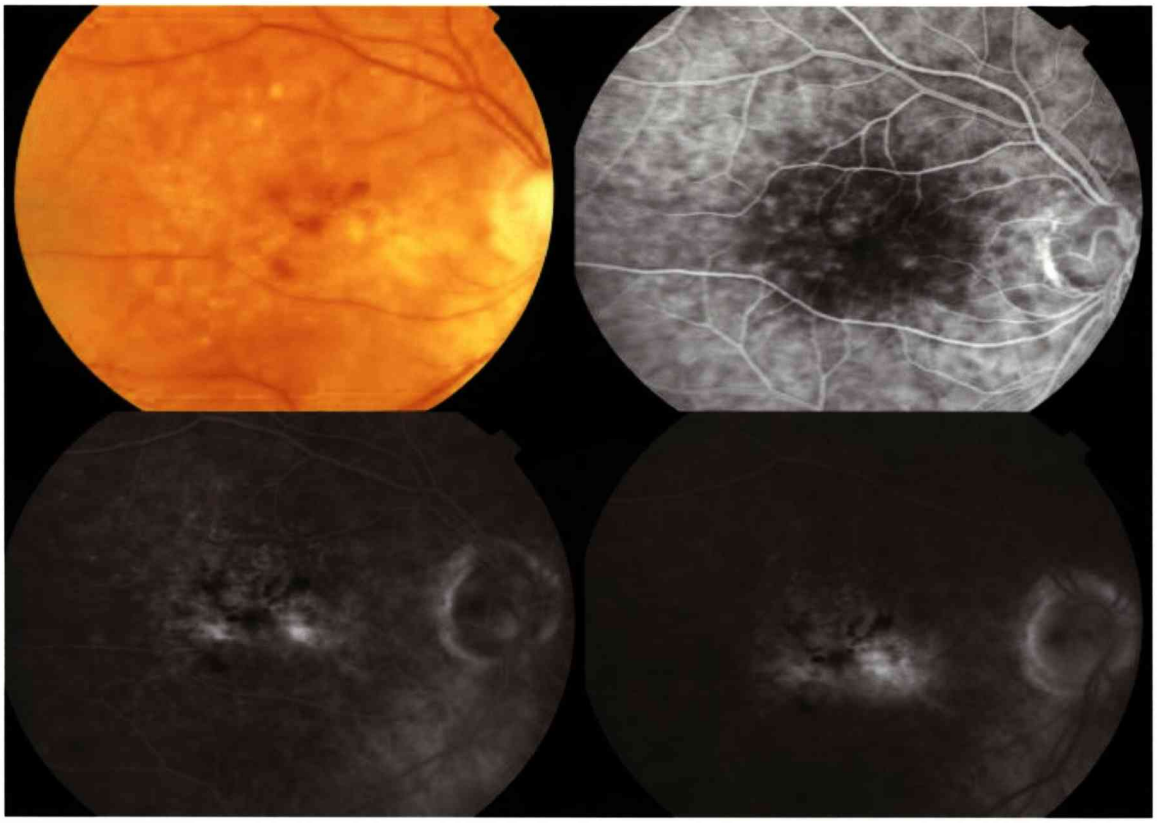

Figure 2.9: Colour fundus and fluorescein angiography (FA) of the right eye of a patient with retinal angiomatous proliferation. The colour fundus shows small multiple intraretinal haemorrhages and hard exudates. FA shows intraretinal haemorrhages and 2 hot spots.

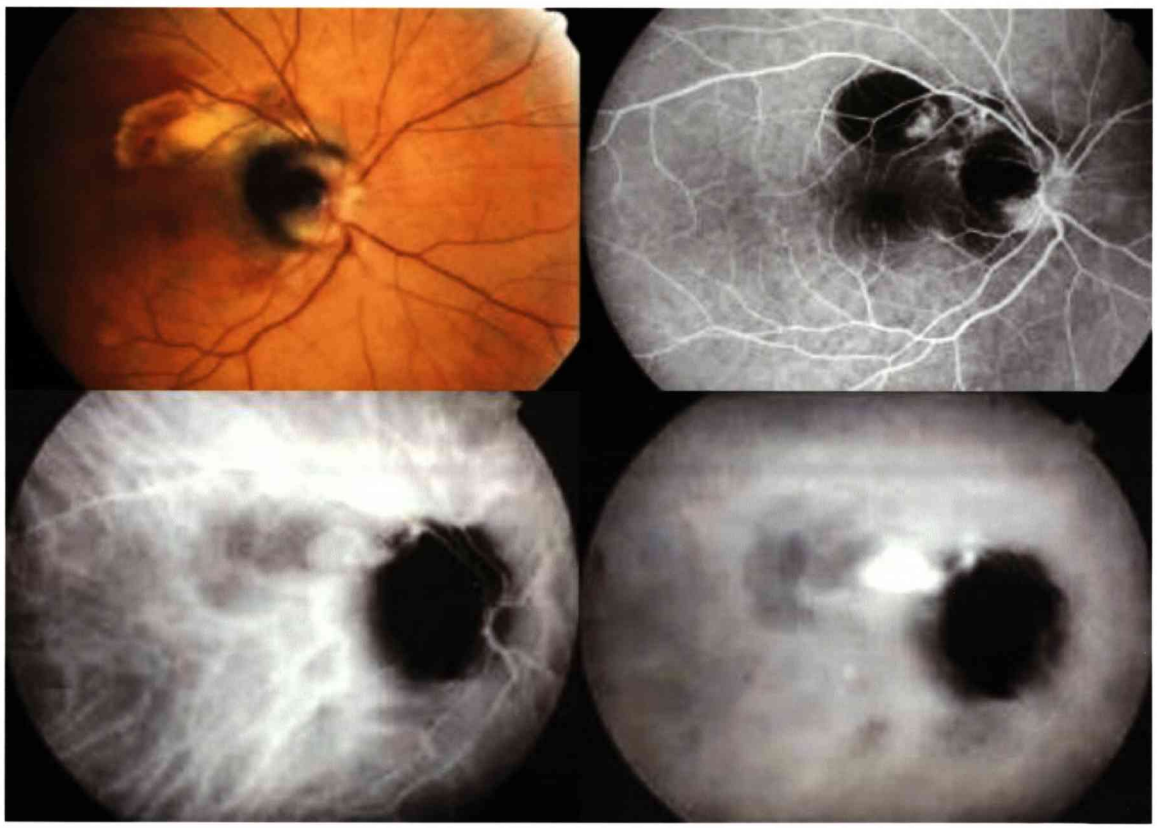

Figure 2.10: These are images from a patient with juxtapapillary polypoidal choroidal vasculopathy. The colour fundus photograph shows a nodular lesion which is polypoidal in appearance in both the fluorescein angiogram and indocyanine green angiography.

2.4.1 Frequency of lesion types in neovascular AMD

FA classification of CNV determines its eligibility for treatment with PDT and laser. Several studies have evaluated the frequency of lesion types in neovascular AMD (Table 2.2).

Table 2.2: Distribution (in percentage) of lesion subtypes in neovascular age-related macular degeneration.

Authors	Year	N	Other lesions	Classic CNV	Predo-minantly Classic CNV	Mini-mally Classic CNV	Occult CNV
Moisseiev et al	1995	100	27%	37%	7%		19%
Margherio et al	2000	474	-	44%		56%	
Bermig et al	2002	191	-	9%	10%	21%	60%
Zawinka et al	2005	168	-	21%		19%	60%
Olsen et al	2004	200	-	26%		6.5%	67.5%
Cohen et al	2007	205	12%	23%		8.0%	57%
Ali et al	2004	98	-	12%	31.6%	35.7%	20.4%

Moisseiev et al tried to determine the percentage of cases that would have been eligible for treatment according to MPS guidelines.[57] They randomly selected 100 FAs of patients with exudative AMD over a 5-year period (1985-1990) and classified them into 4 groups: active lesion, PED, haemorrhage and disciform scar. 63% (63 eyes) had an active lesion further subdivided as classic (37%), occult (19%) and mixed (7%). Only 15 eyes in the classic CNV group were found to be eligible for laser treatment by MPS criteria as the rest (22%) had a subfoveal location.

Margherio et al performed a retrospective study of 474 cases with neovascular AMD to determine their eligibility for PDT.[58] 83% CNV were subfoveal, 44% were

predominantly classic and 56% were minimally classic or occult. Of the eyes with predominantly classic CNV, 36% were eligible for verteporfin PDT (TAP criteria).

In a prospective study Bermig et al recruited 191 patients with acute symptoms due to exudative AMD.[59] They estimated the percentage of patients who would be amenable to either laser photocoagulation as per MPS guidelines or PDT as per TAP guidelines. 9% of the eyes had classic only lesions, 10 % had a predominantly classic CNV, 60% were occult with/ without PED, while 21% were minimally classic lesions. Only 14% eyes were eligible for PDT per TAP criteria and 3% were suitable for argon laser photocoagulation. Majority (83%) were not eligible for either treatment.

Zawinka et al performed a similar study as the Bermig group in 168 eyes of 153 patients.[60] Thirty-five eyes had predominantly classic CNV (21%), 101 eyes had pure occult CNV (60%), and 19% (32 eyes) had minimally classic CNV. 17 % lesions, 28 of the 35 eyes with predominantly classic CNV and 5 out of 101 eyes with pure occult met the TAP and VIP eligibility criteria for PDT treatment. 3% could have been treated with laser photocoagulation according to MPS criteria.

In a cross-sectional study Olsen et al evaluated the frequency of lesion types in 200 cases of neovascular AMD using FA.[61] Lesions were subfoveal in 157 (78.5%), juxtafoveal in 33 (16.5%), and extrafoveal in 10 (5%) and predominantly classic in 52 (26%), occult with no classic in 135 (67.5%), and minimally classic in 13 (6.5%).

Cohen et al prospectively recruited 205 cases to describe the types and location of CNV in newly diagnosed exudative AMD.[62] While all patients had FA, in 50% ICG was also performed. Types and location of CNV were classified by two independent

experts and adjudicated by a third when discordant. In this study 12% had either haemorrhage occupying an area more than 50% of the lesion or a disciform scar, 23% eyes had predominantly classic CNV, 57% had occult CNV and 8% had a minimally classic lesion. 15% of the occult CNV had RAP. 8% lesions were subfoveal. There was only a moderate agreement between the experts in the location (κ=0.52) and type of lesion (κ=0.59).

Ali et al performed a retrospective morphometric analysis of 98 angiograms to study the change in lesion components in untreated exudative AMD at 2 time points separated by an interval of 3 weeks.[63] They excluded eyes with fibrosis >50% of lesion, large lesions >6000 μm and fibrovascular PED- as these features were considered to indicate chronicity. They observed the classic containing CNV tended to be smaller than lesions with occult CNV; increase in the area of lesions with classic CNV is faster than that of lesions with occult CNV; and while most eyes remained in the category to which they were assigned at baseline, 5 eyes with classic only CNV at baseline converted to predominantly classic CNV. At baseline 12%, 31.6%, 35.7% and 20.4% eyes had classic, predominantly classic, minimally classic and pure occult CNV respectively. Twenty-three changes were noted, 10 in the direction of increasing classic CNV, while 13 were in the opposite direction. The distribution of eyes by CNV category at baseline and the first visit for this study is depicted in the table 2.3.

Table 2.3 Change in lesion composition in untreated neovascular AMD at two time points separated by an interval of 3 weeks. Distribution of eyes at baseline and first visit.

	Distribution at baseline			
Distribution at 1st visit	0% Classic (n= 20)	1%- 49% Classic (n= 35)	50-99% Classic (n= 31)	100% Classic (n= 12)
0% Classic	17	2	2	0
1%- 49% Classic	3	26	4	0
50-99% Classic	0	7	25	5
100% Classic	0	0	0	7

The changes in the classification and sub classification of CNV over time and the introduction of new eligibility criteria for treatment are reflected in these studies. It is difficult to make comparisons between these studies as they have been influenced by the different definitions and grading criteria. Studies around the MPS era classified lesions as occult or classic, but since the introduction of PDT the terms predominantly and minimally classic have also become more commonly used. The earlier studies found a high proportion of classic CNV (Moisseiev and Margherio), while later studies have found a higher proportion of occult. The natural history of the disease process also affects the diagnosis and can thus influence the management. As FA is a subjective assessment, the expertise of the graders and the availability of treatment may have also influence the classification in these studies.

2.4.2 Limitations of fluorescein angiography

FA remains the primary investigation for neovascular AMD, but it has several limitations. Although fluorescein is well tolerated by most patients, angiography is an invasive procedure with the risk of adverse reactions. These, though unusual, can

occur in 5 to 10 percent of patients and can range from mild pruritus to anaphylaxis.[64, 65]

Interpretation of the abnormal angiogram relies on the identification of areas that exhibit hypofluorescence or hyperfluorescence. As fluorescein is only 70-85% bound to serum proteins, the extent of the background choroidal fluorescence tends to increase as free fluorescein molecules leak from the highly fenestrated choriocapillaris into the extravascular space. This can obscure the details of choroidal and retinal circulation.

The peak excitation and emission spectra for fluorescein is approximately 490nm and 530nm respectively. Within this range the light absorbed by the dye cannot penetrate the RPE and dense haemorrhage and may mask the underlying pathology.

Stereoscopic angiography and good quality angiograms are essential to accurate lesion classification and interpretation and the technique can be technician/ observer dependent.

Interpretation of the images also requires additional training. Angiographic classification of CNV can vary considerably not only between observers but also for repeated evaluation by the same observer. The fluorescein angiogram in patients with neovascular AMD for PDT eligibility (FLAP) study tried to determine intraobserver and interobserver variation for classifying types of CNV.[66] FA of 40 patients were presented in randomised sequence to 16 independent retinal specialists for classification of type of CNV into classic, occult, or mixed with classic component of less or greater 50%. The mean κ coefficient was 0.64±0.11 for intraobserver variability and 0.55-0.66 for interobserver variability. Zayit-Soudry et al, evaluated 92 FAs of patients with neovascular AMD to determine the variability

among 5 retina specialists in their determination of the location of CNV (subfoveal, juxtafoveal, or extrafoveal), lesion composition (no classic, 0 to 50% classic, predominantly classic, or 100% classic) and eligibility for PDT (recommendations of Verteporfin Roundtable Participants: lesion composition—predominantly classic CNV, occult with no classic CNV with presumed recent disease progression, or relatively small minimally classic lesions; CNV location—subfoveal or so close to the foveal centre that conventional laser photocoagulation treatment almost certainly would extend under the centre; and lesion size—<4 Macular Photocoagulation Study disk areas for minimally classic CNV or occult with no classic lesions). [67, 68] They found only a slight agreement for CNV composition (κ=0.285). The agreement among the graders reduced further when eligibility for PDT was considered and κ was 0.163. Friedman and Curtis evaluated the agreement rate among 21 retina specialists in classifying 6 nonstereoscopic film FA's for CNV type. They reported a moderate interobserver agreement of 0.64.[69] Though these studies show significant variability amongst retina specialists in interpreting FA's, the small numbers and lack of standardised training of the observers limited them. In a small study of 6 patients Kaiser et al (2002) investigated the interrater reliability between 8 retina specialists for retreatment. [70] In grading initial and follow-up visit angiograms, the overall concordance rates were 81% and 82%. In their study, all graders were either TAP study investigators or participants of a fundus imaging reading centre and therefore reflect greater homogeneity in interpretation of FAs. In our own experience with adequate training, graders in a grading centre have up to 90% concordance (Concordance Grading Report, 2007, NetWORC UK meeting, Liverpool).

2.5 NATURAL HISTORY OF NEOVASCULAR AMD

The reported natural history data for untreated neovascular AMD varies according to lesion location, composition and size. Here I discuss the visual prognosis in eyes with untreated subfoveal CNV using evidence from the placebo arms of large randomised clinical trials (Table 2.4).

Studies of subfoveal classic CNV due to AMD indicate a worse prognosis for vision loss in this group. The MPS group enrolled 373 eyes into a randomised controlled clinical trial to investigate the effects of laser photocoagulation for the treatment of subfoveal classic CNV due to AMD (Subfoveal New CNV Study). In the 184 eyes randomised to no treatment, VA decreased by at least 2 lines from baseline in 82% eyes at both 2-year and 4-year examinations. The number of eyes with a loss of ≥6 lines of VA increased from 37% at 2 years to 47% at 4 years. The percentage of eyes with VA of 20/200 or worse increased from 36% at baseline to 88% and 89% at 2 years and 4 years, respectively.[38, 71]

Coscas et al conducted a clinical trial of 160 eyes with subfoveal classic lesions, measuring 0.5 to 2.5 MPS disc areas to investigate the effects of perifoveal laser photocoagulation.[72] At 2 years, 47 (80%) of 59 untreated eyes had lost ≥3 lines of VA, and 29 eyes (49%) had lost ≥6 lines. VA was 20/200 or worse in 53 eyes (90%) at the end of follow-up.

Other studies, TAP study and Verteporfin In Photodynamic Therapy (VIP), also enrolled eyes with subfoveal CNV, but had broader eligibility criteria for lesion size, lesion composition and visual acuity than the MPS study. The TAP study, initiated in 1996, examined the effect of PDT with verteporfin (Visudyne, Novartis Pharma AG, Basel, Switzerland) on the risk of vision loss in patients with subfoveal

CNV (with evidence of classic CNV) due to AMD. 609 patients were randomised in a ratio of 2:1 to verteporfin or placebo (5% dextrose in water). In the placebo group of 207 eyes, 48% had a VA worse than 20/200 at 1 year, and the mean VA loss was 3.5 lines; 54% had a VA loss of ≥3 lines and 24% had a loss of ≥6 lines at 1 year. By 2-year examination, mean VA loss had increased to 3.9 lines, 62% of eyes lost ≥3 lines and 30% lost ≥6lines. 55% had VA<20/200. In this group, 83 had predominantly classic CNV and 104 had minimally classic CNV. The remaining 20 eyes had occult with no classic and should not have been enrolled according to the study criteria. The predominantly classic eyes had a worse visual outcome at 12 and 24 months compared to the eyes with occult CNV.

The VIP study included eyes with subfoveal CNV due to AMD and either occult with no classic CNV and recent disease progression or classic CNV and VA ≥20/40.[73] 114 eyes were assigned to the placebo group; at 2 years 67% had lost ≥3 lines of VA and 47% had lost ≥6 lines of VA. Of 92 eyes with occult with no classic at baseline, 55% had lost ≥3 lines and 33% had lost ≥6 lines at 12 months and 69% and 47% respectively at 24 months. Classic CNV developed in 60% of the 92 eyes and these eyes appeared to have a worse VA outcome at 2 years.

Table 2.4: Visual outcomes for untreated eyes with neovascular AMD classified according to lesion subtype

Study	No. of untreated eyes	Location and type of CNV	Visit (month)	≥ 2 lines loss	≥ 3 lines loss	≥ 6 lines loss	VA≤20/200
MPS (Subfoveal New CNV Study)	184	Subfoveal Classic	0	-	-	-	36%
			24	82%	-	37%	88%
			48	82%	-	47%	89%
Coscas et al.	59	Subfoveal Classic	24	-	80%	49%	90%
TAP	207	Subfoveal CNV	12	-	54%	24%	48%
			24	-	62%	30%	55%
TAP	83	Subfoveal Predominantly Classic	12	-	60%	34%	
			24	-	69%	36%	
TAP	104	Subfoveal Minimally Classic	12	-	45%	16%	
			24	-	56%	27%	
VIP	114	Occult with no classic CNV & Classic CNV with VA>20/40	24		67%	47%	
VIP	92	Occult with no classic CNV	12		55%	33%	33%
			24		69%	47%	45%

In summary, studies of eyes with subfoveal classic CNV (which could also have an occult component) found decreases of ≥3 lines of VA in approximately 60% to 80% over 2 years of follow-up. Also, eyes with predominantly classic CNV or occult with no classic appear to have the worst final VA. In addition, the development or progression of classic CNV had a negative impact on VA outcomes. One of the weaknesses of using natural history data from RCTs is that the eligibility criteria for acceptance into these studies excludes a lot of patients and therefore may not be applicable to the general population.

Fellow eye involvement

AMD is a bilateral disease with a fairly symmetrical presentation and natural history. In the AREDS study, patients with advanced AMD in one eye had a 43% expected probability of progression to advanced AMD in the fellow eye at 5 years. AREDS report 18 developed a simplified scoring system assigning to each eye 1 risk factor for the presence of 1 or more large drusen and 1 risk factor for the presence of any pigment abnormality (Section 2.2.4, Figure 2.2). The risk factor score correlates with the patient's 5-year chance of progression from early to advanced AMD. 0 factors, 0.5%; 1 factor, 3%; 2 factors, 12%; 3 factors, 25%; and 4 factors, 50%.

The MPS group found that 42% of patients with neovascular AMD in one eye developed similar disease in their second eye within 5 years.[74] In their study, patients with subfoveal and juxtafoveal CNV in one eye and fellow eyes with no CNV at baseline, CNV developed in 35% at 5 years. They found 87% of eyes with 4 risk factors: presence of five or more drusen, focal hyperpigmentation, one or more large drusen, and definite systemic hypertension developed CNV at 5 years.

Pauleikhoff et al investigated visual prognosis in fellow eyes in relation to lesion composition in a longitudinal study of 187 patients with newly diagnosed unilateral neovascular AMD.[75] They compared two subgroups; 130 patients (70%) had predominantly classic CNV and 57 (30%) had occult CNV with PED. They found a significantly higher risk of ≥3 lines of vision loss in the fellow eyes of patients with occult CNV. The cumulative risk of ≥3 lines of vision loss in the fellow eyes at 4 years was 31.9% in eyes with predominantly classic CNV as apposed to 69% in eyes with occult CNV with PED ($p<0.001$).

Thus there seems to be consistency across studies and visual prognosis in the fellow eye appears to be worse with greater number of risk factors. This information can be useful for prophylaxis and management of the patients with unilateral disease.

2.6 OPTICAL COHERENCE TOMOGRAPHY

Optical Coherence Tomography (OCT) is a relatively recent medical diagnostic imaging modality that can perform non-invasive, high resolution, micron scale, cross-sectional imaging of the internal microstructure in biological tissues by measuring the echo time delay and intensity of back scattered or back reflected light.[76,77,78,79] It allows real time in-situ imaging of tissue structure or pathology and claims resolutions of 1 to 15 microns (μm). Huang et al first described the technique of OCT for non-invasive cross-sectional imaging in human retina and coronary artery in the journal *Science* in 1991. Owing to the clarity of the optical media, OCT has found an increasing use in ophthalmology. In this section of my thesis I present an overview of the principles of operation of time-domain OCT imaging, factors affecting image quality, interpretation of OCT images of normal retina and a review of the relevant literature for the use of OCT in AMD.

2.6.1 Principles of optical coherence tomography

Optical interferometry

OCT imaging is analogous to ultrasound B-mode imaging, except that it uses light instead of sound. When a light beam is incident onto tissue, it is backreflected from boundaries between different tissues and backscattered differently from tissues that have different optical properties and is attenuated by absorption and scattering as it propagates into the tissue.[80] (Backscatter is the reflection of light waves back to the direction they came from.) The returning or backscattered light is attenuated by absorption and scattering as it propagates out of tissue. The OCT technique currently available in clinical practice and used for this study is referred to as time-domain OCT, because the depth information from the retina is acquired as a

sequence of samples, over time. Because of the speed of light these optical "echoes" cannot be measured directly by the instrument. Therefore the OCT uses low coherence interferometry to perform time and distance measurements for imaging. The coherence length determines the axial resolution of the OCT image. In order to perform distance measurements with tens-of-micron resolution, it is necessary to use an optical instrument that compares or correlates one optical beam or light wave with another reference optical beam or light wave. This is achieved using a fibreoptic Michelson interferometer. Low coherence light (830nm wavelength) from a superluminescent diode (SLD) source is directed onto a partially reflecting mirror functioning as a beamsplitter and is split into measurement and reference beams. One light beam is directed onto the patient's eye and is reflected from intraocular structures at different distances. The light signal from the tissue, consisting of multiple echoes, and the light from the reference mirror consisting of a single echo at a known delay are combined by an interferometer and detected by a photodetector. In order to measure the time delays of light echoes from different structures within the eye, the position of the reference mirror is varied so that the time delay of the reference light pulse is adjusted accordingly. Figure 2.11 shows a schematic representation of the fibreoptic version of the interferometer.

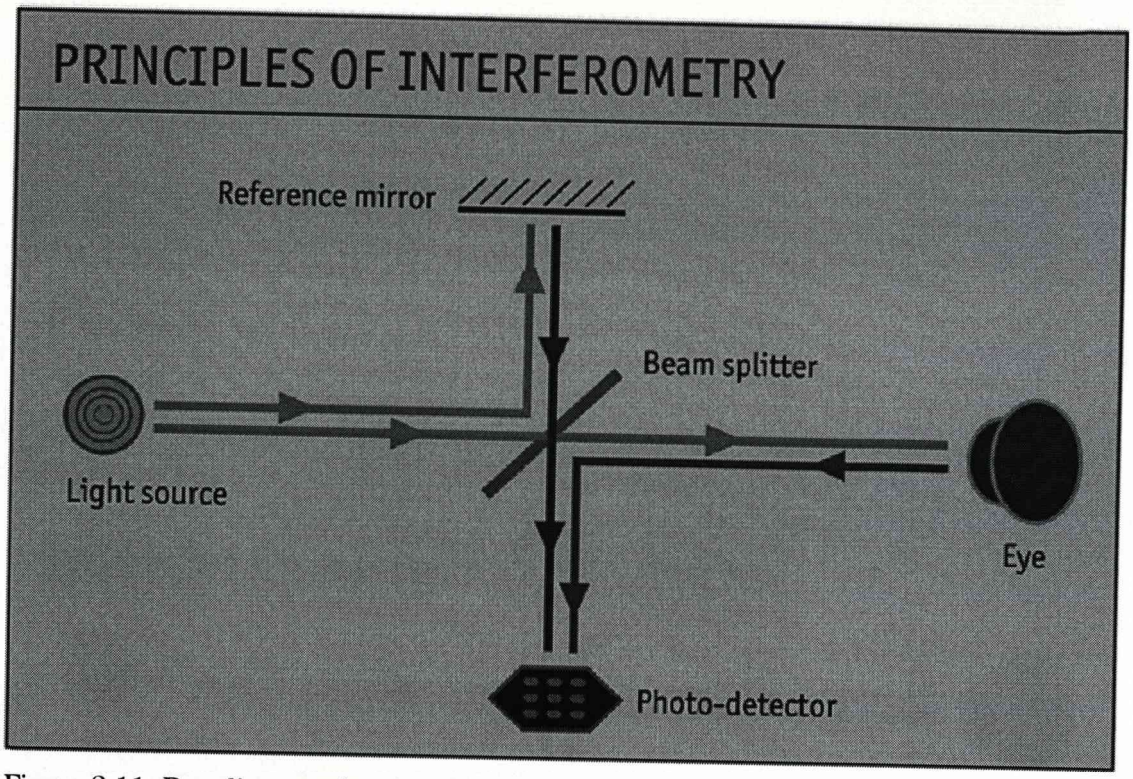

Figure 2.11: Ray diagram showing the principle of interferometry. Light from a source is directed onto the beamsplitter and split into measurement and reference beams. The measurement beam is back reflected from the tissue with different echo time delays, depending on its internal microstructure and the reference beam is reflected at a known distance, which produces a known time delay. The light from these two arms are combined by the interferometer and detected.

Image generation

The simplest type of measurement that can be performed by OCT is information on tissue distances, i.e. axial distance. Once an axial measurement or A-mode scan has been made, the relative position of the different structures is measured by scanning the transverse position of the optical beam within the eye. Cross-sectional imaging of tissue is achieved by performing successive axial measurements or A-mode scans of the tissue at different transverse positions.

Image display

OCT images can be displayed in either a grey scale or a false colour scale (Figure 2.12). On entering the OCT detector system light that is returned from the tissue being examined interferes with that from the reference arm. The resultant intensity of this interference is recorded at 500 points along an individual *z*-axis scan and is represented by a logarithmic pseudocolour scale. The arbitrary units of the signal intensity have a range of 0 to 1600, whereas the pseudocolour scale consists of 16 colours. Tissue structures are mapped into different colours based on their scattering properties, white and red colours designate signals from the most reflective structures, and the black and green designate signals from structures that are the least backscattering. The result of the pseudocolour scale is likely to be a grouping of a wide range of higher signal intensities into single-colour bands of red or white. Thus, significant variations in signal intensity within the inner and outer bands of retinal OCT images may not be displayed. Also, the false colours reflect different optical properties rather than necessarily different tissue morphology and are not analogous to histological staining.[81]

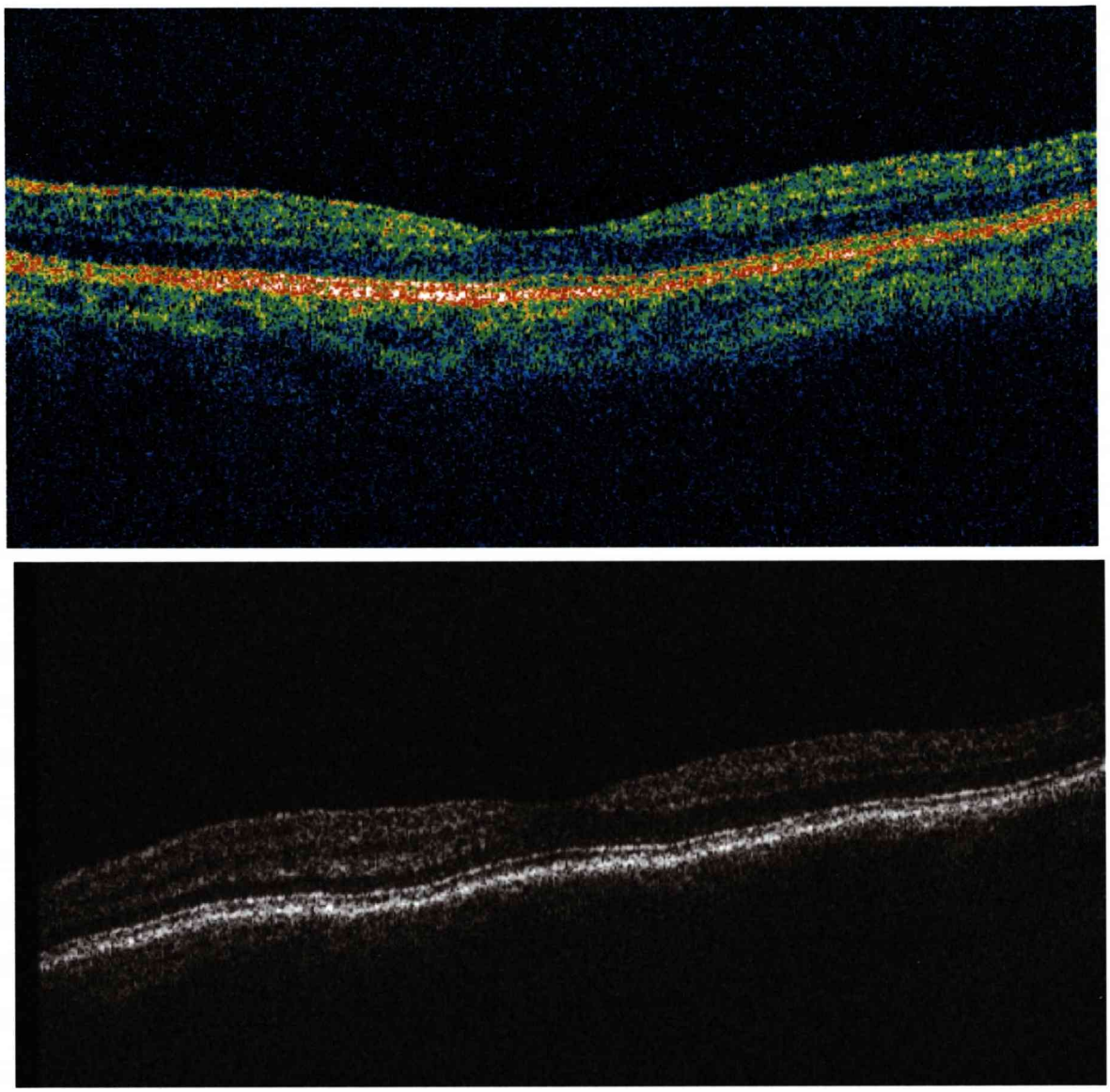

Figure 2.12: Grey-scale and false scale display of OCT images. The grey scale image is displayed using a logarithmic mapping of the signal intensity onto a grey scale ranging from white to black. The amaximum signal is approximately 50db, while the minimum detectable signal is approximately 95db. In the false colour scan, the maximum signal is represented by a red-white colour, while the minimum detectable signal is represented by a blue-black colour.

Image resolution

The *z*-plane is always displayed in the vertical axis, and each pixel has a depth measurement of 4 μm. The spatial resolution of OCT images in the *x*–*y* plane is dependent on both the optical limitations of the ocular media and the design constraints of the instrument. These limitations are apparent when attempting to image over a wide *x*–*y* field. Each OCT image is constructed from 512 equally spaced individual *z*-axis scans, the *x*–*y* dimensions of each being constant, irrespective of the area of retina scanned. Thus, the greater the *x*–*y* field imaged, the greater the spacing between the individual *z*-axis scans, ranging from 10 to 110 μm, and the lower the resolution in the *x*–*y* plane. Thus, for example, when the longest scan is used, the foveola may be missed, because it is only 150 μm across. For the Stratus OCT systems used in our experiments, the lateral (transverse) resolution is also determined by the spot size of the focussed OCT beam. The smallest spot size that can be achieved on the retina is limited by the pupil and the optical aberrations in the eye and is usually ~20-25 μm for the Stratus OCT3. It is therefore evident that, in all three dimensions, the pixelation of images gives rise to both a mismatch between theoretical and practical resolution and indistinct borders on images of tissues.

2.6.2 Optical coherence tomography scanning protocols

In order to create a B-scan, the OCT scanning beam can translate either along a straight line or along a circle. The software provided with the OCT3 offers a number of scanning protocols, which are combinations of these basic scanning options. The scanning protocols used for retinal examination are mainly the line scan protocols (Figure 2.13).

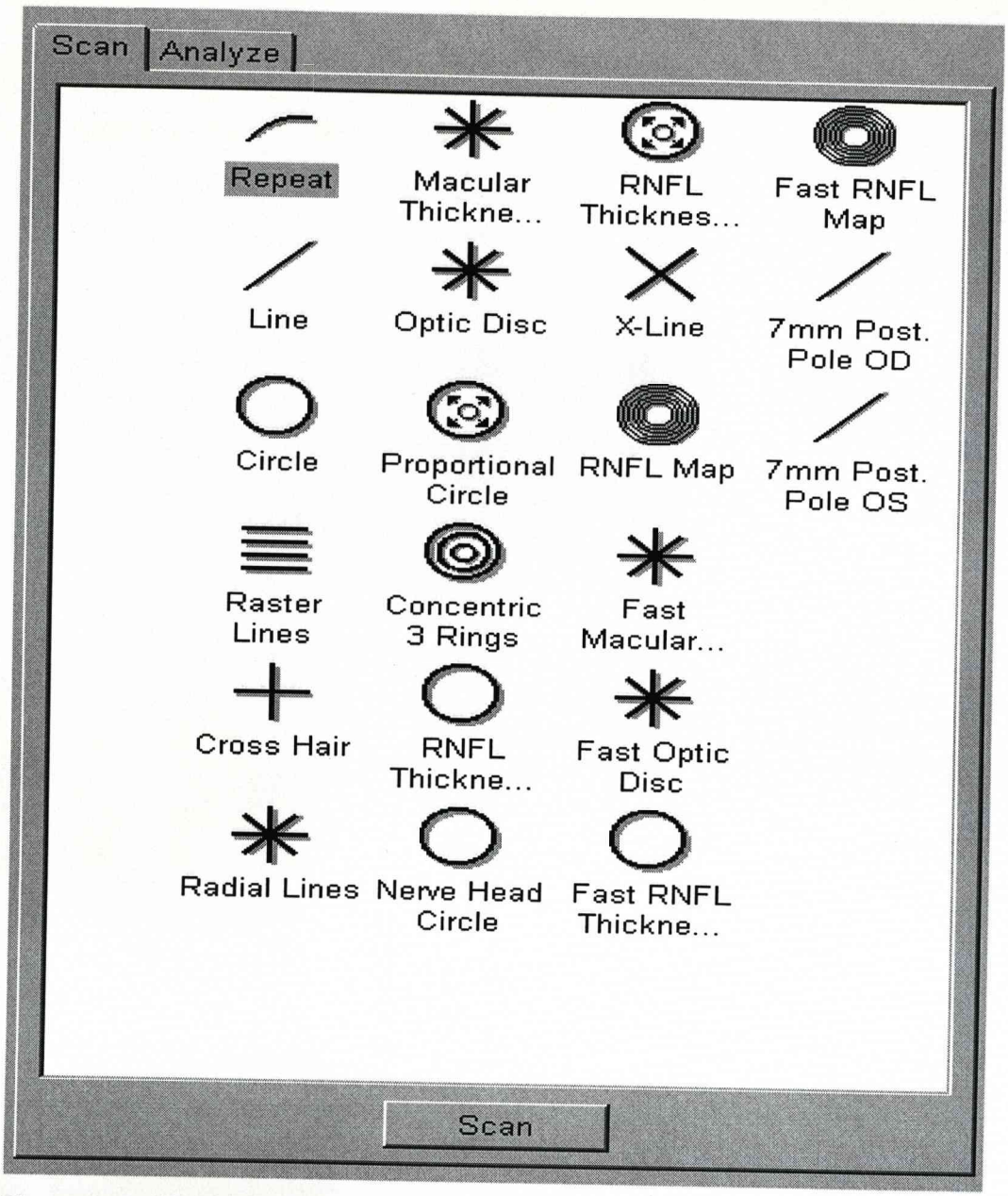

Figure 2.13: The Zeiss OCT 3 has several built-in protocols for scanning the retina and the optic nerve head. A protocol is simply a pre-determined procedure or method. The protocols are represented by descriptive icons in the software, as shown above.

Line scan: The line is a basic scan protocol of the OCT to get a linear scan. The length and angle can be adjusted. The default pattern is a horizontal line 0°, 5mm in length.

Circle scan: The circle protocol is a basic scan form used to acquire multiple circles. The radius of each scan can be adjusted.

Raster lines: This consists of a series of six to 24 equally spaced parallel lines over a rectangular region.[77] The height and width of the aiming box can be adjusted.

Radial lines: This consists of a series of 6 to 24 equally spaced lines through a common centre. The default pattern has 6 lines of 6mm in length.

Fast macular thickness map: This is a time efficient fast scan designed to simplify the process and shorten the acquisition time. The main advantage is that the scan is acquired in 1.92 seconds. This protocol consists of six 6 mm radial line scans that compress the six macular thickness map scans into one scan. All parameters are fixed, the scan alignment and placement area is required only once. The resolution is lower, but the chance of error from patient movement is reduced.

2.6.3 Factors affecting quality of optical coherence tomography scans

Signal to noise ratio

Signal to noise, or the brightness of the retinal features when compared to the background noise, is an important indicator of OCT image quality. This can be affected by ocular media opacities in the cornea, aqueous, lens and vitreous. Improper alignment of the OCT imaging beam can result in the beam being blocked by the iris and is characterised by the loss of signal over a specific portion of the OCT image. Reducing the noise can lead to better quality images that show more intraretinal details and have better delineation of each retinal layer.

Patient fixation

The quality of the scan also depends on the patient's ability to keep the eye steadily fixed on the internal or external fixation light; even the slightest eye movements can cause significant motion artefacts in the scan. The instrument's efficacy is partly limited by the time required for acquiring scans (2.5 seconds). Thus rapid blinking

can also lead to artefacts in the scan. Even in patients with normal fixation, involuntary eye motion amplitudes can be up to several hundred microns at the retina, which is much bigger than the transverse image resolution of the currently available OCT instruments.

Operator factors

Since optical backreflection or backscattering from retinal structures are very weak, reduction in the signal level can occur as a result of operator error during imaging. For optimum scanning, the careful use and adjustment of the focussing control is required during the acquisition sequence.

Retinal morphology

Retinal abnormalities can also be associated with changes in the optical properties that can affect the quality of the OCT images. Focal decreases in backscattering and backreflection may be caused by shadowing from hyperreflective tissues such as haemorrhage, exudates or a detached RPE whereas increased transmission can occur as a result of fibrosis or atrophy. Thus, care is needed in interpreting these images.

2.6.4 Optical coherence tomography image of the normal retina

In a normal eye the OCT scan of the retina shows four pseudocoloured bands that, on passing from the vitreous surface toward the sclera, have the following sequence: red-white, yellow-green, black, and red-white (Figure 2.14). The vitreous appears optically empty. The vitreo-retinal interface, the innermost (red-white) band, is identified by the increase in backscatteringand backreflection between the transparent vitreous and the surface of the inner retina and is thought to correlate with the retinal nerve fibre layer (RNFL). The fovea is identified by its characteristic morphology, i.e. depression or pit, due to the absence of the inner retinal layers. There is also an increase in thickness of the photoreceptor layer at the foveola. The optic disc is recognised by its contour. The RNFL is thicker in the region of the optic disc and becomes thinner towards the macula. The outer high reflectivity band is seen as a double laminar structure. The inner layer is thought to correspond to the junction between the inner and outer segment of the photoreceptors and the outer lamina to the RPE and choriocapillaris and is visible as red-white in the false-colour image demarcating the posterior boundary of the retina. Posterior to the choriocapillaris, relatively weak signals are visible from the deep choroid and sclera due to attenuation of the optical beam after passing through the retina, RPE, and choriocapillaris.

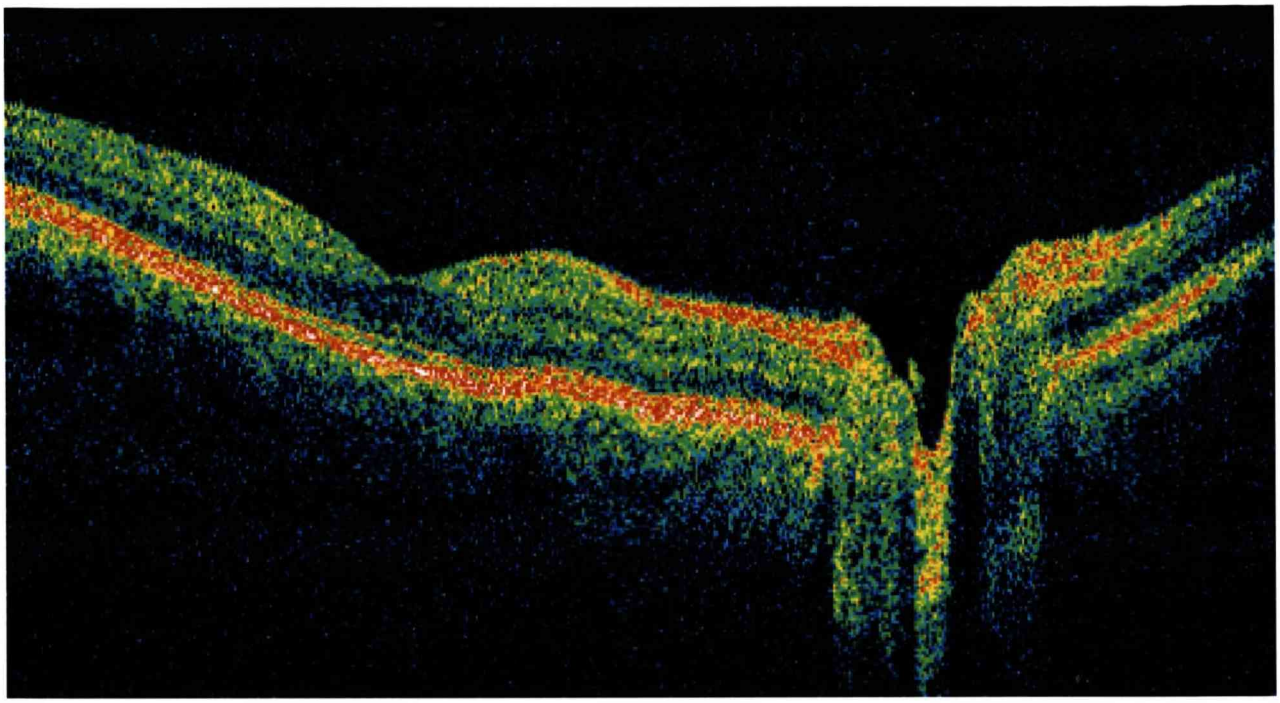

Figure 2.14: OCT tomogram of the normal retina, with a transverse width of 10mm and passing through the fovea and the optic disc.

2.6.5 Comparative histology

OCT scans are usually displayed in a false colour scale. False colour coding represents a plot of the logarithm of the intensity of backreflected or backscattered light. The dimensions of the pseudocolour bands do not display the same ratios as the cell layers in histologic sections. It is therefore extremely difficult to assign the pseudocolour bands in the OCT images to specific anatomic components.

Figure 2.15 shows the microstructure of the various retinal layers that can be differentiated on the OCT images and is correlated with the morphology of the retina.

Toth et al were amongst the first to relate the pseudocolour banding on OCT scans to retinal structural components in primate eyes.[82] In their study they assumed that the innermost aspect of the inner high-signal band corresponded to the inner limiting membrane (ILM) and that the innermost aspect of the outer band corresponded to the apical surface of the RPE. They then compressed the histological images by between 4% and 12%, so that the distance between these two components matched those of their OCT scans. They reported that the outer aspect of the inner band was coincident with the outer aspect of the RNFL. Thus their images had four high-signal bands that corresponded to the RNFL, inner plexiform layer (IPL), the outer plexiform layer (OPL), and the RPE. Although their experimental findings seem to indicate a direct correlation between OCT strata and retinal cellular components, the match is only superficial. For the bands said to correspond to the RNFL and OPL, the ranges of thickness measurements were 3.3 and 7.9 times greater on OCT than light microscopy for the published images.

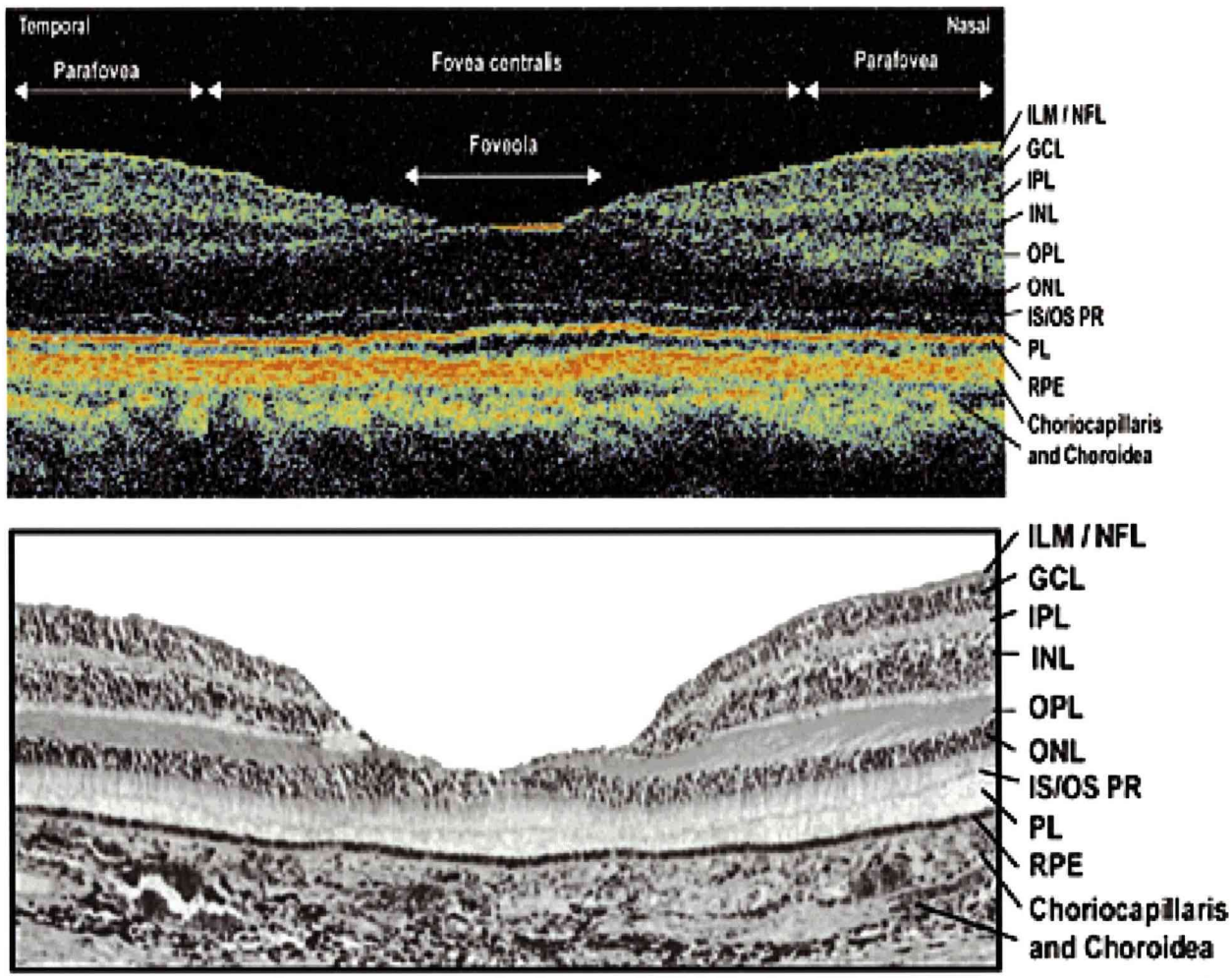

Figure 2.15: Comparison of an in vivo OCT image of the normal human macula to a histological micrograph of the normal human macula. The OCT image has 1:1 aspect ratio to permit comparison to histology. Several layers can be resolved and have been labelled in the image: inner limiting membrane (ILM), nerve fibre layer (NFL), ganglion cell layer (GCL), inner plexiform layer (IPL), inner nuclear layer (INL), junction between the inner and outer segment of the photoreceptors (IS/OS PR), outer nuclear layer (ONL), retinal pigment epithelium (RPE). The foveola, fovea centralis, as well as the parafoveal region, are also indicated. (Nature 2001;7:502-507)

Chauhan and Marshall[83] correlated OCT images with histology using cadaveric human and bovine glutaraldehyde-fixed retina. No image manipulation was performed and matches in retinal thickness were directly correlated to tissue obtained by controlled dissection of superficial retinal layers using excimer laser ablation (mean depth of ablation was 0.49 microns). On correlation with light microscopy, the location and thickness of the inner band of high OCT signal corresponded to the sum of the RNFL, GCL and part of the IPL and was 7.3 times that of the RNFL, while the outer band of high signal corresponded to the RPE, choriocapillaris and half the choroid and was 2.6 times greater than the RPE-choriocapillaris complex. They observed, though reduced in thickness, the inner high reflectivity band persisted even after the deliberate destruction of inner retinal layers contradicting the notion of tissue-specific origin of OCT signal. By comparing the distribution of melanin on OCT images with fundus appearance in in-vivo experiments in patients with retinitis pigmentosa, they attributed the location of the inner limit of the outer high reflectivity band to the apical region of the RPE layer, because it is within this 3-mm layer that melanin granules are concentrated. In their in-vitro experiment the location of the inner border of the outer hyper-reflectivity band remained constant and close to the apical RPE (within 28μm on histological correlation), even with progressive ablation. The thickness of the band was attributed to the RPE, choriocapillaris, and just under half of the choroid in human eyes.

Ghazi et al also tried to address the origin of the outer high reflectivity band on OCT images.[84] 11 formalin-fixed caps of 7 human eyes enucleated for choroidal melanoma were used. Outer high reflectivity band, which they termed "outer red line (ORL)", was evaluated by sequential surgical elimination of RPE, Bruch's

membrane and choroid and OCT images through these areas were correlated with corresponding histological sections. The ORL was partially altered in areas from which the RPE only was removed, and there was increased signal transmission to deeper layers; discontinuous in areas from which the RPE/BM was excised with a residual, irregular, hyper-reflective band external to it, and increased signal transmission and abolished in areas where all three layers were taken out, leaving a sharply demarcated residual hyper-reflective band at an even more external level and increased signal transmission. Their findings suggested a predominant contribution from the Bruch's membrane and the inner choroid to the outer high reflectivity band, compared with the RPE (Figure 2.16).

To date most attempts to correlate optical stratification with retinal histology has had important limitations. In the studies discussed here, differing conclusions regarding the origin of the inner and outer bands were reached. Also, none of the papers have addressed the double laminar structure of the outer high reflectivity band or assessed the contribution of the neurosensory retina to the anterior limit of the band. This may be because the aforementioned studies were performed using the OCT2 (Toth et al, 1997; Chauhan et al, 1999) or an earlier prototype with limited resolution and this led to incorrect interpretation of this structure as the RPE. Further understanding of this retinal microstructure has been possible since the advent of ultrahigh-resolution (UHR-OCT). A comparison study on macular imaging with UHR-OCT and OCT3 exhibited similar performance in differentiation of the thicker and more hyperreflective intraretinal layers. In addition, UHR-OCT permitted enhanced resolution of some of the finer retinal structures such as external limiting membrane, photoreceptor inner and outer segments and possible Bruch's membrane and choriocapillaris. UHR-OCT uses femto-second laser as a light

source and axial imaging resolutions have been claimed to be approximately 3 μm in the human eye.[85] This technology is only available for research use at present. Though human studies are not available, animal studies performed comparing UHR OCT imaging to retinal histology from the pig and monkey, and intraretinal features on UHR OCT have shown good correspondence and also helped to delineate the junction between the photoreceptor inner and outer segment.[86, 87] On UHR-OCT, the photoreceptor outer segment (OS) is ~ 40 μm thick at the foveola and accounts for 18% thickness of the total retina.[88] A recent histological study using glutaraldehyde as a fixative, measured the OS length at about 20 to 30 μm in the human foveola and about 20% of the total retinal thickness.[89]

UHR-OCT imaging has demonstrated possible artifactual modification of the RPE/photoreceptor border tissue in the course of histological processing. Thus, it may be that in the absence of pathology, the inner high reflective band represents the RNFL and the outer high reflective band has a bilaminar structure; the inner representing the photoreceptor IS/OS junction and the outer the RPE/ Bruch's membrane/choriocapillaris complex. The degree to which these findings can be applied to macular degeneration is not known. Accumulation of fluid within and under the retina and RPE, fibrosis, RPE abnormalities, drusen, etc may result in change or displacement of the reflective interfaces, associated alterations in incident and backscattered light, and changes in refractive index adjacent to the interface compared to normal.

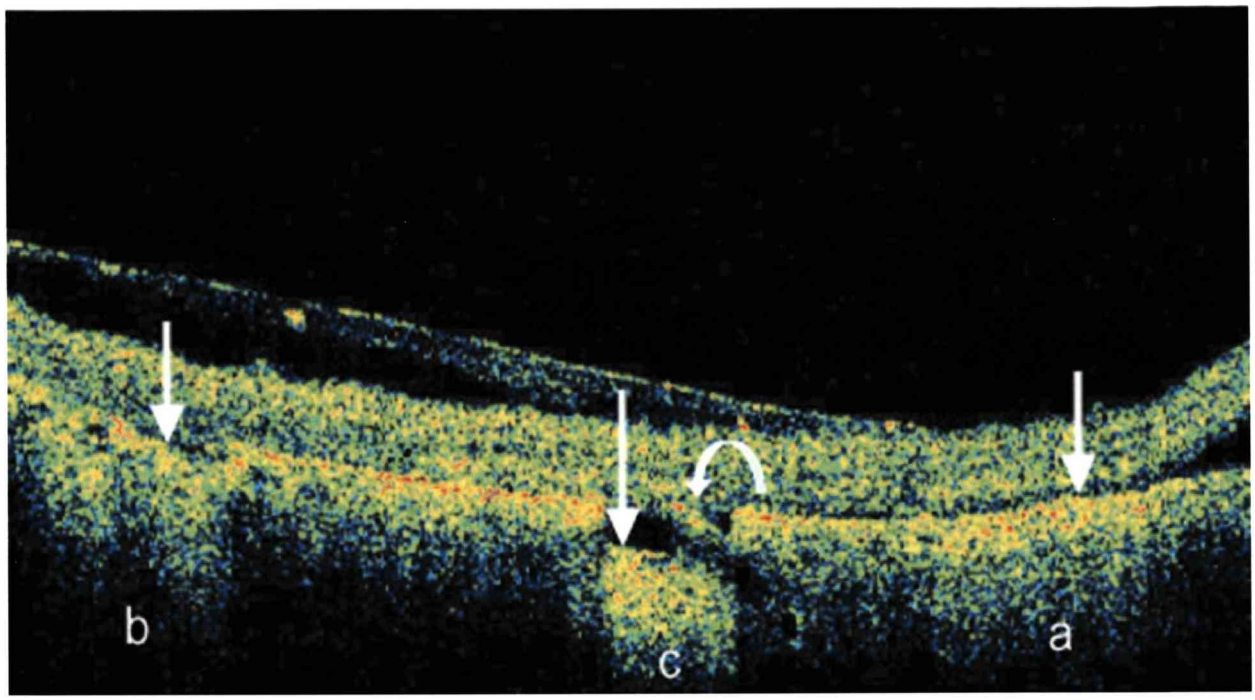

Figure 2.16: Relative contribution of the layers to the outer "red line" (ORL) in OCT3 images of the peripheral retina. Areas a, b, and c, respectively, represent areas from which retinal pigment epithelium (RPE); RPE and Bruch's membrane; and RPE, Bruch's membrane and choroid were surgically removed. The ORL is partially altered (arrow) in (a) with increased signal transmission to deeper layers compared with surrounding surgically unaltered areas. The ORL is discontinuous in (b) with a residual irregular hyper-reflective band (arrow) external to its position in surgically unaltered areas, with increased signal transmission. The ORL is abolished in (c) with a residual sharply demarcated hyper-reflective band (arrow) at an even more external level and increased signal transmission. The curved arrow points to an artefact of the surgical dissection. (Reproduced from: Ghazi NG, Dibernardo C, Ying HS, et al.)

2.6.6 Optical coherence tomography in neovascular AMD

Retinal diseases usually manifest as a structural disruption of the normal retinal architecture and can lead to changes in retinal thickness and optical properties. In 1995, Puliafito et al published their findings using OCT for the examination of macular diseases in 51 eyes of 44 patients. In this observational study they described OCT characteristics of macular hole, epiretinal membrane, cystoid macular oedema and PED and demonstrated the feasibility of applying this technology in macular pathologies.

Toth et al[90] & Fukuchi et al[91] have separately compared OCT images with histology in laser induced CNV in monkey and rat retinas respectively. Their studies showed that OCT may demonstrate the positional relationship between neovascularisation and RPE and that CNV is imaged in the intraretinal space as a highly reflective red signal. This high reflective band is attributed to RPE cells enveloping the CNV. Comparative histology showed that on OCT, retinal fluid collections appear as hyporeflective black spaces whether subretinal or intraretinal.

Although, OCT is now widely applied in the diagnosis of various macular diseases its role in patients with AMD is less well established. Until recently, the management of neovascular AMD and treatment criteria have been based on the classification of CNV on FA. AMD studies such as the MPS, TAP and VIP used FA to determine the need for treatment. Numerous studies have recently emerged piloting the use of OCT in this category of patients both in the detection and classification of lesions and in the guidelines for follow-up and retreatment of patients.

In 1994, Hee et al were the first to report the use of OCT in 391 patients with non-exudative and exudative AMD. Initial diagnosis was made using slit-lamp biomicroscopy and FA.[92] Comparisons between OCT and FA were performed on 90 eyes with exudative AMD and no previous laser, drusen, geographic atrophy or disciform scarring. CNV's were classified on FA as classic, occult, mixed, serous PED and haemorrhagic PED. On OCT the lesions of exudative AMD were described as: 1) well-defined CNV in the presence of a fusiform thickening of the outer high reflectivity band (OHRB) with well defined boundaries, 2) poorly defined CNV when the disruption of the OHRB was diffuse with ill-defined boundaries, 3) serous PED in the presence of a sharp elevation of the RPE reflection over an optically clear space and shadowing the reflections from the choroid below, 4) fibrovascular PED when the elevation of the RPE is over a moderately backscattering region, and 5) haemorrhagic PED where the elevated reflection of the RPE is over a highly backscattering region with complete shadowing of the choroidal reflection. In this study the majority of the angiographically classic CNV appeared as well-defined CNV on OCT, whereas occult CNV were poorly defined, fibrovascular PED or serous PEDs on OCT. This was mainly a descriptive study with a mixed case series and the only conclusion reached was that OCT classifications did not correspond directly to FA descriptions.

Sandhu et al assessed the diagnostic accuracy of OCT in predicting FA findings in patients suspected of having CNV due to multiple causes. [93] In this observational study, FA and OCT scans of 131 eyes were assigned a diagnosis by 2 masked observers. MPS, TAP and VIP protocols were used to classify the lesions on FA, as classic, occult, serous PED and an additional category of no CNV and were expected to correspond to OCT scans showing a well-defined OHRB, a poorly

defined OHRB, a dome shaped elevation of the OHRB and no signs of CNV respectively. Using FA as the reference standard, OCT was good at detecting the presence of CNV (sensitivity 96.4%). But, the authors reported that OCT was less accurate at identifying the components of the CNV (specificity 66%), especially with occult lesions as these were hard to characterise, appearing to have components of classic CNV, cystoid and PED. They were also unable to distinguish serous from vascularised PED on OCT.

In a retrospective study using OCT, Ting et al found CMO in 46% of the 61 eyes with subfoveal CNV secondary to AMD.[94] They reported a statistically significant association between CMO and reduced vision and between the presence of classic CNV on FA and CMO on OCT. They found a weak association between retinal thickness at the fovea and vision ($p=0.02$).

The studies presented here were pilot studies exploring the feasibility of using OCT in the management of neovascular AMD. The universal limitation of the above studies was in using FA as the reference standard. The difference in the macular examination techniques with OCT imaging the retina in the z-plane in addition to the x-y plane, the difficulty in distinguishing between staining and leakage and the presence CMO and SRF angiographically in the setting of leakage from the CNV on FA, may further add to these discrepancies.[95] Also none of the studies validated their technique for the interpretation of the scans.

Rogers et al described OCT findings following PDT of predominantly classic CNV based on a retrospective review of 79 eyes of 77 patients.[96] They created a 5-stage OCT classification in an attempt to monitor the response of eyes with subfoveal CNV treated with PDT. Stage 1 was described in 2 eyes as an increase in SRF due to an inflammatory response within the first week of treatment. Stage 2 was

recognised in 28 eyes by the reduction in SRF between 1 to 4 months. Stage 3 was divided into 3a and 3b based on the ratio of fluid to fibrosis at 4 to 12 weeks after treatment. 15 stage 3a eyes had greater SRF to subretinal fibrosis ratio. 64 eyes with stage 3b leaked less actively on FA and had more prominent fibrosis with minimal intraretinal fluid. Eyes with CMO on OCT and staining only of the CNV on FA were defined as stage 4 and was identified in 11 eyes; this appearance was seen at an average of 5 months following PDT. In 19 stage 5 eyes there was no SRF and the retina showed fibrosis and atrophy. There are several limitations to this study, the majority stemming from the retrospective nature of the data collection with no standardised method of follow-up. The authors have not defined the OCT features and due to the small numbers in each category (except 3b), the value of this classification in the follow-up of patients is difficult to determine. For example, only 2 patients demonstrated stage 1, leading to doubts about its existence. The data is descriptive and the patterns described are not consistent at each time point, with a wide variation in the time at which any of these stages can present. There has been no attempt to identify the factors on OCT that may lead to reactivation of the lesion or poor response to treatment. The data appears to be incomplete, while the authors give the number of patients in stage 3, 4 and 5 who had undergone retreatment, a table detailing the OCT changes in the different eyes following PDT would have served to explain some of the inconsistencies. Their classification, though OCT based, is still dependent on FA and does not change the management of patients undergoing PDT.

2.6.7 Developments in optical coherence tomography imaging of the retina

Since OCT was introduced into ophthalmology a decade ago there have been tremendous progress in the development of the technology.[97]

Ultrahigh resolution OCT

Ultra-high resolution OCT (UHR OCT), developed using a broader bandwidth light source and femtosecond titanium:sapphire light sources, achieves a claimed axial resolution of 3 microns. It permits enhanced visualisation of the intraretinal layers that could not be resolved with the standard OCT, including the ganglion cell layer, inner and outer plexiform and nuclear layers, external limiting membrane and inner and outer segments of the photoreceptor layer. The technology in its current state is restricted by slow image acquisition speed (it takes 4 seconds to acquire a 6x2 mm scan) and the high cost of the light source.

En-face OCT

This method combines high-resolution tomographic images with the surface imaging capability of the scanning laser ophthalmoscope (SLO). Similar to the standard resolution, conventional OCT, this system is built around a Michelson interferometer, and uses a super luminescent diode (SLD) with a central wavelength of 820nm and a spectral bandwidth of 20 nm. An important advantage of the OCT/SLO system over the Stratus OCT is that the OCT C-scans allow for a quick overview of the area involved in a particular retinal disease. In the field of AMD imaging, it may help in the discrimination between the different types of PEDs, It may also be useful as a reliable reference image to assist in overlay with other en-face imaging techniques such as FA.

Spectral domain OCT

Spectral domain OCT utilises the 'Fourier or spectral detection' technique by which magnitude and echo time delay are measured by acquiring the Fourier transformation of the interference spectrum of the light signal using a spectrometer, without mechanically moving the position of the reference mirror. This dramatically increases the scanning speed and imaging sensitivity. Compared to the standard time-domain OCT, spectral OCT has a faster acquisition time (by approximately 50 times), superior sensitivity, a lower amount of energy directed into the eye (less than 600 microwatt) and enables three dimensional mapping of tissue structures. It appears to be the most promising recent development. Because of the greatly increased scanning speed it is far less vulnerable to involuntary eye-movements, and should prove beneficial in patients with neovascular AMD who have fixation problems. Spectral OCT is now commercially available as SOCT Copernicus (Optopol Technology Sp, Zawiercie, Poland), Cirrus HD-OCT (Carl Zeiss Meditec, Dublin, CA, USA), RTVue100 (Optovue, Fremont, CA, USA), Spectralis (Heidelberg Technologies, Germany) and Topcon 3D OCT (3D OCT-1000, Tokyo, Japan).

Molecular imaging with OCT

Functional changes precede morphological ones. Therefore, diagnostic modalities that combine conventional imaging with quantitative visualisation of the involved molecular processes may be of value. Molecular imaging (MI) aims to combine molecular contrast agents with traditional imaging techniques. Two ways to image a specific chemical or protein distribution within a sample with OCT are being investigated.[98]Attenuation based molecular-contrast OCT (MC-OCT) examines the capability of OCT to quantitatively measure changes in the spectral attenuation

characteristics of tissue, localised and in time. Different types of dyes are being studied and include near infra red dyes and contrast agents like methylene blue. Their transition from one state to another causes a change in their absorption profile that may be subtracted from OCT A-scans taken over time. The second approach called coherent-emission based MC-OCT, which relies on intrinsic contrast agents that can convert incident light into different emitting wavelengths. Which molecules within retinal structures have sufficiently distinct contrast properties is still being explored.

Adaptive optics

The transverse resolution of the OCT systems being introduced remains restricted to 15-20 microns. While major strides have been made in improving axial resolution and image acquisition speed, less has been achieved in transverse image resolution. Transverse resolution depends on the numerical aperture (NA) of the system optics including the eye itself and the spot size on the retina. A smaller spot size on the retina can be achieved by expanding the beam and the pupil diameter to enlarge the effective NA of the eye. However, in pupil diameters over 2mm, image quality is affected progressively by ocular aberrations induced by the cornea and to a lesser extent the lens. These aberrations can be corrected through adaptive optics (AO) by wavefront detection and modulation. Several groups are developing AO in ophthalmic OCT imaging, but this technology is still in its infancy and its application in clinical practice still needs to be established.

2.7 PHOTODYNAMIC THERAPY

The treatment of neovascular AMD has become an important challenge for patients, ophthalmologists and health systems. Several treatment strategies have been clinically approved following large scale clinical trials. Until a decade ago, the only proven treatment for CNV was laser photocoagulation applicable only in a small proportion of patients. With a greater understanding of the aetiology of AMD have come therapeutic strategies that have moved beyond the limited approach of thermal laser photocoagulation. Photodynamic therapy represented such a milestone in new options and is discussed in detail here. I will also present a brief review of the past, current and upcoming treatments for neovascular AMD therapy.

2.7.1 Introduction

The principle of chemical sensitisation of live tissues by light is known as photodynamic therapy (PDT) and was first reported in 1900 by Raab.[99] PDT is a two-step technique in which a light sensitive compound called a photosensitiser is administered and subsequently activated by light exposure to produce photochemical effects in the target area.[100] Several substances, including rose Bengal, methylene blue, eosin, tetracycline, chlorophylls, and porphyrins have been used in vitro and in animal models for the study of mechanisms of photodynamic injury and to develop an agent for PDT. A photosensitising drug (haematoporphyrin derivative) that accumulates preferentially in rapidly dividing cells, particularly in the proliferating neovascular tissue of tumours, has been used in combination with low-energy nonthermal laser light to treat cancers of the liver, spleen, kidneys and skin for a number of years. [101, 102] Because PDT appears to cause vascular occlusion by damaging tumour vascular endothelial cells, a potential use in other conditions

with neovascularisation, including choroidal neovascularisation (CNV) was suggested. [103, 104, 105] In April 2000, following large scale, randomised clinical trials the Food and Drug Administration (FDA) in the USA and the European Medicines Agency (EMEA) approved PDT with verteporfin (Visudyne) for predominantly classic CNV secondary to AMD to reduce the risk of vision loss in selected cases of AMD with subfoveal predominantly classic CNV.

2.7.2 Verteporfin

Verteporfin (Visudyne®), a benzoporphyrin derivative monoacid ring A, is a hydrophobic photosensitiser synthesized from protoporphyrin.[106] It is activated by low intensity nonthermal laser light at a wavelength of 689nm. In its excited state, verteporfin is an efficient generator of singlet oxygen, which is believed to be primarily responsible for cell death after PDT.[107]

In vitro studies suggest that verteporfin is selectively taken up by cells with high levels of low density lipoprotein receptors (including neovascular endothelium) as a result of its affinity for plasma lipoproteins.[108] These receptors are expressed in endothelial cells and their expression is increased in neovasculature.

For choroidal neovascularisation, verteporfin 6mg/m^2 is infused intravenously over a 10-minute period, and 5 minutes later, the lesion is exposed to a 689nm light dose of 50 J/cm^2 for 83 seconds.

Verteporfin therapy (photodynamic therapy with liposomal verteporfin) selectively destroys areas of choroidal neovascularisation within the eye while sparing adjacent normal vasculature.[109, 110] Histopathological examination in verteporfin therapy treated eyes in patients with subfoveal CNV secondary to AMD showed occlusion of vessels by erythrocytes or thrombotic masses, damage to the neovascular

endothelium including vacuolisation and fragmentation of neovascular endothelium and disintegration of the endothelial cell layers, extravasation of erythrocytes and mild damage to the RPE.[111, 112, 113]

Verteporfin is associated with transient skin photosensitivity that is dose dependent. Maximum skin photosensitivity occurred 1.5 hours after administration of IV verteporfin 12 mg/m^2 over 45 min in 8 healthy volunteers; the duration of photosensitivity was dose-dependent (2 to 6.7 days with verteporfin 6–20 mg/m2).[114]

2.7.3 Randomised controlled trials of PDT with verteporfin[21,22, 115,116,73 ,117]

There have been 2 completed randomised controlled clinical trials (RCTs) comparing verteporfin PDT with placebo. The realistic aim of PDT is to slow progression of AMD not to produce normal vision. Outcomes are expressed as risk of a poor outcome rather than as improvements in vision. With relevance to this thesis, only the two completed and published RCTs will be reviewed- the Treatment of Age-related macular degeneration with Photodynamic therapy (TAP) in 1999 and Verteporfin in Photodynamic therapy (VIP) trail in 2001.

2.7.4 TAP Study

The objective of the TAP investigation was to determine whether verteporfin therapy, compared with placebo, could reduce the risk of vision loss in eyes with subfoveal CNV secondary to AMD. A total of 609 participants were randomly assigned to verteporfin (402) or placebo (5% dextrose in water) (207). All patients and treating ophthalmologists were masked to the treatment assignment, as were the visual acuity examiners and photograph graders. The key eligibility criteria for inclusion were a best corrected visual acuity (BCVA) of approximately 73 to 34

letters (20/40 to 20/200; 6/12 to 6/60), subfoveal CNV secondary to AMD with evidence of classic CNV, and a greatest linear dimension (GLD) of the entire lesion on the retina of 5400 μm or less. The mean age was 75 years and the participants were examined at 3 monthly intervals and either treated or not. The outcomes measured at three monthly intervals were visual acuity, contrast sensitivity in the study eye and side effects. The primary outcome was maintenance of vision, defined as loss of less than 15 letters of BCVA.

Significantly more verteporfin therapy than placebo recipients lost <15 letters at 12 and 24 months (the primary efficacy outcome; $p < 0.001$ at both time points) Verteporfin therapy was also superior to placebo at 12 and 24 months for most visual acuity secondary endpoints, including loss of <30 letters ($p < 0.001$ at both time points) and the mean number of contrast sensitivity letters lost ($p \leq 0.001$ at both time points).

Subgroup analysis of the TAP Investigation indicated that therapy was of greater benefit to patients with predominantly classic subfoveal CNV (area of classic CNV≥50% of the area of the entire lesion) compared with those with minimally classic CNV (area of classic CNV >0% but <50% of the area of the entire lesion). For patients with predominantly classic subfoveal CNV, more verteporfin therapy (n= 159) than placebo (n = 83) recipients lost <15 letters of BCVA and fewer had reduced contrast sensitivity loss at 12 and 24 months (both $p < 0.001$ vs placebo).

The efficacy of verteporfin PDT in patients with predominantly classic subfoveal CNV was studied in relative risk reduction (RRR), absolute risk reduction (ARR) and relative risk (RR) analyses.[118] Patients with predominantly classic subfoveal CNV had an RRR of 39% and an ARR of 24% at 12 months; however, the 12 month RRR and ARR values were considerably higher in the subgroup of patients

with predominantly classic subfoveal CNV with no occult component (68% and 50%). RR analysis evaluating the effect of verteporfin therapy or placebo on the loss of ≥15 letters (3 lines) at 24 months showed that verteporfin therapy had greater benefit than placebo in patients with classic-containing subfoveal CNV (RR 54%), particularly if there was no occult component to the CNV (RR 42%). Conversely, an RR of 99% at 12 months confirmed the lack of therapeutic benefit of verteporfin PDT in patients with minimally classic lesions.

The beneficial effect of verteporfin PDT on BCVA was observed for up to 60 months in a subgroup of patients with predominantly classic subfoveal CNV secondary to AMD who had received verteporfin therapy in the TAP Investigation and continued to receive verteporfin therapy in the TAP Extension study.[119] Compared with baseline (24 months after commencing therapy), the number of patients who had lost <15 letters had decreased minimally throughout 60 months' treatment and mean change in BCVA was relatively stable. Between months 24 and 36, the distributions of BCVA scores changed minimally and mean acuity was virtually unchanged (approximate Snellen equivalent 20/160+1 versus 20/160).

Since a single treatment with verteporfin therapy did not usually prevent recurrence of subfoveal CNV in phase I/II trials. 3 monthly treatments were planned. On average, patients in the TAP study treated with verteporfin or placebo respectively required 3.4 and 3.7 treatments (out of a possible 4 treatments) in the first 12 months of the study, and 2.2 and 2.8 treatments between months 12 and 24. Data from the TAP Extension study in 105 patients with predominantly classic CNV who had received verteporfin therapy in the TAP Investigation indicate need for treatment with verteporfin therapy continued to decrease; these patients required an

average of 1.3 treatments at 36 months, reducing to an average of 0.5 treatments in the 93 patients who completed the month 48 examination.

2.7.5 VIP Study

The VIP study comprised 339 patients (225 PDT, 114 placebo) mainly with occult only neovascular AMD, whose initial BCVA was ≥50 letters (20/100 or 6/30). VIP also included patients with mixed classic and occult if BCVA was ≥70 letters, although the numbers in this category were small (59 of 225 and 22 of 114 in PDT and placebo respectively). The VIP trial in patients with AMD (VIP-AMD trial) demonstrated that verteporfin PDT had a treatment benefit for selected patients with occult with no classic subfoveal CNV who had demonstrated recent progression defined as the presence of haemorrhage, ≥10% increase in GLD and/or loss of ≥5 letters of BCVA.

In the VIP-AMD trial, fewer verteporfin PDT than placebo recipients lost <15 letters at 24-month ($p < 0.05$). In addition, at 24 months, the risk of severe loss of BCVA (≥30 letters) was lower ($p = 0.004$) and fewer recipients had BCVA of 20/200 or worse (28% vs 45%; $p = 0.009$) with verteporfin therapy than with placebo. Overall, patients receiving verteporfin PDT lost fewer letters than placebo recipients at 24 months compared with baseline, with a shift in favour of PDT in the frequency distribution of changes in BCVA($p = 0.006$). Change in mean contrast sensitivity letter scores from baseline also favoured patients treated with PDT at 24 months. Loss of contrast sensitivity letters did not differ between the two treatment groups during the first 9 months of the study and was not reported in the 12 month report; at 24 months, a smaller proportion of 161 verteporfin therapy recipients had

lost ≥9 letters compared with the 90 placebo recipients (20% vs 34%; p = 0.01 vs placebo).

The greatest therapeutic benefit of verteporfin therapy in patients who had occult with no classic subfoveal CNV appeared to occur in a subgroup with smaller baseline lesion size (≤4 MPS disc areas) regardless of BCVA, or with an initial BCVA of 20/50–1 or worse (irrespective of lesion size).[120]

2.7.6 Effect of baseline lesion composition, size and visual acuity

Retrospective exploratory analyses[121] of data from TAP and VIP-AMD suggest that baseline lesion size, lesion composition and baseline BCVA are important in predicting the efficacy of PDT. At baseline, patients with predominantly classic CNV had a smaller mean lesion area than those with minimally classic or occult with no classic lesions (3.4 vs 4.7 and 4.3 MPS disc areas). Multiple linear regression analysis that included all lesion types (predominantly or minimally classic, or occult with no classic CNV) showed that baseline lesion size was a more significant indicator of treatment benefit (smaller lesions demonstrated a greater treatment effect; p = 0.01 vs larger lesions) than baseline lesion composition (p = 0.18) or visual acuity (p = 0.53). Analysis by lesion composition showed that the interaction between treatment benefit and lesion size was significant in patients with minimally classic and occult with no classic CNV (p = 0.03 for both lesion types), but was not evident in patients with predominantly classic CNV. Nevertheless PDT patients with a baseline lesion size of ≤4 MPS disc areas had a greater improvement in BCVA at 24 months compared with placebo recipients, irrespective of lesion composition (predominantly classic, minimally classic or occult with no classic subfoveal CNV; all p < 0.05). Furthermore, PDT recipients with smaller lesions retained greater BCVA than those with larger lesions at 24 months, irrespective of

lesion composition. Conversely, baseline BCVA did not appear to be a significant predictor of treatment efficacy for any lesion type in these analyses.

Table 2.5: Key results for the TAP and VIP studies at 2 years.

Outcome at 2 years	TAP			VIP		
	PDT	Placebo	RR	PDT	Placebo	RR
	N=402	N=207	(95% CI)	N=225	N=114	(95% CI)
Loss of 15 or more letters	47%	62.3%	0.75 (0.65-0.88)	53.8%	66.7%	0.81 (0.68-0.96)
Mean number of contrast sensitivity letters lost	1.3	5.2	Not applicable	Not reported		

The key results of the TAP and VIP trials indicate that PDT with verteporfin is more effective than placebo in terms of the primary outcome (loss of <15 letters or more of BCVA) and it is very unlikely that this is a chance finding. Though drug company sponsored and run, both were high quality studies with a very similar study design. They have a maximum Jadad score[122] of 5 and allocation to these studies was truly random and appears to be concealed. (Jadad score is a numerical score between 0 & 5 assigned as a measure of the design and reporting quality of a study with 0 being the weakest and 5 being the strongest.) For the two RCTs there is consistency between the results, particularly on relative effects such as RR of the primary outcome measure at two years. The subgroups were pre-specified in the RCT protocol and statistical plan. Also the analysis adhered to the statistical guidelines and the subgroup effect also has a strong biological plausibility.[123]

However, there are a number of weaknesses. Both the RCT's were pharmaceutical industry funded and there have been no independent studies. There are also several arguments for the subgroup effect being a chance finding. This effect needs to be considered in light of the number of subgroups examined. There were 14 subgroups

defined and it would be expected that one statistically significant interaction might occur by chance alone. In the TAP study two were obtained. But the percentage of classic and the presence of occult are interdependent. It was only after the TAP study that predominantly classic as a subgroup was defined. If predominantly classic is more aggressive and sight threatening and so more susceptible to PDT treatment, a gradient of effect between 100% classic and 100% occult would be expected. The TAP subgroup analysis suggests that occult has a similar effect size as predominantly classic, with minimally classic having a worse outcome than both. The VIP trial suggests a similar effect size in minimally classic as occult. Based on their analysis, the Cochrane review committee and Meads et al have suggested that the subgroup effect in the TAP trial was a chance finding.[124]

2.7.7 Our experience

Our centre reported on the clinical efficacy of verteporfin PDT in the treatment of predominantly classic and classic/ no occult CNV in a NHS setting.[125] 170 eyes of 159 patients with subfoveal CNV of mixed aetiology (147 eyes with AMD) were enrolled. At 12 months, 73% overall, 76% in AMD, 70% in classic/no occult, and 89% in predominantly classic, lost< 15 letters. The mean number of treatments in the first year was 2.7 and fewer than reported in the literature.

A recently published paper reports on the visual outcomes observed in patients treated with verteporfin PDT based on prospectively collected data for audit under the UK PDT Users Group (PDTUG) national surveillance programme.[126] All patients commencing a course of verteporfin PDT for CNV for any aetiology in 13 UK clinical treatment centres were followed prospectively within the PDTUG surveillance programme. Between November 1999 and May 2004, data were collected from 1894 eyes. 75.7% eyes had AMD. The results of AMD patients

under the surveillance programme compared favourably with the TAP study; the mean loss of 7.4 letters at 12 months compares favourably with a loss of 9.9 letters in TAP (predominantly classic and classic/no occult groups). The advantage of this study and surveillance programme is the large numbers and the ability to measure the effectiveness of a new treatment in routine clinical practice. Data were available at 12 months on 1010 (53.3%) and at 24 months on 310 (16.4%) eyes. The proportion of eyes losing <15 letters was 71% (716/1010) at 12 months and 70% (217/310) at 24 months. At 12 months 91% (917/1010) of patients lost <30 letters. In the PDTUG surveillance programme the mean number of treatments for the cohort was 2.4 in the first 12 months and over the 24 month follow-up at 3.4 was less than the 5.6 in the treatment arm of the TAP study. This reduction in the number of treatments has potentially favourable implications for the cost-effectiveness of verteporfin therapy.

At the time of conducting this research the best researched treatment for neovascular AMD was PDT. PDT montherapy was shown to slow progressive vision loss in patients with subfoveal and relatively small lesion types. But the therapy was shown to offer only a modest treatment benefit and improvement in visual function was not achieved.

2.8 OTHER TREATMENTS

2.8.1 Laser Photocoagulation

The Macular Photocoagulation Study (MPS) was the first prospective, randomised, multicentre clinical trial that looked at the treatment of exudative AMD. Three sets of randomised, controlled clinical trials were set up to evaluate laser treatment of symptomatic CNV: the Argon Macular Photocoagulation Study (1979–1988)

studied extrafoveal CNV; the Krypton Macular Photocoagulation Study (1982–1991) for juxtafoveal CNV; and the Foveal Photocoagulation Study (1986–1994) for subfoveal (new or recurrent) CNV.

The MPS Group showed that laser photocoagulation reduced the risk of severe vision loss (≥6 lines of visual acuity loss) caused by neovascular AMD in eyes with extrafoveal or juxtafoveal CNV compared with observation.[127] Laser photocoagulation was recommended only for new, small (<3 MPS disc areas), or recurrent (≤6 MPS disc areas) subfoveal lesions with well-demarcated boundaries and evidence of classic CNV, or for symptomatic extrafoveal or juxtafoveal lesions with well-demarcated boundaries.[128] Only a small proportion of patients with neovascular AMD are eligible for laser treatment because most lesions have poorly demarcated boundaries, are too large, or have no classic CNV involving the fovea on presentation. Many patients with subfoveal CNV experience an immediate and irreversible loss of vision because of thermal damage to the overlying retinal tissue, especially when presenting with a visual acuity better than 20/200.[129] In addition there is a high (≥50% within 2 years) chance that CNV will persist or recur to the foveal centre following laser photocoagulation to a nonsubfoveal lesion.

2.8.2 Radiotherapy

Both plaque and external beam irradiation have been used in the treatment of CNV. Low dose radiation selectively inhibits proliferating vascular endothelium in experimental studies. In contrast, mature retinal vessels demonstrate a much lower level of mitotic activity and are therefore relatively radioresistant up to 25 Gy. In 1993, Charkravarthy et al reported a case series of 19 patients with subfoveal AMD-related CNV treated with external beam radiation. Patients received 10 or 15 Gy in 5 divided doses. At 1 year, angiography revealed regression of CNV in 77% of

treated eyes compared with progressive enlargement of CNV in all 7 control eyes. Visual acuity was maintained or improved in 63% of treated versus 14% of control eyes.[130] One of the largest studies to date, the Radiation Therapy for Age-related Macular Degeneration (RAD) study, enrolled 205 patients in a prospective trial of 16 Gy versus sham treatment of AMD-related CNV of <6 MPS disc areas. No treatment benefit as measured by change in visual acuity was found at 1 year.[131] A multicentre, prospective, randomised clinical trial Age-related Macular Degeneration Radiation Trial (AMDRT) sponsored by the National Eye Institute evaluated the use of 20 Gy external beam radiation in treatment of classic, mixed, and occult subfoveal that were not eligible for laser photocoagulation by MPS guidelines.[132] Among AMDRT patients, there was a trend toward a modest and short-lived beneficial effect of radiotherapy compared to observation. At six months follow-up, 26% of radiated and 50% of eyes not radiated demonstrated a loss of ≥3 visual acuity lines ($p = 0.04$). However, this early beneficial trend faded by 12 months follow-up, as 43% of radiated and 50% of observed eyes demonstrated loss of ≥3 visual acuity lines ($p = 0.61$). Radiotherapy was associated with smaller lesion size and far less fibrosis and scarring.

2.8.3 Transpupillary Thermotherapy (TTT)

TTT involves the use of a long-pulse, 810 nm near infrared diode laser irradiation and relatively large spot size, low irradiance, and long exposure times with an infrared laser to deliver hyperthermia to the choroid and retinal pigment epithelium, theoretically causing a targeted choroidal neovascular lesion to involute.[133] The potential benefit of TTT for the treatment of subfoveal CNV has been suggested by preliminary, retrospective, open-label, uncontrolled, noncomparative case studies. Newsom et al treated 44 eyes (12 predominantly classic CNV; 32 predominantly

occult CNV) with TTT. 77% of the membranes were closed at 6 months and only 7.1% developed recurrence.[134] Reichel et al found that 75% of eyes in a study of occult CNV treated with TTT had stabilisation of vision and resolution of the membrane at 13 months. [135]

The TTT4CNV Clinical Trial was a multi-centre, prospective, double-masked, placebo controlled clinical trial conducted at 22 centres in the United States. The trial was designed to look at eyes with wet AMD and randomised eyes with small (less than or equal to 3 mm diameter) subfoveal occult membranes and symptomatic vision (ETDRS visual acuity between 20/50 and 20/400). An intent-to-treat evaluation of the primary visual outcome data in 303 enrolled patients showed that TTT, as applied in this trial, did not result in a significant vision benefit.[136] The results showed that in a subgroup of patients with baseline visual acuity of 20/100 or worse, 22% of treated eyes improved vision by one or more lines compared with none of the eyes in the untreated control group. At 18 months, there was a 2 line benefit in preserving vision in this subgroup. Specifically, TTT treated eyes on average lost 2 lines of visual acuity while control eyes lost 4 lines. Caution has to be exercised when interpreting these data because most of the patients included had very poor visual acuity at baseline. This could increase the probability of stable vision even in the absence of treatment in these patients. In practice, TTT had the advantage of being inexpensive and one of the few treatments available for occult CNV. But, it is not without complications, with significant post-treatment haemorrhage, RPE tears, progression of occult to classic membranes and macular infarction having been reported.

2.8.4 Anti-angiogenic Therapy

Expression of vascular endothelial growth factor (VEGF) and VEGF receptors have been demonstrated histopathologically in choroidal neovascular lesions that have been excised from surgical patients and also from autopsy eyes. Since the completion of this research, a number of anti-angiogenic treatment options have become available for neovascular AMD. Therapies aimed at the angiogenic processes underlying CNV possess the unique advantage of addressing the most destructive feature of AMD. At present the available treatments include steroids and anti-VEGF agents.

Intravitreal Triamcinolone

Steroids are potent anti-inflammatory agents. Several papers have reported increases in visual acuity or decreased rates of severe visual loss in patients with AMD-related CNV after intravitreal triamcinolone injection. [137, 138,139] However, a large, randomised clinical trial of a single intravitreal triamcinolone injection as treatment of neovascular AMD documented no difference in severe visual loss (loss of ≥30 ETDRS letters) between treated and placebo groups at 12 months.[140] The adverse effects associated with intravitreal steroids may also limit their use in some patients. Gillies et al reported significantly higher rates of cataract and increased intraocular pressure (IOP) necessitating topical glaucoma therapy in patients treated with intravitreal triamcinolone versus placebo groups (24% vs. 0% and 28% vs. 1.3%, respectively). Several studies have documented both infectious and noninfectious cases of endophthalmitis after triamcinolone injection as well.

Anecortave acetate

Anecortave acetate is a steroid derivative with little to no glucocorticoid or mineralocorticoid effect. It inhibits proliferation and migration of vascular endothelial cells through its effects on the proteolytic cascade of angiogenesis. It is administered through a juxtascleral subtenon's depot injection. Drug efficacy from a single injection lasts 6 months. The Anecortave Acetate Clinical Study is an ongoing, multicentre, double-masked, controlled trial that randomises patients to one of 3 levels (3 mg, 15 mg, 30 mg) of drug dosage or to placebo given up to every 6 months at the discretion of an investigator. Surprisingly, at both 6 months and 1 year, a non-traditional dose response curve was found with the 15 mg dose being the most efficacious. At 6 months, treatment with anecortave acetate was statistically superior to placebo when evaluating mean change from baseline vision. The drug showed a significant effect in improving vision by 2 or more logMAR lines and inhibiting lesion growth on FA. It was also significantly better at preserving vision in the subgroup of patients with predominantly classic lesions.[141] One year results were compromised by poor patient follow up (41% of patients dropped out of the study between 6 and 12 months), but showed benefit from anecortave acetate (15 mg) compared with placebo for 3 outcomes: mean change from baseline vision, stabilisation of vision (<3 logMAR lines of vision loss), and prevention of severe vision loss (≤6 logMAR lines of vision loss). The subgroup of predominantly classic lesions showed the same statistically significant benefits from treatment with anecortave acetate. Despite a problem with patient follow up after 6 months, the early anecortave acetate study results suggest that further investigation of this agent is warranted. There are two additional, ongoing clinical trials of anecortave acetate. One pivotal phase III study will compare depot

administration of anecortave acetate versus verteporfin PDT in patients with predominantly classic CNV. The results of another clinical study, the Anecortave Acetate Risk Reduction Trial (AART), are also awaited to evaluate anecortave acetate versus placebo in reducing the risk of disease progression from dry to wet AMD in patients who have fellow eyes with CNV.[142]

Intravitreal pegaptanib sodium

Pegaptanib is a synthetic oligonucleotide that binds to the pathological isoform of VEGF, VEGF165, in the extracellular space.[143] The molecule is then prevented from interacting with the VEGF receptor, which in turn neutralises this effect. Pegaptanib was approved by the FDA on December 17, 2004, for treatment of all neovascular AMD. This approval was based on a phase 3 trial, VEGF inhibition study in ocular neovascularisation, or the VISION trial. 70% of patients treated with pegaptanib sodium injection (0.3 mg, n=294) lost fewer than 15 letters of BCVA, compared with 55% in the control group (n=296) ($P<0.001$). 10% of patients treated with pegaptanib sodium (0.3 mg, n=294) had a severe visual acuity loss (30 letters or more), compared to 22% in the control group (n=296) ($P<0.003$). The beneficial effect was seen for all types of neovascularisation.

It is similar to PDT in its ability to reduce the risk of severe vision loss. Visual improvement is limited although it may work better for early detected lesions that are smaller in size. Even so it has been largely supplanted by ranibizumab and bevacizumab when an injection of an anti-VEGF agent is planned.

Ranibizumab

Ranibizumab (Lucentis; Genentech Inc, South San Francisco, California, USA) is a fragmented antibody engineered to bind all active forms of VEGF-A. The Minimally Classic/Occult Trial of the Anti-VEGF Antibody Ranibizumab in the

Treatment of Neovascular AMD (MARINA) study demonstrated the safety of monthly injections over 12 months. [144] The vision improved or stabilised in 95% of ranibizumab-treated patients compared with 62% of sham-treated patients. Nearly one quarter of eyes treated with 0.3mg of the drug and a third of eyes treated with 0.5mg improved their vision (defined as a gain of 15 or more letters) compared with 5.0% of eyes receiving a sham injection. The mean acuity in the sham injection group decreased by 10 letters. The mean increase in BCVA for the treatment groups was over 6 letters and this benefit was sustained at 24 months.

In the Anti-VEGF Antibody for the Treatment of Predominantly Classic Choroidal Neovascularisation in AMD (ANCHOR) study ranibizumab was compared directly to PDT in the treatment of subfoveal, predominantly classic CNV secondary to AMD. [145] Ranibizumab treated patients again were more likely to improve or at least stabilize their vision (94% in those treated with the 0.3mg dose, and 96% in those with the 0.5 mg dose) compared with PDT treated patients (64%) during the first year of this study. The mean acuity improved from baseline in patients treated with ranibizumab, but declined in patients treated with PDT. This was the first treatment proven beneficial over PDT for neovascular AMD. It was also the first treatment producing a meaningful gain in visual acuity in AMD

patients. Ranibizumab has a relatively safe side-effect profile although five patients (1.0%) in the MARINA trial developed endophthalmitis.[146]

The PIER study was designed to study the effects of lengthening the interval between injections of ranibizumab. The PIER study included 182 patients with all lesion subtypes. The aim of this study was to evaluate the efficacy and safety of ranibizumab initially administered monthly for three injections followed by a fixed regimen of maintenance injections at three month intervals. Overall, patients treated

with ranibizumab remained stable at baseline visual acuity for 12 months, while sham-treated patients lost a mean of three lines suggesting that 3 monthly injections were successful. However, analysis of the proportion of gainers over time demonstrated that only 40% of eyes achieved an initial and permanent benefit. For the majority of eyes, the fixed quarterly regimen was not sufficient and recurrence was not treated adequately. This observation clearly highlights the importance of an individualised re-treatment regimen based on an individualised diagnostic monitoring.[147]

The Prospective Optical Coherence Tomography Imaging of Patients with Neovascular Age-related Macular Degeneration Treated with Intra-Ocular Lucentis (PrONTO) study was designed to determine whether retreatment decisions can be made on the basis of criteria involving OCT.[148] Forty patients were enrolled. The improvements in VA and OCT measurements observed by month 3 were maintained through month 7 using an OCT-guided variable dosing regimen. These visual acuity results are very similar to the results observed in the Phase III trials at 7 months. By month 3, 1 month after the last scheduled injection, the mean central thickness measurement decreased by 190 microns ($p<0.001$). By month 7, 5 months after the last scheduled injection, the average number of retreatments per eye was 0.2 with 50% of eyes receiving no additional treatment.

Ranibizumab therapy is the first treatment for neovascular AMD to claiming to improve vision for most patients. The benefits were found to apply to all angiographic subtypes of neovascular AMD and across all lesion sizes. Although the pivotal phase III trials (MARINA and ANCHOR) used monthly injections of ranibizumab for 2 years, the ongoing PIER and PrONTO suggest that less frequent dosing regimens may be effective.

Bevacizumab

Bevacizumab is a full length recombinant, humanized antibody of a molecular weight of 149-kDa binding to all VEGF isoforms. Like ranibizumab, the drug reduces angiogenesis and vascular permeability rapidly following intravitreal administration. The drug was originally developed to target pathological angiogenesis in tumours and was approved by the FDA for the treatment of metastatic colorectal cancer.

Bevacizumab appears to have a beneficial effect in the off label treatment of intraocular neovascularisation at least based on retrospective, non-comparative case series. As prospective randomised studies are missing, no solid proof of the level of efficacy is available. Dosage, re-treatment intervals and durability of the treatment as well as the systemic safety are unknown factors. Lower costs and the general availability are the major arguments to consider an off label use of bevacizumab.

2.8.5 Combination of anti-VEGF therapy with PDT

Intravitreal anti-VEGF therapy appears to be an efficient approach to achieve elimination of extravasated fluid in neovascular AMD with resolution of retinal oedema and vision recovery in at least 25% of cases. However, for optimal results the treatment may need to be continued on a monthly regimen during years of follow-up and the patient needs long-term clinical monitoring. On the other hand, PDT offers an effective modality to directly target CNV with a permanent effect once the lesion becomes atrophic. Re-treatments with PDT monotherapy appear to be the consequence of an increased expression of VEGF and inflammatory mediators. Combining an anti-VEGF approach with PDT may have a synergistic long-term effect potentially reducing the frequency of re-treatments.

The PROTECT trial, a prospective, open-label phase I/ II study, examined the safety of same day administration of standard PDT and an intravitreal injection of ranibizumab.[149] The initial treatment was followed by three subsequent monthly injections of ranibizumab. After 4 months 92% of eyes had stable vision, improved by a mean of 7 letters was found in the overall population and 25% of patients improved by more than three lines. Angiography revealed a complete absence of leakage from CNV in most patients for as long as 9 months of follow-up.

2.8.6 Future treatments

Recent advances in understanding the pathogenesis of AMD have led to the quest for more effective strategies and agents interacting with various steps in the angiogenic cascade. Some of these are under clinical or pre-clinical evaluation and include the following.

VEGF-Trap

VEGF-Trap (Regeneron, Tarrytown, New York, USA) is an anti-VEGF agent and functions as a receptor decoy to bind and disable VEGF. Preclinical studies have demonstrated its ability to prevent angiogenesis as well as tumorigenesis. The Clinical Evaluation of Antiangiogenesis in the Retina (CLEAR) AMD-1 study demonstrated VEGF Trap's ability to decrease retinal thickness in neovascular AMD patients. When administered intravenously, however, it is associated with an increase in blood pressure. The development of VEGF-Trap for intravitreal application is currently ongoing. In a phase I/II trial with increasing dosing from 0.05 to 4 mg, VEGF-Trap was well tolerated with no ocular or systemic side effects. Stabilisation or improvement in vision was found in 95% of patients lasting over the 6 week observation period and VA improved by a mean of 4.8 letters at 6 weeks. A phase II study is currently recruiting patients.

RNA interference

RNA interference is a method of inhibiting the intracellular production of proteins, such as VEGF and VEGF-R, by silencing the gene coding for that specific protein. This is mediated by a double stranded RNA homologous to the targeted protein. Clinical phase I and II studies evaluating small interfering RNA (siRNA) have already been performed. Bevasiranib, a siRNA targeted against VEGF production, was tested intravitreally in concentrations ranging from 0.1 to 3.0 mg. No local or systemic serious adverse events were found. However, there was evidence of continuing deterioration during the first 3 weeks of treatment with subsequent stabilisation of the disease from week 3–15. This may be because siRNA has no effect on VEGF that has already been produced, it may well be a promising treatment strategy for consequent and long lasting blockade of VEGF. Further studies will have to proof the efficacy of this concept. ALN-VEG01 (Alnylam, Cambridge, Massachusetts, USA) is another agent targeting RNA coding of VEGF.

Receptor tyrosine kinase inhibitor

The receptor tyrosine kinase inhibitor (RTPi) class of compounds consists of small, organic molecules that are competitive inhibitors of ATP for a subset of receptor tyrosine kinases (RTPs), including all VEGF receptors (VEGFR1, VEGFR2 and VEGFR3) as well as closely related tyrosine kinase receptors, e.g. platelet derived growth factor (PDGF) receptors, which also contribute to angiogenesis in the eye. Furthermore, these compounds block receptor activation by various other receptor agonists, not only VEGF-A. The small molecular weight of these compounds may enhance their inter- and intracellular distribution and offers the potential for formulations increasing their intravitreal half life time. AG-013958 (Pfizer, San

Diego, California, USA) is currently being evaluated in subfoveal CNV due to AMD.

Squalamine

Squalamine lactate is a small molecule isolated from the cartilage of dogfish shark, Squalus acanthus, a species known for its resistance to bacterial and viral infections. The molecule belongs to a class of compounds called aminosterols, a steroid chemically linked to an amino acid. Squalamine can block various angiogenic cytokines such as VEGF, as well as the expression of integrin and cytoskeleton by chaperoning calmodulin. The principle efficacy of squalamine in inhibiting angiogenesis has been shown in various animal models such as laser induced CNV in the rat and oxygen induced retinopathy in the mouse.

A phase II study evaluated the effect of squalamine in combination with PDT treatment in 46 patients. Squalamine was administered in doses of 10, 20 or 40 mg intravenously at weeks one, two, four and five and were treated with PDT at week three. The control group was treated with PDT at week three, but received a sham injection. Vision stabilised in both groups and no drug related serious adverse event occurred. A phase III clinical study is currently enrolling patients.[150]

Gene Therapy

Angiogenesis is a multifactorial process with multiple actors and counteractors. Several cytokines, such as pigment epithelium derived growth factor (PEDF), endostatin and angiostatin, are known to act as anti-angiogenic agents. LentiVector, a gene delivery system, was used to introduce the angiostatic genes of endostatin and angiostatin, only being turned on under hypoxic conditions, into the retinal pigment epithelium of mice. The size of the resulting CNV in treated as compared

to untreated eyes was reduced by 60% for endostatin and 50% for angiostatin. Gene therapy is still in experimental stages, but holds promise to improve treatment outcomes in the future.[150]

These rapidly growing number of therapeutic options and hypotheses will have to be proven in randomised controlled clinical trials, a growing challenge in respect to the evolving field of knowledge about the pathogenic background of AMD.

2.9 CONCLUSION

Epidemiologic data shows that AMD is the leading cause for substantial and irreversible vision loss among the populations of the industrialised nations. Although neovascular AMD only accounts for about 10–20% of the overall AMD incidence, this subtype is responsible for 90% of cases of severe vision loss. Due to the increasing age of these population, this number is expected to double by the year of 2020.

Despite extensive past and ongoing research in AMD, there is currently no universally accepted classification of AMD in the literature. The problem is further compounded by differences in methodology used in the various epidemiological studies, making comparisons between them difficult. As future studies provide further insight into the pathogenesis of the disease and new imaging techniques permit more accurate and quantitative analysis of the retina and subretinal deposits, there will be a need to incorporate new subcategories or change the classification. In this thesis, I have adopted the AREDS classification system. All patients had neovascular AMD and therefore fall within the classification of advanced AMD (AREDS category 4).

The pathogenesis of neovascular AMD is poorly understood with several possible mechanisms of causation. The RPE is thought to orchestrate the initiation, stabilisation and involution of CNV. Presence of functioning RPE may be important in the maintenance of the photoreceptor cell layer, especially in the setting of disciform degeneration. Increased cross-sectional thickness of the involuted CNV's subretinal component is correlated with greater loss of photoreceptors. This suggests that therapies that aim to restrict the dimensions of the CNV may help by reducing the distance between the RPE and the photoreceptor layer, thus helping it to maintain its nutrition.

At the time of conducting the research presented in this thesis, PDT was the best available approved treatment for neovascular AMD (especially classic/ no occult and predominantly classic CNV). Unfortunately, it was shown to benefit only a modest subgroup of patients and there were several arguments for the subgroup effect being a chance finding.

Existing practices based on MPS and TAP studies, rely on FA for the classification of CNV and to monitor the response to treatment. Though fluorescein is well tolerated by most patients, angiography is an invasive procedure, cannot penetrate RPE or blood and is reliant on the expertise of the technician and specialist for reliable interpretation.

OCT on the other hand is a non-invasive technique that offers high resolution cross-sectional images of anatomical features with 3-dimensional capabilities. Limited work has been done using this technique in the field of neovascular AMD. Studies so far have been descriptive (Hee et al, 1996; Rogers et al, 2002) in poorly described groups and experiments, and were not backed by statistical data.

Chapter 3

PATIENTS AND METHODS

In this chapter I present the backdrop against which the investigations presented in this research were commenced. I describe the patient characteristics for inclusion into the study, the protocol for optical coherence tomography (OCT) scanning developed for this study and the treatment protocol for patients with subfoveal predominantly classic choroidal neovascularisation (CNV) secondary to age-related macular degeneration (AMD).

3.1 BACKGROUND

My work commenced in June 2002 when, based on the Treatment of Age-Related Macular Degeneration with Photodynamic Therapy (TAP) study,[21, 22] photodynamic therapy (PDT) was being introduced into the UK as a novel treatment for classic and predominantly classic CNV secondary to AMD. At the time, there was very little evidence of the effect of PDT on the morphology and function of the macula. Fluorescein angiography (FA) and argon laser photocoagulation, with their associated limitations, were the mainstay of diagnosis and management. A commercial OCT (Stratus OCT3) had just been made available for clinical use. While there were a few anecdotal and descriptive papers on its usefulness in macular diseases, there was no literature of its application in macular degeneration. It was thought that the Stratus OCT3, with its ability to take high resolution cross-sectional images of the retina, could measure retinal and CNV thickness and identify and quantitatively assess intra retinal oedema and subretinal fluid more

effectively than biomicroscopy or angiography and the response to PDT could be objectively monitored.

Treatment for wet AMD is provided by centres that are part of a national research study. The medical retina unit at St Paul's is the tertiary referral centre for patients from the North West with wet AMD and there was an established NHS service already in existence.

The research presented in this thesis was undertaken in the Clinical Eye Research Centre (CERC) of St Paul's Eye Unit. The CERC is a dedicated area within the Royal Liverpool University Hospital, purpose built to allow clinical research. It houses all the instrumentation required for advanced macular imaging.

3.2 DEFINITIONS

Anatomy: In this thesis the macula is defined as the area within the temporal vascular arcades and the fovea as the central retinal depression, 1.5 mm in diameter and within the foveal avascular zone. The foveal centre, foveola, was defined as the maximum depression within the depression of the fovea, the diameter of which was 500μm.[151]

Location: The location of the CNV is defined in relation to the proximity of the lesions nearest edge to the geometric centre of the foveal avascular zone (FAZ). Extrafoveal CNV is defined as a lesion situated at least 200μm from the FAZ; juxtafoveal CNV's occur between 1μm and 199μm from the fovea and subfoveal CNV is located directly beneath the geometric centre of the FAZ.

Classic CNV is defined as an area of choroidal hyperfluorescence with well-demarcated boundaries visible in the early transit phase of the angiogram and continues to leak during the mid and late phase with progressive increase in

hyperfluorescence. In the later phases, pooling of the dye occurs in the overlying subretinal space and usually obscures the boundaries of the CNV.

Predominantly classic CNV if the area of classic is greater than or equal to 50% of the area of the entire lesion

TAP criteria: Based on the TAP study, eyes with classic only or predominantly classic CNV secondary to AMD, < 199 microns from the foveal centre with vision equal to or better than 6/60 and greatest linear dimension (GLD) of the entire lesion on the retina of 5400 μm or less at presentation were eligible to receive PDT at baseline.

Retreatment criteria: At Liverpool the patients underwent retreatment if there was persistent sub retinal fluid (SRF) under the foveal centre, drop in vision (< 20 letters), extension of CNV, leakage on FA or a new haemorrhage. Patients did not receive PDT if the SRF had cleared or if there was >20 letters of BCVA lost.[125]

3.3 PATIENTS

All patients with AMD attending CERC for PDT as part of an established NHS service were included in this research. Those with a classic or predominantly classic subfoveal CNV and eligible for PDT as per TAP criteria formed the core of this thesis. The study was conducted between June 2002 and June 2004.

3.4 METHODS

Patients attending CERC with neovascular AMD were identified in the admissions area from their referral letters and notes. The majority of patients had had FA at the referral centre, helping to identify those with subfoveal predominantly classic CNV.

Information regarding the study was provided and consent for ophthalmoscopy and ocular investigations (FA, OCT) was obtained. Ethical approval for the research of new imaging techniques in AMD was obtained from the Liverpool Research Ethics Committee (LREC ref 02/051). None of the research investigations interfered with the clinical care of the patient, which took precedence at all times. No changes were made to the established treatment plan with PDT and patients continued to receive treatment within this programme as per the TAP protocol.

The patient course for the clinical examinations and procedures performed during the study was as follows:

- Refraction protocol best corrected visual acuity (BCVA)
- Optical coherence tomography (OCT)
- Fluorescein angiography (FA)
- Slit lamp biomicroscopy and fundus examination
- Photodynamic therapy (PDT)

3.4.1 Visual acuity protocol

The best corrected visual acuity (BCVA) of patients was measured based on a retroilluminated Lighthouse for the Blind (New York, NY) distance visual acuity test chart (using modified Early Treatment Diabetic Retinopathy Study charts 1, 2, and R). Charts 1 and 2 are used for testing the right and left eye, respectively, chart R is used for refraction. The features of the chart are 14 lines of letters to be read at a distance of 2 meters and 3 lines of letters to be read at a distance of 1 meter for patients with reduced vision. The distance VA charts have 5 letters per line and a doubling of the minimum angle of resolution every 3 lines.

At the baseline examination, a TAP certified VA examiner refracted both eyes and measured distance BCVA according to a protocol designed to encourage the patient to achieve the best identification of each letter. BCVA acuity was scored based on the total number of correct letters identified at 2 m plus 15. If the patient read fewer than 20 letters at 2 m, the patient was tested on the top 3 lines at 1 m and the score was the total number of letters read at 2 m plus the total number of letters read at 1 m. For each of the 2 vision tests, the 2 eyes of a patient were tested using different charts.

3.4.2 Optical coherence tomography protocol

The commercially available Stratus OCT, Model 3000 (OCT3) manufactured by Carl Zeiss Meditec, Dublin, California was used for the research presented in this thesis (Figure 3.1).

Scan acquisition

Pupils were dilated with 2.5% phenylephrine eye drops and 1% tropicamide eye drops. It was ensured that the patient was sitting comfortably with his/her chin on the chin rest, forehead against the band and teeth clenched. Prior to beginning the protocol scan sequence the polarisation setting was optimised by rotating the corresponding dial on the control panel while observing the scans on the computer monitor. The goal was to try to standardise the scans by compensating for individual variations in the birefringent properties of the eye. The endpoint was when the image appeared the brightest. All scans were performed by a single examiner (JS) (Figure 3.2).

The following line scans were acquired

- 5 mm horizontal line at 0° centred on the fovea (the default pattern).

Figure 3.1: The Stratus Optical Coherence Tomographer, Model 3000 (OCT3) manufactured by Carl Zeiss Meditec, Dublin, California.

Figure 3.2: Performing optical coherence tomography scan of a patient.

- 5 X 5mm Raster lines centred on the fovea
- 6mm radial scans positioned on fovea
- Fast macular thickness map at the fovea

For patients with impaired fixation the scans were positioned manually on the anatomical fovea as viewed on the black and white video image. The scans were analysed immediately after acquisition to ensure that signal strength was greater than 7; if less than 7, the scan was repeated. If good quality scans were not possible, the reason- e.g. media opacity or poor fixation, was entered on the data chart.

Analysis

First terminology to analyse the scans was designed, then validated (Chapter 4). Each scan was analysed quantitatively and qualitatively (Appendix 1). Measurements on the line scans were performed by the manual positioning of callipers and using the retinal thickness (single eye) analysis protocol offered by OCT3. The callipers were placed in a vertical line at the centre of the fovea on the retinal thickness algorithm.

3.4.3 Colour fundus and fluorescein angiography

Stereoscopic colour photographs of the macula and disc of each eye and a stereoscopic FA with photographs of the macula of the study eye were performed at each visit as part of the standard management. 5cc of 10% fluorescein was used. The photographs acquired for the study were red-free, stereoscopic black and white fundus photographs, rapid sequence photographs of the macula taken during fluorescein dye transit, including stereoscopic pairs of the macula taken approximately 30, 40, 60, 90, 120, and 180 seconds after dye injection and late

phase stereoscopic pair of the macula taken 5 and 10 minutes after dye injection; and stereoscopic colour fundus photographs of the macula.

The table below describes the standardised method for classifying CNV used in this study.[152]

Identify morphological features	Assess total lesion size	Categorise lesion subtype
1. CNV lesion components Fluorescein leakage associated with CNV Classic CNV Occult CNV: fibrovascular PED, late leakage of undetermined origin Features contiguous with CNV and constitute part of the lesion Blood Elevated blocked fluorescence (EBF)- may be due to RPE hyperplasia, thick exudates, fibrous tissue Serous PED	1. Define boundaries of lesion 2. Define boundaries of the areas of classic leakage 3. Estimate proportion of classic relative to total lesion size 4. Ineligible for PDT if less than 50% of lesion is classic	1. Classic with no occult (NICE FAD 1.1) 1A. Classic leakage = 100% of lesion 1B. Classic leakage = 50-90% but lesion has no occult component 2. Predominantly classic with occult (NICE FAD 1.2) Classic leakage = 50-99% of lesion with some occult 3. Minimally classic Classic leakage< 50% lesion 4. Occult with no classic 0% classic. 100% occult.
2. Features associated with CNV not used to define the boundaries of the lesion Atrophy: Geographic atrophy and non GA Flat blocked fluorescence Fibrosis not contiguous to CNV boundary Thick exudates not contiguous to CNV		
3. Other features Retinal angiomatous proliferation Chorio-retinal anastomoses Idiopathic polypoidal choroidopathy		

3.4.4 Slit-lamp biomicroscopy

A complete ophthalmological examination was performed at each visit. This included both anterior and posterior segment examination. The presence of media opacity was recorded.

A dilated detailed fundus examination was performed with a 60 dioptre Volk lens and the following data was collected:

- subretinal fluid (SRF)
- cystoid macular oedema (CMO)
- fibrosis
- haemorrhage
- pigment epithelial detachment (PED)

3.4.5 Photodynamic therapy

Patients with active subfoveal predominantly classic CNV were treated with Verteporfin photodynamic therapy (PDT) according to the standard TAP protocol. A diode laser at 689 nm with a slit lamp delivery system (Coherent Inc, Palo Alto, Calif, or Zeiss Jena GmbH, Jena, Germany) designed to deliver 50 J/cm^2 at an intensity of 600 mW/cm^{2}over 83 seconds was used. Since the light application causes no visible changes on biomicroscopic examination during treatment, the power output of the laser at the slit lamp was confirmed and calibrated prior to each treatment session for the day by using a handheld power meter (Laser Check; Coherent Inc). The treatment spot size was determined after measuring the greatest linear dimension (GLD) of the entire CNV lesion using a software function on the Visupac viewer and placed on the digital FA. An additional 1000 μm was added to the GLD to provide a 500 μm margin of additional treatment around the lesion. This increased the chance that the lesion would be treated in its entirety and would compensate for any slight movements of the study eye during light application. Verteporfin (6 mg per square meter of body surface area) after calculating the body surface area from a nomogram based on the height and weight of the patient on the

day of treatment was infused through intravenous access over a 10 minute period. Fifteen minutes after the start of the infusion, the laser light was applied for 83 seconds to the CNV lesion through a fundus contact lens of known magnification to result in a light exposure of 50 J/cm^2. Patients were instructed to avoid direct sunlight as much as possible and, while outdoors, to wear glasses with a low (4%) transmittance of visible light for 48 hours after treatment.

3.4.6 Patient follow-up

All patients were scheduled to return approximately 3 months after each treatment (within 2 weeks before or after that date). The patients in the longitudinal arm of the study were examined at baseline, 3, 6, 9 and 12 months following treatment. At each regularly scheduled follow-up visit, a protocol refraction, BCVA measurement, OCT, ophthalmoscopic examination, stereoscopic colour fundus photography and fluorescein angiography were performed in both eyes before retreatment. Retreatment was considered if there was no serious adverse event judged to be associated with any previous photodynamic therapy. Retreatment with verteporfin was administered to the patient if the treating ophthalmologist noted any leakage from any CNV (classic or occult) on a fluorescein angiogram.

3.4.7 Data documentation and analysis

Data was entered on an Excel spreadsheet. Statistical analysis of the data was performed using SPSS for windows Version 11 (SPSS Inc, Chicago, IL, USA). Patient details were kept confidential in accordance with the data protection act 1998 and the Research Governance Framework for Health and Social Care (March 2001) and each patient was given his or her own unique code during the period of the study.

3.5 SUMMARY

This thesis is based on observational studies conducted between June 2002 and June 2004 to assess the value of the new imaging technique, OCT, in the management of patients with neovascular AMD. Patients were drawn from an aging population and underwent treatment for neovascular AMD based on best clinical evidence at the time. To address the research questions, the project was divided into four observational studies. Findings were related to clinical parameters and outcome. There were minor differences in the research design between the studies and these will be discussed in the following chapters where the results and discussions of each study will be presented.

Chapter 4

INTEROBSERVER CONCORDANCE IN GRADING OCT SCANS

4.1 INTRODUCTION

When this research started in 2002, the latest commercially available model of the OCT, Stratus OCT, Model 3000 (OCT3) (manufactured by Carl Zeiss Meditec, Dublin, California) had only just become available. While there were reports of its use for retinal imaging, no standardised terminology for the assessment of the scans had been introduced and there was no evidence of the concordance amongst independent readers in evaluating the scans for morphology and measurements.

Instruments developed for new quantifiable measurements must be shown to be reliable before they can be applied in a clinical or research setting. Reliability means that the measurements that the instrument records are reproducible at different time intervals (test–retest reliability) and that those observers making the measurements produce repeatable results, both for the same observer over a period of time (intraobserver reliability) and between different observers on the same subject (interobserver reliability).

In order to successfully implement OCT scanning in the clinical environment, new terminology was defined and a protocol for interpreting OCT images was developed.

4.2 AIM

This study aimed to validate the protocol used for the research in eyes with neovascular AMD undergoing photodynamic therapy (PDT) at the Clinical Eye Research Centre (CERC), St Paul's Eye Hospital. In order to do this we prospectively determined the level of agreement between 3 independent observers.

4.3 PATIENTS AND METHODS

Consecutive patients with neovascular AMD undergoing PDT at the CERC, St Paul's Eye Hospital were prospectively recruited into this study from June 2002 to August 2002.

The following line scans were acquired (see page 102 for detailed description)

- 5 mm horizontal line at 0° centred on the fovea (the default pattern).
- 6mm, 6 radial scans in fast macular thickness (FMT) mode at the fovea

The scans acquired were divided into two groups and analysed by 3 observers. Observer 1 (myself) and observer 2 (P Stanga) analysed group 1 and observer 1 (JS) and observer 3 (S Harding) analysed group 2. Data was recorded on an Excel spreadsheet. The data to be included for this study had been previously agreed upon and was developed by expert consensus between the 3 observers. Observers first independently recorded if the scans were readable. If readable, each 6mm FMT scan and the 5mm default line scan at 0° was assessed for the presence or absence of intra-retinal fluid (IRF), sub-retinal fluid (SRF), posterior vitreous detachment (PVD) and vitreo-macular hyaloid attachment (VMHA). The neuro-retinal foveal thickness (NFT), bilaminar foveal thickness (BFT) and outer high reflectivity band thickness (OHRBT) measurements on the OCT scans were done at the fovea by

manual positioning of the callipers using the retinal thickness (single eye) quantitative analysis protocol offered by Stratus OCT3 on the 5mm line scan.

Terminology used to interpret and measure the scans are defined in Table 4.1 and shown in Figures 4.1, 4.2 and 4.3.

Table 4.1: Terms and definitions used for interpreting optical coherence tomography scans in this thesis.

Term	Definition
Neuroretinal foveal thickness (NFT)	Distance between the inner high reflectivity band and the inner margin of the outer lamina of the outer high reflectivity band at the foveal centre
Bilaminar foveal thickness (BFT)	Distance between the inner high reflectivity band and the inner margin of the outer lamina of the outer high reflectivity band at the foveal centre in the presence of subretinal hyporeflective space at the fovea (NFT=BFT in the absence of SRF)
Outer high reflectivity band thickness (OHRBT)	Distance between the inner margin of the outer lamina of the outer high reflectivity band and the outer margin of the outer high reflectivity band at the fovea
Vitreo-macular hyaloid attachment (VMHA)	Incomplete separation of the posterior hyaloid with attachment at the macula in the OCT scan
Posterior vitreous detachment (PVD)	Complete separation of the posterior hyaloid from the macula in the OCT scan
Intra-retinal fluid (IRF)	Well-defined intraretinal hyporeflective spaces separated by reflective septae
Sub-retinal fluid (SRF)	Separation of the neuroretina from the outer high reflectivity band by a well defined hyporeflective space

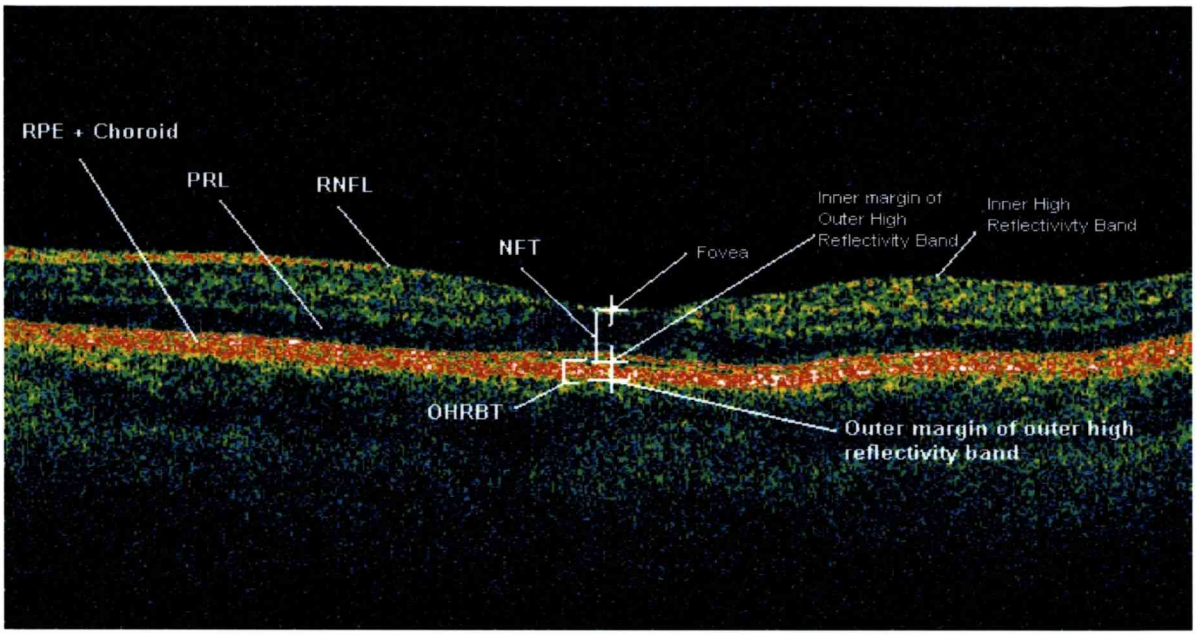

Figure 4.1: Optical coherence tomogram passing through the fovea of a normal eye illustrating retinal layers and terminology developed for the study. RNFL, retinal nerve fibre layer; PRL, photoreceptor layer; RPE, retinal pigment epithelium; NFT, neuroretinal foveal thickness (distance between inner high reflectivity band and inner margin of outer high reflectivity band at foveal centre); OHRBT, outer high reflectivity band thickness; NFT = 181 μm and OHRBT = 58μm in this scan.

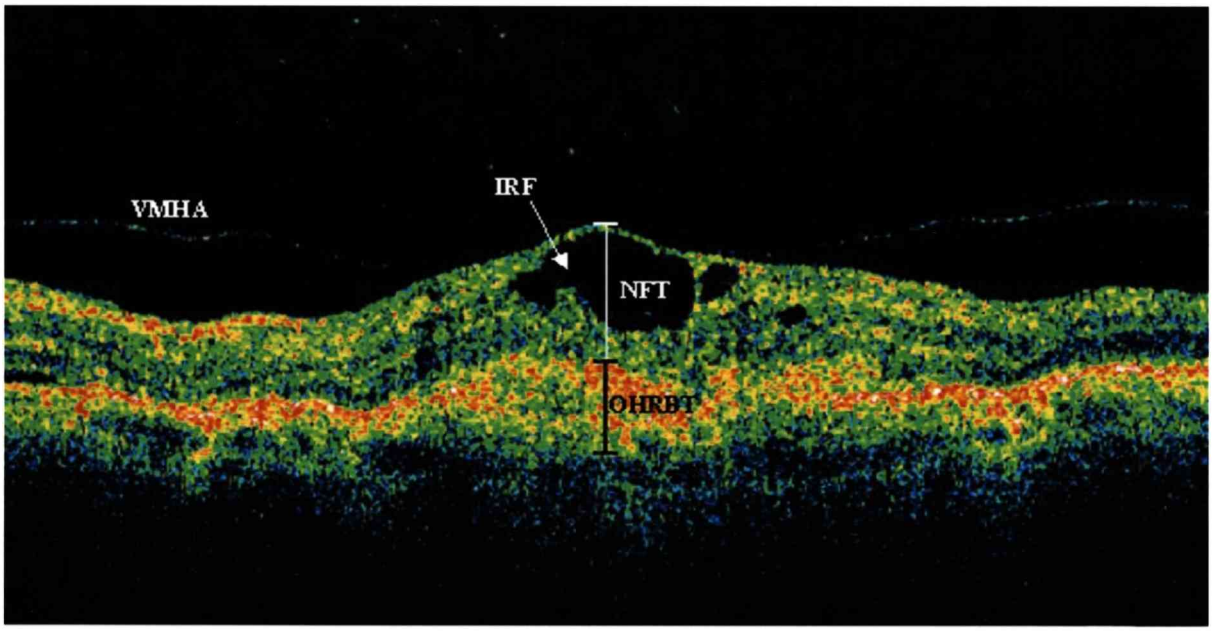

Figure 4.2: OCT image demonstrates loss of foveal depression with cystoid spaces and vitreomacular hyaloid attachment (VMHA). NFT, neuroretinal foveal thickness; OHRBT, outer high reflectivity band; IRF, intraretinal fluid. NFT = 406 μm and OHRBT = 307 μm in this scan.

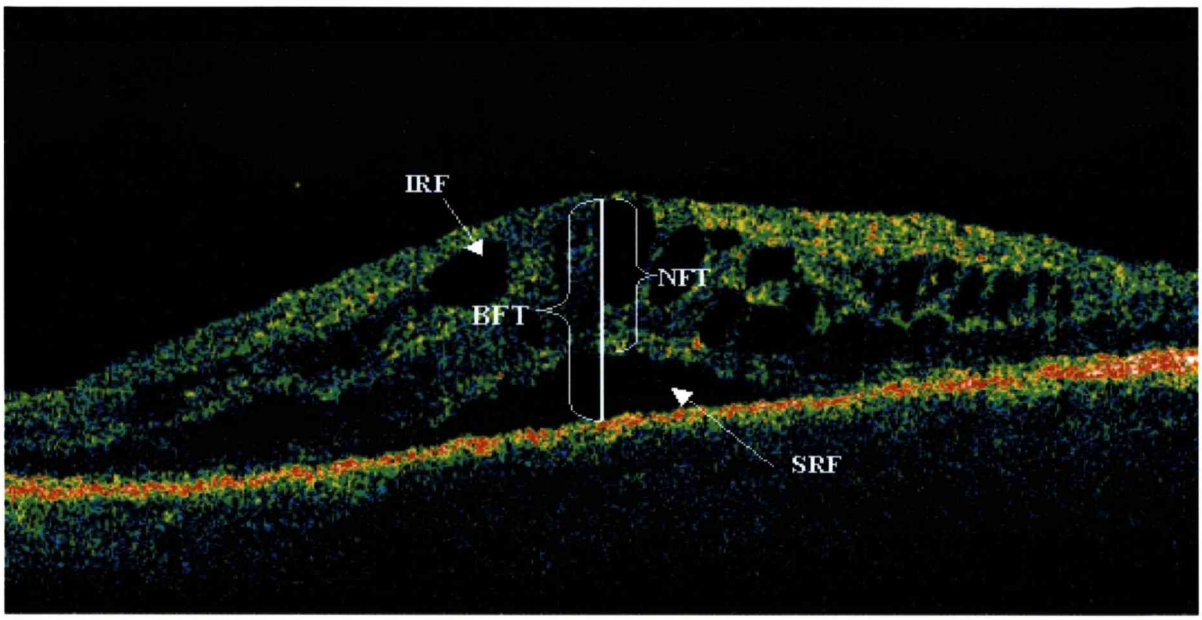

Figure 4.3: OCT passing through the fovea illustrating bilaminar foveal thickness (BFT), intraretinal fluid (IRF), and subretinal fluid (SRF). BFT is the distance between the inner high reflectivity band and the inner margin of the outer high reflectivity band at the foveal centre in the presence of subretinal hyporeflective area. NFT = 473 μm and BFT = 722 μm in this scan.

Statistics

For categorical data, agreement between the observers was compared by Cohen's kappa statistic. The kappa statistic gives a value that is an indication of the amount of agreement present, corrected for that which would have occurred by chance. The values of *K* can range from -1 to +1 (zero translates as agreement no better than that which would have occurred by chance). While no absolute definitions for agreement are possible we used the following by Landis and Koch (1977) to interpret the kappa values:

Table 4.2[153]: Interpretation of kappa values (Landis and Koch, 1977)

Value of κ	Strength of agreement
< 0.20	Poor
0.21-40	Fair
0.41-60	Moderate
0.61-0.80	Good
0.81-1	Excellent

Analysis of the agreement between continuous measurements was assessed by the intraclass correlation coefficient ratio (ICC).[154] The ICC varies from +1 (perfect agreement) to 0 (no agreement). I have also calculated the mean of the difference between the observers and used the Bland and Altman plot to graph the mean difference against the average of the two ratings on the horizontal. This plot demonstrates whether the agreement between the observers is related to the underlying value, for instance, if the two observers agree closely when estimating the normal retina as apposed to thicker retina.

4.4 RESULTS

Scans of 40 eyes of 40 patients with subfoveal predominantly classic CNV secondary to AMD were divided into 2 groups of 20 scans. Observers 1 and 2

analysed group1 and 16 scans (80%) were readable. Observers 1 and 3 analysed group 2 and graded all 20 scans (100%).

Tables 4.3 to 4.8 are cross tabulations showing the classification of categorical data (i.e. IRF, SRF and VMHA) by the groups and give the relevant kappa statistic

Group1: Observers 1 & 2.

Table 4.3: Cross tabulation showing the number of eyes with intra-retinal fluid (IRF) defined by the grouping variables (observer 1 and observer 2). $\kappa = 0.87$

		Observer 2 (IRF)		Total
Observer 1 (IRF)		Yes	No	
	Yes	6	1	7
	No	1	8	9
Total		7	9	16

Table 4.4: Cross tabulation showing the number of eyes with sub-retinal fluid (SRF) defined by the grouping variables (observer 1 and observer 2). $\kappa = 1$

		Observer 2 (SRF)		Total
Observer 1 (SRF)		Yes	No	
	Yes	9	0	9
	No	0	7	7
Total		9	7	16

Table 4.5: Cross tabulation showing the number of eyes with vitreo-macular hyaloid attachment (VMHA) defined by the observers 1 and 2. $\kappa = 0.75$

		Observer 2 (VMHA)		Total
Observer 1 (VMHA)		Yes	No	
	Yes	7	1	8
	No	1	7	8
Total		8	8	16

Group 2: Observers 1 & 3

Table 4.6: Cross tabulation showing the number of eyes with intra-retinal fluid (IRF) defined by the grouping variables (observer 1 and observer 3). κ= 0.69

		Observer 3 (IRF)		Total
Observer 1 (IRF)		Yes	No	
	Yes	6	3	9
	No	0	11	11
Total		6	14	20

Table 4.7: Cross tabulation showing the number of eyes with sub-retinal fluid (SRF) defined by the grouping variables (observer 1 and observer 3). κ= 0.73

		Observer 3 (SRF)		Total
Observer 1 (SRF)		Yes	No	
	Yes	4	1	5
	No	1	14	15
Total		5	15	20

Table 4.8: Cross tabulation showing the number of eyes with vitreo-macular hyaloid attachment (VMHA) defined by the grouping variables 1 & 3. κ= 1

		Observer 3 (VMHA)		Total
Observer 1 (VMHA)		Yes	No	
	Yes	3	0	3
	No	0	17	17
Total		3	17	20

For the continuous variables, NFT, BFT and OHRBT, mean, standard deviation and ICC were calculated (table 4.9).

Table 4.9: Mean difference between the observers of each group, correlation coefficient (CC) and standard deviation (SD) of the mean.

	Group 1			Group 2		
Measurement	Mean difference	CC	SD	Mean difference	CC	SD
NFT	11.3	0.98	9	11.2	0.97	13
BFT	14.9	0.98	15.7	15.3	0.97	13
OHRBT	37	0.76	29.4	23.1	0.93	17.5

Group 1: The ICC for NFT was 0.98 with an interobserver SD of 9; for BFT, ICC was 0.98 with SD±15.7 and for OHRBT the ICC was 0.76 and SD±29.4.

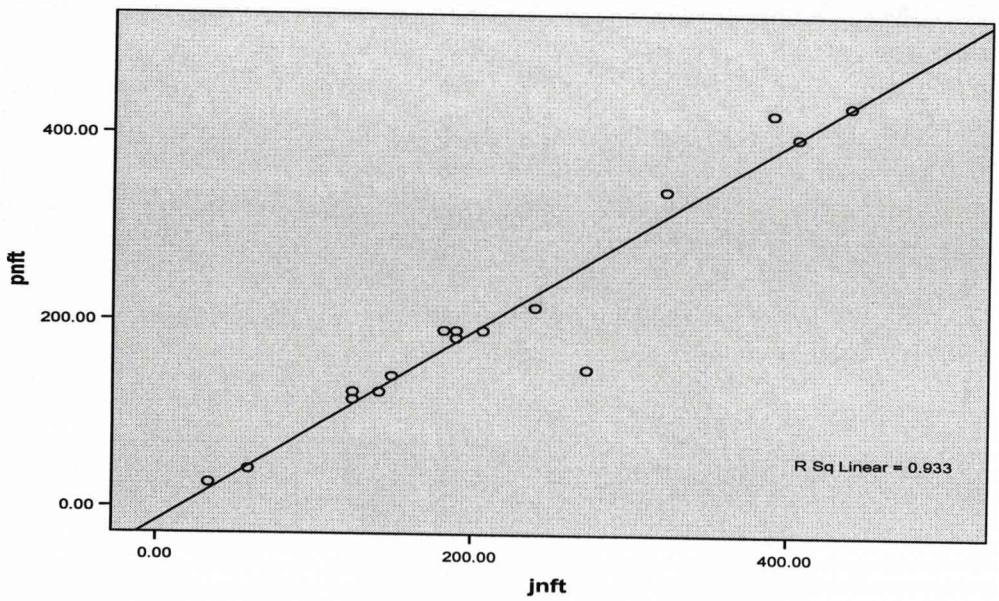

Figure 4.4: Scatter plot showing the linear correlation between observer 1 and 2 in rating neuroretinal foveal thickness (NFT). Pearson's correlation = 0.98.

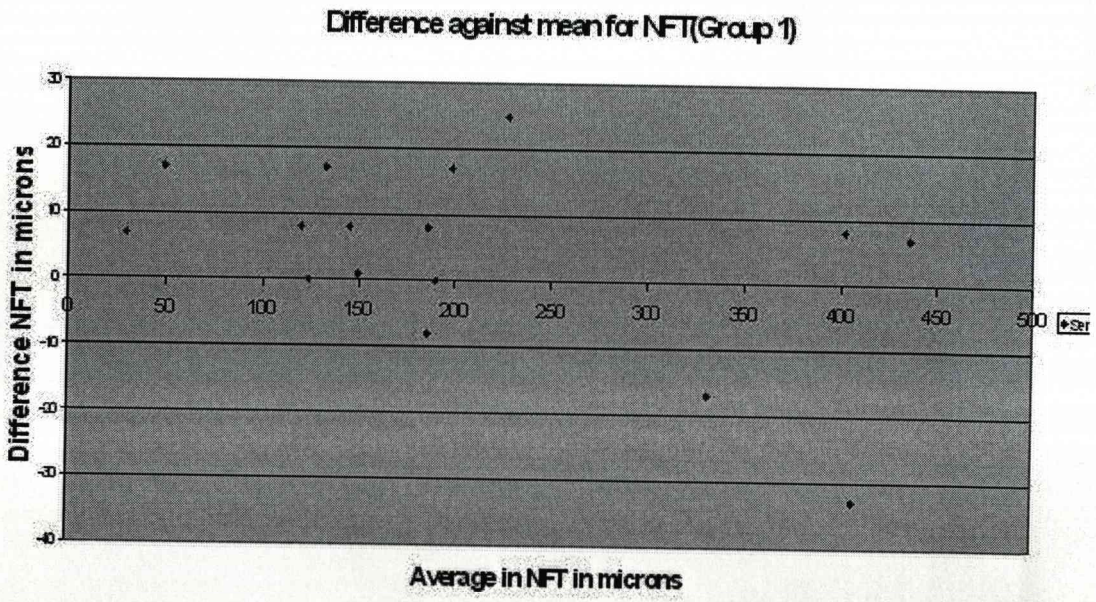

Figure 4.5: Bland- Altman plot for neuro-retinal foveal thickness (NFT). The mean NFT for each patient is plotted on the x-axis against the difference in NFT between the two observers, on the y-axis.

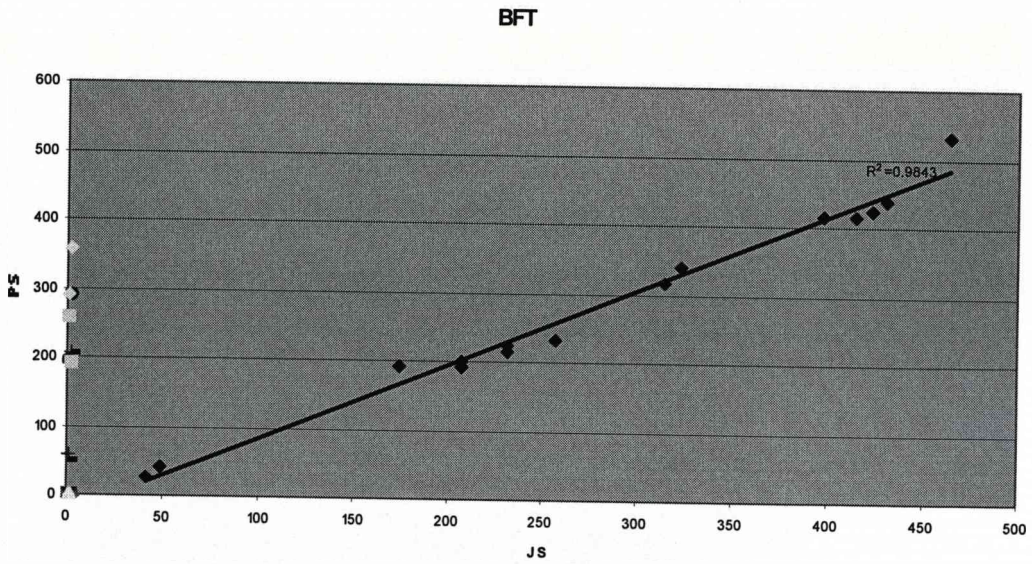

Figure 4.6: Scatter plot showing the linear correlation between observer 1 and 2 in rating bilaminar foveal thickness (BFT). Pearson's correlation = 0.98.

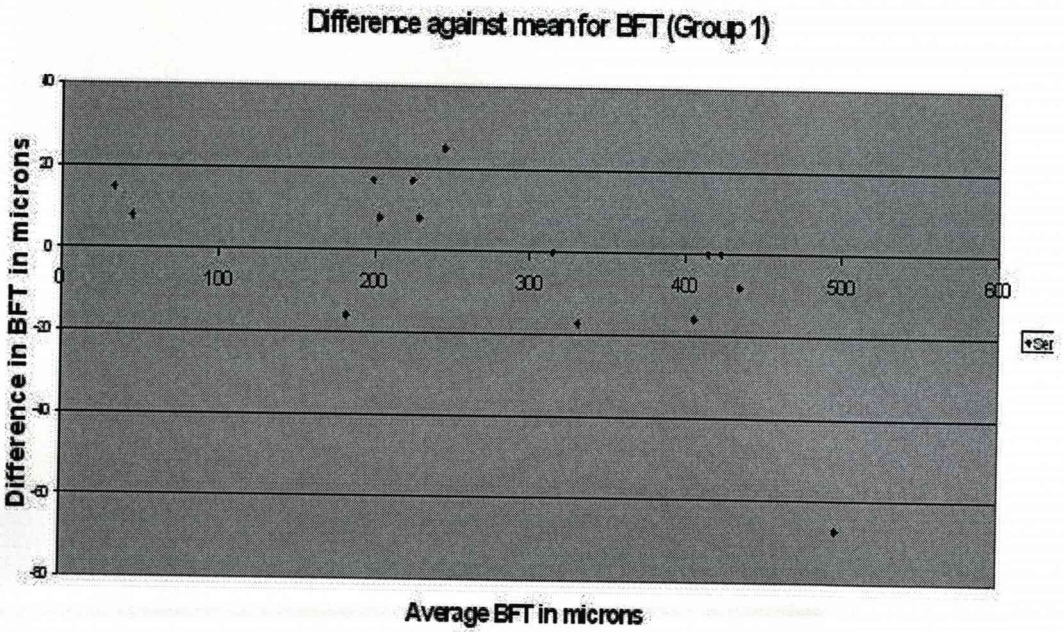

Figure 4.7: Bland-Altman plot for bilaminar foveal thickness (BFT). The mean BFT for each patient is plotted on the x-axis against the difference in BFT between the two observers, on the y-axis.

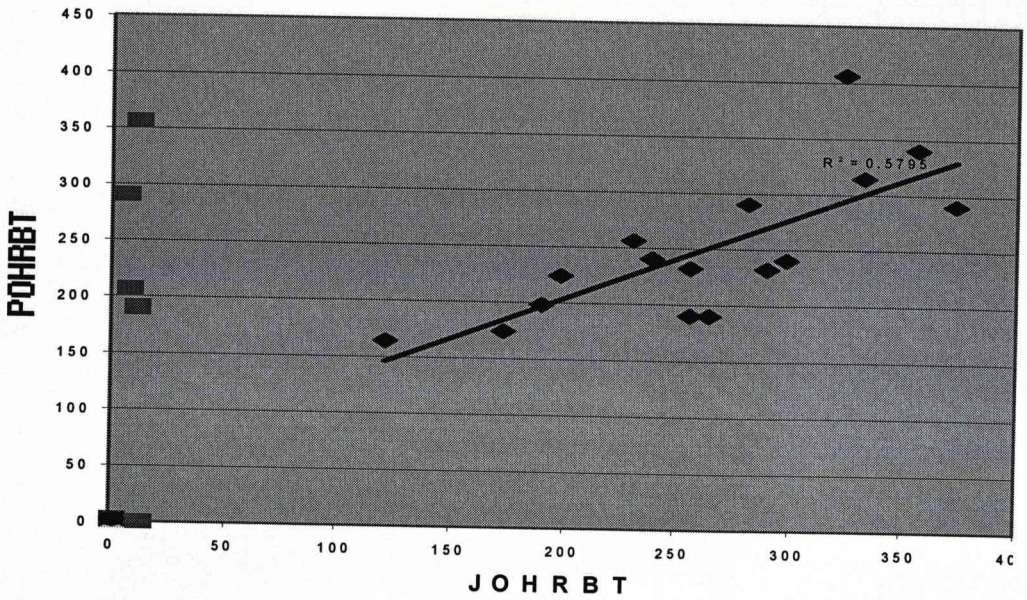

Figure 4.8: Scatter plot showing the linear correlation between observer 1 and 2 in rating outer high reflectivity band thickness (OHRBT). Pearson's correlation = 0.76.

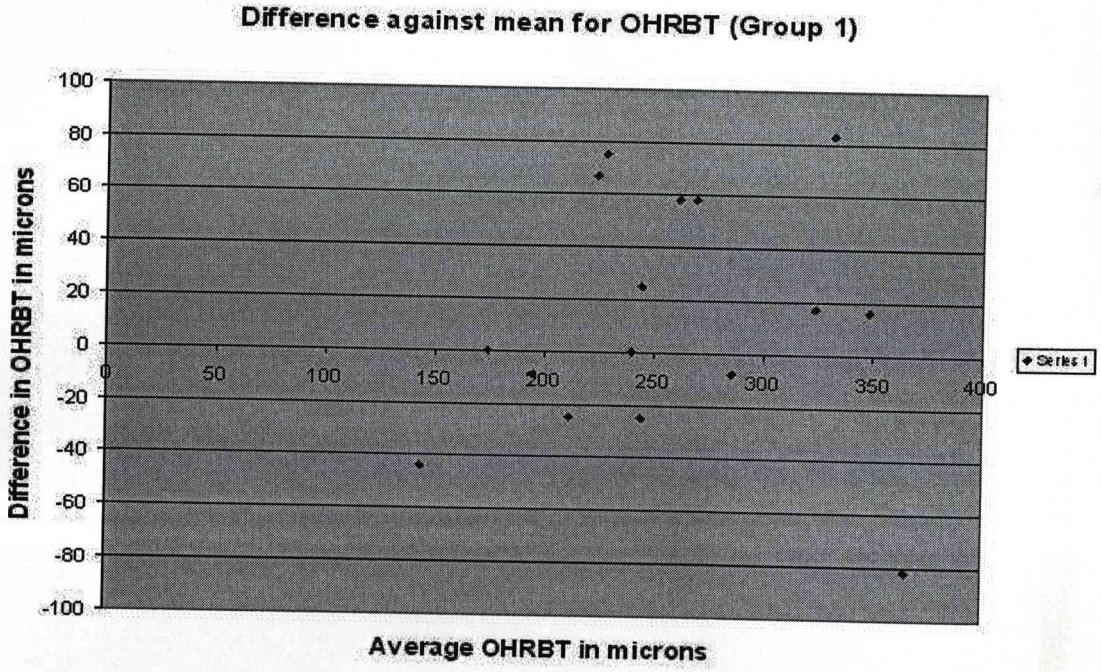

Figure 4.9: Bland-Altman plot for outer high reflectivity band thickness (OHRBT). The mean OHRBT for each patient is plotted on the x-axis against the difference in OHRBT between the two observers, on the y-axis.

Group 2: ICC for NFT was 0.97 with an interobserver SD of 13; for BFT, ICC was 0.97 with SD±13 and for OHRBT the ICC was 0.93 and SD±17.5.

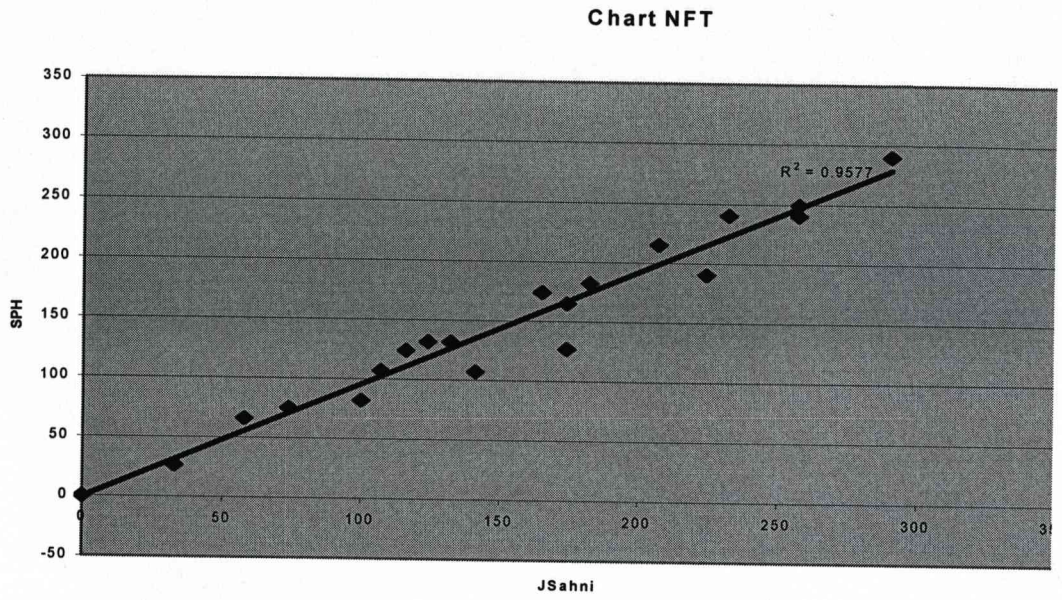

Figure 4.10: Scatter plot showing the linear correlation between observer 1 and 3 in rating neuroretinal foveal thickness (NFT). Pearson's correlation = 0.97.

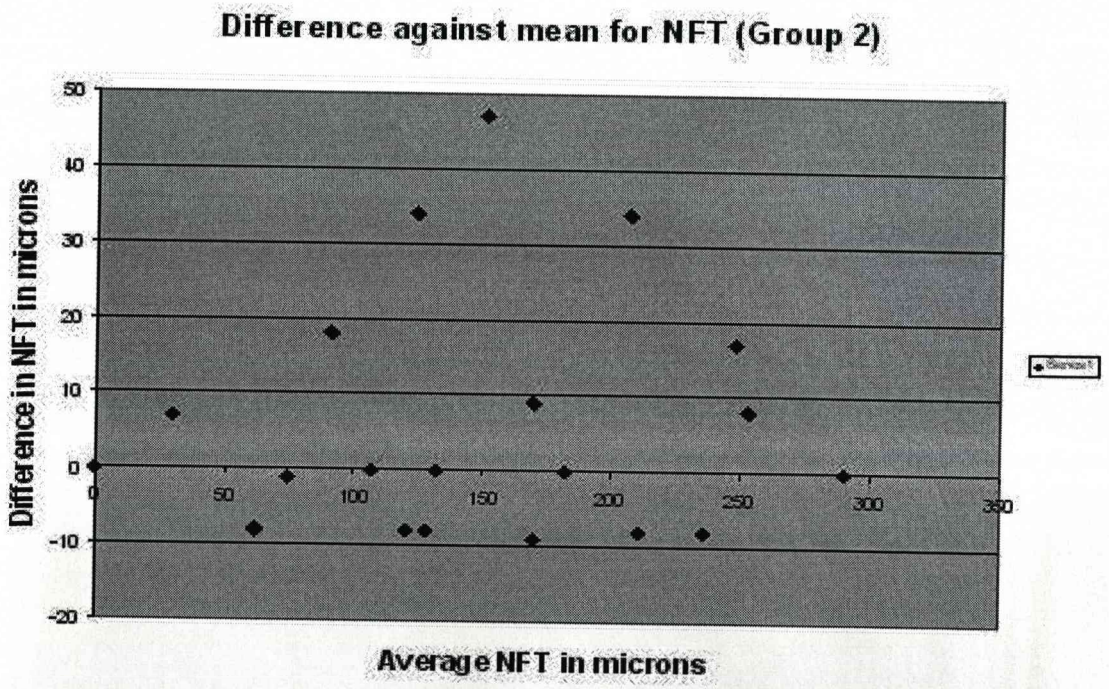

Figure 4.11: Bland-Altman plot for neuro-retinal foveal thickness (NFT). The mean NFT for each patient is plotted on the x-axis against the difference in NFT between the two observers (1 & 3), on the y-axis.

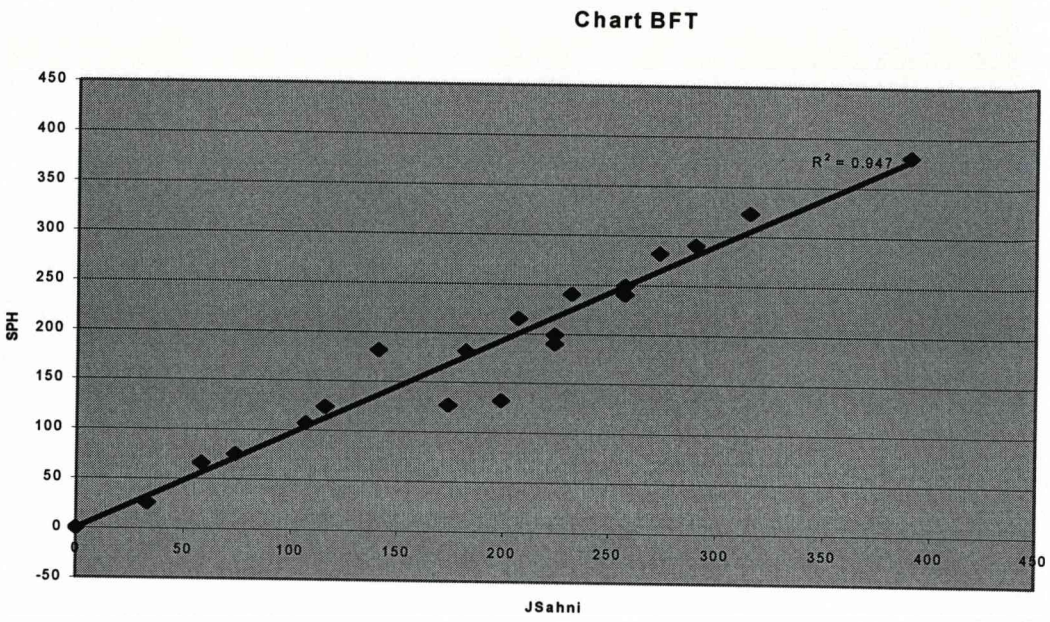

Figure 4.12: Scatter plot showing the linear correlation between observer 1 and 3 in rating bilaminar foveal thickness (BFT). Pearson's correlation = 0.97.

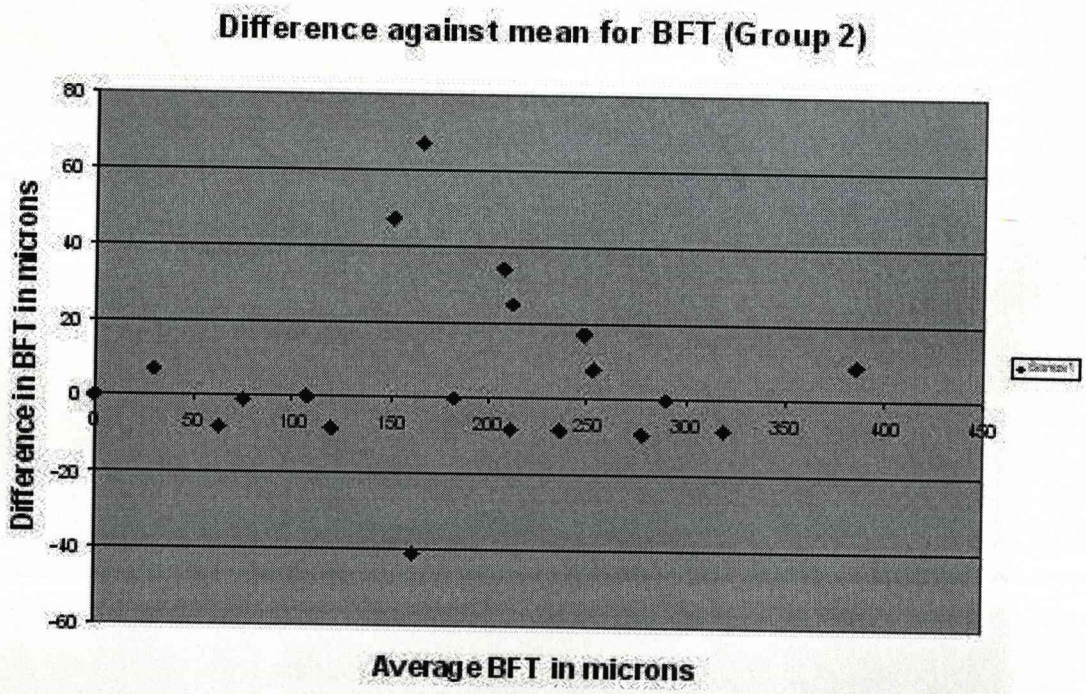

Figure 4.13: Bland-Altman for bilaminar foveal thickness (BFT). The mean BFT for each patient is plotted on the x-axis against the difference in BFT between the two observers, on the y-axis.

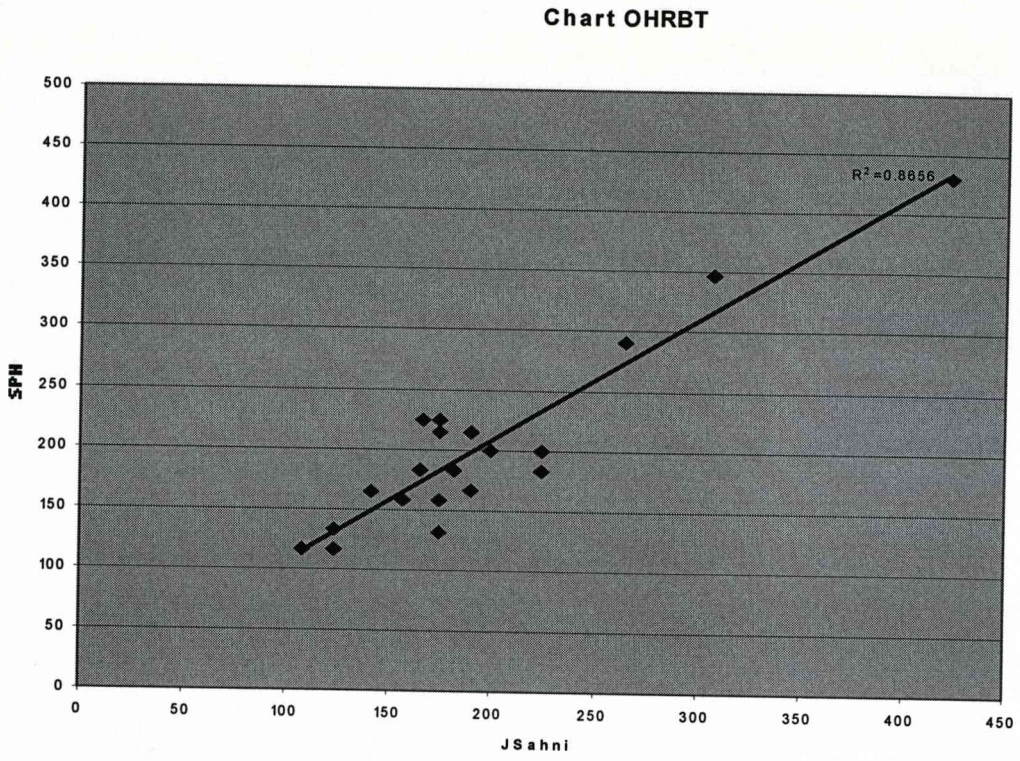

Figure 4.14: Scatter plot showing the linear correlation between observer 1 and 2 in rating outer high reflectivity band thickness (OHRBT). Pearson's correlation = 0.93.

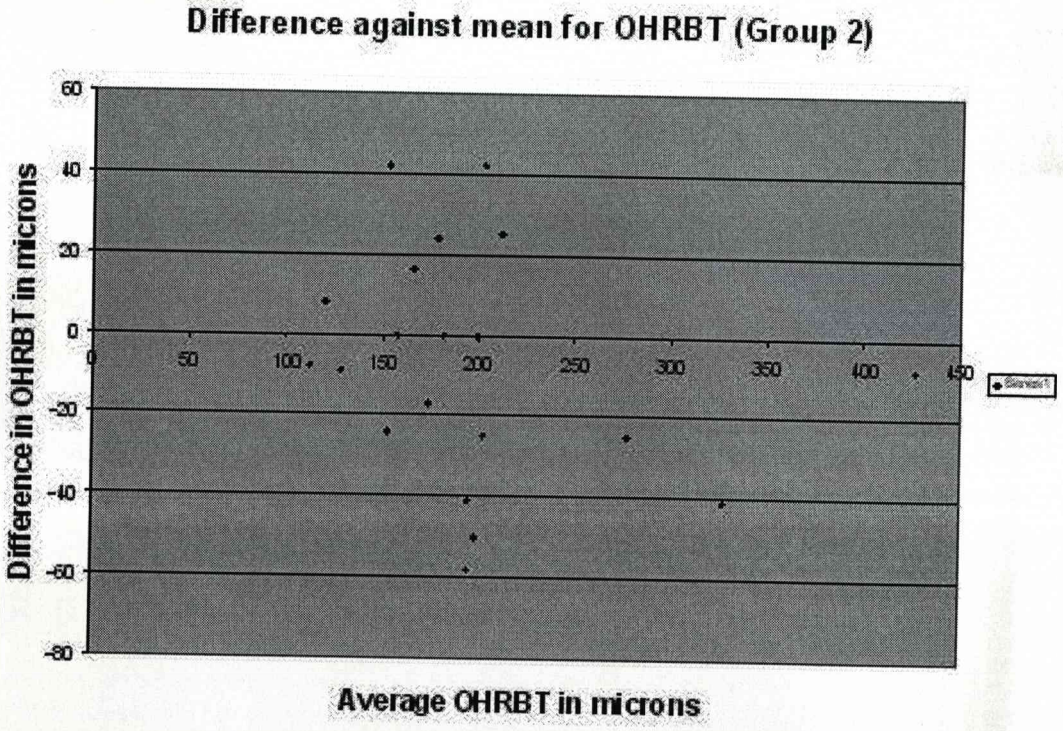

Figure 4.15: Bland-Altman for outer high reflectivity band thickness (OHRBT). The mean OHRBT for each patient is plotted on the x-axis against the difference in OHRBT between the two observers, on the y-axis.

4.5 DISCUSSION

When we started this study, there were no standardised terminologies available for the interpretation of the OCT scans in the literature. In this study we first developed specific terminology and then validated them by testing for interobserver concordance in its application in the clinical situation of neovascular AMD. We use the term IRF for describing well-delineated hypo-reflective spaces separated by reflective septae within the neuroretina and SRF when there is a well-demarcated hyporeflective separating the neuroretina from the outer high reflectivity band. Retinal thickness measurements were done from the inner high reflectivity band to the inner margin of the outer lamina of the outer high reflectivity band. As previously described in chapter 2, on OCT3 the outer high reflectivity band is seen have a double laminar structure; the inner lamina has been attributed to the junction of the photoreceptor inner and outer segments and technically is part of the neuroretina. Therefore, our measurements of retinal thickness were done from the inner high reflectivity band to the inner margin of the outer lamina of the outer high reflectivity band. We defined two measurements of foveal thickness, NFT and BFT, to allow for differences depending on the absence or presence respectively of sub retinal hyporeflectivity on OCT.[155, 156] We introduced the term OHRBT to measure the thickness of the sub retinal hyperreflectivity which could represent the RPE-CNV complex at the fovea.[91, 157] Finally we have introduced the term VMHA where partial separation of the posterior hyaloid with attachment at the macula was noted on the OCT. We avoided calling this traction, as tractional forces cannot be measured with the OCT.

Overall, this study found good agreement between the observers in the detection of IRF, SRF and VMHA (κ>0.61) (table 4.2). In the concordance study, reproducibility of NFT and BFT had high ICC's and low SD's, which are essential for accurate and reliable measurements of retinal thickness. OHRBT reproducibility was lower with lower ICC and higher SD in-group 1. This high variability may be due to difficulty in identification of the true outer margin of the outer high reflectivity band.

In this study, all measurements on the OCT3 scans were done by positioning the callipers manually. The automated retinal thickness measurement tool of the OCT3 software obtains retinal thickness measurements automatically by means of a computer algorithm that searches for the changes in reflectivity observed at the superficial and deep retinal boundaries. We therefore tested the algorithm that is supplied within the software suite of the OCT3. In our experience, in most cases it failed to distinguish between the detached posterior hyaloid and the true inner high reflectivity band corresponding to the inner retinal border. The software is guided by the presence of the inner lamina of the outer high reflectivity band, i.e. the photoreceptor inner/ outer segment junction, consistently underestimating the thickness of the neuroretina.[158, 159] Sadda et al observed errors of outer retinal boundary detection and thickness measurement in 92% of eyes in an observational study of 200 eyes with varying macular pathologies.[160] This was worse in the presence of a SRF and CNV. Thus better software algorithms and anatomic knowledge will be needed before clinicians can fully rely on the quantitative output from these devices.

But manual placement of callipers is a subjective technique and as we have demonstrated this can lead to interobserver and intraobserver variability in the

measurements. Sadda et al have described a technique of computer assisted OCT grading using custom-made software (termed OCTOR). OCTOR was developed by the Doheny Image Reading Centre (DIRC) (Doheny Eye Institute, University of Southern California) software engineers.[161] The software, which operates as a painting program and calculator, imports data exported from the Stratus OCT machine and allows the grader to use a computer mouse to draw various boundaries in the retinal cross-sectional image, including: the inner retinal surface, the outer retinal boundary, the RPE-choriocapillaris interface (if different from the outer retinal boundary, as in cases with subretinal fluid), and the estimated level of the normal RPE (if different from the RPE-choriocapillaris interface, as in cases of pigment epithelial detachment). The software then calculates the distance in pixels between the manually drawn inner and outer retinal boundary lines. There was good intra- and intergrader reproducibility in manually drawing retinal boundaries using a computer mouse. Manual correction of OCT boundary detection errors and the delineation of boundaries of other structures (such as subretinal fluid) are only potentially useful, short-term solutions to the limitations of the existing OCT software. Automated segmentation algorithm may be able to give more consistent accurate detection of retinal boundaries. These have been described but are not yet available.[162] These techniques of measuring the scans have been only been described in research settings and reproducibility data are only available for certified reading centre graders. At present manual calliper placement currently remains the method of choice.

One of the weaknesses of this study is the relatively short training and lead in time for the three observers who graded the scans. Three independent observers with different levels of grading expertise graded the images. Observer 2 (Stanga) had

previous experience in interpreting OCT 2 images. He supervised me in the acquisition, interpretation and measurement of the OCT scans, and I then supervised observer 2 (Harding) in the same training process. We had 2 weeks of training each. It is likely that with more experience other features on the scans could be identified. For example, concordance on the details of the RPE/ choriocapillaris layer, including identification and differences between haemorrhagic and serous PED could have been studied. Another limitation is the relatively small data set available for validation. A sample size calculation was not done in the study planning because there was no data on OCT findings in neovascular AMD on which to base such a calculation. This study examined interobserver concordance, but did not address intraobserver concordance. Also repeatability of grading was not analysed in normal eyes.

4.6 CONCLUSION

The results of our study indicate that clinicians and researchers using a standardised protocol and with adequate training can independently grade, with a high level of interreader agreement, multiple morphologic parameters and can reproducibly quantify neuroretinal, SRF, and CNV thickness on OCT scans obtained from eyes with neovascular AMD.

Chapter 5

OCT IN NEOVASCULAR AMD
A CROSS-SECTIONAL STUDY

5.1 INTRODUCTION

In 2002, optical coherence tomography (OCT) was a relatively new imaging technique only just entering the clinical domain. The Stratus OCT3, the latest commercially available model offered increased resolution and its role in the assessment of patients with neovascular AMD was yet to be established. There were a few anecdotal reports in the literature that were mainly descriptive and retrospective studies with no standardisation or validation of the technique used in the assessment of the scans.[92, 94] The diagnostic accuracy of the OCT when compared to the existing modalities of investigation had not been evaluated. It was felt that the ability of the OCT to take cross-sectional images of the retina would enable the study of the effect of photodynamic therapy (PDT) on the morphology and function of the macula

5.2 AIM

The aim of this study was to assess the diagnostic accuracy of OCT in detecting cystoid macular oedema (CMO) and subretinal fluid (SRF) in eyes undergoing PDT for subfoveal CNV. Secondly it aimed to determine if there was a relationship between foveal morphology on OCT and vision in eyes undergoing PDT.

5.3 PATIENTS AND METHODS

This was a prospective cross-sectional study of eyes with predominantly classic subfoveal CNV secondary to AMD attending the St Paul's Clinical Eye Research Centre.

All patients underwent refraction protocol best corrected visual acuity (BCVA) measurement on a retroilluminated Lighthouse for the Blind (New York, NY) distance visual acuity test chart (using modified Early Treatment Diabetic Retinopathy Study charts 1, 2, and R).

Clinical and fluorescein angiography (FA) evaluation was performed by a retina specialist. The presence or absence of CMO and SRF was documented on slit lamp biomicroscopy using a 60-dioptre Volk (Volk Opticals, Mentor, OH, USA) lens and on FA by interpretation of 10 minute late frames.

OCT was performed and analysed by a single observer (JS) on the OCT3 masked to visual acuity (VA), clinical and FA findings. All scans were performed prior to FA and slit lamp biomicroscopy. Pupils were dilated with tropicamide (1%) and phenylephrine (2.5%) drops. Internal fixation guided by the video image was used to ensure that scans passed through the fovea. Scans that did not pass through the fovea were excluded. Horizontal single line A-scans through the fovea of default length 5 mm at 0° and a fast macular thickness map consisting of six simultaneous 6 mm radial line scans were obtained. With each single line scan pass, 512 longitudinal range samples were captured—each consisting of 1024 data points over 2 mm of depth, giving 524288 data points, which are integrated to construct a cross sectional anatomical image (tomogram). In cases with poor central fixation, the scan was manually positioned on the anatomical fovea as viewed on the black and white

video image. All thickness measurements were made on the single line horizontal scans. The measurements were done at the foveal centre (foveola) by manually positioning the callipers on the scans and using the retinal thickness (single eye) quantitative analysis protocol offered by Stratus OCT3.

The OCT scans were interpreted and measured using the terminology described in Chapter 4 (page 110). The retinal thickness measurements at the fovea were neuro-retinal foveal thickness (NFT) and bilaminar foveal thickness (BFT) in the presence of subretinal fluid (SRF). Outer high reflectivity band thickness (OHRBT) was measured between the inner margin of the outer lamina and outer margin of the outer lamina at the fovea. Presence/ absence of intra retinal fluid (IRF), SRF and vitreo- macular hyaloid attachment (VMHA) on the scans was recorded. Scans were also studied for features, which could confound the interpretation and measurement of the images.

Statistics

Statistical analysis of the data was performed using SPSS for windows version 11.0 (SPSS Inc, Chicago, IL, USA). Agreement between clinical examination and OCT in the detection of CMO and SRF were investigated on 2 x 2 tables and kappa statistic (κ) was calculated. The relation between the thickness measurements (NFT, BFT and OHRBT) respectively and VA was analysed using the Pearson correlation coefficient. P-value <0.05 was taken to be significant.

5.4 RESULTS

Sixty-eight eyes of 65 patients attending St. Paul's Eye Unit, Royal Liverpool University Hospital between Aug 2002 and Feb 2003 were recruited.

Twelve eyes (17%) were excluded, as scans passing through the fovea could not be obtained due to erratic and inaccurate fixation leaving 56 eyes for analysis.

The median age was 76 years. Mean duration since baseline visit was 9.5 months (range 0 to 30; M 24, F 32). 3 patients were scanned at baseline prior to receiving any treatment. 16 had undergone 1 PDT treatment application, 11 had 2, 10 had 3, 6 had 4, 9 had 5 and 1 patient had 7 treatment applications prior to the OCT scanning.

IRF was found in 23 (42%) eyes on OCT imaging and CMO was found in 13 (23%) eyes on slit-lamp and FA examination. Kappa was 0.29 signifying a fair agreement between the two tests. (Table 5.1) There was poor agreement between slit lamp biomicroscopy and OCT in the detection of SRF ($\kappa = 0.17$). (Table 5.2) The mean VA in eyes with IRF was 41.6 letters (SD±16) and in eyes without IRF was 46.2 letters (SD±11). There was no significant difference in the distance VA in eyes with and without IRF and SRF at the fovea ($p>0.5$).

Table 5.1: Classification of cystoid macular oedema by clinical examination (CMO) and OCT examination (IRF). (κ=0.29)

		IRF		
CMO		No	Yes	Total
	No	29	14	43
	Yes	4	9	13
	Total	33	23	56

Table 5.2: Classification of subretinal fluid by clinical examination (SRF) and OCT examination (oSRF). (κ =0.17)

		oSRF		
SRF		No	Yes	Total
	No	26	1	27
	Yes	23	6	29
	Total	49	7	56

The mean NFT was significantly greater in patients with IRF at 223 μm compared to those without at 154 μm ($p=0.005$). The correlation between the NFT and BCVA ($p>0.5$) and NFT and the number of PDT applications ($r = -0.23$, $p=0.09$) was not statistically significant.

The correlation between BFT and BCVA was also not significant ($p>0.05$). There was a statistically significant correlation between BFT and the number of PDT applications ($r=-0.28$; $p=0.04$). BCVA was significantly better in eyes with a thinner OHRBT ($r=-0.331$; $p=0.013$) (Figure 5.1). A VMHA was present in 20 of the 56 patients (35.7%). No statistically significant association was found between IRF and VMHA ($p=0.4$).

Confounding features interfering with the interpretation of the scans were found to be RPE atrophy and the presence of sub-retinal pigment epithelial (RPE) haemorrhage. In cases with atrophy of the RPE (on slit-lamp or FA) an optical shadow was cast making it difficult to identify the outer limit of the OHRBT. Sub RPE fluid and haemorrhage also disrupted the architecture of the OHRBT and made the measurement impossible. In cases with a large amount of intra- or sub retinal fluid or haemorrhage signal attenuation appears to reduce the apparent OHRBT.

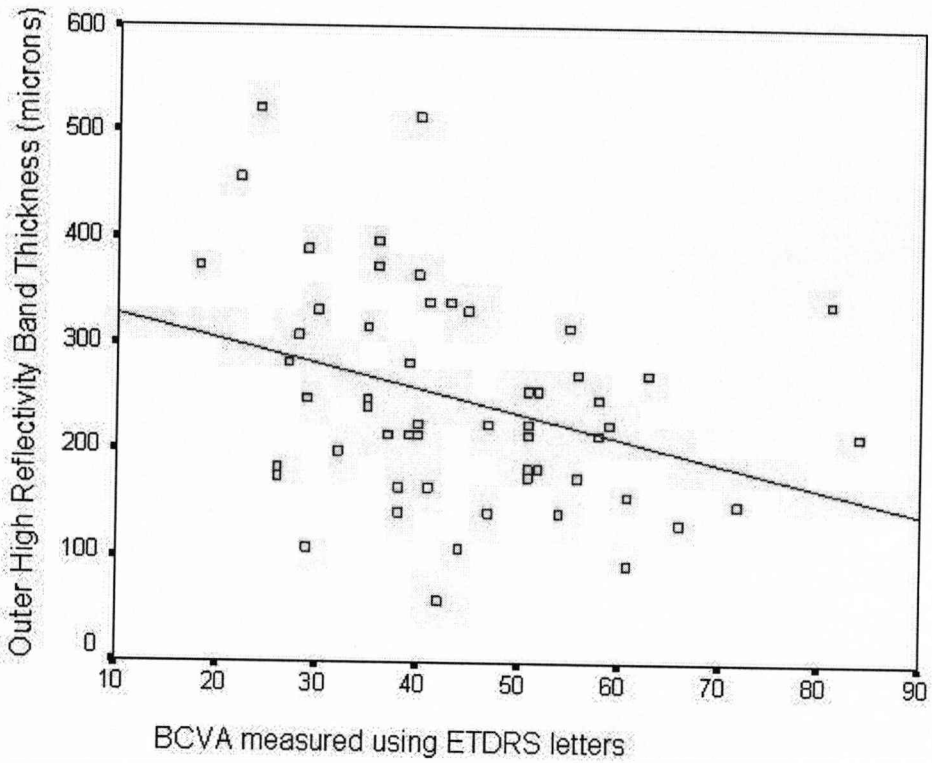

Figure 5.1: Relation between visual acuity (ETDRS letters) units plotted against outer high reflectivity band (OHRBT) in μm in 56 eyes. The linear regression line is y=22.3352x+350.58 (r =20.331, p = 0.02).

5.5 DISCUSSION

In this study new terminologies and scan measurement definitions developed in the previous study were applied to a group of patients with subfoveal predominantly classic CNV at various stages of their treatment with PDT. This study found that favourable visual outcome following PDT was associated with a thinner OHRBT.

Twelve (17%) of 68 eyes could not be reliably scanned through the fovea. Reliability of scans was limited by poor fixation, excessive eye movements and difficulty identifying the true location of the fovea due to morphological changes caused by disease. Two other studies have reported on the difficulty of obtaining scans. In a study on diabetic maculopathy patients Hee et al failed to obtain

adequate quality scans in 4.2%.[77] Rogers et al[96] reported a higher percentage (12.2%) of scans to be unobtainable/unreliable in a population of patients with AMD, a result more similar to but still lower than ours. In both studies as the OCT scans were reviewed retrospectively, the authors would have had no way of knowing if the scans had definitely passed through the fovea due to distortion of the retinal architecture in the more advanced cases. Also data on VA are not available for these studies. Unlike these authors our population was consecutive and prospective, often with quite low levels of vision and poor fixation and accounting for a 17% exclusion rate: the mean VA score was 42 letters (roughly equivalent to 20/120) and scans that did not pass through the foveal centre were excluded.

The presence/absence of leakage is integral to treatment and retreatment decision making during a course of PDT.[163] Bressler et al[95] have commented on the difficulty of correctly identifying leakage due to CNV in the presence of co-existing CMO, which can confound interpretation of FA images. FA and slit lamp biomicroscopy are the standard examinations used for the diagnosis of CNV in patients with AMD and these examinations are relatively insensitive at detecting small changes in retinal thickness.[164] Hee et al noted that slit lamp biomicroscopy was unreliable in detecting an increase in thickness smaller than 250 μm in diabetic macular oedema. Browning et al [165] calculated κ to be 0.63 in their cohort of diabetic patients for the agreement between slit lamp biomicroscopy and OCT in the detection of macular oedema. In the present study OCT detected IRF in more than 50% of patients in whom CMO was not seen on slit lamp biomicroscopy or FA, but the agreement between the two methods was only fair (κ=0.29). There was also poor agreement between the two methods in the detection of SRF (κ=0.165). The majority of patients (94.6%) had undergone previous PDT making it difficult to identify the

fluid on slit lamp biomicroscopy and FA and this may have led to the lower level of detection using these traditional diagnostic methods. Studying the relationship between VA and retinal thickness / fluid is important in increasing the understanding of retinal pathophysiology in exudative maculopathy. In our study of patients with AMD who had undergone PDT, there was no statistically significant association between the presence or absence of IRF and SRF and VA or between VA and NFT or BFT. In a study using OCT at the baseline visit, Ting et al reported a poorer VA with the presence of CMO.[94] This difference between the studies may be because of the difference in patient populations, 95% of the patients in our study had undergone PDT, while all the patients in their study were scanned at baseline. Therefore other factors such as the baseline VA and size of CNV affect the final VA. Also, the retinal thickness may not be a direct measure of the viability of the retinal photoreceptors.

This study found an important relationship between RPE-CNV complex thickness, i.e. OHRBT, and VA. Histological studies have suggested that increased thickness of the CNV may be associated with increased loss of photoreceptors.[51] Thus the anti-angiogenic effect of PDT may preserve VA in patients with AMD by modifying the natural history of the scarring process which may reduce the photoreceptor loss. [111, 113] There was no association between the OHRBT and the number of PDT treatments or the duration since initial treatment.

Vitreo-macular traction has been implicated in progression of diabetic maculopathy.[166] VMHA was present in 20 patients, but there was no statistically significant correlation between CMO and VMHA. It may be that in AMD disruption of RPE metabolism by the associated CNV is responsible for the changes

in the retinal architecture and CMO as opposed to vitreo-macular traction as has been implicated in the other conditions such as diabetes.[167]

A limitation of this study is that scans were not possible in 17% of the patient population. The time required for the acquisition of an OCT scan (1.92 seconds) is the main rate-limiting step in these patients with poor vision and fixation difficulties. Until new technology, which permits faster acquisition times, becomes available, OCT will not be feasible in certain patient groups.

Errors in the interpretation and measurement of the OHRBT can arise because of disruption in the architecture of the RPE/ CNV complex as a result of disease and treatment. Hee et al described the distinguishing characteristics of serous, haemorrhagic and fibrovascular PED. In practise however, OCT features of these three pathologies show considerable overlap, causing difficulty in the interpretation and measurement of the scans. Retinal and RPE atrophy can also cause increase transmission of light and lead to similar errors. Although we have taken great care to accurately delineate the outer high reflectivity band, errors in measuring true RPE-CNV thickness may have arisen because of light attenuation or amplification properties of the tissue.

Another limitation of the study is that although we have only sought correlations between vision and OCT features, baseline VA, diameter of the CNV, presence of fibrosis, atrophy, and blood may have also influenced the VA results.

5.6 CONCLUSION

This study demonstrates that OCT provides an objective alternative to FA and clinical examination in the detection of CMO and SRF.

This is also the first report correlating OCT thickness measurements with vision. The visual acuity was reduced in eyes with a thicker RPE/ CNV complex. This may reflect an increase loss of photoreceptors in these eyes and is consistent with histological studies that showed increased loss of photoreceptors with increased thickness of the disciform scar.

Thus the new terminology we have developed in the interpretation of the OCT scans may prove particularly valuable in monitoring the response of the retina and CNV to a course of PDT and may also be applicable in the emerging anti-VEGF medical therapies.

Chapter 6

OCT OF BILATERAL END-STAGE CNV

6.1 INTRODUCTION

Age-related macular degeneration (AMD) is a bilateral condition that tends to be fairly symmetrical in its presentation and natural course. Retinal scars resulting from bilateral untreated cases of exudative AMD are known to be similar in fellow eyes.[168, 169] The risk of developing a neovascular lesion in the second eye has been reported to be approximately 35% at 3.5 years by Gass[170] and 35% at 5 years by Macular Photocoagulation Study (MPS) group.[171] Loss of vision in AMD has been attributed to loss of retinal photoreceptors.[172, 173, 174, 175] Green and Enger correlated histologically the thickness of fibrovascular scars and the extent of cell loss in the retina.[51] Scars thicker than 0.2 mm were associated with severe photoreceptor loss. Kim et al found a 69.4% reduction in the number of outer nuclear layer cells in eyes with end-stage fibrosis due to AMD compared with control eyes.[52]

6.2 AIM

The previous cross-sectional study showed a correlation between scar thickness measured with Stratus optical coherence tomography (OCT3) and vision in patients undergoing photodynamic therapy (PDT). In this study, retinal thickness, subretinal hyper-reflectivity and best corrected visual acuity (BCVA) were compared between PDT treated eyes with a stable fibrotic scar and fellow untreated eyes with an end-stage fibrosis and showing no signs of active choroidal neovascularisation (CNV) in either eye (i.e. leakage on fluorescein angiography (FA) and subretinal fluid (SRF)

or intra retinal fluid (IRF) on OCT3). The aim of the study was to examine the relationship between end-stage scar and retinal thickness using OCT and to see if the histological findings of Green et al and Kim et al hold true in vivo.

6.3 PATIENTS AND METHODS

Patients with bilateral neovascular AMD with end-stage subfoveal fibrosis (disciform scar) and who had a PDT-induced stable fibrotic scar in one eye and end-stage scar in the fellow eye were recruited. A stable lesion in treated eyes was defined as a lesion with fibrosis not requiring PDT for at least 6 months. On slit-lamp biomicroscopy, subfoveal fibrosis was observed as a yellow-grey area blocking details of the underlying choroid.

Patients were excluded if OCT scans passing through the centre of the fovea could not be obtained and/ or the scan showed the presence of SRF, IRF or retinal pigment epithelial detachment because the presence of fluid was taken as an indicator of continuing lesion activity.

Study design

This was a prospective, cross-sectional study in patients with neovascular AMD attending St Paul's Eye Unit as part of an established PDT treatment service. If the patients were deemed to have a PDT-treated inactive scar in one eye and an inactive untreated fibrosed scar in their fellow eye based on slit-lamp biomicroscopy and FA, they were referred for OCT3 scan. All patients also underwent: refraction protocol Early Treatment Diabetic Retinopathy Study (ETDRS) visual acuity measurement using the TAP Protocol, colour fundus photographs and stereoscopic FA. Horizontal single line A-scans through the fovea of default length 5mm at 0° angle were obtained. OCT3 was performed using an internal fixation beam. In cases

with unstable or eccentric fixation, the scan was manually positioned on the anatomical fovea as viewed on the black and white video image and multiple horizontal line scans were acquired passing through and above and below the fovea.

Colour fundus images were analysed and the greatest linear dimension (GLD) of the fibrotic lesion was calculated using commercial imaging software (Figure 6.1). For the purpose of this study the lesions were categorised as small <3500 μm, medium 3500–5000 μm and large >5000 μm. One grader (JS) performed all the scans on the day of recruitment after informed consent. Neuroretinal foveal thickness (NFT) and outer high reflectivity band thickness (OHRBT) were measured using the definitions and technique described in chapter 4. All measurements were performed by positioning the callipers manually and using the retinal thickness analysis protocol offered by Stratus OCT3. Figures 6.2 and 6.3 demonstrate the measurement of the OHRBT and NFT in the treated eye and fellow eye of a patient with bilateral end-stage disciform scarring on an OCT3 scan through the fovea. Patients with IRF or SRF on OCT3 were excluded as defined in the exclusion criteria. Measurements from OCT3 scans were performed in a masked fashion, the examiner (JS) being unaware of which eye had been treated.

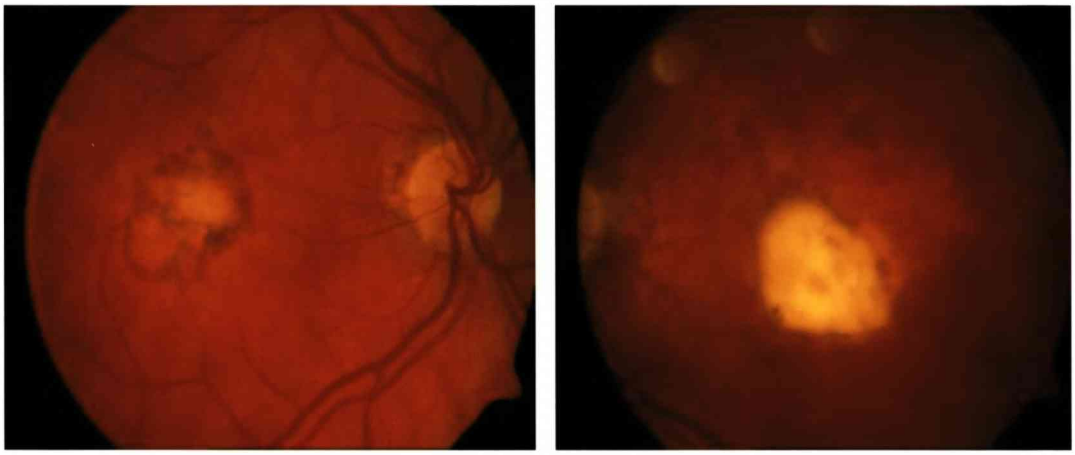

Figure 6.1: Colour fundus photograph of the treated right eye with best corrected visual acuity(BCVA) of 54 letters showing a translucent scar 15 months after photodynamic therapy (PDT) and the untreated left eye with BCVA of 24 letters showing end-stage disciform scarring.

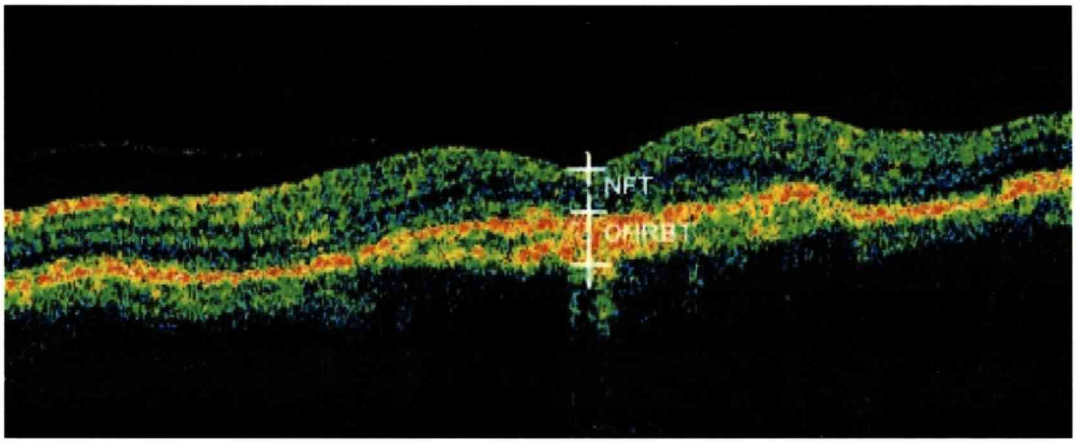

Figure 6.2: Stratus optical coherence tomogram passing through the scar at the fovea of the PDT-treated right eye in the above image. Neuroretinal foveal thickness (NFT) = 132 μm; outer high reflectivity band thickness (OHRBT) = 240 μm.

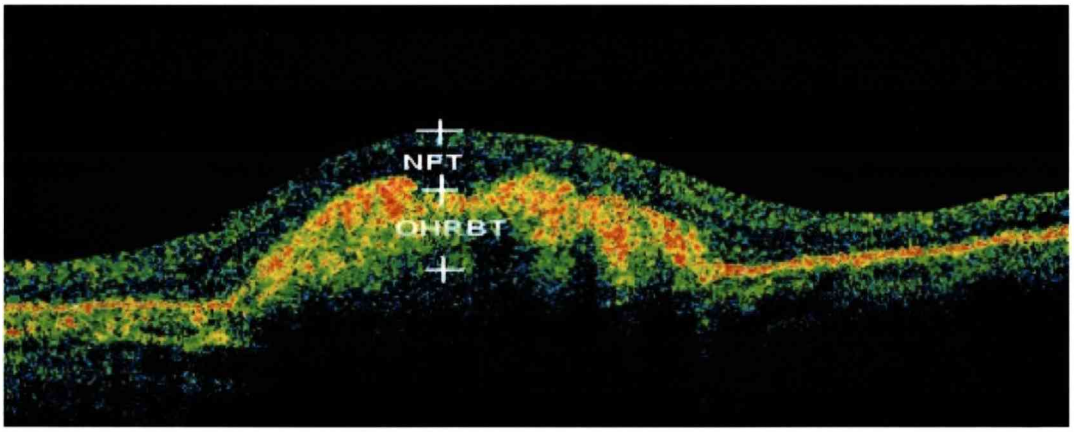

Figure 6.3: Stratus optical coherence tomogram passing through the scar and the fovea of the untreated left eye. Neuroretinal foveal thickness (NFT) = 97 μm; outer high reflectivity band thickness (OHRBT) = 489 μm.

Statistics

Statistical analysis of the data was performed using SPSS for windows Version 11.0 (SPSS Inc, Chicago, IL, USA). VA, OHRBT, NFT and morphology between the eyes of the study patients were compared using the paired samples Student's *t*-test. Linear correlation between independent variables was analysed using the Pearson correlation coefficient (*r*). All correlations were two-tailed.

6.4 RESULTS

Thirty-eight patients with a PDT treated inactive scar in one eye and an inactive untreated fibrosed scar in their fellow eye were initially recruited based on slit lamp biomicroscopy and FA findings. Eighteen had SRF on OCT, suggesting active CNV and were excluded.

Twenty patients (mean age=76.3 years; range=65 - 85) had bilateral AMD meeting the enrolment criteria. In 4 patients (20%) OCT scans passing through the fovea could not be obtained due to erratic fixation. 16 patients fulfilled all recruitment criteria.

The mean duration since first PDT treatment (baseline) was 20.7 months (range 12-30 months); patients had received a mean 4.5 PDT treatments (range 2-9). Dating of disease onset in the fellow eye with end-stage fibrotic scarring was not possible. The mean BCVA of the treated eye was 42.0 letters. The mean BCVA for the fellow eye was 15.0 letters. The difference of the mean was significant between the two groups ($p<0.005$). Based on the GLD 50% of patients had symmetrical scars. Of these eight patients, four had scars <3500 μm in both eyes (i.e. small) and four

had scars with GLD between 3500 and 5000 μm (i.e. medium). All large scars belonged to the untreated eyes.

Mean OHRBT was 255.6 microns in the treated eye and 350.8 microns in the untreated fellow eye (p=0.001). Mean NFT was 130.25 microns in the treated eye and 79.88 microns in the fellow untreated eye (p=0.017) (Table 6.1). There was no statistically significant correlation between NFT and OHRBT, NFT and VA or OHRBT and VA in both treated and untreated eye. However if the OHRBT and VA of both eyes were pooled and analysed together the relationship between the two groups showed a trend association (p=0.06) (Figure 6.4). There was no statistically significant relationship between NFT and VA even when the data was collated.

Table 6.1: Mean of outcome measures between eyes with bilateral end-stage CNV.

Measurements	PDT eye (Treated)	Fellow eye (Untreated)	P-value
Mean VA (letters)	42±14	15±18	<0.005
Mean NFT (microns)	130.3±61	79.9 ±61	<0.05
Mean OHRBT (microns)	255.6±76	350.8 ±124	<0.005

NFT, neuroretinal foveal thickness; OHRBT, outer high reflectivity band thickness; PDT, photodynamic therapy; VA, visual acuity.

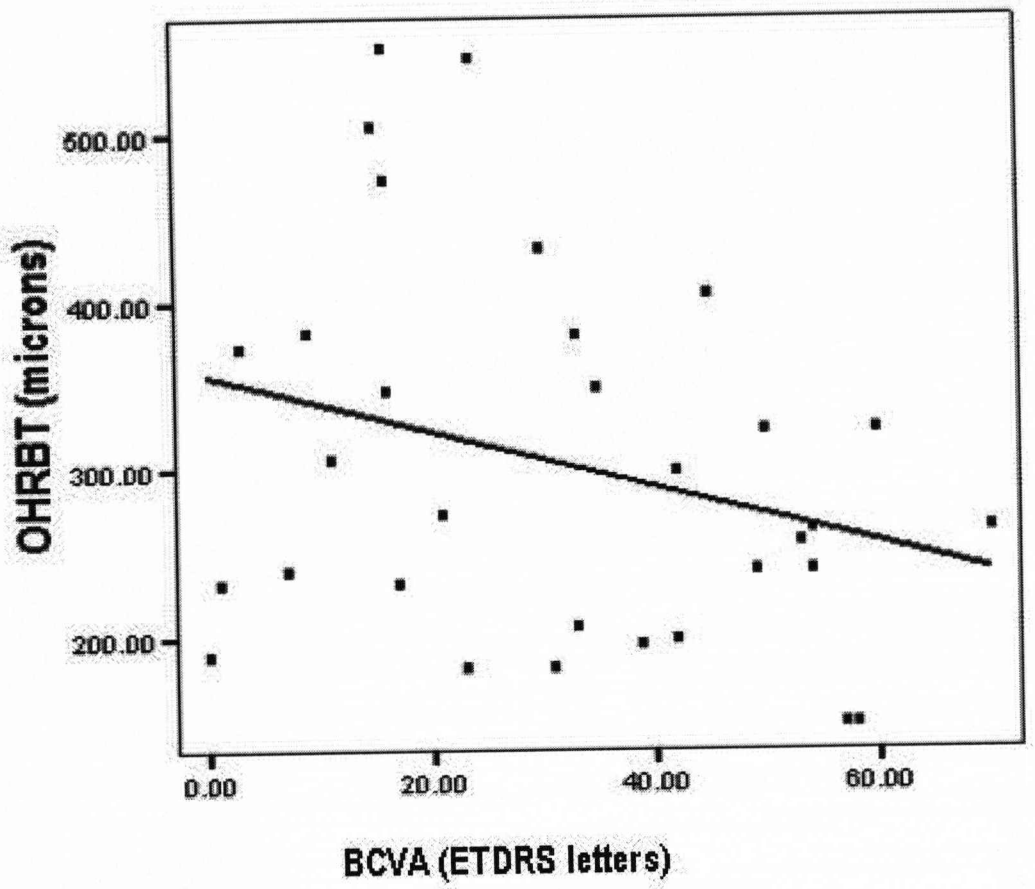

Figure 6.4: Relationship between best corrected visual acuity (BCVA) (in letters) plotted against outer high reflectivity band thickness (OHRBT) in microns. The linear regression line is $y = -1.68x + 356.39$, $P = 0.06$.

6.5 DISCUSSION

There was a statistically significant difference in the VA, NFT and OHRBT between eyes treated with PDT and untreated fellow eyes. The VA in the treated eyes was significantly better. The scars in the treated eyes were thinner in cross-section and the neuroretina was better preserved. These observations on OCT are supported by histopathological studies that have shown that eyes with thicker disciform scars were associated with more severe photoreceptor loss.[51, 52] Verteporfin PDT is thought to cause selective occlusion of the subretinal capillary layer with minimal involvement of the overlying retina and choroid in various

animal experiments.[111, 113] Based on this study it can be hypothesised that the benefit in vision preservation may also be due to the reduction in the thickness of the fibrosed scar which may prevent further neuroretinal damage and photoreceptor loss.

While the choice of the fellow eye as a control may introduce an inter-eye correlation bias, in this study the use of the fellow eye as a control group is justified because of the following reasons: (i) AMD is a bilateral condition that tends to be fairly symmetrical in its presentation and natural course. A number of studies have assessed the overall risk of development of CNV in the fellow eye. In the MPS study, 42% of fellow eyes progressed to neovascular AMD at 5 years. (ii) Although it is possible that the lesion composition may differ between the two eyes, most studies suggest that the type of CNV in the first eye predicts the type of CNV in the second eye. Sixty-three per cent of eyes with classic-only CNV in one eye developed a classic-only CNV in the fellow eye in the MPS study.[176] Chang *et al.* found that 84–87% patients with occult CNV developed the same type of occult CNV in their other eye.[177] (iii) Evidence from Lavin et al and Bird et al suggests that the final outcome in bilateral neovascular AMD tends to be similar.[168, 169] Lavin et al found that the degree of concordance increased from 54% to 68% with a 12 month follow up. Although the size of the scar was not a factor for inclusion into this study, 50% of patients had symmetrical scars in terms of GLD. (iv) This study did not attempt to correlate scar thickness with the horizontal dimension of the scar.

6.6 CONCLUSION

The aim of this study was to show that scar thickness is an independent risk factor for visual loss secondary to photoreceptor loss. Before the advent of the OCT3, it has not been possible to study the thickness of the scar in an *in vivo* situation. Hence, there have been no previous studies to show that scar thickness tends to be symmetrical. As 50% of our patients had symmetrical GLD, it is possible that the thickness of the disciform scar may be an independent factor for visual outcome.

Chapter 7

OCT IN NEOVASCULAR AMD A LONGITUDINAL STUDY

7.1 INTRODUCTION

Until recently, age-related macular degeneration (AMD) studies such as the Macular Photocoagulation Study, the treatment of age-related macular degeneration with photodynamic therapy (TAP), and others have used fluorescein angiography (FA) to determine the need for treatment. The introduction of optical coherence tomography (OCT), with its ability to take high resolution cross-sectional images, into the field of retinal imaging was thought to herald a new era which would allow appreciation of disease origin and early detection. As the OCT is less invasive than the FA, pharmaceutical trials are now beginning to use OCT to monitor the response to treatment in neovascular AMD. They base their decision on reports of the OCTs ability to detect the presence of retinal and macular oedema in neovascular AMD, which have mainly been descriptive. There have been no studies that compare retinal morphologic features and quantitative measures of thickness over time in a given patient's eye or among patients within a study, or that critically evaluate the specificity and sensitivity of OCT when compared to FA.

7.2 AIMS

The purpose of this study was to evaluate the role of OCT in the detection and follow-up of patients with neovascular AMD. This study was designed to i) investigate the response of the retina and choroidal neovascularisation (CNV) to a course of photodynamic therapy (PDT); ii) evaluate the role of OCT in decision making for PDT; iii) identify OCT features associated with worse outcome; iv) to study if there is a specific pattern of evolution/ regression of the retina and CNV on OCT following PDT.

7.3 PATIENTS AND METHODS

Consecutive patients with subfoveal predominantly classic choroidal neovascularisation (CNV), eligible for PDT as per TAP criteria, were recruited into this study at baseline and followed up prospectively at 3 monthly intervals up to 12 months. All patients also underwent refraction protocol best corrected visual acuity (BCVA) measurement, FA and fundus examination at each visit. Six, radial scans passing through the fovea of default length 6mm were obtained and serial evaluation with OCT was performed at baseline, 3, 6, 9 and 12 months. All patients received verteporfin PDT at baseline and at follow-up examinations every 3 months if angiography showed fluorescein leakage.

Based on the OCT appearance of the outer high reflectivity band at baseline the CNV was defined as: type A if there was a well-defined fusiform thickening of the outer high reflectivity band (Figure 7.1); type B in the presence of a poorly defined thickening of the outer high reflectivity band (Figure 7.2); and type C if there was pigment epithelial detachment (PED) (Figure 7.3).

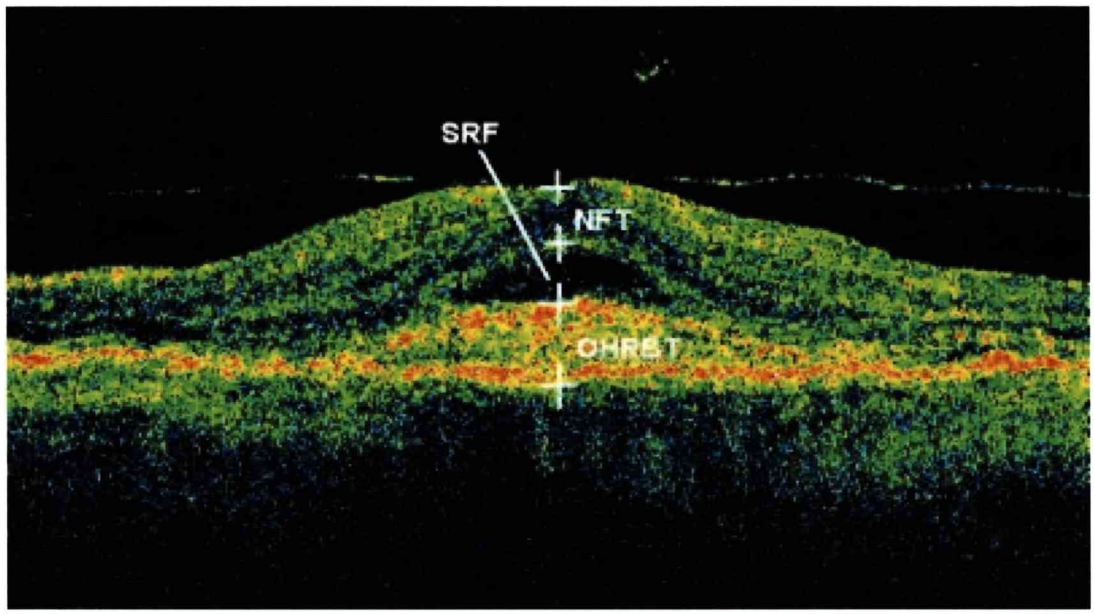

Figure 7.1: Type A choroidal neovascularisation showing well defined fusiform thickening of the outer high reflectivity band.

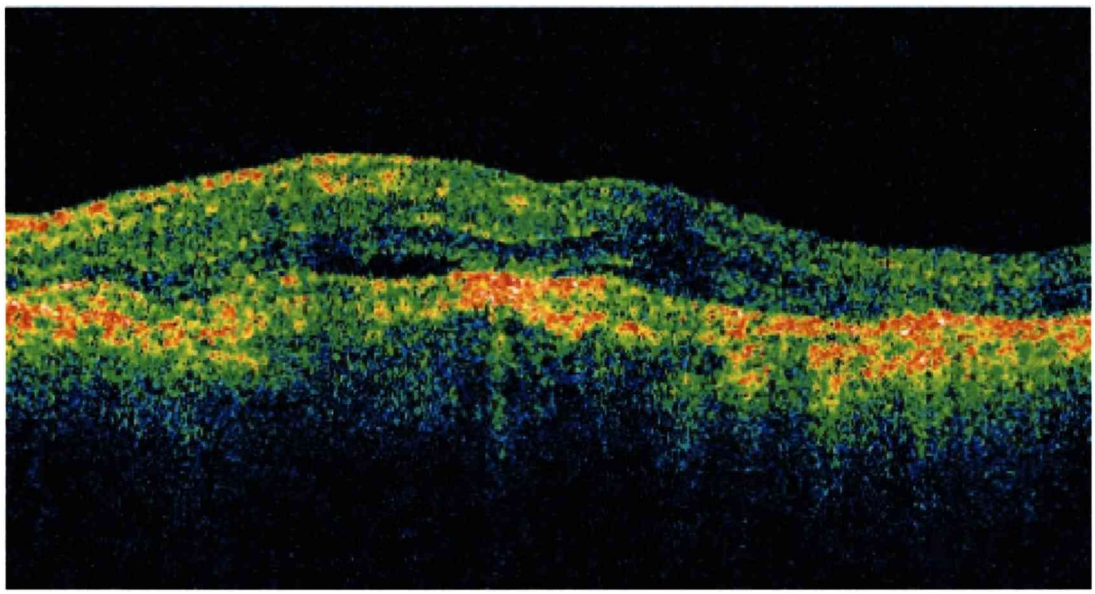

Figure 7.2: Type B choroidal neovascularisation shows a poorly defined thickening of the outer high reflectivity band (OHRB) and the posterior limit of the OHRB cannot be delineated.

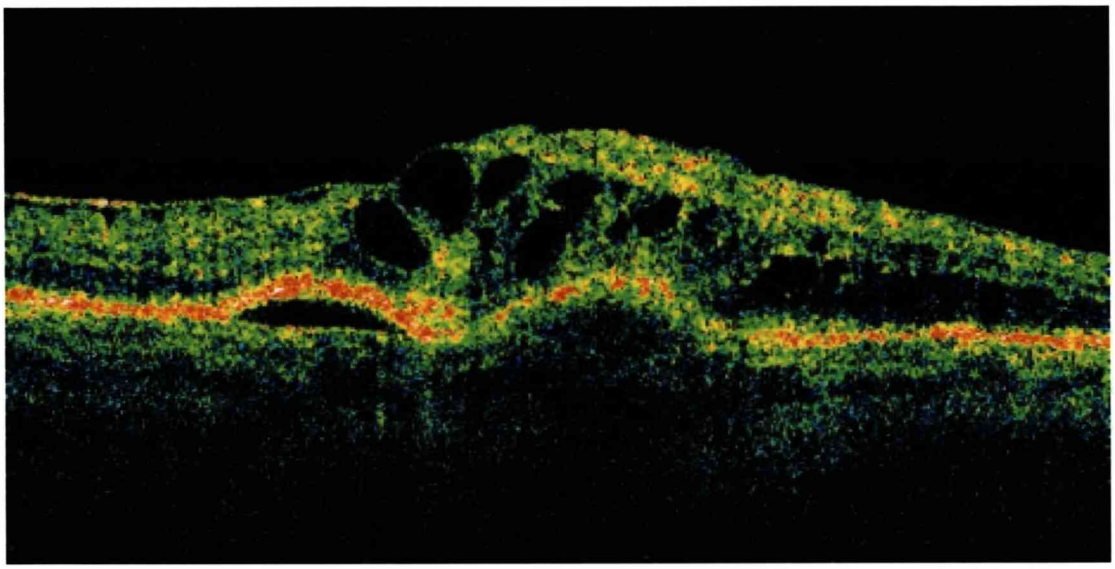

Figure 7.3: An example of Type C choroidal neovascularisation showing a bilobed elevation of the outer high reflectivity band (arrows) and shadowing of the choroidal reflections due to retinal pigment epithelial detachment.

The mean central foveal thickness in healthy eyes using the Stratus OCT (OCT3) has been shown to be approximately 180±20 μm.[178] If the NFT was >200μm, and/ or if IRF and/ or SRF was present, the OCT was recorded as positive for the presence of fluid. These parameters were then independently correlated with FA evidence of leakage.[179]

Well defined intraretinal hyporeflective spaces within the neuroretina at the fovea separated by reflective septae were identified as intra-retinal fluid (IRF) and separation of the neuroretina from the outer high reflectivity band by a well defined hyporeflective space at the fovea was taken to indicate the presence of sub-retinal fluid (SRF).

Neuro-retinal foveal thickness (NFT), bilaminar foveal thickness (BFT) and outer high reflectivity band thickness (OHRBT) were measured at the foveal centre by manually positioning the callipers on the scans and using the retinal thickness (single eye) quantitative analysis protocol offered by Stratus OCT3 as previously described.

In order to record the response of the retina and CNV to PDT longitudinally over a period of 12 months, OCT features were analysed and a 3-stage classification system proposed.

Inorder to ensure that the overall chance of making a type I error is less than 0.05, the Bonferroni multiple comparison correction was made. Therefore, as I was testing 10 outcomes, the Bonferroni adjusted p-values were obtained by multiplying the obtained value by 10. This is reflected in the values described in this section.

7.4 RESULTS

Eighty eyes of 74 patients with subfoveal CNV secondary to AMD and meeting the study eligibility criteria at presentation were included in this study. In 6 patients both eyes were involved. 70 eyes had "classic without occult" subfoveal CNV and 10 eyes had "predominantly classic" subfoveal CNV. Thirty-four patients were male and forty patients were female. The average age was 78 ± 6.8 SD years.

Thirty-nine eyes had type A CNV (well-defined fusiform thickening of the outer high reflectivity band), 40 had type B (i.e. ill-defined thickening of the outer high reflectivity band) and only 1 eye had type C CNV (PED).

7.4.1 OCT and BCVA

At baseline there was a statistically significant difference between the mean BCVA of eyes with type A (54±11 letters) compared to type B CNV (48±10 letters) ($p=0.01$). BCVA was worse in eyes with IRF ($p<0.02$), thicker NFT ($p<0.05$) and thicker OHRBT ($p<0.05$).

There were no statistically significant associations between BCVA and any of the OCT measurements post-treatment. Table 7.1 and Figure 7.4 summarise the change in the OCT measurements over time, i.e. the response of the retina and CNV to PDT at 3 monthly intervals for a year. Overall, there was a restoration to a near normal foveal contour and retinal thickness with the maximum reduction occurring in the first 3 months. BFT approached 180 microns by around 9 months indicating clearance of SRF. There was no statistically significant change in OHRBT over the 12 month period.

Table 7.1: Mean absolute OCT measurements (±95% confidence limits) and BCVA (letters) with mean change (δ) from month 0 (baseline visit for PDT treatment). P values relate to paired t-test performed on data collected from the same eye on both occasions. * $p<0.005$, † $p<0.05$.

Measurement	0 month	3 months	6 months	9 months	12 months
NFT (μ)	227 (±79)	184 (± 77)	190 (± 95)	176 (± 122)	131 (± 26)
	δ	-42.2 *	-29.6	-65.2†	-91.4†
BFT (μ)	309 (± 172)	217 ± 102	224 ± 102	183 ± 125	131 ± 26
	δ	-97.7*	-119.6 †	-145.0*	-68.5†
OHRBT (μ)	246 (± 131)	243 ± 99	250 ± 106	245 ± 105	216 ± 75
	δ	-16.9	-98	-69	-57.8
BCVA (no. of letters)	52 ± 11	47 ± 14	43 ± 15	42 ± 19	40 ± 13
	δ	-5.5 *	-11*	-12†	-9.5

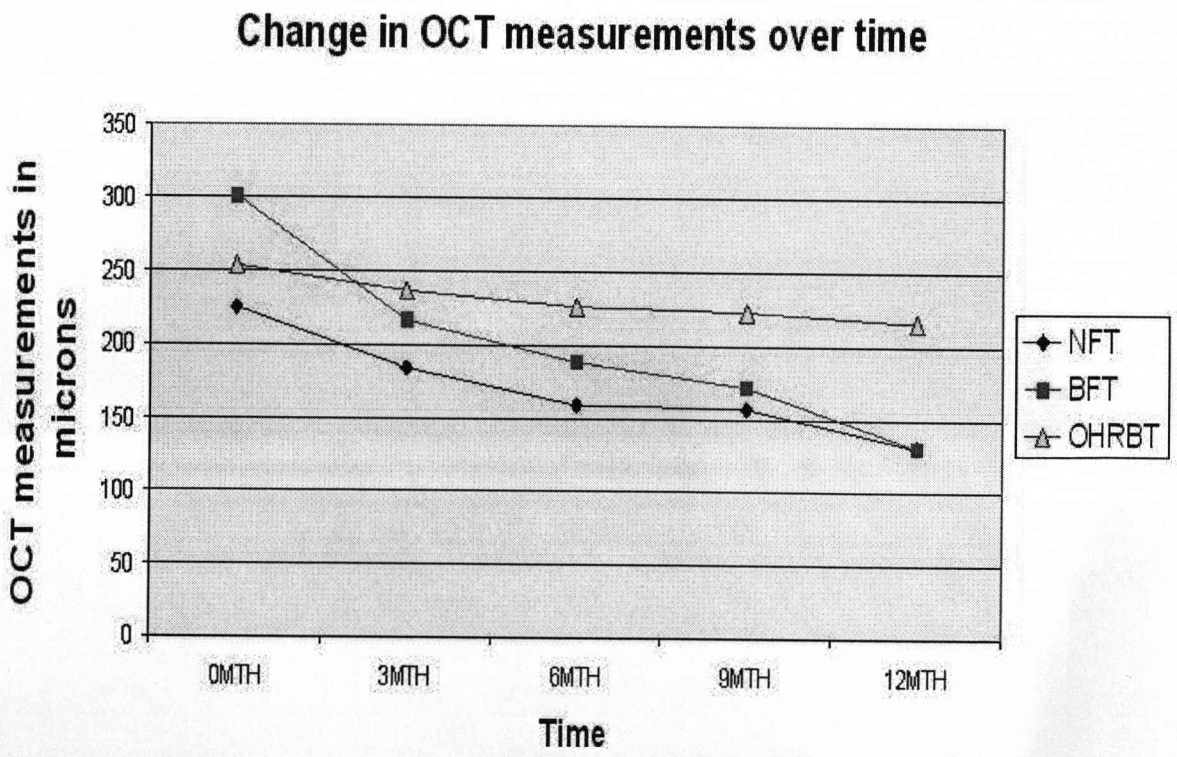

Figure 7.4: Shows the change in OCT measurements over a period of 12 months. (OCT, Optical coherence tomography; NFT, Neuroretinal foveal thickness; BFT, Bilaminar foveal thickness; OHRBT, Outer high reflectivity band thickness)

7.4.2 Macular oedema on OCT

Treatment with PDT is based on FA presence of leakage, which can accumulate in the sub-retinal space or within the retina resulting in CMO and increased retinal thickness. At baseline, 95% (76 of 80 eyes) eyes had fluid on OCT, 59.2% had SRF and 98.7% had IRF and/or NFT >200 μm. At 3, 6, 9 and 12 months this had fallen to 81.2%, 65.9%, 56.5% and 37.5% respectively. The distribution of fluid is summarised in Table 7.2. By 3 months, IRF had reduced to 44.2% and SRF to 48%. At 6 months, although there was an overall reduction in fluid, there was reaccumulation of SRF and IRF in some eyes where the fluid had previously disappeared resulting in 54.8% eyes with SRF and 51.6% with IRF. Further resolution of fluid took place over the next 3 months with restoration of the foveal contour and at 9 months SRF was present in only 46.1% and IRF in 30.7%. Majority of eyes had resolution of fluid and stabilisation of vision by 12 months although 37.5% eyes continued to have IRF. During this period there was no corresponding change in the OHRBT. Another observation was that with repeat PDT, there was a reduction in the NFT even in the absence of IRF.

Table 7.2: Number of eyes (expressed in percentage) showing subretinal fluid (SRF) and intraretinal fluid (IRF) and/ or diffuse thickening with neuroretinal foveal thickness (NFT) >200 μm at each follow-up visit.

Months after treatment	Fluid	IRF and/or NFT >200μm	SRF
0	95%	98.7%	59.2%
3	81.2%	44.2%	48%
6	65.9%	51.6%	54.8%
9	56.5%	30.7%	46.1%
12	37.5%	37.5%	0%

7.4.3 OCT and FA

Pre-treatment, all eyes had leakage on FA. Four eyes in whom leakage was present on FA did not demonstrate any fluid on OCT. Post treatment FA for the eighty eyes was done at 3, 6, 9 and 12 months. After treatment there were 320 data points at which the eyes were examined with FA and OCT. 218 of 320 (68.1%) times there was leakage on FA requiring PDT treatment. At the same time OCT was positive for fluid in 226 eyes (70.6%). In 36 eyes with leakage on FA, OCT did not detect IRF, SRF or increased NFT (Table 7.3). And in 44 eyes with fluid at the fovea on OCT, there was no evidence of leakage on FA. With FA as the current reference standard, OCT had a sensitivity of 83.3% in detecting CNV activity after treatment. However, OCT had a low specificity of 56.4%. The likelihood ratio for a positive test was 1.91 and for a negative test was 0.29. The positive predictive value (PPV) for OCT with FA as reference standard was 0.80. The parameter on OCT with highest predictive value for leakage on FA was IRF (0.87). PPV for SRF and increased NFT was 0.77 and 0.86 respectively.

Table 7.3: Cross tabulation displaying the number of eyes with leakage on FA and OCT following baseline treatment.

		Leakage on FA		Totals
		Absent	Present	
Fluid on OCT	Absent	58	36	94
	Present	44	182	226
Totals		102	218	320

7.4.4 OCT classification

We tried to identify features that would place the eyes in the Rogers et al.[96] described 5 stage classification system to monitor the response of the eyes undergoing PDT. But we found the Rogers et al classification difficult to use in a clinical situation of 3 monthly visits. None of the eyes at the post-treatment visits corresponded to the Rogers et al stage 1 or stage 2.

Hence I developed a 3-stage classification that can be applied in a clinical scenario for patients undergoing novel treatments for neovascular AMD. This was a modification of the existing Rogers et al classification.

Stage 1: If the scans showed any fluid (i.e. IRF/ or NFT>200 μm or SRF) (Figure 7.5). This stage was further sub classified as 1A and 1B based on fluid to fibrosis ratio, i.e. NFT/ OHRBT or BFT/ OHRBT.

1A: If NFT/ OHRBT or BFT/ OHRBT >1.

1B: If NFT/ OHRBT or BFT/ OHRBT <1.

Stage 2: When there was no evidence of SRF and IRF on OCT and the retinal thickness approximated to normal (180±20) (Figure 7.6).

Stage 3: If there was no evidence of SRF and IRF on OCT and the retinal thickness was less than normal i.e. NFT <150 μm, suggesting retinal atrophy (Figure 7.7).

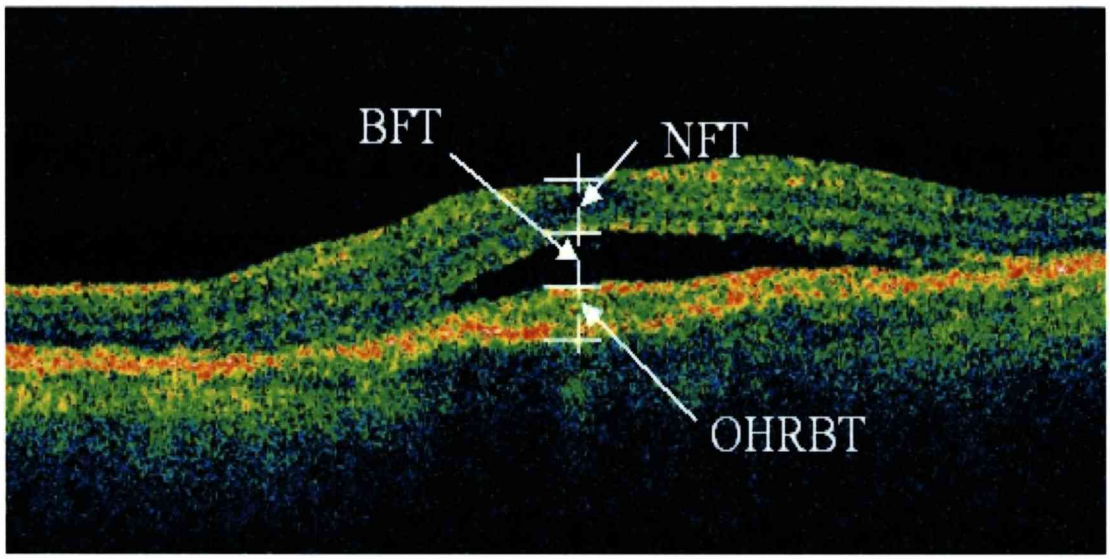

Figure 7.5: Stage 1A: Optical coherence tomography scan taken at 3-month follow-up in an eye with subfoveal predominantly classic CNV. In this image the neuroretinal foveal thickness (NFT) = 190 μm, bilaminar foveal thickness (BFT) = 365 μm and the outer high reflectivity band thickness (OHRBT) = 216 μm. BFT/OHRBT >1 and therefore the choroidal neovascularisation is still active.

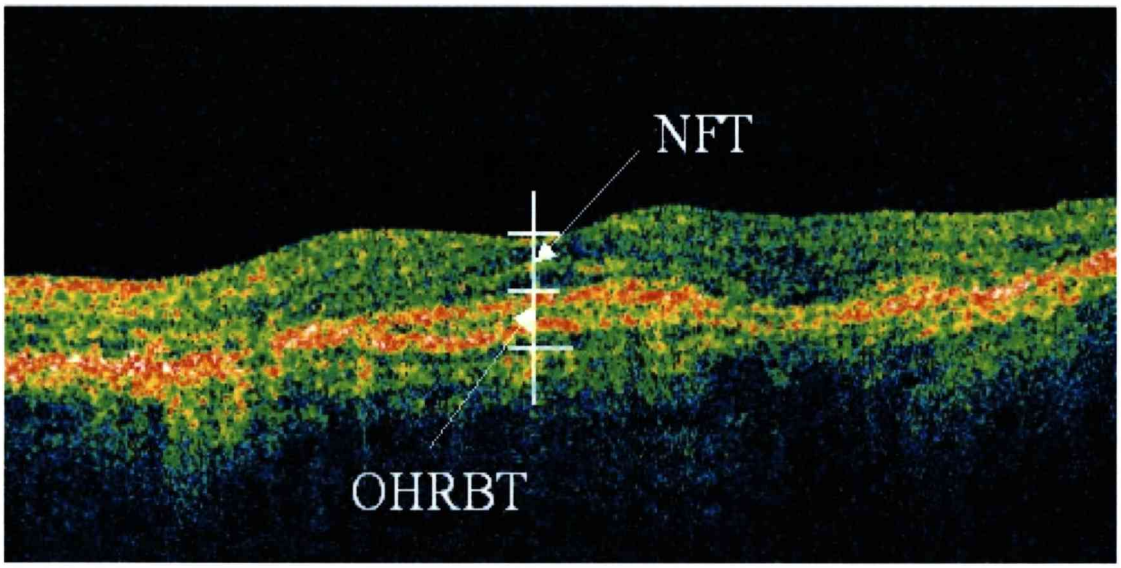

Figure 7.6: Stage 2: Optical coherence tomography scan from the same patient at 6 month follow-up shows absence of hyporeflective spaces (intraretinal fluid (IRF) or subretinal fluid (SRF)). The neuroretinal foveal thickness (NFT) = 190 μm and is within normal range. There is no sign of any active choroidal neovascularisation.

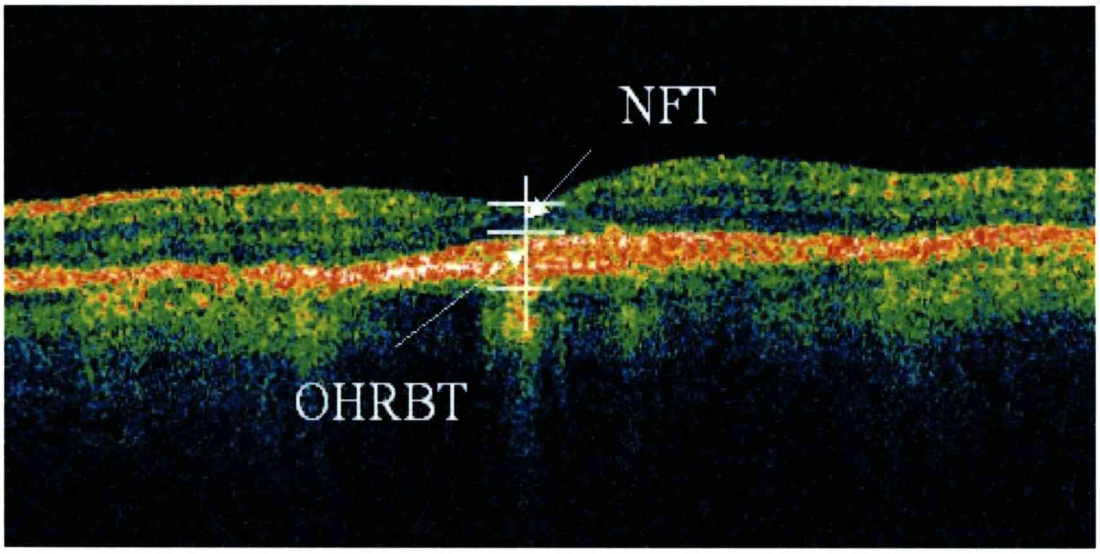

Figure 7.7: Stage 3: Optical coherence tomography scan at the 12-month follow-up visit shows a thin and atrophic neuroretina (neuroretinal foveal thickness (NFT) = 100 μm).

On assessing the scans, this classification system was easily applicable (Table 7.4). At 3 months, majority (53.75%) of the eyes belonged to stage 1A with fluid to fibrosis ratio >1. 27.5% were in stage 1B. 12.5% showed no evidence of fluid on the OCT scan and had a normal retinal thickness, i.e. stage 2, and 6.25% already showed signs of retinal atrophy (stage 3). At 6 months, there were 47.5%, 18.75%, 6.25% and 27.5% in stage 1A, 1B, stage 2 and stage 3 respectively. By 9 months there were 35 eyes (43.75%) in stage 1A, 10 eyes (12.5%) in stage 1 B, 10 eyes (12.5%) in stage 2 and 25 eyes (31.25%) showing retinal atrophy and stage 3. At 12 months the numbers in each category were 20 eyes (25%) in stage 1A, 10 eyes (12.5%) in stage 1B, 10 eyes (12.5%) in stage 2 and 40 eyes (50%) in stage 3. Vision in eyes with stage 3 was on an average worse than the vision in the group as a whole at each of the post-PDT visits. At 3, 6, 9 and 12 months the VA (in letters) was 36.3±18.78, 38.07±20.15, 29.22±16.58 and 28.75±7.63 respectively.

Table 7.4: Number of eyes (expressed in percentage) at each stage of the OCT classification at each follow-up visit.

Months since baseline	Stage 1A	Stage 1B	Stage 2	Stage 3
3	53.75	27.5	12.5	6.25
6	47.5	18.75	6.25	27.5
9	43.75	12.5	12.5	31.25
12	25	12.5	12.5	50

7.5 DISCUSSION

This was a prospective longitudinal study on eyes undergoing PDT for subfoveal predominantly classic CNV secondary to AMD.

At baseline, seventy-nine out of the eighty eyes (98.75%) recruited on FA findings, and meeting the TAP criteria, had an increase in the OHRBT, suggesting the presence of CNV on OCT. There were equal numbers of eyes with well-defined type A (48.75%) and poorly defined type B (50%) appearance of the CNV. In 56 eyes with predominantly classic CNV on FA, Sandhu et al[93] reported that 78.5% had our type A and the rest had type B on OCT. In a population such as ours Salinas et al[180] identified a well-defined CNV complex on OCT in 60% of the 62 eyes at baseline and 6-month follow-up visits. PDT disrupted the OCT appearance of the lesions and after a few sessions of PDT, the appearance had altered.

At baseline, VA was worse in eyes with type B compared to type A CNV ($p=0.01$). VA was worse in eyes with IRF ($p<0.02$), thicker NFT ($p<0.05$) and thicker OHRBT ($p<0.05$). Unlike expected, vision was not worse in eyes with SRF (i.e. thicker BFT). Ting et al (2002) reported similar findings in a cohort of 61 eyes. Salinas et al (2005) could not find an association between their retinal thickness measurements and vision in their pre-treatment group. This may be because unlike Ting et al, and us they did not distinguish between intra and subretinal fluid and their retinal thickness measurements included both the IRF and SRF.

There was a statistically significant reduction in the retinal thickness (NFT and BFT) following PDT. The maximum resolution of IRF took place in the first 3 months. SRF took a longer time to disappear, 9 months. During the same period, there was no statistically significant increase or decrease in the CNV thickness.

Salinas et al also reported an overall reduction in macular thickness measurements at 6 and 12-month follow-up. They do not however differentiate between NFT and BFT.

Following PDT a statistically significant relationship between NFT and OHRBT and VA could not be demonstrated. In the cross-section of patients at various stages of their PDT treatment, (chapter 4) a statistically significant relationship between OHRBT and VA was present. A likely explanation for this is that while patients in that study had a mean of 2.57 PDT treatments as opposed to this group where the mean number of treatments was 3.25 (range, 1 to 4) (mean TAP group 3.4). This may have caused greater atrophy of the retina and disruption of the RPE/ CNV complex in turn leading to errors in the measurement of the OHRBT or a thinner OHRBT and hence the results are not similar.

Pre-treatment OCT correctly identified presence of fluid in 95%. With FA as the current reference standard, OCT had a sensitivity of 83.3% and a low specificity of 56.4% in detecting CNV activity after treatment. These values are similar to Salinas et al's findings of 95.65% and 59.01% respectively.[180] We found the positive predictive value (PPV) for OCT with FA as reference standard was 0.80. The parameter on OCT with highest predictive value for leakage on FA was IRF (0.87). PPV for SRF and increased NFT was 0.77 and 0.86 respectively. While comparing OCT with FA, it will be prudent to remember that OCT scans show collection of fluid as IRF, SRF and PED, which may be the FA equivalent of pooling of the dye while leakage on FA without collection of fluid may not be actually demonstrable on OCT.

We tried to identify features that would place the eyes in the Rogers et al. described 5 stage classification system to monitor the response of the eyes undergoing PDT.

Rogers et al. imaged their patients between 1 hour and 1 week following PDT. This is unlike what happens in a clinical setting where the patients are examined at 3 monthly intervals.[21, 22] We found the Rogers et al classification difficult to use in a clinical situation. Also it is dependant on FA features and cannot be used in isolation. None of the eyes at the post-treatment visits corresponded to the Rogers et al stage 1 or stage 2. Hence we proposed a modification which included retinal and OHRB thickness measurements, which we found, was easily applicable in order to monitor the response of the eyes undergoing PDT. Fluid and fibrosis are the main indicators of CNV activity and hence stage 1 represented persistent CNV activity with presence of IRF and / or SRF and was divided based on fluid to fibrosis ratio greater and less than 1 as stage 1A and stage 1B respectively. Our stage 2 may have included some of the eyes that would have been classified as stage 4 by Rogers et al. We classified eyes with no fluid on OCT and retinal thickness approximating normal as stage 2. In stage 3 eyes the atrophic retina measured as <150 microns on the OCT. Over a period of 12 months, there was a steady decline in the number of eyes with IRF/SRF on OCT. 37.5% showed persistent fluid on OCT at 12 months and were in stage 1 while 62.5% eyes had complete resolution of SRF and IRF. PDT appears to cause neuro-retinal atrophy and 50% exhibited stage 3 at 12 months. While there was no statistically significant association between vision and NFT, eyes with stage 3 had worse vision. We believe this modified OCT classification may have a clinical application in eyes undergoing treatment, PDT and others, for exudative AMD. Eyes in stage 1 require treatment while those in stage 2 and 3 can be observed.

The strengths of this study lie in the prospective nature of data collection. All scans were performed by me and all the eyes reviewed had good quality scans. As the

vision deteriorates and fixation becomes unstable, acquisition of the scans can become difficult. The patients in this study were scanned only up to 12 months post-treatment and it is possible with further follow-up, scans may not have been acquirable or readable. The main limitation of this study is that the patients were treated on FA parameters. Hence, it is difficult to accurately predict the OCT features signifying worse outcome.

7.6 CONCLUSION

In summary, I have demonstrated that OCT classification of lesions at baseline does not follow currently known FA definitions. There was a reduction in retinal thickness with resolution of IRF and SRF following PDT. There was no corresponding change in thickness of the RPE/CNV complex. Worse outcome appears to be associated with retinal atrophy and persistent fluid.

I have also described a 3 stage OCT based classification system that is independent of FA and can be used to monitor the response of the retina and CNV to a course of treatment. As we move into the realm of anti-VEGF treatment, and OCT is gaining wider application, with some places using only OCT to manage patients following the initial diagnosis, the classification system proposed here could be valuable.

Chapter 8

DISCUSSION

In this final chapter I will summarise the previous literature on the use of optical coherence tomography (OCT) in neovascular age-related macular degeneration (AMD), and review the aims of this thesis. I will then discuss the findings of my studies in relation to these aims. I will also discuss the role of other emerging ophthalmic imaging technologies in the detection and management of AMD.

8.1 SYNOPSIS OF PREVIOUS LITERATURE

Prior to the work included in this study Toth et al and Fukuchi et al had shown in animal experiments that OCT could demonstrate the positional relationship between choroidal neovascularisation (CNV) and the retina.[82, 91] Hee at al had documented and published photographic examples of OCT features of AMD.[92] Ting et al reported that the presence of CMO on OCT was associated with worse vision.[94] Rogers et al described a 5 stage classification system based on OCT findings of the retina and CNV following photodynamic therapy (PDT) with verteporfin.[96] All these studies were retrospective, used unvalidated, non standardised techniques in interpreting the scans and were mainly descriptive.

A histological study by Green and Enger in 1992 suggested that photoreceptor cell degeneration was progressively greater as the diameter and thickness of the end-stage CNV (disciform scar) increased.[51] In disciform scars greater than 0.2mm in thickness, only approximately 25% of the surface of the scar had some remaining photoreceptor cells. Further histological work by Kim et al in 2002 showed a

reduction in the outer nuclear layer, but a good preservation of cells in the inner nuclear layer and ganglion cell layer, overlying disciform scars.[52]

Prior to the studies presented in this thesis, standardised definitions of OCT features and measurements were not available. The relationship between OCT characteristics and FA features, OCT measurements and visual outcome had not been fully elucidated. The change in OCT over a course of treatment had not been investigated in a prospective study.

8.2 REVIEW OF AIMS

The overall aim of my MD thesis is to evaluate the role of OCT in the management of patients with subfoveal neovascular AMD. Specific objectives were:

(i) To test the feasibility of doing OCT in an aging population with this disabling eye disease.

(ii) To define macular features of neo-vascular AMD on OCT and validate the technique of acquiring and interpreting OCT scans in AMD.

(iii) To define the relationship of the findings on OCT to overall disease process by relating the scans to visual outcome and FA.

(iv) To determine if OCT can be used to monitor the response of the retina to a course of treatment.

(v) To develop diagnostic and analysis criteria for OCT based on our observations.

8.3 FACTORS AFFECTING QUALITY OF OCT SCANS

Measurements on the OCT scan and their test-retest reliability in subfoveal neovascular AMD depend on the ability to acquire good quality scans that consistently pass through the fovea. Since OCT is a non-invasive technique, scanning was well tolerated by the majority of patients and good quality scans could be acquired quickly and easily from 90% of the patients. However in 10% of patients good quality scans could not be acquired in this population. Rogers et al also had similar findings.[96] The quality of the scan also depends on the patient's ability to keep the eye steady; even the slightest eye movements can cause significant motion artefacts in the scan. Data using microperimetry have shown that patients with subfoveal CNV due to AMD have a progressive deterioration of retinal fixation (unstable fixation) and macular sensitivity.[181] The Stratus OCT3's efficacy in these eyes was also partly limited by the time taken for the acquiring a line scan (1.92 seconds).

OCT is an optical system which constructs transverse retinal images from light reflected from within the eye. Any factor that affects the ability of light to travel through to the retina is likely to compromise image quality. Corneal drying, cataract and posterior capsular opacification may be associated with reduced intensity per pixel of the scans, lower returning signal strength and loss of intraretinal details and can cause difficulty with retinal thickness measurements.[182, 183] While the inner high reflectivity band could be observed in all patients, errors in delineating the outer limit of the outer high reflectivity band were a confounding feature in the interpretation and measurement of scans. The reflection from fluid such as seen in haemorrhagic or serous PED can attenuate the reflections from the choroid. In the presence of atrophy there is increased reflectivity from this layer due to increased

transmission of the light through an atrophic RPE. It can also be difficult to distinguish serous from haemorrhagic PED on OCT. (Appendix 2)

Thus, a technology such as the OCT that is highly precise under ideal conditions may be subject to large and long term fluctuations due to subject factors.

8.4 OCT SCAN GRADING PROTOCOL

A protocol to assess the OCT scans was developed and validated. Multiple morphological parameters were observed in patients with neovascular AMD. Terminology developed to interpret these features on the scans included definitions for intra and sub retinal fluid (IRF, SRF), retinal thickness measurements (NFT and BFT) and RPE/CNV thickness measurement (OHRBT) and was found to have a high degree of interobserver concordance in its grading and quantification.

Manually positioned computer callipers were used to perform thickness measurements on cross-sectional line scans. This was because of artefacts induced by misidentification of the retinal surfaces by the computer algorithm provided with the OCT software.[184] Recommendations from the results of studies in this thesis are that this is the most appropriate method of quantification. The terminologies developed for this study have been adopted by the Network of Ophthalmic Reading Centres UK (NetwORC).

Overall, our results suggest that data obtained from the OCT scans were reproducible and could be used in longitudinal studies to monitor response to treatment. Manually placed callipers are the method of choice at present, but care needs to be taken while interpreting the features and measurement of the outer high reflectivity band.

8.5 ASSESSMENT OF MACULAR OEDEMA

Retinal and macular oedema in patients with neovascular AMD can cause one or all of the following three structural patterns on OCT: i) intra-retinal fluid identified by well defined hyporeflective spaces within the neuroretina separated by hyperreflective septae, ii) subretinal fluid seen as an hyporeflective space separating the neuroretina from the outer high reflectivity band or iii) a diffuse thickening of the neuroretina (normal thickness ~180± 20μm).[178]

FA evidence of leakage is currently the reference standard for indication of CNV activity in neovascular AMD. This is usually detected as a progressive increase in hyperfluorescence during the transit of the dye in classic CNV. Using FA as the current reference standard OCT had a sensitivity of 83% and specificity of 57% in detecting fluid. The low specificity may be due to the inherent difference between the two techniques; for OCT to detect the presence of fluid there must be collection of the fluid within either the intra or subretinal space, whereas, FA is a dynamic process and, in the presence of a functioning RPE, fluid may not collect giving rise to the discrepancy. Also, difficulty distinguishing between staining and leakage on FA may underestimate the incidence of fluid at the macula.

When the findings on OCT were separately characterised as CMO and SRF and compared to FA and clinical findings the agreement between the two methods was only fair for the detection of CMO and poor for the detection of SRF. Other studies have commented on the difficulty in distinguishing between SRF and CMO angiographically in the setting of leakage from the CNV.[95]

These findings suggest that while OCT may be useful for detecting and monitoring the presence of macular oedema in neovascular AMD, care must be taken in

interpreting the results, as a disruption of RPE metabolism rather than leakage from an active CNV may be responsible.

8.6 OCT IN RELATION TO VISUAL OUTCOME

The MPS group reported that visual acuity (VA) in eyes with neovascular AMD can vary widely, even in groups with similar angiographic components and duration of disease. A reasonable hypothesis is that retinal thickness measurements should correlate with estimates of retinal dysfunction better than non-quantifiable fluorescein leakage. In addition, increase in retinal thickness may occur in the absence of detectable fluorescein leakage.

In untreated patients in our studies NFT and presence of CMO were correlated with VA. However no association was detected between SRF and VA. Ting et al reported similar findings.[94] However Salinas et al could not find this association in their treatment naïve patients. This may be because they failed to separate retinal thickness measurement from the height of SRF at the fovea. Following treatment with PDT we could not demonstrate an association between retinal thickness measurements and VA. There are three possible explanations why VA may not correlate with retinal thickness measurements in eyes treated with PDT: (i) the relationship between VA and retinal thickness maybe bimodal, with poorer VA with both increase and decrease in thickness compared to normal, (ii) patients with subfoveal CNV due to AMD may have eccentric fixation and therefore retinal thickness measurement at the fovea may not be reflective of the locus for their VA, and (ii) eyes with extensive disruption of the retinal architecture due to CMO can still have a normal retinal thickness measurement and thus retinal thickness measurement may not be a direct measure of the viability of the photoreceptors.

An interesting finding was the association between RPE/CNV complex thickness, as measured by OHRBT, at the fovea on OCT and VA. This observation on OCT is supported by histological studies that have shown that eyes with thicker disciform scars were associated with more severe photoreceptor loss. Eyes that had achieved a stable outcome following PDT were found to have thinner scar dimension on OCT suggesting that in addition to its anti-angiogenic effect, PDT may preserve VA in patients with AMD by modifying the natural history of the scarring process resulting in thinner scars, which in turn may prevent photoreceptor loss.

8.7 ROLE OF OCT IN THE MANAGEMENT OF CNV

The treatment options of CNV due to AMD have expanded in recent years. Prior to PDT the only available treatment was laser photocoagulation. Several studies now report on the use of OCT in the follow-up of patients undergoing novel therapies for wet AMD.[96, 185] However, standardised longitudinal studies have not been reported.

At the baseline visit, while OCT features such as IRF, SRF, increased retinal and RPE/CNV complex thickness are able to detect the presence of a potentially treatable lesion, it is not possible to define the exact components. This study showed that predominantly classic CNV could present either as a well-defined fusiform thickening or an ill-defined thickening of the outer high reflectivity band.

The decision to re-treat during a course of PDT is reliant in large part on FA.[186] Based on OCT 11.25% of eyes with evidence of leakage on FA would have been missed and 13.75% would have received inappropriate treatment. Unless the treatment parameters are specifically formulated based on OCT features, this confusion arising from the difference in the imaging techniques will remain.

Following treatment, OCT was found to be useful in objectively measuring the resolution of macular oedema and retinal thickness. It was possible to devise a 3 stage classification system based on the observations of the response of the retina and CNV to PDT. Stage 1 eyes show signs of active CNV and may require treatment, stage 2 eyes may be observed and followed up without treatment and stage 3 eyes showed signs of stability, including retinal and RPE atrophy. This classification system was independent of FA findings. Several studies are currently using OCT to monitor the response of CNV to intravitreal anti-VEGF therapy for CNV.[187, 188] The main outcome measures in these studies is the resolution of macular oedema and retinal thickness measurements on OCT. But confounding features such as the difference between leakage and pooling or collection without leak, as well as the integrity of the RPE have not been taken into account. In this study only 2 patients had a PED at presentation, and the underlying CNV could not be identified in them. While these numbers are small there have been similar reports of the difficulty in identifying the CNV when it is located under a serous or haemorrhagic PED (Eter et al, 2005). Further study of the two techniques in a RCT is needed to establish its usefulness in a clinical situation.

In summary, in its current form and with the available evidence, OCT cannot supplant FA in decision making for PDT treatment. However, use of OCT in conjunction with FA will likely result in improved clinical guidelines when determining the need for re-treatment with PDT and anti-angiogenic therapies.

8.8 FURTHER RESEARCH

The management of AMD has changed dramatically over the past 10 years. Although AMD continues to be a major threat to visual function, there is exciting progress in the development of new and effective treatments for this condition (chapter 2 (section 2.8)). New imaging modalities for the detection and management of AMD have evolved significantly over the past few decades. The impetus for their development stems from the growing body of research that suggests that the current methods of neovascular AMD detection such as FA and Amsler grid and visual acuity testing identify AMD too late in its course.

Visual acuity alone depends on many factors such as media opacity and is a psychophysical measurement with limited reliability. Angiography is an invasive modality not suitable for a monthly follow-up including other problems such as the inability to differentiate between leakage and staining.

The aim of further research in this field will be to develop new diagnostic strategies for treatment and follow-up adapted according to medical needs.

Although OCT offers many advantages as it is non-invasive and allows an objective measurement of extravasated fluid and retinal thickening, it does not offer much in terms of functional imaging. I believe the future direction for research in this field will be to combine the morphometric measurements obtained from the new generation spectral-OCT, fundus autofluorescence (AF) and laser doppler flowmetry (LDF) with localised objective functional information obtained from multifocal electroretinography (mfERG) and microperimetry (MP).

MfERG can provide an estimate of local retinal function, MP can chart retinal fixation to macular sensitivity, AF imaging can provide information about the health

and function of the RPE at the macula, and LDF can investigate the choroidal circulation.

8.8.1 Multifocal electroretinography (MfERG)

MfERG can be used to assess focal macular function objectively. This technique developed by Sutter and Tran allows comparative analysis between photoreceptor responses from within the visible lesion and outside the lesion, as it derives responses from a large number (usually either 61 or 103) of small retinal areas (stimulus size between one degree to five degrees) within the central 30 degrees.[189]

Initial studies in our centre have shown that central photoreceptor and bipolar cell dysfunction associated with AMD can be detected using mfERG.[190] A study by our electrophysiologists found that mfERG amplitude density in the central 5.3° was the most sensitive of the electroretinographic parameters to neovascular AMD.[191] These studies have reported the mfERG features of patients with neovascular AMD but did not compare the electrophysiologic responses with retinal thickness or OCT features. The Roland Consult Retiscan system will be used for the stimulation and acquisition of mfERG responses. A pilot study suggested that obtaining responses from the central segment might be difficult.

8.8.2 Microperimetry (MP)

Distance visual acuity is the gold standard of visual function examination. Unfortunately, visual acuity is inadequate to quantify the natural history of visual function in patients with AMD and does not provide information about retinal fixation, and presence and density of central scotoma.[192]

The MP allows reliable non invasive examination of fixation and scotoma characteristics in patients affected by macular diseases, even when visual acuity is

poor, and fixation is unstable and eccentric, as is usual in patients with neovascular AMD. With this technique, retinal fixation, foveal or extrafoveal (preferred retinal locus) and macular sensitivity may be accurately tested with strict correspondence of visual parameters to macular morphology.[193]

MP will be performed using a new automatic fundus related perimeter: the MP1 microperimeter (Nidek Technologies, Vigonza, Italy).

8.8.3 Fundus autofluorescence (AF) and laser doppler flowmetry (LDF)

AF is a property derived from lipofuscin which accumulates in aging RPE cells. The formation of lipofuscin occurs as an oxidative end product of the RPE phagocytosis of photoreceptor outer segments and consists of retinoids, fatty acids, and proteins.

LDF is a noninvasive method of measuring microvascular blood flow, which can be applied to the exposed surface of any tissue and has been previously investigated to study the microcirculation of the optic nerve head in glaucoma and malaria retinopathy.[194] Recently Metelitsina et al investigated foveolar choroidal blood flow changes associated with the development of CNV. In a longitudinal study over a 5 year period, of 135 patients with AMD and no CNV at baseline, they reported lower average choroidal blood flow and volume in eyes that developed CNV.[195]

The accumulation of waste products and drusen, between the RPE and Bruch's membrane is thought to be the clinical hallmark of AMD. Two theories on their occurrence are: (i) a primary choriocapillaris dysfunction or dropout initiates the accumulation of waste associated with Bruch's membrane;[196] (ii) a primary RPE senescence leads to decreased activity of the RPE lysosomes and accumulation of deposits.[197] Support for the vascular theory in AMD comes from: (i) delayed choroidal filling demonstrated using conventional angiographic techniques (ICG &

FA); (ii) LDF studies suggesting that decrease in the foveolar choroidal circulation, and ischaemia, precede the development of CNV.[198] On the other hand, choriocapillaris have been shown to atrophy after RPE cell loss in clinical and experimental studies.[199] Also there is histopathological evidence to suggest that aging RPE cells promote the progression of CNV by the expression of various growth factors.[200] This proposed relationship between choroidal circulation and RPE has not been previously investigated in a clinical study. Studies are planned in this area commencing in 2008. The imaging of AF will be accomplished in a noncontact and noninvasive manner using a scanning laser ophthalmoscope (Heidelberg Retinal Angiograph). Oculix Sarl LDF, developed by the Institute of Ophthalmology, Sion, Switzerland, will be used for choroidal blood flow measurements.

8.9 CONCLUDING REMARKS

OCT has heightened our awareness of the pathogenesis in AMD and represents a useful method by which re-treatment can be evaluated. This study has demonstrated that resolution of intra and subretinal fluid does not lead to vision recovery or stabilisation in all eyes. Progressive subretinal fibrosis impairs photoreceptor function and may impair the overall visual prognosis. Continuous inflammatory processes may contribute to creating a focal milieu, which is damaging to RPE cells and photoreceptors.

The encouraging results from clinical trials and preclinical evaluations have shifted the goal post from simply preventing moderate or severe vision loss to those of restoring and improving vision in our patients. Neovascularisation as a late symptom of AMD disease involves multiple cytokines and cell types and blocking

only VEGF may not be adequate to completely and effectively promote healing. There is extensive room for improvement and the search for more effective strategies and agents is still ongoing.

We are in an exciting era in the development of retinal imaging. The use of new imaging technologies is likely to increase further over the next few decades. Despite the fact that many of the emerging technologies show great potential, they need to be carefully evaluated before being widely used in clinical practice. Studies on the clinical relevance and effectiveness are needed to create an evidence to base clinical judgement.

REFERENCES

[1] Keeler R. Antique ophthalmic instruments and books: the Royal College Museum. Brit J Ophthalmol. 2002;86:602-3.

[2] Loring EG. Text-Book of Ophthalmology, Part 1. London: Henry Kimpton; 1892.

[3] Nordensen JW. Allvar Gullstrand (1862-1930). Doc Ophthalmol. 1962;16:283-337.

[4] Duke-Elder S. System of Ophthalmology Volume II. St. Louis: CV Mosby; 1961.

[5] Duke-Elder S. System of Ophthalmology Volume X. London: Henry Kimpton; 1967.

[6] Jackman WT, Webster JD. Notes and news. Science. 1886;12:455-60.

[7] Bedell AJ..Stereoscopic fundus photography. JAMA. 1935;105:1502-5.

[8] Novotny HR, Alvis DL. A method of photographing fluorescence in circulating blood in the human retina. Circulation. 1961;24:82-6.

[9] Gass JDM. Stereoscopic atlas of macular diseases: diagnosis and treatment. St.Louis: CV Mosby; 1970.

[10] Leibowitz HM, Krueger DE, Maunder LR, et al. The Framingham Eye Study monograph: an ophthalmological and epidemiological study of cataract, glaucoma, diabetic retinopathy, macular degeneration, and visual acuity in a general population of 2631 adults, 1973–1975. Surv Ophthalmol. 1980;24:335–610.

[11] Rosenberg T, Klie F. The incidence of registered blindness caused by age-related macular degeneration. Acta Ophthalmol Scand. 1996;74:399–402.

[12] Fletcher A, Donoghue M, Owen C. Low vision services for people with age-related macular degeneration in the UK: a review of services needed and pro-vision. Denbigh: Macular Disease Society, 2001.

[13] Bressler SB, Bressler NM, Fine SL. Age-related macular degeneration. Surv Ophthalmol. 1988;32:375-413.

[14] Macular Photocoagulation Study Group. Risk factors for choroidal neovascularisation in the second eye of patients with juxtafoveal or subfoveal choroidal neovascularisation secondary to age-related macular degeneration. Arch Ophthalmol. 1997;115:741-7.

[15] Ivers RQ, Cumming RG, Mitchell P, et al. Visual impairment and falls in older adults: the Blue Mountains Eye Study. J Am Geriatr Soc. 1998;46:58-64.

[16] Klein BE, Klein R, Lee KE, et al. Performance-based and self assessed measures of visual function as related to history of falls, hip fractures, and measured gait time. The Beaver Dam Eye Study. Ophthalmology. 1998;105:160–4.

[17] West SK, Munoz B, Rubin GS, et al. Function and visual impairment in a population-based study of older adults. Invest Ophthalmol Vis Sci. 1997;38:72–82.

[18] Stevenson SR, Hart PM, McCulloch DW, et al. Reduced vision in older adults with age related macular degeneration interferes with ability to care for self and impairs role as a carer. Br J Ophthalmol. 2004;88:1125–30.

[19] Rovner BW, Casten RJ, Tasman WS. Effect of depression on vision function in age-related macular degeneration. Arch Ophthalmol. 2002;120:1041–4.

[20] Brown GC, Brown MM, Sharma S et al. The burden of age-related macular degeneration: a value-based medicine analysis. Trans Am Ophthalmol Soc. 2005;103:173-86.

[21] Treatment of Age-related Macular Degeneration with Photodynamic Therapy Study Group. Photodynamic therapy of subfoveal choroidal neovascularisation in age-related macular degeneration with verteporfin: one year results of 2 randomized clinical trials – TAP Report 1. Arch Ophthalmol. 1999;117:1329-45.

[22] Treatment of Age-Related Macular Degeneration with Photodynamic Therapy (TAP) Study Group. Photodynamic therapy of subfoveal choroidal neovascularization in age-related macular degeneration with verteporfin: two-year results of 2 randomized clinical trials – TAP Report 2. Arch Ophthalmol. 2001;119:198-207.

[23] Nussbaum JJ, Pruett RC, Delori FC. Historic perspectives. Macular yellow pigment. The first 200 years. Retina. 1982;1:296-310.

[24] Hogan MJ, Alvarado J, Wendell JE. Histology of the human eye: An atlas and textbook. Philadelphia: Saunders; 1971.

[25] Pagenstecher H, Genth CP. Atlas der pathofischen Antomie des Augapfels. Wiesbaden: CW Kreiden; 1875.

[26] Hutchinson, J, Tay, W. Symmetrical central choroidoretinal disease occurring in senile persons. R. London Ophthal. Hosp. 1875;8:231-244.

[27] Oeller JN. Atlas Seltener Ophthalmoskopischer Befunde. Zugleich Evga¨nzungstateln zu dem Atlas der Ophthalmoskopie. Weisbaden: JF Bergeman; 1900–1905.

[28] Haab O. Erkrankungen der Macula Lutea. Zentralbl Augenheilkd 1885;9:384-91.

[29] Age-Related Eye Disease Study Research Group. The Age-Related Eye Disease Study system for classifying age-related macular degeneration from stereoscopic color fundus photographs: the Age-Related Eye Disease Study Report Number 6. Am J Ophthalmol. 2001;132:668–81.

[30] Ryan SJ, Mittl RN, Maumenee AE. The Disciform Response: An historical perspective. Albrecht von Graefes Arch. Klin. Ophthalmol 1980;215:1-20.

[31] Bird AC, Bressler NM, Bressler SB, et al. An international classification and grading system for age-related maculopathy and age-related macular degeneration. The International ARM Epidemiological Study Group. Surv Ophthalmol. 1995;39:367–74.

[32] Age-Related Eye Disease Study Research Group. A simplified severity scale for age-related macular degeneration:AREDS Report No.18. Arch Ophthalmol. 2005;123:1570-4.

[33] Seddon J, Sharma S, Adelman RA. Evaluation of the Clinical Age-Related Maculopathy Staging System. Ophthalmology. 2006;113:260–6.

[34] van Leewen R, Klaver CC, et al. Epidemiology of age-related maculopathy: a review. Eur J Epidemiol. 2003;18:845-54.

[35] Klein R, Klein BK, et al. The five-year incidence and progression of age-related maculopathy. Ophthalmol 1997;104:7-21.

[36] Smith W, Assink J, Klein R, et al. Risk factors for age-related macular degeneration: pooled findings from three continents. Ophthalmology. 2001;108:697–704.

[37] Green WR, Wilson DJ. Choroidal neovsacularisation. Ophthalmol. 1986;93:1169-76

[38] Macular Photocoagulation Study Group. Subfoveal neovascular lesions in age-related macular degeneration: guidelines for evaluation and treatment in the macular photocoagulation study. Arch Ophthalmol. 1991;109:1242-57.

[39] Ambati J, Ambati BK, Yoo SH, et al. Age-related macular degeneration: etiology, pathogenesis and therapeutic strategies. Suvr Ophthalmol. 2003;48:257-93.

[40] Holz FG. Autofluorescence imaging of the macula. Ophthalmologe. 2001;98:10–8.

[41] Kopitz J, Holz FG, Kaemmerer E, Schutt F. Lipids and lipid peroxidation products in the pathogenesis of age-related macular degeneration. Biochimie. 2004;86:825–31.

[42] Beatty S, Koh H-H, Henson D, Boulton M. The role of oxidative stress in the pathogenesis of age-related macular degeneration. Surv Ophthalmol. 2000;45:115-134.

[43] Ambati J, Ambati BK, Yoo SH, Ianchulev S, Adamis AP. Age-related macular degeneration: etiology, pathogenesis and therapeutic strategies. Suvr Ophthalmol. 2003;48:257-93.

[44] Zarbin MA. Current concepts in the pathogenesis of age-related macular degeneration. Arch Ophthalmol. 2004;122:598-614.

[45] Grossniklaus HE, Green WR. Choroidal neovascularisation Perspective. Am J Ophthalmol. 2004;137:496-503.

[46] Patel N, Adewoyin T, Chong NV. Age-related macular degeneration: a perspective on genetic studies. Eye. 2007 May 11.

[47] Gass JDM. Biomicroscopic and histologic considerations regarding the feasibility of surgical excision of subfoveal neovascular membranes. Am J Ophthalmol. 1994;18:285–98.

[48] Grossniklaus HE, Gass JDM. Clinicopathologic correlation of surgically-excised type 1 and type 2 choroidal neovascular membranes. Am J Ophthalmol. 1998;126:59-69.

[49] Bressler SB, Silva JR, Bressler NM, et al. Clinicopathologic correlation of occult choroidal neovascularisation in age-related macular degeneration. Arch Ophthalmol. 1992;110:827-32.

[50] LaFaut BA, Bartz-Schmidt KU, van den Broeecke C, et al. Clinicopathologic correlation in exudative age-related macular degeneration: Histological

differentiation between classic and occult choroidal neovascularisation. Br J Ophthalmol. 2000;84:239-43.

[51] Green WR, Enger C. Age-Related Macular Degeneration Histopahtologic Studies. The 1992 Lorenz E. Zimmerman Lecture. Ophthalmology. 1993;100:1519-35.

[52] Kim SY, Sadda S, Pearlman J et al. Morphometric analysis of the macula in eyes with disciform age-related macular degeneration. Retina. 2002;22:471–7.

[53] Yannuzzi LA, Negrao S, Iida T, et al. Retinal angiomatous proliferation in age-related macular degeneration. Retina. 2001;21:416–34.

[54] Yannuzzi LA, Sorenson J, Spaide RF, Lipson B. Idiopathic polypoidal choroidal vasculopathy (IPCV). Retina 1990;10:1–8.

[55] Spaide RF, Yannuzzi LA, Slakter JS, et al. Indocyanine green videoangiography of idiopathic polypoidal choroidal vasculopathy. Retina. 1995;15:100–10.

[56] Lip PL, Hope-Ross MW, Gibson JM. Idiopathic polypoidal choroidal vasculopathy: a disease with diverse clinical spectrum and systemic associations. Eye. 2000;14:695–700.

[57] Moisseiev J, Alhalel A, Masuri R, et al. The impact of the macular photocoagulation study results on the treatment of exudative age-related macular degeneration. Arch Ophthalmol. 1995;113:185–9.

[58] Margherio RR, Margherio AR, DeSantis ME. Laser treatments with verteporfin therapy and its potential impact on retinal practices. Retina. 2000;20:325–30.

[59] Bermig J, Tylla H, Jochmann C et al. Angiographic findings in patients with exudative age-related macular degeneration. Graefe's Arch Clin Exp Ophthalmol. 2002;240:169–75.

[60] Zawinka C, Ergun E, Stur M. Prevalence of patients presenting with neovascular age-related macular degeneration in an urban population. Retina. 2005;25:324-31.

[61] Olsen TW, Feng X, Kasper TJ, et al. Fluorescein angiographic lesion type frequency in neovascular age-related macular degeneration. Ophthalmology. 2004;111:250-5.

[62] Cohen SY, Creuzot-Garcher C, Darmon J et al. Types of choroidal neovascularisation in newly diagnosed exudative age-related macular degeneration. Br J Ophthalmol. 2007;91:1173-76.

[63] Ali F, Chan WC, Stevenson MR et al. Morphometric analysis of angiograms of exudative lesions in age-related macular degeneration. Arch Ophthalmol. 2004;122:710-5.

[64] Kwan AS, Barry C, McAllister IL, Constable I. Fluorescein angiography and adverse drug reactions revisited: the Lions Eye experience. Clin Experiment Ophthalmol. 2006;34:33-8.

[65] Musa F, Muen WJ, HancockR, Clark D. Adverse effects of fluorescein angiography in hypertensive and elderly patients. Acta Ophthalmol Scand. 2006;84:740-2.

[66] Holz FG, Jorzik J, Schutt F, et al. Agreement among ophthalmologists in evaluating fluorescein angiograms in patients with neovascular age-related macular degeneration for photodynamic therapy eligibility (FLAP-study). Ophthalmology. 2003;110:400-5.

[67] Zayit-Soudry S, Alfasi M, Goldsteinn M, Et al. Variability among retina specialists in evaluating fluorescein angiograms of patients with neovascular agerelated macular degeneration. Retina. 2007;27:798-803.

[68] Verteporfin Roundtable Participants. Guidelines for using verteporfin (Visudyne) in photodynamic therapy for choroidal neovascularisation due to age-related macular degeneration and other causes: update. Retina. 2005;25:119–34.

[69] Friedman SM, Margo CE. Choroidal neovascular membranes: reproducibility of angiographic interpretation. Am J Ophthalmol. 2000;130:839-41.

[70] Kaiser RS, Berger JW, Williams GA, et al. Variability in fluorescein angiography interpretation for photodynamic therapy in age-related macular degeneration. Retina. 2002;22:683-90.

[71] Macular Photocoagulation Study Group. Laser photocoagualtion of subfoveal neovascular lesions of age-related macular degeneration. Updated findings from two clinical trials. Arch Ophthalmol. 1993;111:1200-9.

[72] Coscas G, Soubrane G, Ramahefasolo C, Fradeau C. Perifoveal laser treatment for subfoveal choroidal new vessels in age-related macular degeneration. Results of arandomised clinical trial. Arch Ophthalmol 1991;109:1258-1265.

[73] Verteporfin in Photodynamic Therapy (VIP) Study Group. Verteporfin therapy of subfoveal choroidal neovascularisation in age-realted macular degeneration: two

year results of a randomised clinical trial including lesions with occult with no classic choroidal neovascularisation- report 2. Am J Ophthalmol. 2001;131:541-60.

[74] Macular Photocoagulation Study Group. Risk factors for choroidal neovascularistaion in the second eye of patients with juxtafoveal or subfoveal choroidal neovascularisation secondary to age-related macular degeneration. Arch Ophthalmol. 1997;115:741-7.

[75] Pauleikhoff D, Radermacher M, Spital G, et al. Visual prognosis of second eyes in patients with unilateral late exudative age-related macular degeneartion. Graefes Arch Clin Expt Ophthalmol. 2002;240:539-42.

[76] Huang D, Swanson EA, Lin CP, ET AL. Optical Coherence Tomography. Science. 1991; 254:1178-81.

[77] Hee MR, Izatt JA, Swanson EA, et al. Optical Coherence Tomography of the human retina. Arch Ophthalmol 1995;113:325-32.

[78] Puliafito CA, Hee MR, Lin CP, et al. Imaging of macular diseases with optical coherence tomography. Ophthalmology. 1995;102:217-29.

[79] Fujimoto JG, Pitris C, Boppart SA,Brenzinski ME. Optical Choherence Tomography: an emerging technology for biomedical imaging and optical biopsy. Neoplasia. 2000;2:9-25.

[80] Cheong WF, Prahl SA, Welch AJ. A review of the optical properties of biological tissues. IEEE Journal of Quantum Electronics. 1990;26:2166-85.

[81] Fujimoto JG, Hee MR, Huang D, et al. Optical coherence tomography of ocular diseases. 2nd ed. NJ: SLACK; 2004.

[82] Toth CA, Narayan DG, Boppart SA, et al. A comparison of retinal morphology viewed by optical coherence tomography and by light microscopy. Arch Ophthalmol. 1997;115:1425-8.

[83] Chauhan DS, Marshall J. The Interpretation of Optical Coherence Tomography Images of the Retina. Invest Ophthalmol Vis Sci. 1999;40:2332-42.

[84] Ghazi NG, Dibernardo C, Ying HS, et al. Optical Coherence Tomography of enucleated human eye specimens with histological correlation: Origin of the Outer Red Line. Am J Ophthalmol 2006;141:719-726.

[85] Drexler W, Morgner U, Ghanta RK, et al. Ultrahigh resolution ophthalmic optical coherence tomography. Nat Med. 2001;7:502–7.

[86] Gloesmann M, Hermann B, Schubert C, et al. Histologic correlation of pig retina radial stratification with ultrahigh-resolution optical coherence tomography. Invest Ophthalmol Vis Sci. 2003;44:1696–703.

[87] Anger EM, Unterhuber A, Hermann B, et al. Ultrahigh resolution optical coherence tomography of the monkey fovea. Identification of retinal sublayers by correlation with semithin histology sections. Exp Eye Res. 2004;78:1117–25.

[88] Ko TH, Fujimoto JG, Paunescu LA, et al. Comparison of ultrahigh- and standard-resolution optical coherence tomography for imaging macular pathology. Ophthalmology. 2005;112:1922.

[89] Hoang QV, Linsenmeier RA, Chung CK, Curcio CA. Photoreceptor inner segments in monkey and human retina: mitochondrial density, optics, and regional variation. Vis Neurosci. 2002;19:395–407.

[90] Toth CA, Birngruber R, Boppart SA, et al. Argon laser retinal lesions evaluated in vivo by optical coherence tomography. Am J Ophthalmol. 1997;123:188–98.

[91] Fukuchi T, Takahashi K, Uyama M, Matsumura M. Comparative study of experimental choroidal neovascularization by optical coherence tomography and histopathology. Jpn J Ophthalmol. 2001;45:252-8.

[92] Hee MR, Baumal CR, Puliafito CA, et al. Optical Coherence Tomography of age-related macular degeneration and choroidal neovascualrisation. Ophthalmology. 1996;103:1260-70.

[93] Sandhu SS, Talks SJ. Correlation of optical coherence tomography, with or without additional colour fundus photography, with stereo fundus fluorescein angiography in diagnosing choroidal neovascular membranes. Br J Ophthalmol. 2005;89:967-70.

[94] Ting TD, Oh M, Cox TA, et al. Decreased visual acuity associated with cystoid macular oedema in neovascular age-related macular degeneration. Arch Ophthalmol. 2002;120:731-7.

[95] Bressler NM, Bressler SB, Alexander J, et al. Macular Photocoagulation Study Reading Center. Loculated fluid: a previously undescribed fluorescein angiographic finding in choroidal neovascularization associated with macular degeneration. Arch Ophthalmol. 1991;109:211-215.

[96] Rogers AH, Martidis A, Greenberg PB, Puliafito CA. Optical coherence tomography findings following photodynamic therapy of choroidal neovascularisation. Am J Ophthalmol. 2002;134:566-76.

[97] Van Velthoven ME, Faber DJ, Verbraak FD et al. Recent developments in optical coherence tomography for imaging the retina. Prog Retin Eye Res. 2007;26:57-77.

[98] Yang, C. Molecular contrast optical coherence tomography: a review. Photochem Photobiol. 2005;81:215–237.

[99] Raab O. Uber die Wirkung fluoresziender staaf auf infuroriea. Z Biol. 1900;19:524.

[100] Schmidt-Erfurth U, Hasan T. Mechanisms of action of photodynamic therapy with verteporfin for the treatment of age-related macular degeneration. Surv Ophthalmol. 2000;45:195-214.

[101] Dougherty TJ, Gomer CJ, Henderson BW, et al. Photodynamic therapy. J Natl Cancer Inst 1998;90:889-905.

[102] Hasan T, Parrish JA. Photodynamic therapy of cancer. Holland JF (ed): Baltimore, Williams & Wilkins; 1997.

[103] Donati G, Kapetanios AD, Pournaras CJ. Principles of treatment of choroidal neovascularisation with phtotodynamci therapy. Semin Ophthalmol. 1999;14:2-10.

[104] Schmidt-Erfurth U, Hasan T, Gragoudas E, et al. Vascular targeting in photodynamic occlusion of subretinal vessels. Ophthalmology. 1994;101:1953-61.

[105] Soubrane G, Bressler NM. Treatment of subfoveal choroidal neovascularisation in age related macular degeneration: focus on clinical application of verteporfin photodynamic therapy. Br J Ophthalmol. 2001;85:483-95.

[106] Richter AM, Waterfield E, Jain AK, et al. In vitro evaluation of phototoxic properties of four structurally related benzo- porphyrin derivatives. Photochem Photobiol. 1990;52:495-500.

[107] Henderson BW, Dougherty TJ. How does photodynamic therapy work? Photochem Photobiol. 1992;55:145-57.

[108] Schmidt-Erfurth U, Hasan T, Schomacker K, et al. In vivo uptake of liposomal benzoporphyrin derivative and photothrombosis in experimental corneal neovascularization. Lasers Surg Med. 1995;17:178-88.

[109] Michels S, Schmidt-Erfurth U. Sequence of early vascular events after photodynamic therapy. Invest Ophthalmol Vis Sci. 2003;44:2147-54.

[110] Miller JW, Schmidt-Erfurth U, Sickenberg M, et al. Photodynamic therapy with verteporfin for choroidal neovascularisation by age-related macular degeneration: results of a single treatment in a phase I and 2 study. Arch Ophthalmol. 1999;117: 1161-73.

[111] Ghazi NG, Jabbour NM, De La Cruz ZC, et al. Clinicopathologic studies of age-related macular degeneration with classic subfoveal choroidal neovascularization treated with photodynamic therapy. Retina. 2001;21:478-86.

[112] Schmidt-Erfurth U, Laqua H, Schlotzer-Schrehard U, et al. Histopathological changes following photodynamic therapy in human eyes. Arch Ophthalmol. 2002; 120:835-44.

[113] Schlo¨tzer-Schrehardt U, Viestenz A, Naumann GOH, et al. Dose-related structural effects of photodynamic therapy on choroidal and retinal structures of human eyes. Graefes Arch Clin Exp Ophthalmol 2002;240:748-57.

[114] Houle J-M, Strong HA. Duration of skin photosensitivity and incidence of photosensitivity reactions after administration of verteporfin. Retina. 2002;22:691-7.

[115] Treatment of Age-Related Macular Degeneration with Photodynamic Therapy (TAP) Study Group. Verteporfin therapy of subfoveal choroidal neovascularisation in patients with age- related macular degeneration: additional information regarding baseline lesion composition's impact on vision outcomes – TAP Report no. 3. Arch Ophthalmol. 2002;120:1443-54.

[116] Rubin GS, Bressler NM, and the Treatment of Age-Related Macular Degeneration with Photodynamic Therapy (TAP) Study Group. Effects of verteporfin therapy on contrast on sensitivity: results From the Treatment of Age-Related Macular Degeneration With Photodynamic Therapy (TAP) Investigation – TAP Report no. 4. Retina. 2002;22:536-44.

[117] Verteporfin in Photodynamic Therapy (VIP) Study Group. Photodynamic therapy of subfoveal choroidal neovascularization in pathologic myopia with verteporfin: 1-year results of a randomized clinical trial – VIP report no. 1. Ophthalmology 2001;108:841-52.

[118] Cochrane Database of Systematic Reviews. Wormald R, Evans J, Smeeth L. Photodynamic therapy for neovascular age-related macular degeneration. Oxford: Update Software, 2003.

[119] Treatment of Age-Related Macular Degeneration with Photodynamic Therapy (TAP) Study Group. Verteporfin therapy for subfoveal choroidal neovascularization in age-related macular degeneration: three-year results of an open-label extension of 2 randomized clinical trials – TAP Report no. 5. Arch Ophthalmol. 2002;120:1307-14.

[120] Bressler NM. Verteporfin therapy of subfoveal choroidal neovascularisation in age-related macular degeneration: two-year results of a randomized clinical trial including lesions with occult with no classic choroidal neovascularization – Verteporfin in photodynamic therapy report 2. Am J Ophthalmol. 2002;133:168-9.

[121] Treatment of Age-Related Macular Degeneration with Photodynamic Therapy (TAP) and Verteporfin In Photodynamic Therapy (VIP) Study Groups. Effect of lesion size, visual acuity, and lesion composition on visual acuity change with and without verteporfin therapy for choroidal neovascularisation secondary to age-related macular degeneration: TAP and VIP Report No. 1. Am J Ophthalmol. 2003;136:407-18.

[122] Moher D, Jadad AR, Tugwell P.Assessing the quality of randomised clinical trials. Current issues and future directions. Int J Technol Assess Health Care. 1996;12:195-208.

[123] Macular Photocoagulation Study Group. Occult choroidal neovascularisation. Influence on visual outcome in patients with age related macular degeneration. Arch Ophthalmol. 1996;114:400–12.

[124] Meads C, Hyde C. Photodynamic therapy with verteporfin is effective, but how big is its effect? Results of a systematic review. B J Ophthalmol. 2004;88:212-7.

[125] Barnes RM, Gee L, Taylor S, Briggs MC, Harding SP. Outcomes in verteporfin photodynamic therapy for choroidal neovascularisation--'beyond the TAP study'. Eye. 2004;18:809-13.

[126] Ghanchi FD, Fullarton J, Blake J, Harding SP. The introduction of verteporfin photodynamic therapy in the UK: PDT users group (PDTUG) surveillance programme report 1. Eye. 2008;22:671-7.

[127] Macular Photocoagulation Study Group. Argon laser photocoagulation for neovascular maculopathy. Five-year results from randomized clinical trials. Arch Ophthalmol. 1991;109:1109–14.

[128] Macular Photocoagulation Study Group. Laser photocoagulation for juxtafoveal choroidal neovascularization. Five-year results from randomized clinical trials. Arch Ophthalmol. 1994;112:500–9.

[129] Macular Photocoagulation Study Group. Laser photocoagulation of subfoveal neovascular lesions in age-related macular degeneration. Results of a randomized clinical trial. Arch Ophthalmol. 1991;109:1220–31.

[130] Chakravarthy U, Houston RF, Archer DB. Treatment of age-related subfoveal neovascular membranes by teletherapy: a pilot study. Br J Ophthalmol. 1993;77:265-73.

[131] The Radiation Therapy for Age-related Macular Degeneration Study Group. A prospective, randomized, double-masked trial on radiation therapy for neovascular age-related macular degeneration (RAD Study). Ophthalmology. 1999;106:2239-47.

[132] Marcus DM, Peskin E, AMDRT research group. The age-related macular degeneration radiotherapy trial (AMDRT): One year results from a pilot study. Am J Ophthalmol. 2004;138:818-28.

[133] Lanzetta P, Michieletto P, Pirracchio A, Bandello F. Early vascular changes induced by transpupillary thermotherapy of choroidal neovascularisation. Ophthalmology. 2002;109:1098– 104.

[134] Newsom RS, McAlister JC, Saeed M, McHugh JD. Transpupillary thermotherapy (TTT) for the treatment of choroidal neovascularisation. Br J Ophthalmol. 2001;85:173–8.

[135] Reichel E, Berrocal A, Ip M, et al. Transpupillary thermotherapy of occult subfoveal choroidal neovascularisation in patients with age related macular degeneration. Ophthalmology. 1999;106:1908-14.

[136] Myint K, Armbrecht AM, Mon S, Dhillon B. Transpupillary thermotherapy for the treatment of occult CNV in age-related macular degeneration: a prospective randomized controlled pilot study. Acta Ophthalmol Scand. 2006;84:328-32.

[137] Jonas JB, Akkoyun I, Budde WM, et al. Intravitreal reinjection of triamcinolone for exudative age-related macular degeneration. Arch Ophthalmol. 2004;122:218-22.

[138] Danis RP, Ciulla TA, Pratt LM, et al. Intravitreal triamcinolone acetonide in exudative age-related macular degeneration. Retina. 2000;20:244-50.

[139] Challa JK, Gillies MC, Penfold PL, et al. Exudative macular degeneration and intravitreal triamcinolone: 18 month follow up. Aust N Z J Ophthalmol. 1998;26:277-281.

[140] Gillies MC, Simpson JM, Luo W, et al. A randomized clinical trial of a single dose of intravitreal triamcinolone acetonide for neovascular age-related macular degeneration: one-year results. Arch Ophthalmol. 2003;121:667-73.

[141] The Anecortave Acetate Clinical Study Group. Anecortave acetate as monotherapy for the treatment of subfoveal lesions in patients with exudative age-related macular degeneration (AMD): interim (month 6) analysis of clinical safety and efficacy. Retina. 2003;23:14-23.

[142] Russell SR, Slakter JS, Ho AC, et al. Anecortave Acetate Study Group. Anecortave acetate treatment of "dry" AMD to reduce risk of progression to "wet" AMD-The Anecortave Acetate Risk Reduction Trial (AART). Invest Ophthalmol Vis Sci. 2004;45:3134.

[143] Gragoudas ES, Adamis AP, Cunningham ET Jr, et al. Pegaptanib for neovascular age-related macular degeneration. N Engl J Med. 2004;351:2805-16.

[144] MARINA Study group: Rosenfeld PJ, Brown DM, Heier JS, et al. Ranibizumab for neovascular age-related macular degeneration. N Engl J Med. 2006;355:1419-31.

[145] ANCHOR Study group: Brown DM, Kaiser PK, Michels M, et al. Ranibizumab versus verteporfin for neovascular age-related macular degeneration. N Engl J Med. 2006;355:1432-44.

[146] Smith BT, Joseph DP, Grand MG. Treatment of neovascular age-related macular degeneration: past, present and future directions. Curr Opin Opthalmol. 2007;18:240-4.

[147] Schmidt-Erfurth U. Results from the PIER study. Asian Pacific Association of Ophthalmologists Annual Meeting (APAO). Singapore: June 2006.

[148] Fung A, Rosenfeld PJ, Puliafito C, et al. One Year Results of the PrONTO Study: An OCT-Guided Variable-Dosing Regimen with Ranibizumab (Lucentis™) In Neovascular AMD. Vitreoretinal Symposium. Frankfurt:2006.

[149] Schmidt-Erfurth UM, Gabel P, Hohman T. PROTECT Study Group. Preliminary Results from an Open-Label, Multicenter, Phase II Study Assessing the Effects of Same Day Administration of Ranibizumab (Lucentis) and Verteprofin PDT (PROTECT Study). Invest Ophthalmol Vis Sci. 2006;47:2960.

[150] Schmidt-Erfurth U, Pruente C. Management of neovascular age-related macular degeneration. Prog Retin Eye Res. 2007;26:437-51.

[151] Fine BS, Yanoff M. Ocular histology. A text and atlas, 2nd edition. Hagerstown: Harper & Row; 1979:61–127.

[152] Yang YC, Chakravarthy U, Harding S. Classifying choroidal neovascularisation in the macula. Liverpool local guidelines. April 2004.

[153] DG Altman. Practical Statistics for Medical Research. 1st edition. London: Chapman & Hall; 1991:404.

[154] Patton N, Aslam T, Murray G. Statistical strategies to assess reliability in ophthalmology. Eye. 2006;20:749-54.

[155] Gloesmann M, Hermann B, Schubert C, et al. Histologic correlation of pig retina radial stratification with ultrahigh-resolution optical coherence tomography. Invest Ophthalmol Vis Sci. 2003;44:1696–703.

[156] Anger EM, Unterhuber A, Hermann B, et al. Ultrahigh resolution optical coherence tomography of the monkey fovea. Identification of retinal sublayers by correlation with semithin histology sections. Exp Eye Res. 2004;78:1117–25.

[157] Toth CA, Narayan DG, Boppart SA, et al. A comparison of retinal morphology viewed by optical coherence tomography and by light microscopy. Arch Ophthalmol. 1998;115:1425-8.

[158] Costa RA, Calucci D, Skaf M, et al. Optical coherence tomography 3: Automatic delineation of the outer neural retinal boundary and its influence on retinal thickness measurements. Invest Ophthalmol Vis Sci. 2004;45:2399-406.

[159] Pons ME, Garcia-Valenzuela E. Redefining the limit of the outer retina in optical coherence tomography scans. Ophthalmology. 2005;112:1079–85.

[160] Sadda SR, Wu Z, Walsh AC et al. Errors in retinal thickness measurements obtained with optical coherence tomography. Ophthalmology. 2006; 113:285-93.

[161] Sadda SR, Joeres S, Wu Z et al. Error correction and quantitative subanalysis of optical coherence tomography data using computer-assisted grading. Invest Ophthalmol Vis Sci. 2007;48:839-48.

[162] Ishikawa H, Stein DM, Wollstein G, Beaton S, Fujimoto JG, Schuman JS. Macular segmentation with optical coherence tomography. Invest Ophthalmol Vis Sci. 2005;46:2012–2017.

[163] Harding S. Photodynamic therapy in the treatment of subfoveal choroidal neovascularisation. Eye. 2001;15:407-12.

[164] Shahidi M, Ogura Y, Blair NP, et al. Retinal thickness analysis for quantitative assessment of diabetic macular edema. Arch Ophthalmol 1991;109:1115-9.

[165] Browning DJ, McOwen MD, Bowen RM et al. Comparison of the clinical diagnosis of diabetic macular oedema with diagnosis by optical coherence tomography. Ophthalmology 2004;111:712-715

[166] Giovannini A, Amato GP, Mariotti C, Ripa E. Diabetic maculopathy induced by vitreo-macular traction: evaluation by optical coherence tomography (OCT). Doc Ophthalmol. 1999;97:361-6.

[167] Gallemore RP, Jumper JM, McCuen BW 2nd, Jaffe GJ, Postel EA, Toth CA. Diagnosis of vitreoretinal adhesions in macular disease with optical coherence tomography. Retina. 2000;20:115-20.

[168] Lavin MJ, Eldem B, Gregor ZJ. Symmetry of disciform scars in bilateral AMD. Br J Ophthalmol 1991;75:133–6.

[169] Gregor Z, Bird AC, Chisholm IH. Senile disciform degeneration in the second eye. Br J Ophthalmol. 1977; 61: 141–7.

[170] Gass JD. Drusen and disciform macular detachment and degeneration. Arch Ophthalmol. 1973;90:206–17.

[171] Macular Photocoagulation Study Group. Five-year follow-up of fellow eyes of patients with age-related macular degeneration and unilateral extrafoveal choroidal neovascularisation. Arch Ophthalmol. 1993;111:1189–99.

[172] Green WR, McDonell PJ, Yeo JH. Pathologic features of senile macular degeneration. Ophthalmology. 1985;92:615–27.

[173] Green WR, Key SN. Senile macular degeneration: a histopathologic study. Trans Am Ophthalmol Soc. 1977;75:180–254.

[174] Gartner S, Henkind P. Aging and degeneration of the human macula. Outer nuclear layer and photoreceptors. Br J Ophthalmol. 1981;65:23–8.

[175] Curcio CA, Medeiros NE, Millican CL. Photoreceptor loss in age-related macular degeneration. Invest Ophthalmol Vis Sci. 1996;37:1236–49.

[176] Macular Photocoagulation Study Group. Risk factors for choroidal neovascularisation in the second eye of patients with juxtafoveal or subfoveal choroidal neovascularization secondary to age-related macular degeneration. Arch Ophthalmol. 1997;115:741–7.

[177] Chang B, Yanuzzi LA, Ladas ID et al. Choroidal neovascularisation in second eyes of patients with unilateral exudativeage-related macular degeneration. Ophthalmology. 1995;102:1380–6.

[178] Chan A, Duker J, Ko TH, et al. Normal macular thickness measurements in healthy eyes using stratus optical coherence tomography. Arch Ophthalmol. 2006;124:193-8.

[179] Otani T, Kishi S. Correlation between optical coherence tomography and fluorescein angiography findings in diabetic macular oedema. Ophthalmology. 2007;14:104-7.

[180] Salinas- Alaman A, Garcia-layana A, Maldonado MJ et al. Using optical coherence tomography to monitor photodynamci therapy in age-related macular degeneration. Am J Ophthalmol. 2005;140:23-8.

[181] Midena E, Radin PP, Pilotto E et al. Fixation pattern and macular sensitivity in eyes with subfoveal choroidal neovascularisation secondary to age-related macular degeneration. A microperimetry study. Semin Ophthalmol. 2004;19:55-61.

[182] Hougaard JL, Wang M, Sander B, Larsen M. Effects of pseudophakic lens capsule opacification on optical coherence tomography of the macula. Curr Eye Res. 2001;23:415-21.

[183] Stein DM, Wollstein G, Ishikawa H et al. Effect of corneal drying on optical coherence tomography. Ophthalmology. 2006;113:985-91.

[184] Ray R, Stinnett S, Jaffe GJ. Evaluation of image artifact produced by optical coherence tomography of retinal pathology. Am J Ophthalmol. 2005;139:18-29.

[185] Rosenfeld PJ, Moshfeghi AA, Puliafito CA. Optical coherence tomography findings after an intravitreal injection of bevacizumab (avastin) for neovascular age-related macular degeneration. Ophthalmic Surg Lasers Imaging. 2005;36:331–335.

[186] Eter N, Spaide RF. Comparison of fluorescein angiography and optical coherence tomography for patients with choroidal neovascularization after photodynamic therapy. Retina. 2005;25:691–696.

[187] Rosenfeld PJ, Moshfeghi AA, Puliafito CA. Optical coherence tomography findings after an intravitreal injection of bevacizumab (avastin) for neovascular age-related macular degeneration. Ophthalmic Surg Lasers Imaging. 2005;36(4):331-5.

[188] Fung A, Rosenfeld PJ, Puliafito C, et al. One Year Results of the PrONTO Study: An OCT-Guided Variable-Dosing Regimen with Ranibizumab (Lucentis™) In Neovascular AMD. Vitreoretinal Symposium Frankfurt: 2006.

[189] Sutter E, Tran D. The field topography of ERG components in man-I. The photopic luminance response. Vision Res. 1992;32:433-46.

[190] Mackay AM, Brown MC, Grierson I, Haridng SP. Multifocal electroretinography as a predictor of maintenance of vision after photodynamic therapy for neovascular age-related macular degeneration. Doc Ophthalmol. 2008;116:13-8.

[191] Mackay, AM, Brown, MC, Hagan, RP, Fisher, AC, Harding, SP. Deficits in the electroretinogram in neovascular age-related macular degeneration and changes during photodynamic therapy. Doc Ophthalmol. 2007;115:69-76.

[192] McClure ME, Hart PM, Jackson A, Stevenson MR. Macular degeneration: do conventional measurements of impaired visual function equate with visual disability? Br J Ophthalmol. 2000;84:244–250.

[193] Fletcher DC, Schuchard RA. Preferred retinal loci relationship to macular scotoma in a low-vision population. Ophthalmology. 1997;104:632–638.

[194] Beare NAV, Riva CE, Petrig BL et al. Changes in optic nerve head blood flow in children with cerebral malaria and acute papilloedema. J Neurol Neurosurg Psych. 2006;77:1288-190.

[195] Metelitsina TI, Grunwald JE, DuPont JC, et al. Foveolar choroidal circulation and choroidal neovascularization in age-related macular degeneration. Invest Ophthalmol Vis Sci. 2008;49:358-63.

[196] Friedman, E. and Krupsky, S. et al. Ocular blood flow velocity in age-related macular degeneration. Ophthalmology. 1995;102:640-46.

[197] Young, R. Pathophysiology of age-related macular degeneration. Surv Ophthalmol. 1987;31:291-306.

[198] Grunwald JE, Metelistina TI, Dupont JC et al. Reduced foveolar choroidal blood flow in eyes with increasing AMD severity. Invest Ophthalmol Vis Sci. 2005;46:1033-38.

[199] Sarks JP, Sarks SH, Killingsworth MC. Evolution of geographic atrophy of the retinal pigment epithelium. Eye. 1988; 2:552-77.

[200] Uyama M. [Choroidal neovascularisation, experimental and clinical study]. Nippon Ganka Gakkai Zasshi. 1991; 95:1145-80.

Appendix 1

OCT GRADING PROTOCOL

1) Image quality:

1. Orientation of scan
2. Signal Strength
3. Type of scan: 5mm horizontal scan, FMT, Raster line, 6mm radial scan
4. Scan passing through fovea on video image

2) Qualitative analysis of neuroretina

1. Foveal contour visible
2. Subretinal fluid (SRF) at fovea
3. Any areas of intra-retinal fluid (IRF)
    - Cystoid/ Non-cystoid
4. Any vitreo-macular hyaloid attachment (VMHA)
5. Any other pathology: ERM, macular hole, pseudohole, exudates

3) Qualitative analysis of the outer high reflective band (OHRB)

1. OHRB: well-defined or poorly defined
2. Outer margin of the OHRB elevated
3. Type of elevation
    a. Serous PED
    b. Haemorrhagic PED
    c. Fibrovascular PED
    d. Drusenoid PED

4) Morphometry

(All measurements performed using manual positioning of callipers in a vertical line at the centre of the fovea on the retinal thickness algorithm)

1. NFT (Neuro-retinal foveal thickness): Distance between inner high reflectivity band and the inner margin of the outer lamina of the OHRB. (SRF not included)
2. BFT (Bilaminar foveal thickness): Distance between the inner high reflectivity band and the inner margin of the outer lamina of the OHRB in the presence of SRF.
3. OHRBT (Outer high reflectivity band thickness): Distance between the inner margin and the outer margin of the outer lamina of the OHRB.

Appendix 2

EXAMPLES

This section shows some examples of features on OCT that can confound the interpretation of scans. These images belong to patients who underwent PDT for subfoveal predominantly classic CNV secondary to AMD. I have included the following examples:

1. Intra and subretinal fibrosis
2. Retinal and retinal pigment epithelial atrophy
3. RPE rip
4. Retinal angiomatous proliferation
5. Full thickness macular hole with operculum
6. Haemorrhagic pigment epithelial detachment.
7. Pseudohole with epi-retinal membrane.

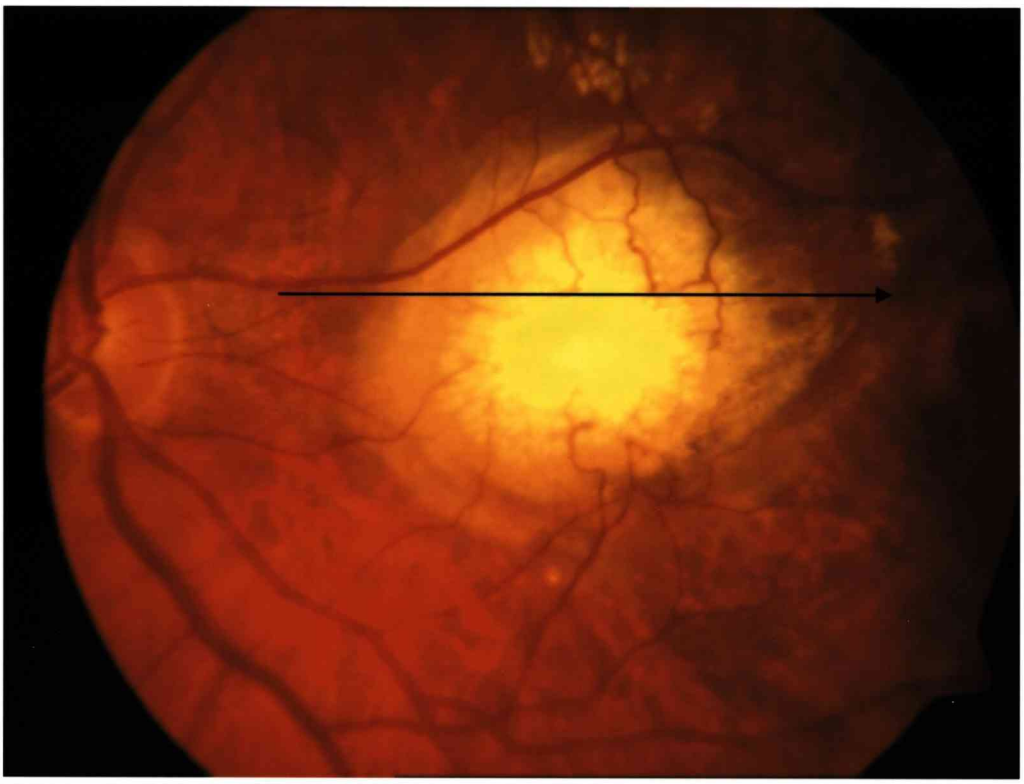

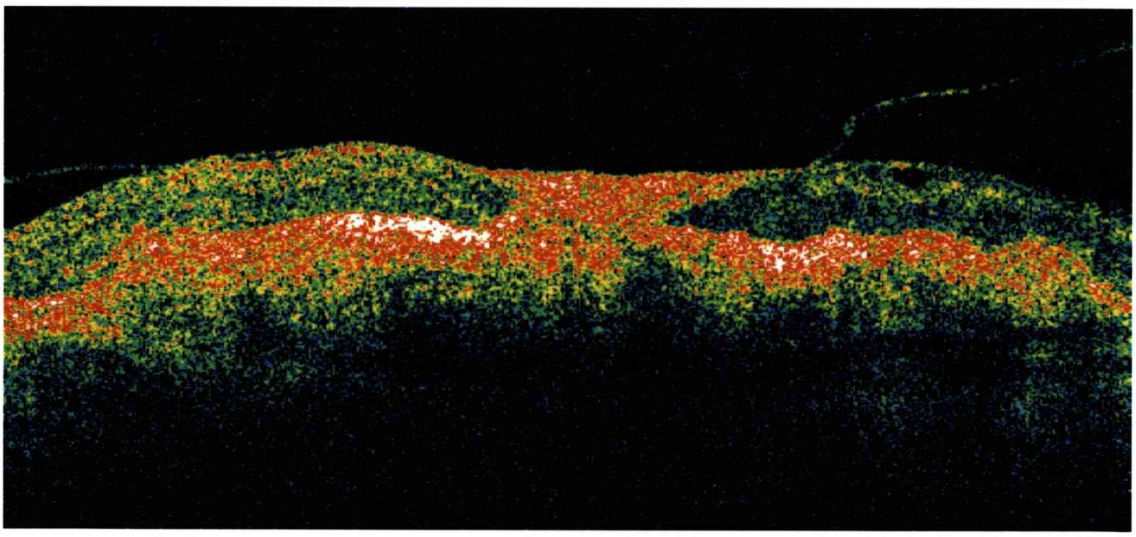

OCT scan through the fovea in an eye with end-stage disciform scarring showing intra and subretinal fibrosis. The outer margin of the outer high reflectivity band cannot be not well delineated. The scan also shows some areas of intra-retinal hyporeflectivity temporally. There is a taut adherent vitreo-macular hyaloid attachment.

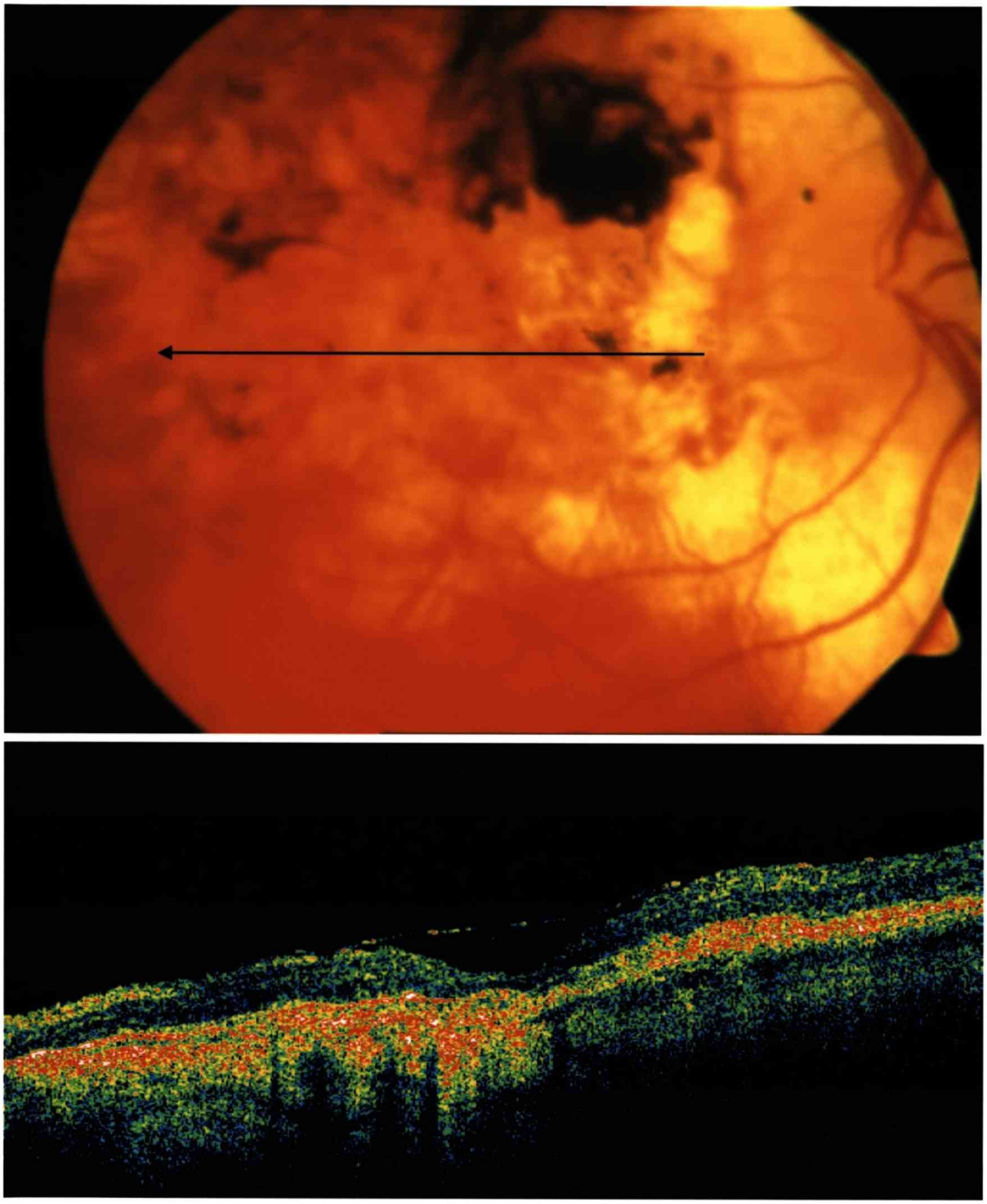

OCT scan through the fovea in an eye with end-stage neovascular AMD showing neuro-retinal thinning, subretinal fibrosis and RPE atrophy. The outer margin of the outer high reflectivity band cannot be not well delineated temporal to the foveal depression due to increased transmission through the atrophic RPE. The scan also shows an intact vitreo-macular hyaloid attachment bridging over the fovea.

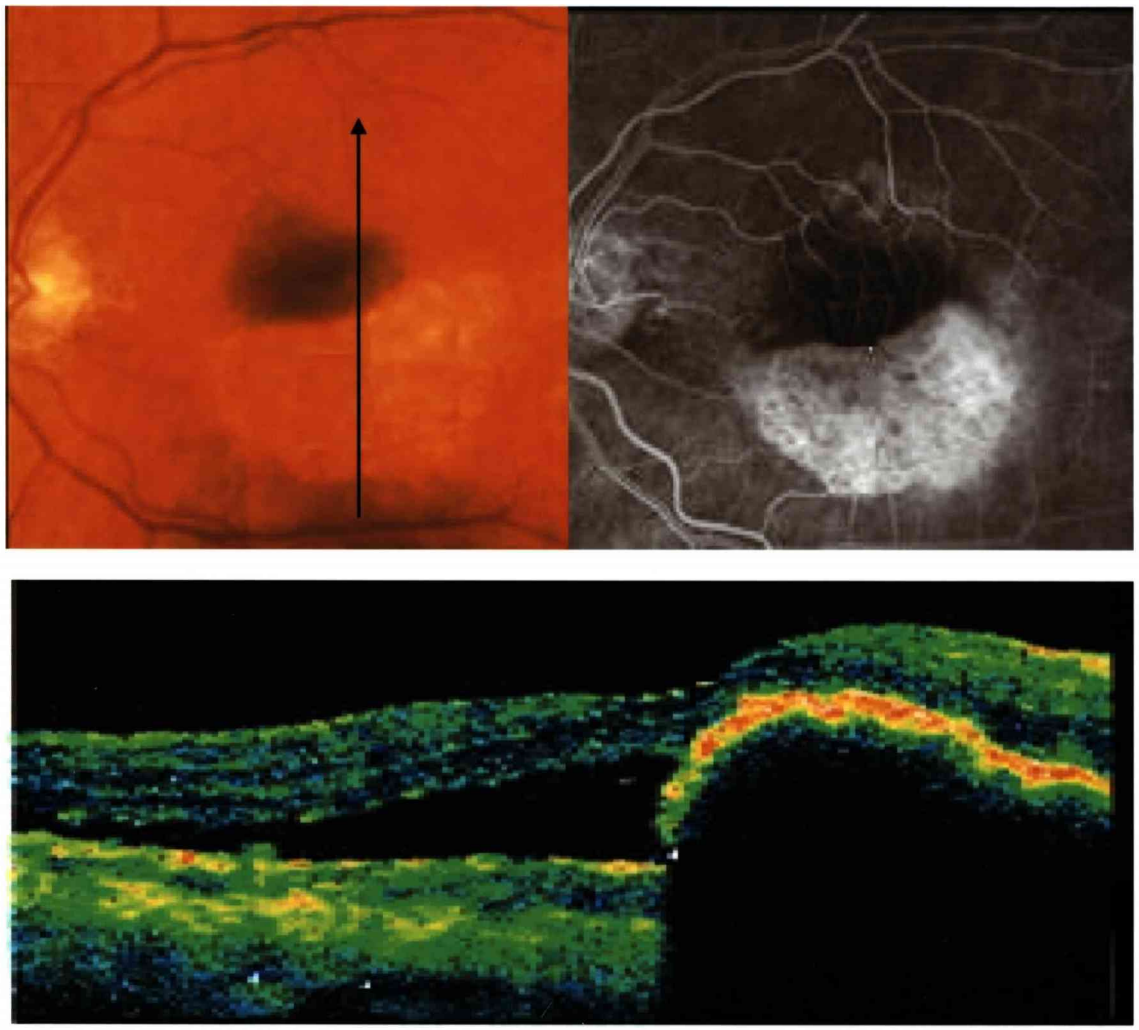

OCT scan oriented in an inferior to superior direction through the fovea in an eye with retinal pigment epithelial (RPE) tear following PDT in an eye with serous pigment epithelial detachment (PED). There is enhanced transmission through the outer high reflectivity band (OHRB) in the region of the RPE loss (left side of the scan) In the region of the folded RPE , the OHRB is elevated and thickened. There is residual subretinal fluid overlying the region of the denuded RPE

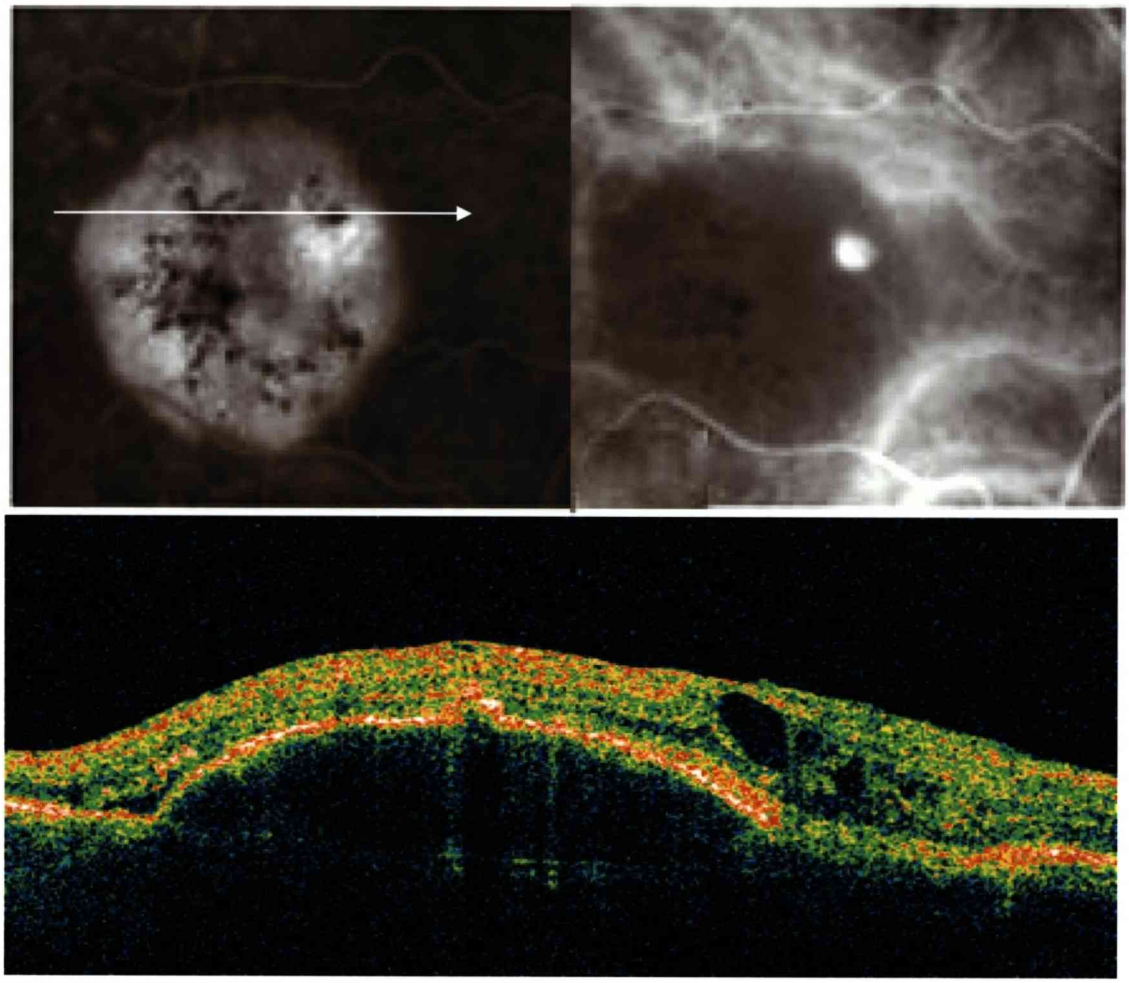

Fluorescein angiogram (FA), indocyanine green angiogram (ICG) and optical coherence tomogram (OCT) in an eye with stage IIB retinal angiomatous proliferation (RAP). The FA shows a smooth pigment epithelial detachment (PED). ICG shows a focal hotspot corresponding to the intra-retinal anastomoses. OCT scan in a temporal to nasal orientation shows a serous PED. In the region of the intra-retinal anastomoses the neuroretina shows the presence of intra-retinal fluid.

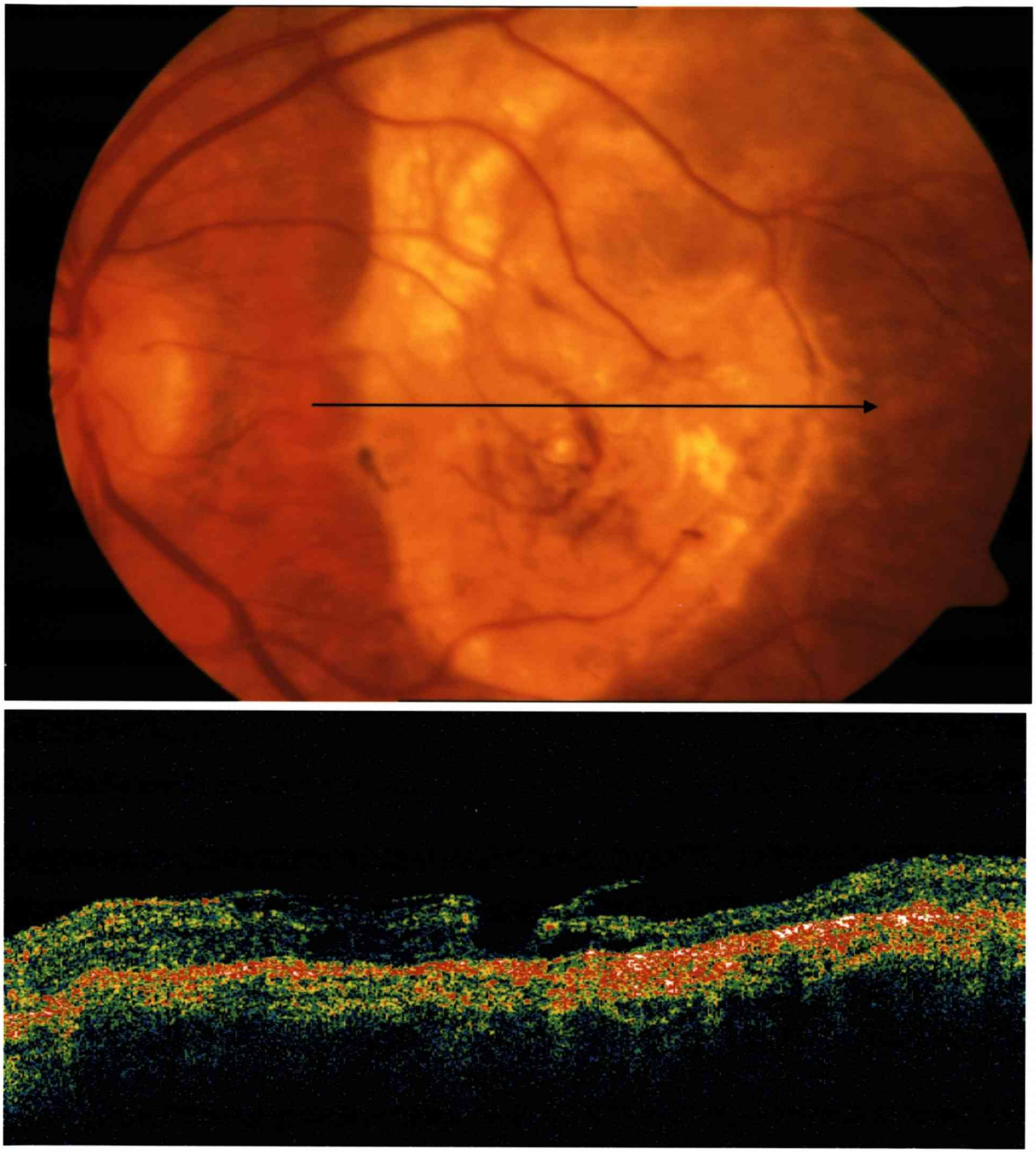

OCT scan a full thickness macular hole overlying a thick subretinal fibrosis in an eye with end-staged fibrosed disciform scar. The lack of retinal tissue at the base of the fovea confirms a full thickness hole. It is unclear whether the vitreous remains attached to the retinal operculum.

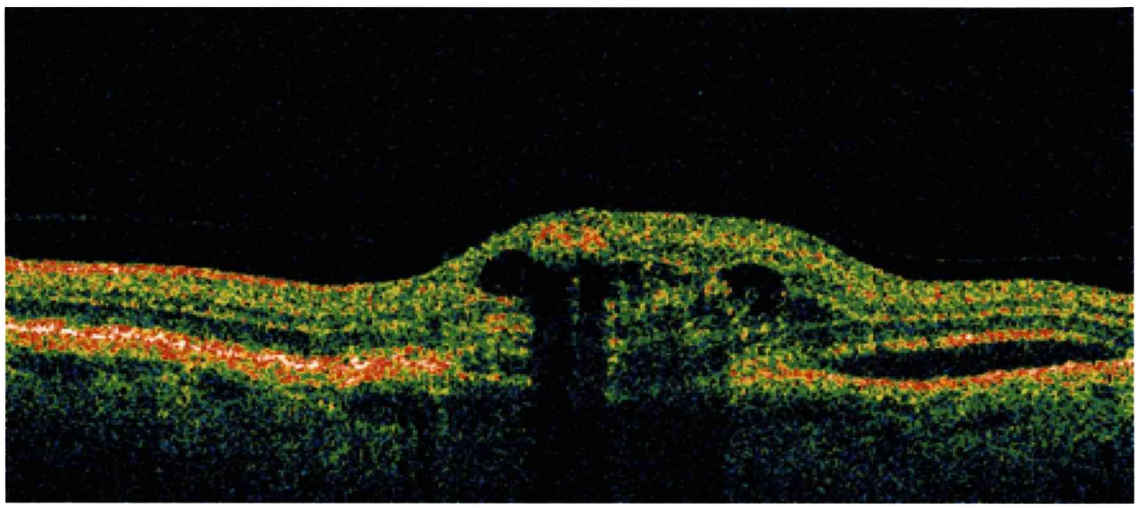

OCT scan of a patient with classic choroidal neovascularisation showing intra-retinal fluid, subretinal fluid and a focal area of increased hyperreflectivity within the neuroretina corresponding to the the haemorrhage. This area of hyperreflectivity has resulted in extensive shadowing of the underlying signal.

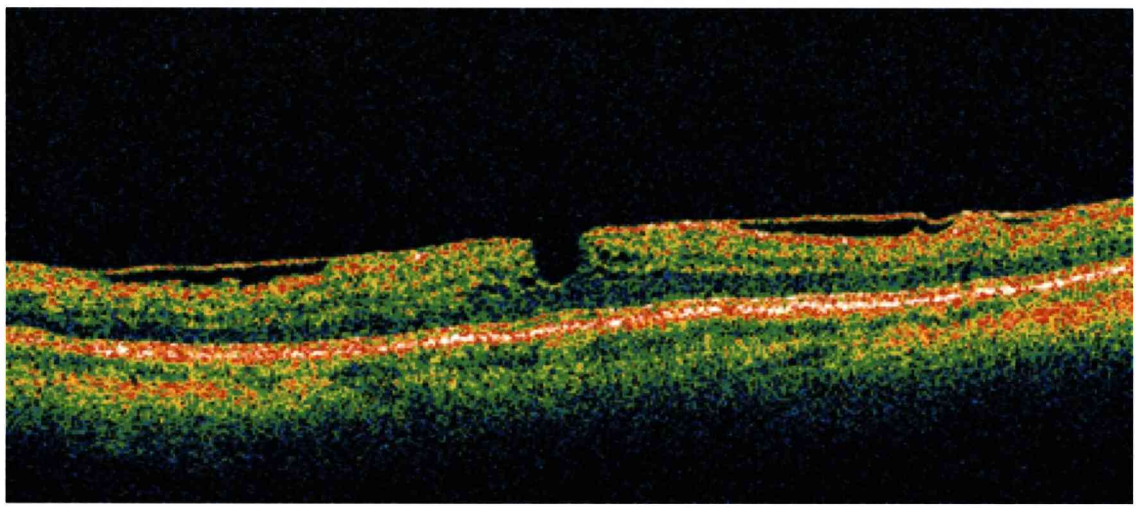

OCT scan shows an abnormally deep and wide foveal pit contour caused by a taut epiretinal membrane. The reflective retinal tissue at the base of the fovea confirms a pseudohole

Appendix 3

LIST OF PUBLICATIONS AND PRESENTATIONS

PUBLICATIONS

1. Sahni J, Stanga PE, Wong D, Harding SP. Optical coherence tomography in photodynamic therapy for subfoveal choroidal neovascularisation secondary to age-related macular degeneration: a cross-sectional study. Br J Ophthalmol. 2005;89:316-20.
2. Sahni J, Harding SP. Optical coherence tomography of the vitreomacular interface in photodynamic therapy. Br J Ophthalmol. 2005;89:929.
3. Sahni J, Stanga PE, Kent D, Wong D, Harding SP. Morphometric analysis of end-stage choroidal neovascularisation after photodynamic therapy for age-related macular degeneration using optical coherence tomography. Clin Experiment Ophthalmol. 2007;35:13-7.

PRESENTATIONS

1. Sahni J. Optical Coherence Tomography. Invited speaker. North of England Ophthalmology Society. Liverpool: Mar 2003.
2. Sahni J, Stanga P, Wong D, Harding SP. Optical coherence tomography in patients treated with photodynamic therapy for subfoveal choroidal neovascularisation secondary to age related macular degeneration: a cross-sectional study. Roy Mapstone prize presentation. Liverpool: Nov 2003.
3. Sahni J, Stanga PE, Kent D, Wong D, Harding SP. Morphometric analysis of end-stage choroidal neovascularisation after photodynamic therapy for age-related macular degeneration using optical coherence tomography. North of England Ophthalmology Society. Manchester: Mar 2005.
4. Sahni J, MacKay A, Stanga P, Brown M, Grierson I, Wong D, Harding SP. Relationship between optical coherence tomography features and multifocal electroretinography in patients with subfoveal choroidal neovascularisation. Royal College of Ophthalmologists Annual Congress. Birmingham: May 2005.

5. Wong D, Heimann H, Dhawahir F, Sahni J. Results of a longitudinal study of autofluorescence in a consecutive series of patients treated with mt360. EVRS. Sweden: Aug 2005.

6. Sahni J. Value of OCT3 in the management of neovascular AMD. Liverpool Grading Conference. Liverpool: June 2007.

PUBLISHED POSTERS AND ABSTRACTS

1. Sahni JN, MacKay A, Stanga P, Brown M, Grierson I, Wong D, Harding SP. Relationship between optical coherence tomography characteristics and multifocal electroretinography in patients with subfoveal choroidal neovascularisation. Invest Ophthalmol Vis Sci. 2005;46:1581.

2. Dhingra N, Sahni J, Shipley J, Harding SP, Groenewald C, Pearce IA, Stanga PE, Wong D. Vitrectomy and internal limiting membrane removal for diabetic macular oedema in eyes with absent vitreo–macular traction fails to improve visual acuity: results of a 12 months prospective randomised controlled clinical trial. Invest Ophthalmol Vis Sci. 2005;46:1467.

3. Sahni JN, Stanga PE, Wong D, Harding SP Optical coherence tomography evaluation following photodynamic therapy of subfoveal choroidal neovascularisation: a longitudinal study. Invest Ophthalmol Vis Sci. 2004;45:3169.

4. Sahni JN, Stanga PE, Wong D, Harding SP. Optical coherence tomography evaluation of baseline choroidal neovascularisation in patients undergoing photodynamic therapy. Invest Ophthalmol Vis Sci. 2004;45:2980.

5. Sahni JN, Stanga PE, Wong D, Taylor S, Harding SP. Correlation of stratus optical coherence tomography with clinical and fluorescein angiography findings in retreatment of subfoveal choroidal neovascularisation with photodynamic therapy. Invest Ophthalmol Vis Sci. 2003;44:4867.

EXTENDED REPORT

Optical coherence tomography in photodynamic therapy for subfoveal choroidal neovascularisation secondary to age related macular degeneration: a cross sectional study

J Sahni, P Stanga, D Wong, S Harding

Br J Ophthalmol 2005;**89**:316–320. doi: 10.1136/bjo.2004.043364

See end of article for authors' affiliations

Correspondence to: Mrs J Sahni, St Paul's Eye Unit, Royal Liverpool University Hospital, Liverpool L7 8XP UK; jayashree2001@hotmail.com

Accepted for publication 17 July 2004

Aims: To introduce new terminology and validate its reliability for the analysis of optical coherence tomography (OCT) scans, compare clinical detection of cystoid macular oedema (CMO) and subretinal fluid (SRF) with OCT findings, and to study the effect of photodynamic therapy (PDT) on the foveal morphology.

Methods: Patients with subfoveal, predominantly classic choroidal neovascularisation (CNV) secondary to age related macular degeneration (AMD) undergoing PDT were evaluated with refraction protocol best corrected logMAR visual acuity (VA), slit lamp biomicroscopy, stereoscopic fluorescein angiography (FFA), and OCT. New terminologies introduced to interpret the OCT scans were: neuroretinal foveal thickness (NFT), bilaminar foveal thickness (BFT), outer high reflectivity band thickness (OHRBT), intraretinal fluid (IRF), subretinal fluid (oSRF), and vitreomacular hyaloid attachment (VMHA).

Results: Fifty six eyes of 53 patients were studied. VA was better in eyes with a thinner outer high reflectivity band (OHRBT) ($p = 0.02$) and BFT ($p = 0.05$). BFT was less in eyes that had undergone a greater number of PDT treatments ($p = 0.04$). There was poor agreement between OCT and clinical examination in the detection of CMO and subretinal fluid ($\kappa = 0.289$ and $\kappa = 0.165$ respectively). To validate the interpretation and measurements on OCT, two groups of 20 scans were analysed by two independent observers. There was good agreement between the observers in the detection of IRF, oSRF, and VMHA ($p < 0.001$). Measurements of NFT and BFT had a high reproducibility, and of OHRBT reproducibility was low.

Conclusions: New terminology has been introduced and tested. OCT appears to be superior to clinical examination and FFA in the detection of CMO. In this study, better vision was associated with a thinner OHRBT and/or the absence of SRF giving insight into the biological effect of PDT.

Age related macular degeneration (AMD) is a leading cause of registerable blindness in the developed world in people over the age of 65 and subfoveal choroidal neovascularisation (CNV) is the major cause of severe visual loss.[1–3] The Treatment of AMD with Photodynamic therapy (TAP) study[4 5] reported a reduction in visual loss in subfoveal predominantly classic CNV.

Routine methods of assessing macular morphology, including fluorescein angiography (FA) and slit lamp biomicroscopy, allow only limited evaluation of the three dimensional relation between the CNV and retinal pigment epithelium.

Optical coherence tomography (OCT) is a relatively new tool and its role in the assessment of AMD has yet to be fully established in clinical practice. Fukuchi *et al*[6] and Toth *et al*[7] have demonstrated that the pseudocolour banding of retinal OCT images correlates well with histology. To date the literature has been descriptive and qualitative, concentrating on the detection of intraretinal and subretinal fluid[8–10] and the assessment of vitreomacular traction.[11] Objective measures from OCT images in AMD have yet to be developed or validated.

In our study we used the Zeiss Optical Coherence Tomographer Model 3000 (OCT3) (Zeiss-Humphrey, Dublin, CA, USA) to study the retinal morphology in patients with AMD undergoing photodynamic therapy (PDT) with the following aims: (1) to develop a relevant descriptive terminology to analyse OCT scans; (2) to test its reproducibility between observers; (3) to analyse clinical findings compared with OCT, and (4) to study the effect of PDT on the foveal morphology in patients with subfoveal CNV secondary to AMD using OCT in order to relate findings to the number of applications of PDT.

PATIENTS AND METHODS

This was a non-randomised prospective cross sectional study of eyes with predominantly classic subfoveal CNV secondary to AMD attending the St Paul's Clinical Eye Research Centre. All patients underwent refraction and visual acuity measurement using TAP protocol. The Early Treatment Diabetic Retinopathy Study (ETDRS) chart (Lighthouse Television Products, NY, USA) was used. Best corrected visual acuity was measured at 2 m. The score was the total number letters read correctly plus 15. If the patients saw fewer than 20 letters, they were tested with the top three lines at 1 m. The score then was the total number of letters read at 2 m plus the number of letters read at 1 m. Clinical and fundus fluorescein angiography (FFA) evaluation was by a retina specialist or a fellow experienced in clinical studies. The presence or absence of cystoid macular oedema (CMO) and subretinal fluid (SRF) was determined on slit lamp biomicroscopy using a 60 dioptre Volk (Volk Opticals, Mentor, OH, USA) lens and a standard Mainster (Ocular Intruments Inc, Bellevue, USA) contact lens with 1.5 magnification and on FFA by interpretation of 10 minute late frames. Patients with CNV secondary to non-AMD aetiologies were excluded.

Abbreviations: AMD, age related macular degeneration; BFT, bilaminar foveal thickness; CMO, cystoid macular oedema; FFA, fundus fluorescein angiography; ICC, intraclass correlation coefficient; IRF, intraretinal fluid; NFT, neuroretinal foveal thickness; OCT, optical coherence tomography; OHRBT, outer high reflectivity band thickness; PDT, photodynamic therapy; RPE, retinal pigment epithelium; SRF, subretinal fluid; TAP, Treatment of AMD with Photodynamic therapy study; VA, visual acuity; VMHA, vitreomacular hyaloid attachment.

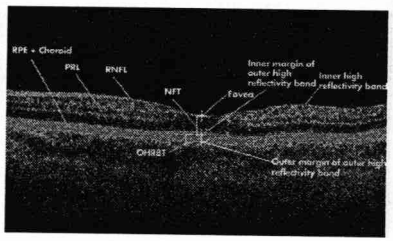

Figure 1 Optical coherence tomogram passing through the fovea of a normal eye illustrating retinal layers and terminology developed for the study. RNFL, retinal nerve fibre layer; PRL, photoreceptor layer; RPE, retinal pigment epithelium; NFT, neuroretinal foveal thickness (distance between inner high reflectivity band and inner margin of outer high reflectivity band at foveal centre); OHRBT, outer high reflectivity band thickness; NFT = 181 μ and OHRBT = 58 μ in this scan.

OCT was performed and analysed by a single observer (JS) on the OCT3 masked to visual acuity (VA) clinical and FFA findings. All scans were performed prior to FFA and slit lamp biomicroscopy. Pupils were dilated with tropicamide (1%) and phenylephrine (2.5%) drops. Internal fixation guided by the video image was used to ensure that scans passed through the fovea. Scans that did not pass through the fovea were excluded. Horizontal single line A scans through the fovea of default length 5 mm at 0° and a fast macular thickness map consisting of six simultaneous 6 mm radial line scans were obtained. With each single line scan pass, 512 longitudinal range samples were captured—each consisting of 1024 data points over 2 mm of depth, giving 524 288 data points, which are integrated to construct a cross sectional anatomical image (tomogram). In cases with poor central fixation, the scan was manually positioned on the anatomical fovea as viewed on the black and white video image.

All thickness measurements were made on the single line horizontal scans. The measurements were done by manual positioning of the callipers using the retinal thickness (single eye) quantitative analysis protocol offered by Stratus OCT3.

New terminology was defined and used in interpreting OCT images as shown in table 1 and figures 1, 2, and 3. The foveal centre was defined as the maximum depression within the depression or pit within the neuroretina[12] and the fovea was defined as the surrounding area, the diameter of which was 500 μm. Measurements were obtained from acquired scans using these definitions and compared against clinical

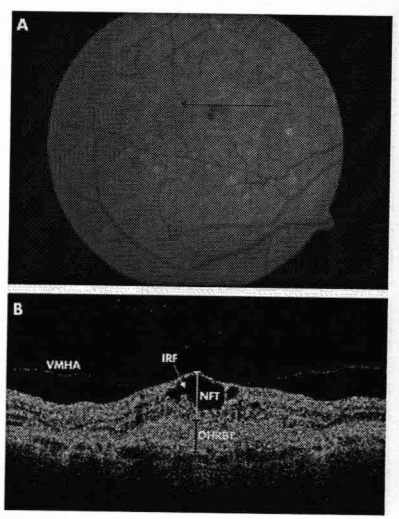

Figure 2 (A) Colour fundus photograph of the right eye of an 83 year old male patient demonstrates a green-grey subfoveal lesion with haemorrhage. The arrow indicates the location and direction of the optical coherence tomographic (OCT) scan. (B) OCT image demonstrates loss of foveal depression with cystoid spaces and vitreoretinal hyaloid attachment. NFT, neuroretinal foveal thickness; OHRBT, outer high reflectivity band; IRF, intraretinal fluid. NFT = 406 μm and OHRBT = 307 μ in this scan.

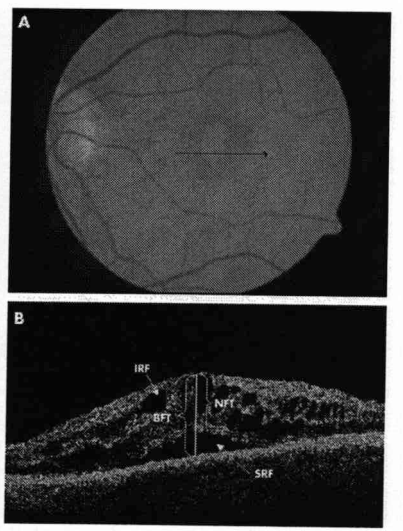

Figure 3 (A) Colour fundus photograph of the left eye of a 54 year old female patient shows a subfoveal green-grey lesion with minimal haemorrhage. The arrow indicates the location and direction of the optical coherence tomographic (OCT) scan. (B) OCT passing through the fovea illustrating bilaminar foveal thickness (BFT), intraretinal fluid (IRF), and subretinal fluid (SRF). BFT is the distance between the inner high reflectivity band and the inner margin of the outer high reflectivity band at the foveal centre in the presence of subretinal hyporeflective area. NFT = 473 μ and BFT = 722 μ in this scan.

Table 1 Terms and definitions used within this paper

Term	Definition
Neuroretinal foveal thickness (NFT)	Distance between the inner high reflectivity band and the inner margin of the outer high reflectivity band at the foveal centre
Bilaminar foveal thickness (BFT)	Distance between the inner high reflectivity band and the inner margin of the outer high reflectivity band at the foveal centre in the presence of subretinal hyporeflective space at the fovea
Outer high reflectivity band thickness (OHRBT)	Distance between the inner margin of the outer high reflectivity band and the outer margin of the outer high reflectivity band at the fovea
Vitreomacular hyaloid attachment (VMHA)	Incomplete separation of the posterior hyaloid with attachment at the macula in the OCT scan
Posterior vitreous detachment (PVD)	Complete separation of the posterior hyaloid from the macula in the OCT scan
Intraretinal fluid (IRF)	Well defined intraretinal hyporeflective spaces at the fovea separated by reflective septae
Subretinal fluid (oSRF)	Separation of the neuroretina from the outer high reflectivity band by a well defined hyporeflective space at the fovea

observations. Scans were also studied for features which could confound the interpretation and measurement of the images.

Validation

Two groups of 20 scans of patients with subfoveal predominantly classic CNV secondary to AMD were analysed by two groups of independent observers. For each horizontal 5 mm line scan, each observer independently recorded the presence or absence of IRF, oSRF, and VMHA and measured NFT, BFT, and OHRBT by manual positioning of the callipers.

Statistics

Statistical analysis of the data was performed using SPSS for windows version 11.0 (SPSS Inc, Chicago, IL, USA). Intraclass correlation coefficient (ICC) was used as a measure of reliability between the observers for the validation study. To obtain the standard deviation of the differences between the 20 pairs of measurements by the observers, we squared all the differences, added them up, divided by 20 and took the square root.

The relation between NFT, BFT, and OHRBT respectively with VA was analysed using the Pearson correlation coefficient. Agreement between clinical examination and OCT in the detection of CMO and SRF were investigated on 2×2 tables and kappa statistic (κ) was calculated. A p value of $\leqslant 0.05$ was taken to be significant.

VALIDATION RESULTS

Forty eyes of 40 patients (not included in the cross sectional study) with subfoveal predominantly classic CNV undergoing PDT were divided into two groups of 20 each. Observer 1 and observer 2 analysed group 1 and observer 1 and observer 3 analysed group 2.

For observer 1 and observer 2: the ICC for NFT was 0.98 with an interobserver standard deviation of 14.33 μ; for BFT, ICC was 0.98 (SD 21.3) μ and for OHRBT the ICC was 0.76 (SD 46.74) μ. The ICC for IRF was 0.87 ($p<0.001$). For SRF there was high repeatability (ICC = 1, $p<0.001$) and for VMHA the ICC was 0.75 ($p<0.001$)

For observer 1 and observer 3: the ICC for NFT was 0.97 with an interobserver SD of 17 μ; for BFT, ICC was 0.97 (SD 23.5) μ and for OHRBT the ICC was 0.93 (SD 28.8) μ. The ICC for IRF was 0.73 ($p<0.001$). For SRF the ICC was 0.73 ($p<0.001$) and for VMHA there was high repeatability (ICC = 1, $p<0.001$).

RESULTS

Sixty eight eyes of 65 patients attending St Paul's Eye Unit, Royal Liverpool University Hospital between August 2002 and February 2003 were recruited. Twelve eyes (17%) were excluded, as scans passing through the fovea could not be obtained due to erratic and inaccurate fixation leaving 56 eyes for analysis. The median age was 76 years. Mean duration since baseline visit was 9.5 months (range 0 to 30; 24 males, 32 females). Three patients were scanned at baseline prior to receiving any treatment. Sixteen had undergone one PDT treatment application, 11 had two, 10 had three, six had four, nine had five, and one patient had seven treatment applications prior to the OCT scanning.

IRF was found in 23 (42%) eyes on OCT imaging and CMO was found in 13 (23%) eyes in the same group on slit lamp clinical examination. Kappa was 0.29 signifying a poor agreement between the two tests. There was poor agreement between slit lamp biomicroscopy and OCT in the detection of SRF ($\kappa = 0.17$).

There was no significant difference in the distance VA in eyes with and without IRF at the fovea ($p>0.5$).

The mean NFT was significantly greater in patients with IRF at 223 μm compared with those without at 154 μm ($p = 0.005$). There was no correlation between the NFT and VA ($p>0.5$) and NFT and the number of PDT applications ($r = -0.23$, $p>0.05$).

The correlation between BFT and VA was significant ($p = 0.05$). There was a statistically significant correlation between BFT and the number of PDT applications ($r = -0.28$; $p = 0.04$) (fig 4). TAP protocol VA was significantly better in eyes with a thinner OHRBT (fig 5) ($r = -0.331$; $p = 0.013$). A VMHA was present in 20/56 patients (35.7%). No statistically significant association was found between IRF and VMHA ($p = 0.4$).

New observations were made from the scans in these patients. In some cases with atrophy of the retinal pigment epithelium (RPE) (on slit lamp or FFA) an optical shadow was present interfering with the identification of the outer border of the OHRBT. In cases with a large amount of intraretinal or subretinal fluid or haemorrhage, signal attenuation appears to reduce the apparent OHRBT.

DISCUSSION

Optical coherence tomography[9 10] is a relatively new technique for cross sectional imaging of the retina. To date, the

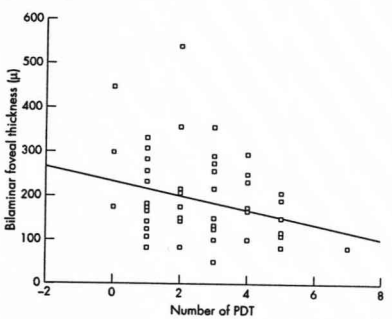

Figure 4 Relationship between bilaminar foveal thickness (BFT) and number of PDT application in 56 eyes. The linear regression line is $y = -15.928x + 231.14$ ($r = -0.275$, $p = 0.04$).

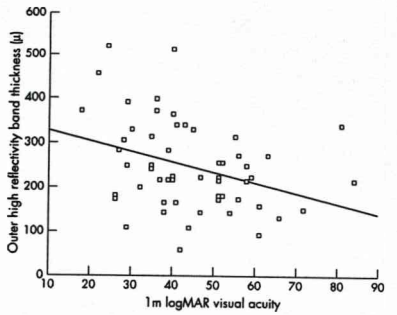

Figure 5 Relation between visual acuity (logMAR letters) units plotted against outer high reflectivity band (OHRBT) in μm in 56 eyes. The linear regression line is $y = -2.3352x + 350.58$ ($r = -0.331$, $p = 0.02$).

published literature has been descriptive and definitions of clinical relevance have not been defined.[9] In our study we used the most recent OCT model with higher data sampling than in previously published reports and have developed specific terms for future use in clinical studies.

In the previous literature there has been no definition to describe the thickness of the central fovea. Firstly, therefore, we defined the centre of the anatomical fovea and went on to define two measures of foveal thickness—BFT and NFT—to allow distinction between measures, depending on the presence or absence respectively of subretinal hyporeflectivity on OCT.

In our study we have used the term IRF for describing well delineated hyporeflective spaces separated by reflective septae within the neuroretina. Otani *et al* have described two distinct OCT appearances of macular oedema in diabetes under the terms "cystoid macular oedema" and "sponge-like retinal swelling".[13] The use of an OCT system providing fewer data points per scan could have influenced the tomographic appearance of the intraretinal fluid in their study. We found considerable interobserver variability in the detection of the second of these terms and believe that an increase in NFT in the absence of IRF may be taken as evidence of diffuse retinal swelling.

We have introduced the term OHRBT to measure the thickness of the subretinal hyperreflectivity at the fovea. Finally we have introduced the term VMHA to describe when partial separation of the posterior hyaloid with attachment at the macula was noted on the OCT. We avoided calling this "traction", as tractional forces cannot be measured with OCT.

As OCT becomes more widely available, debate continues on the relevance and reliability of the images produced. The usefulness of the instrument depends on the reproducibility of its measurements and the ability of the observers to agree on the interpretation of the results. In the validation study, reproducibility of the neuroretinal thickness and bilaminar foveal thickness had high ICCs and low standard deviations, which are essential for accurate and reliable measurements of retinal thickness. OHRBT reproducibility was lower, with lower ICC and higher SD in both groups of observers. This high variability may be because of the difficulty in identification of the true outer margin of the outer high reflectivity band. There was good agreement between the observers in the detection of IRF, oSRF, and VMHA ($p<0.001$).

For OCT to be meaningful in macular disease, scans must pass through the anatomical centre of the fovea, especially if measurements are to be compared with VA. In our study 12 (17%) of 68 eyes could not be reliably scanned through the fovea. Reliability of scans was limited by poor fixation, excessive eye movements, and difficulty identifying the true location of the fovea because of morphological changes caused by disease. Two other studies have reported on the difficulty of obtaining scans. Hee *et al*[14] failed to obtain adequate scans in 4.2% of the study population, comprising mainly patients with diabetes with moderate to good VA (better than 20/80). Rogers *et al*[15] reported a higher percentage (12.2%) of scans to be unobtainable/unreliable in a population of patients with AMD, a result more similar to ours but still lower. Unlike these authors our population was consecutive, often with quite low levels of vision and poor fixation, and accounting for a 17% exclusion rate: the mean VA score was 42 letters (roughly equivalent to 20/120) and scans that did not pass through the foveal centre were excluded. This significant failure rate raises the question of reliability and suitability of OCT as an objective means of measuring and monitoring retinal thickness at the fovea in some patients.

All measurements in our study were obtained by manual positioning of the callipers. Hee *et al*[14] obtained retinal thickness measurements automatically by means of a computer algorithm that searches for the changes in reflectivity observed at the superficial and deep retinal boundaries. We therefore tested the algorithm that is supplied within the software suite of the OCT 3000. In most cases it failed to distinguish between the detached posterior hyaloid and the true inner high reflectivity band corresponding to the inner retinal border. In the presence of a subretinal hyporeflective space, the algorithm usually misread the true NFT. We believe that manual calliper placement currently remains the method of choice.

In the clinical management of AMD the detection of CMO and SRF is important. Bressler *et al*[16] have commented on the difficulty of correctly identifying leakage due to CNV in the presence of coexisting CMO, which can confound interpretation of FFA images. FFA and slit lamp biomicroscopy are the standard examinations used for the diagnosis of CNV in patients with AMD and these examinations are relatively insensitive at detecting small changes in retinal thickness.[17] Hee *et al*[14] reported that slit lamp biomicroscopy was unreliable in detecting an increase in thickness smaller than 250 μm in diabetic macular oedema. Browning *et al*[18] calculated κ to be 0.63 in their cohort of diabetics for the agreement between slit lamp biomicroscopy and OCT in the detection of macular oedema. In our study OCT detected IRF in more than 50% of patients in whom CMO was not seen on slit lamp biomicroscopy. The agreement between the two methods was much less in our study, $\kappa = 0.29$. This may be because the majority of our patients had undergone previous PDT making clinical interpretation difficult. There was also poor agreement between the two methods in the detection of SRF ($\kappa = 0.165$). The presence/absence of leakage is integral to retreatment decision making during a course of PDT.[19] With OCT, a new standard for assessment of CMO and SRF have been set, which is more objective than slit lamp biomicroscopy and fluorescein angiography.

Studying the relation between VA and retinal thickness/fluid is important in increasing the understanding of retinal pathophysiology in exudative maculopathies. The presence of CMO has been reported to be associated with poorer VA in neovascular AMD.[20] However in our study of patients with AMD who had undergone PDT, there was no statistically significant association between the presence or absence of IRF and SRF and VA. We could not show a statistically

significant association between VA and NFT or BFT. This could be because other factors such as the baseline VA and size of CNV may also affect the final VA. Using OCT, we have shown that a higher number of PDT treatments are associated with lower BFT. This observation needs further investigation in longitudinal studies but does suggest that OCT imaging may be helpful. We are currently undertaking a study to develop a new set of retreatment criteria taking these findings into consideration.

Previous studies[6 7] have shown that the outer high reflectivity band corresponds to the RPE and choriocapillaris. Hee *et al*[21] categorised untreated CNV on OCT tomograms as well defined, poorly defined, or as a fibrovascular PED. In our experience these characteristics were lost following PDT. We found a statistically significant inverse association between the RPE-CNV complex thickness, defined in our study as OHRBT, and VA. The suggestion from our study is that in addition to the recognised anti-angiogenic effect,[22 23] PDT may preserve VA in patients with AMD by modifying the natural history of the scarring process,[24] which in turn prevents photoreceptor loss. There was no association between the OHRBT and the number of PDT treatments or the duration since initial treatment. Measurement of OHRBT appears to have some limitations, as the absorption and scattering properties of fluid and fibrosis can attenuate the OCT signal. In contrast, RPE/choroidal atrophy can intensify the transmission of the light and might result in a thicker OHRBT measurement.

Vitreomacular traction has been implicated in the progression of diabetic maculopathy.[25] We looked at the pattern of vitreous interaction with the retinal surface at the fovea. VMHA was present in 20 patients, but we did not find a statistically significant correlation between CMO and VMHA. We propose that in AMD disruption of RPE metabolism by the associated CNV is responsible for changes in the retinal architecture as opposed to vitreomacular traction (as has been implicated in other conditions).[11]

A limitation of this study is that scans were not possible in 17% of our patient population, because of poor vision and fixation. Although we have taken great care to accurately delineate the outer high reflectivity band, errors in measuring true RPE-CNV thickness may have arisen because of light attenuation or amplification properties of the tissue. Although we have only sought correlations between vision and OCT features, baseline VA, diameter of the CNV, presence of fibrosis, atrophy, and blood may have also influenced the VA results.

Power calculations were not performed as there were no preliminary data on which to base them. In any future studies our data will be useful to perform power calculations in this specific population.

Our study shows that OCT can be a useful technique for quantitative retinal measurements in patients undergoing PDT. We were able to show that VA was better in those patients with an absence of SRF following PDT. We also showed that the favourable visual outcome following PDT might be associated with a thinner OHRBT. Thus OCT and the terminology we have developed appears to be useful in evaluating the response of the retina and can aid in interpreting the FFA when evaluating the activity of CNV treated with PDT. Further prospective longitudinal studies are needed to establish retreatment criteria based on these findings, and may improve the efficacy and cost effectiveness of PDT.

ACKNOWLEDGEMENTS

This study was presented in part as a poster at the annual meeting of the Association for Research in Vision and Ophthalmology, Fort Lauderdale, FL, USA, May 2003. The authors do not have any commercial or proprietary interest in the OCT model 3000 (Zeiss-Humphrey, USA). The authors are grateful to the staff of the Clinical Eye Research Centre at St Paul's Eye Unit, Liverpool for their help with the study.

REFERENCES

1 **Klein R**, Klein BE, Linton KL. Prevalence of age-related maculopathy: the Beaver Dam Eye Study. *Ophthalmology* 1992;**99**:933–43.
2 **Vingerling JR**, Dielemans I, Hofman A, *et al*. The prevalence of age-related maculopathy in the Rotterdam study. *Ophthalmology* 1995;**102**:205–10.
3 **Bressler NM**, Bressler SB, Fine SL. Age-related macular degeneration. *Surv Ophthalmol* 1988;**32**:375–413.
4 **TAP study group**. Photodynamic therapy of subfoveal choroidal neovascularisation in age-related macular degeneration with verteporfin: one-year results of 2 randomised clinical trials. TAP report 1. *Arch Ophthalmol* 1999;**117**:1329–45.
5 **Bressler NM**, TAP study group. Photodynamic therapy of subfoveal choroidal neovascularisation in age-related macular degeneration with verteporfin: two-year results of 2 randomised clinical trials. TAP report 2. *Arch Ophthalmol* 2001;**119**:198–207.
6 **Fukuchi T**, Takahashi K, Uyama M, *et al*. Comparative study of experimental choroidal neovascularisation by optical coherenece tomography and histopathology. *Jpn J Ophthalmol* 2001;**45**:252–8.
7 **Toth CA**, Narayan DG, Boppart SA, *et al*. A comparison of retinal morphology viewed by optical coherence tomography and by light microscopy. *Arch Ophthalmol* 1998;**115**:1425–8.
8 **Hee MR**, Izatt JA, Swanson EA, *et al*. Optical coherence tomography of the human retina. *Arch Ophthalmol* 1995;**113**:325–32.
9 **Montero JA**, Ruiz-Moreno JM, Tavolato M. Follow-up of age-related macular degeneration patients treated by photodynamic therapy with optical coherence tomography 3. *Graefes Arch Clin Exp Ophthalmol* 2003;**241**:797–802.
10 **Puliafito CA**, Hee MR, Lin CP, *et al*. Imaging of macular diseases with optical coherence tomography. *Ophthalmology* 1995;**102**:217–29.
11 **Gallemore RP**, Jumper JM, McCuen BW 2nd, *et al*. Diagnosis of vitreoretinal adhesions in macular disease with optical coherence tomography. *Retina* 2000;**20**:115–20.
12 **Fine BS**, Yanoff M. *Ocular histology. A text and atlas*, 2nd edition. Hagerstown: Harper & Row, 1979:61–127.
13 **Otani T**, Kishi S, Mauyama Y. Patterns of diabetic macular edema with optical coherence tomography. *Am J Ophthalmol* 1999;**127**:688–93.
14 **Hee MR**, Puliafito CA, Wong C, *et al*. Quantitative assessment of macular edema with optical coherence tomography. *Arch Ophthalmol* 1995;**113**:1019–29.
15 **Rogers AH**, Martidis A, Greenberg PB, *et al*. Optical coherence tomography findings following photodynamic therapy of choroidal neovascularisation. *American J Ophthalmol* 2002;**134**:566–76.
16 **Bressler NM**, Bressler SB, Alexander J, *et al*. MPS reading center. Loculated fluid: a previously undescribed fluorescein angiographic finding in choroidal neovascularisation associated with macular degeneration, *Arch Ophthalmol* 1991;**109**:211–15.
17 **Shahidi M**, Ogura Y, Blair NP, *et al*. Retinal thickness analysis for quantitative assessment of diabetic macular edema. *Arch Ophthalmol* 1991;**109**:1115–19.
18 **Browning DJ**, McOwen MD, Bowen RM, *et al*. Comparison of the clinical diagnosis of diabetic macular edema with diagnosis by optical coherence tomography. *Ophthalmology* 2004;**111**:712–15.
19 **Harding S**. Photodynamic therapy in the treatment of subfoveal choroidal neovascularisation. *Eye* 2001;**15**:407–12.
20 **Ting TD**, Cox TA, Meyer CH, *et al*. Decreased visual acuity associated with cystoid macular edema in neovascular age-related macular degeneration. *Arch Ophthalmol* 2002;**120**:731–7.
21 **Hee MR**, Baumal CR, Puliafito CA, *et al*. Optical coherence tomography of age-related macular degeneration and choroidal neovascularisation. *Ophthalmology* 1996;**103**:1260–70.
22 **Ghazi NG**, Jabbour NM, De La Cruz ZC, *et al*. Clinicopathologic studies of age-related macular degeneration with classic subfoveal choroidal neovascularization treated with photodynamic therapy. *Retina* 2001;**21**:478–86.
23 **Schlotzer-Schrehardt U**, Viestenz A, Naumann GO, *et al*. Dose-related structural effects of photodynamic therapy on choroidal and retinal structures of human eyes. *Graefes Arch Clin Exp Ophthalmol* 2002;**240**:748–57.
24 **Green WR**, Enger C. Age related macular degeneration histopathologic studies: the 1992 Lorenz E Zimmerman Lecture. *Ophthalmology* 1993;**100**:1519–35.
25 **Giovannini A**, Amato GP, Mariotti C, *et al*. Diabetic maculopathy induced by vitreo-macular traction: evaluation by optical coherence tomography (OCT). *Doc Ophthalmol* 1999;**97**:361–6.

References

1 **Sahni J**, Stanga P, Wong D, *et al.* Optical coherence tomography in photodynamic therapy for subfoveal choroidal neovascularisation secondary to age related macular degeneration: a cross sectional study. *Br J Ophthalmol* 2005;**89**:316–20.
2 **Ting TD**, Oh M, Cox TA, *et al.* Decreased visual acuity associated with cystoid macular edema in neovascular age-related macular degeneration. *Arch Ophthalmol* 2002;**120**:731–7.
3 **Mennel S**, Hausmann N, Meyer CH, *et al.* Transient visual decrease after photodynamic therapy. *Ophthalmologe* 2005;**102**:58–63.
4 **Costa RA**, Farah ME, Cardillo JA, *et al.* Immediate indocyanine green angiography and optical coherence tomography evaluation after photodynamic therapy for subfoveal choroidal neovascularization. *Retina* 2003;**23**:159–65.
5 **Rogers AH**, Martidis A, Greenberg PB, *et al.* Optical coherence tomography findings following photodynamic therapy of choroidal neovascularization. *Am J Ophthalmol* 2002;**134**:566–76.

Optical coherence tomography of the vitreomacular interface in photodynamic therapy

We would like to comment on the excellent article by Sahni *et al.*[1] In their paper, a number of descriptive terms for optical coherence tomography (OCT) analysis are defined in patients with age related macular degeneration (AMD) with subfoveal choroidal neovascularisation undergoing treatment with photodynamic therapy. One term, "vitreomacular hyaloid attachment (VMHA)," was used to refer to incomplete separation of the posterior hyaloid with attachment at the macula. Twenty of 56 patients (35.7%) included in the study had VMHA on OCT. We would like to point out that this vitreomacular configuration is identical to that described in a previous report of normal eyes.[2]

The study by Uchino *et al* reported OCT findings at the vitreoretinal interface in 209 normal eyes. In their study, they defined five individual stages of posterior vitreous detachment (PVD). Two stages represented partial PVD with persistent macular attachment, identical to VMHA as defined by Sahni *et al*. Stage 1 was defined as focal perifoveal PVD in one to three quadrants with persistent vitreofoveal attachment, and stage 2 was defined as perifoveal PVD in all four quadrants with persistent vitreofoveal attachment. Of the 209 normal eyes, 47.8% had stage 1 PVD and 12.6% had stage 2 PVD. Mean age of the patients in the study was 52.3 years (range 31–74 years).[2]

We find it interesting that the percentage of AMD patients with VMHA in the Sahni study is less than the percentage of normal eyes with stage 1 or 2 PVD in the Uchino study.[1 2] This suggests that the vitreomacular configuration defined as VMHA by Sahni *et al* is probably not a finding specific to the AMD patients included in the study.

A J Witkin, J S Duker
New England Eye Center, Tufts-New England Medical Center, Tufts University, Boston, MA, USA

Correspondence to: Jay S Duker, New England Eye Center, Tufts-New England Medical Center, Tufts University, Boston, MA, USA; jduker@tufts-nemc.org

doi: 10.1136/bjo.2005.071100

Accepted for publication 14 March 2005

References

1 **Sahni J**, Stanga P, Wong D, *et al.* Optical coherence tomography in photodynamic therapy for subfoveal choroidal neovascularisation secondary to age related macular degeneration: a cross sectional study. *Br J Ophthalmol* 2005;**89**:316–20.
2 **Uchino E**, Uemura A, Ohba N. Initial stages of posterior vitreous detachment in healthy eyes of older persons evaluated by optical coherence tomography. *Arch Ophthalmol* 2001;**119**:1475–9.

Author's reply

We thank Mennel *et al* and Duker and Witkin for their interesting comments regarding our article.

Mennel *et al* make some interesting points on the immediate structural changes that occur after photodynamic therapy (PDT), a topic that we thought was outside the scope of our study. I agree that the short term and long term changes after treatment are important and need to be taken into account in future studies on patients undergoing PDT.

We are grateful to Duker and Witkin for pointing out the article by Uchino and colleagues.[1] Our patients were older (mean 76 years (range 59–94)) than those reported by these authors (mean 52.3 years). Uchino *et al* had 20 patients in the same age group and only two patients were above 70 years of age. Both these had a complete posterior vitreous detachment (PVD). All our patients had associated pathology and the majority had undergone PDT, all of which may have influenced the outcome. While the finding of vitreomacular attachment may be more common in normal eyes (>50%), our study[2] suggests that the incidence may be may be lower in patients with exudative age related macular degeneration (35.7%).

J Sahni, S Harding
Royal Liverpool University Hospital, Liverpool, UK

Correspondence to: J Sahni, Royal Liverpool University Hospital, Liverpool, UK; jayashree2001@hotmail.com

doi: 10.1136/bjo.2005.072827

Accepted for publication 8 April 2005

References

1 **Uchino E**, Uemura A, Ohba N. Initial stages of posterior vitreous detachment in healthy eyes of older persons evaluated by optical coherence tomography. *Arch Ophthalmol* 2001;**119**:1475–9.
2 **Sahni J**, Stanga P, Wong D, *et al.* Optical coherence tomography in photodynamic therapy for subfoveal choroidal neovascularisation secondary to age related macular degeneration: a cross sectional study. *Br J Ophthalmol* 2005;**89**:316–20.

NOTICES

EVER 2005 meeting

This will take place on 5-8 October 2005 in Vilamoura, Portugal. For further details please contact: Christy Lacroix, EVER Secretary, Kapucijnenover 33, B-3000 Leuven, Belgium (tel: +32 (0)16 233 849; fax +32 (0)16 234 097; email:ever@skynet.be).

World Ophthalmology Congress 2006 – Brazil

The World Ophthalmology Congress (which is replacing the International Congress of Ophthalmology) is meeting in February 2006 in Brazil.

For further information on the congress and committees, scientific program and coordinators of different areas are available at the congress website www.ophthalmology2006.com.br

Red eye

The latest issue of *Community Eye Health* (No 53) discusses the role of primary care in the treatment of red eye. For further information please contact: Journal of Community Eye Health, International Resource Centre, International Centre for Eye Health, Department of Infectious and Tropical Diseases, London School of Hygiene and Tropical Medicine, Keppel Street, London WC1E 7HT, UK (tel: +44 (0)20 7612 7964; email: Anita.Shah@lshtm.ac.uk; online edition: www.jceh.co.uk). Annual subscription (4 issues) UK £28/US$45. Free to developing country applicants.

Clinical and Experimental Ophthalmology 2007; **35**: 13–17
doi:10.1111/j.1442-9071.2006.01385.x

Original Article

Optical coherence tomography analysis of bilateral end-stage choroidal neovascularization where one eye is treated with photodynamic therapy

Jayashree Sahni MRCOphth,[1] Paulo Stanga MD,[2] David Wong FRCOphth,[1] Pauline Lenfestey MBBS,[1] David Kent FRCOphth[3] and Simon Harding FRCOphth[1]
[1]St Paul's Eye Unit, Royal Liverpool University Hospital, Liverpool, [2]Manchester Royal Eye Hospital, Manchester, UK, and [3]Eye Service, Aut Even Hospital, Kilkenny, Ireland

ABSTRACT

Background: To compare retinal thickness and subretinal hyper-reflectivity using Stratus optical coherence tomography (OCT3) between the eyes of patients with bilateral end-stage exudative age-related macular degeneration (AMD), where one eye has been treated with photodynamic therapy (PDT).

Methods: Patients with PDT-treated stable choroidal neovascularization (CNV), defined as a fibrotic lesion not requiring treatment for 6 months, in one eye and an untreated end-stage CNV (disciform) scar in their fellow eye, underwent refraction protocol logMAR visual acuity (VA) in letters, slit-lamp biomicroscopy, fluorescein angiography and OCT3 scan. Subretinal scar thickness was measured as Outer High Reflectivity Band Thickness (OHRBT) and retinal thickness as neuroretinal foveal thickness (NFT) on OCT3.

Results: Thirty-two eyes of 16 patients were studied. Mean OHRBT was 255.62 μm in treated eyes and 350.8 μm in untreated eyes ($P = 0.001$). Mean NFT was 130.3 μm in the treated eye and 79.9 μm in the untreated eye ($P = 0.017$). Mean VA was 42 letters in treated eyes and 15 letters in untreated eyes ($P < 0.005$).

Conclusion: Based on OCT3 findings, eyes with AMD treated with PDT have a thinner fibrous scar and better preserved retinal thickness when compared with untreated fellow eyes with end-stage fibrotic scarring.

Key words: age-related macular degeneration, choroidal neovascularization, optical coherence tomography, photodynamic therapy.

INTRODUCTION

Age-related macular degeneration (AMD) is a bilateral condition that tends to be fairly symmetric in its presentation and natural course. Retinal scars resulting from bilateral untreated cases of exudative AMD are known to be similar in fellow eyes.[1,2] The risk of developing a neovascular lesion in the second eye has been reported to be approximately 35% at 3.5 years by Gass[3] and 42% per year at 5 years by Macular Photocoagulation Study (MPS) group.[4]

Loss of vision in AMD has been attributed to the loss of retinal photoreceptors.[5–8] Green and Enger correlated histologically the thickness of fibrovascular scars and the extent of cell loss in the retina.[9] Scars thicker than 0.2 mm were associated with severe photoreceptor loss. Kim *et al.* found a 69.4% reduction in the number of outer nuclear layer cells in eyes with end-stage scars due to AMD compared with control eyes.[10]

In a cross-sectional study, we showed a correlation between scar thickness measured with Stratus optical coherence tomography (OCT3) and vision in patients undergoing photodynamic therapy (PDT).[11] In the current study, we compared retinal thickness, subretinal hyper-reflectivity and visual acuity (VA) between PDT-treated and fellow eyes that were stable or 'end-staged', that is, there was no leakage demonstrated on fluorescein angiography (FFA) and subretinal fluid (SRF) or macular oedema on OCT3 examination. If previous histoloical findings by Green and Enger hold true in this group of patients, we might be able to demonstrate similar findings by morphometric analysis on OCT3 examination.

■ *Correspondence:* Mrs Jayashree Sahni, Link 8 Z, St Paul's Eye Unit, Royal Liverpool University Hospital, Liverpool L7 8XP, UK. Email: jayashree2001@hotmail.com

Received 4 December 2005, accepted 3 August 2006.

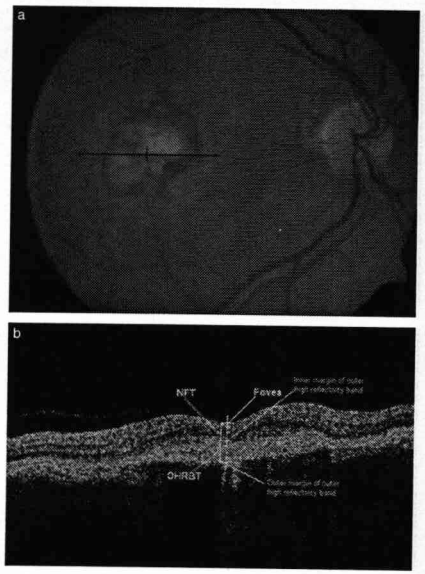

Figure 1. (a) Colour fundus photograph of treated right eye with logMAR visual acuity = 54 letters showing translucent scar 15 months after photodynamic therapy (PDT). (b) Stratus optical coherence tomogram passing through the scar and the fovea of the PDT-treated right eye. Neuroretinal foveal thickness (NFT) = 132 μm; outer high reflectivity band thickness (OHRBT) = 240 μm.

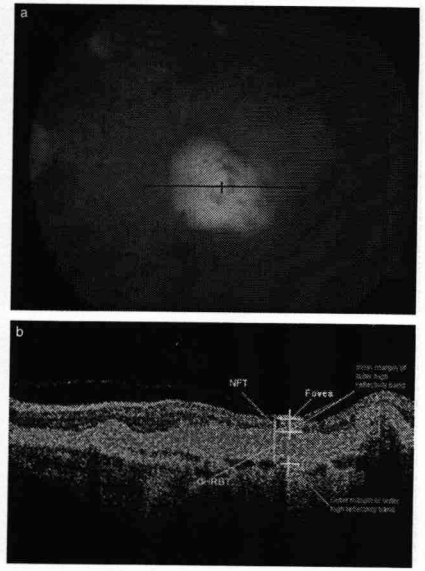

Figure 2. (a) Colour fundus photograph of untreated left eye with logMAR visual acuity = 24 letters showing end-stage disciform scarring. (b) Stratus optical coherence tomogram passing through the scar and the fovea of the untreated left eye. Neuroretinal foveal thickness (NFT) = 97 μm; outer high reflectivity band thickness (OHRBT) = 489 μm.

METHODS

Patients

Patients with bilateral neovascular AMD with end-stage subfoveal fibrosis (disciform scar) and who had a PDT-induced stable scar in one eye and end-stage scar in the fellow eye were recruited (Figs 1,2). A stable lesion in treated eyes was defined as a lesion with fibrosis not requiring PDT for at least 6 months. On slit-lamp biomicroscopy, subfoveal fibrosis was observed as a yellow-grey area related that blocked the details of underlying choroid.

Patients were excluded in the presence of:

- Inaccurate scan location through the centre of the fovea
- SRF on biomicroscopy or on OCT3 because of possible confounding effects on VA and the presence of fluid taken as an indicator of continuing lesion activity
- Severe cystoid macular oedema (CMO) causing distortion of retinal architecture and interfering with identification of the fovea
- Retinal pigment epithelial detachment

Study design

This was a prospective, cross-sectional study in patients with neovascular AMD attending St Paul's Eye Unit (Royal Liverpool University Hospital, UK) as part of an established PDT treatment service. If the patients were deemed to have a PDT-treated inactive scar in one eye and an inactive untreated fibrosed scar in their fellow eye based on slit-lamp biomicroscopy and FFA, they were referred for OCT3 scan. All patients also underwent: refraction protocol Early Treat-

ment Diabetic Retinopathy Study (ETDRS) logMAR VA using TAP Protocol,[1] colour fundus photographs and stereoscopic FFA.

Fluorescein angiography and colour fundus images were analysed and using the routine PDT protocol software, the greatest linear dimension (GLD) of the scar was calculated. For the purpose of this study the scars were divided as small <3500 μm, large 3500–5000 μm and very large > 5000 μm.

One grader (JS) performed all the scans on the day of recruitment after informed consent. Pupils were dilated with tropicamide (1%) and phenylephrine (2.5%) drops. Horizontal single line A scans through the fovea of default length 5 mm at 0° were obtained. OCT3 was performed using an internal fixation beam. In cases with unstable or eccentric fixation, the scan was manually positioned on the anatomical fovea as viewed on the black and white video image and multiple horizontal line scans were acquired passing through and above and below the estimated fovea. In these cases, colour fundus photographs and FFA centred on the macula were studied by another grader (PL), and the location of the fovea was marked (Figs 1a,2a). These images were then used to ensure that only a scan through the fovea was included for analysis. Neuroretinal foveal thickness (NFT) and outer high reflectivity band thickness (OHRBT) were measured using the definitions and technique described in our earlier paper.[11] All measurements were performed by positioning the callipers manually and using the retinal thickness (single eye) quantitative analysis protocol offered by Stratus OCT3. Figures 1b and 2b demonstrate the measurement of the OHRBT and NFT in the treated eye and fellow eye of a patient with bilateral end-stage disciform scarring on an OCT3 scan through the fovea. NFT was defined as the distance between the inner high reflectivity band and the inner margin of the outer high reflectivity band at the foveal centre. OHRBT was defined as the distance between the inner margin of the outer high reflectivity band and the outer margin of the outer high reflectivity band at the fovea. Patients with CMO or SRF on OCT3 were excluded as defined in the exclusion criteria. Measurements from OCT3 scans were performed in a masked fashion, the examiner (JS) being unaware of which eye had been treated.

The study had the approval of the Liverpool research ethics committee. Informed consent was obtained from all subjects and data were handled in accordance with the Data Protection Act (1984).

Statistics

Statistical analysis of the data was performed using SPSS for windows Version 11.0 (SPSS Inc, Chicago, IL, USA). VA, OHRBT, NFT and morphology between the eyes of the study patients were compared using the paired samples Student's *t*-test. Linear correlation between independent variables was analysed using the Pearson correlation coefficient (*r*). All correlations were two-tailed.

[1]ETDRS chart (Lighthouse Television Products, NY11101) was used. Best corrected visual acuity was measured at 2 m. The score was the total number of letters read correctly plus 15. If patients saw less than 20 letters, they were tested with the top 3 lines at 1 m. The score then was the total number of letters read at 2 m plus the number of letters read at 1 m.

Results

Thirty-eight patients (76 eyes) with a PDT-treated inactive scar in one eye and an inactive untreated fibrosed scar in their fellow eye were initially recruited based on slit-lamp biomicroscopy and FFA findings. In four patients OCT3 scans passing through the fovea could not be obtained because of erratic fixation. Eighteen untreated eyes had SRF or CMO at the fovea on OCT3. We felt that this suggested active choroidal neovascularization (CNV) and hence they were excluded. Sixteen patients had bilateral AMD that fulfilled all recruitment criteria.

Of the patients, 13 were women and 3 were men. Their mean age was 76.3 years (range 65–85 years).

The mean duration since first PDT treatment (baseline) was 20.7 months (range 12–30 months); patients had received a mean 4.5 PDT treatments (range 2–9). Dating of disease onset in the fellow eye with end-stage fibrotic scarring was not possible. The mean VA of the treated eye was 42.0 letters. The mean VA for the fellow eye was 15.0 letters. The difference of the mean was significant between the two groups ($P < 0.005$). Based on the GLD 50% of patients had symmetrical scars. Of these eight patients, four had scars <3500 μm in both eyes (i.e. small) and four had scars with GLD between 3500 and 5000 μm (i.e. large). All very large scars belonged to the untreated eye.

Mean OHRBT was 255.6 μm (range 149–406 μm) in the treated eye and 350.8 μm (range 182–553 μm) in the untreated fellow eye ($P = 0.001$). Mean NFT was 130.25 μm in the treated eye and 79.88 μm in the fellow untreated eye ($P = 0.017$) (Table 1). There was no statistically significant correlation between NFT and OHRBT, NFT and VA or OHRBT and VA in both treated and untreated eye. However, if the OHRBT and VA of both eyes were pooled and analysed together the relationship between the two groups showed a trend association ($P = 0.06$) (Fig. 3). There was no statistically significant relationship between NFT and VA even when the data were collated.

Table 1. Mean of outcome measures

Measurements	PDT eye (treated)	Fellow eye (untreated)	*P*-value
Mean VA (letters)	42 ± 14	15 ± 18	<0.005
Mean NFT (μm)	130.3 ± 61	79.9 ± 61	<0.05
Mean OHRBT (μm)	255.6 ± 76	350.8 ± 124	<0.005

NFT, neuroretinal foveal thickness; OHRBT, outer high reflectivity band thickness; PDT, photodynamic therapy; VA, ETDRS visual acuity.

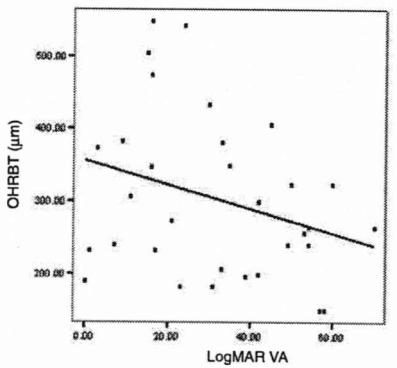

Figure 3. Relationship between logMAR visual acuity (VA) (in letters) units plotted against outer high reflectivity band thickness (OHRBT) in microns (μm). The linear regression line is $y = -1.68x + 356.39$, $P = 0.06$.

Discussion

In our present report, the relationship between VA and macular morphometry in PDT-treated eyes and untreated eyes with end-stage fibrosis was studied using the Stratus OCT3. Cross-sectional images were analysed and the NFT and OHRBT calculated from the scans. We found a statistically significant difference in outcome in terms of VA, NFT and OHRBT between eyes treated with PDT and untreated fellow eyes. The VA in the treated eyes was significantly better. The scars in the treated eyes were thinner in cross-section and the neuroretina was better preserved. These observations on OCT3 are supported by histopathological studies, which suggest that thicker fibrovascular (disciform) scarring can be responsible for photoreceptor atrophy.[6–10,12,13]

Verteporfin PDT has been shown to cause selective occlusion of the subretinal capillary layer with minimal involvement of the overlying retina and choroid in various animal experiments.[12,13] Our study suggests that in addition to this PDT may ultimately preserve the vision by modifying the natural history of the disciform scarring process. This in turn may prevent further neuroretinal damage and photoreceptor loss.[9]

To reduce a bias in the case selection, we recruited all sequential patients who had a PDT-treated inactive scar in one eye and an untreated fibrosed scar in their fellow eye based on slit-lamp biomicroscopy and FFA. For the purpose of this study, a stable lesion in the treated eye was defined as a lesion with fibrosis not requiring PDT for at least 6 months. However, 18 untreated fellow eyes had SRF on OCT3 suggesting an active exudative pathology. To minimize the confounding effect of variables such as the presence of fluid and to minimize errors in interpretation of the OCT3 scans, only patients with well-defined subfoveal fibrotic scarring were included in the study. As the 18 patients were excluded because of the OCT3 features in their untreated eye, we believe that the patients left in the study are a representative sample of PDT-treated eyes. Hence, the findings of the study can be applied to the understanding of all the patients undergoing this treatment.

For OCT3 to be meaningful in macular disease, scans must pass through the anatomical centre of the fovea. In our study 25% could not be reliably scanned through the fovea. Reliability of scans was limited by poor fixation, excessive eye movements and difficulty identifying the true location of the fovea because of morphological changes caused by disease. Three other studies have reported on the difficulty of obtaining scans. Hee *et al.* failed to obtain adequate scans in 4.2% of the study population, comprising mainly patients with diabetes with moderate to good VA (better than 6/24).[14] Rogers *et al.* reported a higher percentage (12.2%) of scans to be unobtainable/unreliable in a population of patients with AMD.[15] We found a 17% exclusion rate in an earlier study and found a higher rate in this study.[11] This is because our patients had worse vision and very poor fixation.

We chose the fellow eye as a control. We recognize that a potential inter-eye correlation may introduce bias. We believe that the use of the fellow eye as a control group is justified because of the following reasons: (i) AMD is a bilateral condition that tends to be fairly symmetric in its presentation and natural course. A number of studies have assessed the overall risk of development of CNV in the fellow eye. In the MPS study, 42% of fellow eyes progressed to neovascular AMD at 5 years. (ii) Although it is possible that the lesion composition may differ between the two eyes, most studies suggest that the type of CNV in the first eye predicts the type of CNV in the second eye. Sixty-three per cent of eyes with classic-only CNV in one eye developed a classic-only CNV in the fellow eye in the MPS study.[16] Chang *et al.* found that 84–87% patients with occult CNV developed the same type of occult CNV in their other eye.[17] (iii) Evidence from Lavin *et al.* and Bird *et al.* suggests that the final outcome in bilateral neovascular AMD tends to be similar.[1,2] Lavin *et al.* found that the degree of concordance increased from 54% to 68% with a 12-month follow up. Although the size of the scar was not a factor for inclusion into our study, 50% of patients had symmetrical scars in terms of GLD. (iv) Our paper does not attempt to correlate scar thickness with the horizontal dimension of the scar. We aimed to show that scar thickness is an independent risk factor for visual loss secondary to photoreceptor loss. Before the advent of the OCT3, it has not been possible to study the thickness of the scar in an *in vivo* situation. Hence, there have been no previous studies to show that scar thickness tends to be symmetrical. However, there is histopathological evidence for symmetry in scar thickness and the relationship between thickness of the disciform scar and photoreceptor loss.[9] As 50% of our patients had symmetrical GLD, it is possible to conclude that the thickness of the disciform scar may be an independent

factor for visual preservation. This study only included patients who had responded to PDT as demonstrated on clinical, FFA and OCT examination. Therefore, this conclusion can be applied to only those patients responsive to PDT.

We could not find a statistically significant association between visual outcome and central retinal or scar thickness. This may be because our strict inclusion criteria resulted in a small number of patients being included. Power calculations were not performed, as there were no preliminary data on which to base them on. With a larger number of patients, as seen when the results from the two eyes were pooled, there was a definite trend association between the scar thickness and VA. Also, some error in the measurements could have arisen because of the patients' unstable fixation. As a result, although the measurements on OCT3 were performed at the fovea, vision might have been measured from the extrafoveal retina.

In summary, we have demonstrated that in comparison with untreated eyes with end-stage disciform scars, the subretinal scar tend to be thinner in eyes treated with PDT and the retina tends to be thicker. In eyes with thicker scar, in the absence of SRF and CMO, the retina tends to be atrophic because of loss of photoreceptors and neural elements. In PDT-treated eyes, on the other hand, the rapid organization of the scar results in a thinner scar, which in turn may result in the preservation of the neuroretina and a retinal thickness closer to normal (180 μm). If subretinal hyper-reflectivity refers to the subretinal scar, then one of the benefits of PDT is the modification of the wound healing process, such that the visual benefit of treatment may be derived from preservation of the foveal morphology and alteration of the subfoveal scarring. Thus, patients who have a thick established scar in one eye and present with a subfoveal classic CNV in their second eye may benefit from early treatment with PDT.

ACKNOWLEDGEMENTS

This study was supported by The Foundation for the Prevention of Blindness, UK (registered charity no: 1047988). We are grateful to the staff of the Clinical Eye Research Centre at St Paul's Eye Unit, Liverpool for their help with the study.

REFERENCES

1. Lavin MJ, Eldem B, Gregor ZJ. Symmetry of disciform scars in bilateral AMD. *Br J Ophthalmol* 1991; **75**: 133–6.
2. Gregor Z, Bird AC, Chisholm IH. Senile disciform degeneration in the second eye. *Br J Ophthalmol* 1977; **61**: 141–7.
3. Gass JD. Drusen and disciform macular detachment and degeneration. *Arch Ophthalmol* 1973; **90**: 206–17.
4. Macular Photocoagulation Study Group. Five-year follow-up of fellow eyes of patients with age-related macular degeneration and unilateral extrafoveal choroidal neovascularization. *Arch Ophthalmol* 1993; **111**: 1189–99.
5. Green WR, McDonell PJ, Yeo JH. Pathologic features of senile macular degeneration. *Ophthalmology* 1985; **92**: 615–27.
6. Green WR, Key SN. Senile macular degeneration: a histopathologic study. *Trans Am Ophthalmol Soc* 1977; **75**: 180–254.
7. Gartner S, Henkind P. Aging and degeneration of the human macula. Outer nuclear layer and photoreceptors. *Br J Ophthalmol* 1981; **65**: 23–8.
8. Curcio CA, Medeiros NE, Millican CL. Photoreceptor loss in age-related macular degeneration. *Invest Ophthalmol Vis Sci* 1996; **37**: 1236–49.
9. Green WR, Enger C. Age related macular degeneration histopathologic studies: the 1992 Lorenz E Zimmerman Lecture. *Ophthalmology* 1993; **100**: 1519–35.
10. Kim SY, Sadda S, Pearlman J *et al.* Morphometric analysis of the macula in eyes with disciform age-related macular degeneration. *Retina* 2002; **22**: 471–7.
11. Sahni J, Stanga P, Wong D, Harding S. Optical coherence tomography in photodynamic therapy for subfoveal choroidal neovascularisation secondary to age related macular degeneration: a cross sectional study. *Br J Ophthalmol* 2005; **89**: 316–20.
12. Ghazi NG, Jabbour NM, De La Cruz ZC, Green WR. Clinicopathologic studies of age-related macular degeneration with classic subfoveal choroidal neovascularization treated with photodynamic therapy. *Retina* 2001; **21**: 478–86.
13. Schlotzer-Schrehardt U, Viestenz A, Naumann GO *et al.* Dose-related structural effects of photodynamic therapy on choroidal and retinal structures of human eyes. *Graefes Arch Clin Exp Ophthalmol* 2002; **240**: 748–57.
14. Hee MR, Puliafito CA, Wong C *et al.* Quantitative assessment of macular edema with optical coherence tomography. *Arch Ophthalmol* 1995; **113**: 1019–29.
15. Rogers AH, Martidis A, Greenberg PB *et al.* Optical coherence tomography findings following photodynamic therapy of choroidal neovascularisation. *Am J Ophthalmol* 2002; **134**: 566–76.
16. Macular Photocoagulation Study Group. Risk factors for choroidal neovascularization in the second eye of patients with juxtafoveal or subfoveal choroidal neovascularization secondary to age-related macular degeneration. *Arch Ophthalmol* 1997; **115**: 741–7.
17. Chang B, Yanuzzi LA, Ladas ID *et al.* Choroidal neovascularization in second eyes of patients with unilateral exudative age-related macular degeneration. *Ophthalmology* 1995; **102**: 1380–6.